Investigation and comparison of the regulation of ATOH1 in the mammalian and avian inner ear

Miriam Gómez Dorado

Submitted for the degree of PhD

University College London

2017

Declaration

"I, Miriam Gómez Dorado, confirm that the work presented in this thesis is my own. Where information has been derived from other sources, I confirm that this has been indicated in the thesis. Where work has been conducted by other members of our laboratory, this has been indicated by their initials or an appropriate reference"

SD = Dr. Sally Dawson

JG = Dr. Jonathan Gale

ND = Dr. Nicolas Daudet

NH = Mrs. Naila Haq

CG = Miss Ana Cláudia Gonçalves

Abstract

Atonal homolog 1 (*Atoh1*) is a basic helix-loop-helix (bHLH) transcription factor required for the formation of sensory hair cells in the inner ear (Bermingham et al. 1999). Understanding the *Atoh1* regulatory network is crucial for the development of new therapies to treat hearing loss. However, to date, little is known about the mechanisms controlling ATOH1 expression.

The loss of sensory hair cells can cause deafness and balance disorders. In the mammalian inner ear, the loss of ATOH1 expression in adults has been linked with a limited capacity to regenerate hair cells (Wang et al. 2010). However, in non-mammalian vertebrates, ATOH1 expression re-activates spontaneously after hair cell damage and new hair cells can be formed throughout life (Cafaro et al. 2007) (Daudet et al. 2009).

In this thesis, I aimed to identify regulatory elements responsible for ATOH1 expression through a comparative analysis of avian and mammalian ATOH1 gene loci. A bioinformatic approach was used to identify evolutionary conserved non-coding ATOH1 DNA sequences including those that are conserved between avian and mammals and those that are specific to both groups. Putative transcription factor binding sites predicted within these conserved elements were then investigated using EMSA analysis and reporter gene assays. These experiments suggest that the E2F1 transcription factor activates the chick ATOH1 gene and that this activation occurs predominantly via a direct interaction with a regulatory region that is conserved between avian species but absent from mammals. E2F transcription factors control cell cycle progression so the identification of this family as novel regulators of the chick ATOH1 expression links avian ATOH1 re-activation to cell proliferation. If confirmed, this would provide a possible mechanism to explain the different regenerative capabilities of mammalian and non-mammalian sensory cells and therefore contribute to the design of therapies for the regeneration of hair cells after damage.

Table of Contents

1 GENERAL INTRODUCTION 18

1.1 THE STUDY OF THE INNER EAR AND HEARING LOSS 18

1.2 GENERAL ANATOMY AND FUNCTION OF THE MAMMALIAN EAR 19

1.2.1 The outer ear 19

1.2.2 The middle ear 19

1.2.3 The inner ear 21

1.3 HAIR CELLS AND MECHANOELECTRICAL TRANSDUCTION 25

1.4 INNER EAR DEVELOPMENT 26

1.4.1 Early inner ear development 26

1.4.2 From the otic placode to the otocyst 28

1.4.3 Late morphogenesis and sensory development of the inner ear 31

1.4.4 Summary of inner ear development 32

1.5 DEVELOPMENT OF AUDITORY HAIR CELLS 33

1.5.1 Early cellular differentiation of the primordium cochlear epithelium 33

1.5.2 Specification of hair cells and supporting cells: Id proteins and Notch signalling 36

1.5.3 Hair cell differentiation 37

1.5.4 Maturation of the hair cells 41

1.6 *ATOH1* 41

1.6.1 Initial studies 42

1.6.2 Expression of *Atoh1* in the developing inner ear 45

1.6.3 The role of *Atoh1* in the inner ear 49

1.6.4 *Atoh1* function in other tissues 50

1.7 TRANSCRIPTION FACTORS AND REGULATORY MECHANISMS OF GENE EXPRESSION 52

1.7.1 Transcriptional control of gene expression 54

1.7.2 Regulation of *Atoh1* 56

1.7.3 Transcription factors binding *Atoh1* enhancers 59

1.7.4 Signalling pathways, ATOH1 expression and sensory cell fate in the inner ear 63

1.7.5 Can *Atoh1* restore hearing? 64

1.8 NEW PERSPECTIVES AND TREATMENTS FOR HEARING LOSS 67

1.9 INVESTIGATION OF INNER EAR BIOLOGY 68

1.9.1 The challenge of studying the inner ear 68

1.9.2 The use of cell lines as a model to study gene regulation 69

1.10 PROJECT AIMS 70

2 MATERIAL AND METHODS 72

2.1 MATERIAL 72

2.1.1 General Equipment 72

2.1.2 Stock solutions 73

2.1.3 Safety 73

2.1.4 Primers 73

2.2 METHODS 74

2.2.1 DNA purification 74

2.2.2 Plasmid construction 78

2.2.3 Screening of bacterial recombinants 82

2.2.4 Sequencing of plasmid constructs 83

2.2.5 Reverse Transcriptase Polymerase Chain Reaction (RT-PCR) 83

2.2.6 Cell culture 85

2.2.7 *In vitro* transcription and translation procedure 87

2.2.8 The electrophoretic mobility shift assay (EMSA) 87

2.2.9 Reporter Gene Assay 91

2.2.10 Quick Change Site-Directed Mutagenesis 99

2.2.11 Dissections of animal material 100

2.2.12 Tissue processing for cryo-sections 101

2.2.13 Immunohistochemistry 102

2.2.14 *In ovo* electroporation 104

2.2.15 *In situ* hybridization (ISH) 107

3 BIOINFORMATIC ANALYSIS 110

3.1 STRATEGY OF THE INVESTIGATION 110

3.2 IDENTIFICATION OF CONSERVED ELEMENTS BY COMPARATIVE GENOME ANALYSIS 111

3.2.1 Comparative alignment of the human and mouse *Atoh1* locus 111

3.2.2 Comparative alignment of the chick and zebra finch *Atoh1* locus 114

3.2.3 Multi-species alignment of the *Atoh1* genomic sequence 117

3.3 IDENTIFICATION OF PUTATIVE TRANSCRIPTION BINDING SITES WITHIN ECRS 120

3.3.1 Predictions within *Atoh1* Enhancer A and Enhancer B 120

3.3.2 Predictions within putative Enhancer C 125

3.3.3 Predictions within other evolutionary conserved regions 125

3.4 REFINEMENT OF PREDICTIONS 128

3.5 PRIORITIZATION OF YY1, NFKB, E2F AND ATOH1 131

3.5.1 YY1 131

3.5.2 NF-κB 132

3.5.3 E2F 133

3.5.4 ATOH1 133

3.6 BINDING PROFILES FOR YY1, NF-κB AND ATOH1 TRANSCRIPTION FACTORS 134

3.7 BINDING PROFILES FOR THE E2F TRANSCRIPTION FACTOR FAMILY 137

3.8 DISCUSSION 142

4 INVESTIGATION OF PUTATIVE CANDIDATE REGULATORS OF ATOH1 144

4.1 EMSA ANALYSIS OF CANDIDATE BINDING SITES 144

4.2 TRANSCRIPTIONAL ACTIVATION OF *ATOH1* CONSERVED REGIONS BY CANDIDATE REGULATORS 149

4.2.1 Cloning of the mouse and chick *Atoh1* conserved elements 149

4.2.2 Effect of YY1 on the *Atoh1* conserved non-coding elements 150

4.2.3 Effect of NF-κB on the *Atoh1* conserved non-coding elements 152

4.2.4 Effect of ATOH1 on the *Atoh1* conserved non-coding elements 154

4.2.5 Investigation of the effect of E47, the ATOH1 co-factor 159

4.3 DISCUSSION 163

5 INVESTIGATION OF THE E2F TRANSCRIPTION FACTOR FAMILY AS A PUTATIVE CANDIDATE REGULATOR OF ATOH1 168

5.1 INTRODUCTION TO THE E2F FAMILY 168

5.1.1 Initial studies 168

5.1.2 E2F family members 169

5.1.3 E2F co-factors: The DP family 170

5.1.4 E2F functions 171

5.1.5 E2F and the inner ear 174

5.1.6 The E2F family and the study of *Atoh1* regulation 176

5.2 REGULATION OF THE MAMMALIAN AND AVIAN *ATOH1* CONSERVED REGIONS BY E2F1 177

5.3 EMSA ANALYSIS OF THE PREDICTED E2F BINDING SITES IN THE CHICK *ATOH1* CONSERVED REGIONS. 181

5.3.1 Analysis of E2F1 expression in UB/OC2 cells 181

5.3.2 Binding of E2F in EMSA experiments 185

5.3.3 Characterization of binding affinities of the predicted E2F sites in the *Atoh1* regulatory elements 189

5.3.4 Further analysis of *Atoh1* probes 2 and 6 as putative E2F binding sites 193

5.4 SITE DIRECTED MUTAGENESIS OF SITES 2 AND 6 WITHIN THE AVIAN *ATOH1* CONSERVED REGIONS 199

5.4.1 Design of mutagenesis sites 199

5.4.2 Site-directed mutagenesis of sites 2 and 6 201

5.5 RESPONSE OF THE *ATOH1* CONSERVED REGIONS TO E2F1 WHEN PUTATIVE E2F SITES ARE MUTATED 203

5.6 TRANSCRIPTIONAL REGULATION OF THE *ATOH1* CONSERVED REGIONS BY OTHER E2F TRANSCRIPTION FACTORS 205

5.7 CHARACTERIZATION OF E2F1 EXPRESSION IN THE MAMMALIAN AND AVIAN DEVELOPING INNER EAR EPITHELIUM 209

5.7.1 E2F1 expression in the developing chick inner ear epithelium 210

5.7.2 E2F1 expression in the developing mouse inner ear epithelium 216

5.8 SUMMARY AND DISCUSSION 221

6 IN VIVO INVESTIGATION OF THE ROLE OF PUTATIVE ENHANCER C AND E2F1 ON THE REGULATION OF CHICK ATOH1 228

6.1 INTRODUCTION TO THE TOL2 SYSTEM 228

6.2 *IN VIVO* CHARACTERIZATION OF THE CHICK *ATOH1* CONSERVED REGIONS BY THE USE OF THE TOL2 SYSTEM. 230

6.2.1 Effect of the relative position of the *Atoh1* conserved regions on the Tol2 reporter activity 238

6.3 *IN VIVO* EFFECT OF E2F1 IN THE CHICK INNER EAR AT EARLY STAGES 242

6.4 SUMMARY AND DISCUSSION 246

7 GENERAL DISCUSSION 250

8 CONCLUSIONS 259

APPENDIX 261

BIBLIOGRAPHY 266

List of Figures

Figure 1.1. Anatomy of the mammalian ear. 20
Figure 1.2. General anatomy of the cochlea. 23
Figure 1.3. Anatomy of the mammalian vestibular system 24
Figure 1.4. Development of the inner ear 27
Figure 1.5. Morphogenesis of the inner ear. 29
Figure 1.6. Early cellular differentiation of the primordium cochlear epithelium. 35
Figure 1.7. The Notch signalling pathway 37
Figure 1.8. *Atoh1* is required for the formation of hair cells 44
Figure 1.9. *Atoh1* expression in mouse and chick 48
Figure 1.10. Initiation of transcription 55
Figure 1.11. Schematic representation of the mouse *Atoh1* locus on chromosome 6. 61
Figure 2.1. pDrive vector. 78
Figure 2.2. pGEM®-T Easy Vector 79
Figure 2.3. pGL4.23[luc2/minP] 92
Figure 2.4. pSI Mammalian expression vector 93
Figure 2.5. pcDNA3 expression construct 94
Figure 3.1. Alignment comparison between the human and mouse *Atoh1* genome sequences 113
Figure 3.2. Alignment comparison between the chick and zebra finch *Atoh1* genome sequences 115
Figure 3.3. Alignment comparison between the chick, human, mouse and zebra finch *Atoh1* genome sequences 118
Figure 3.4. Common transcription factor binding sites predicted within *Atoh1* enhancer A and B. 122
Figure 3.5. Common transcription factor binding sites predicted within *Atoh1* putative enhancer C in chick and zebra finch.. 126
Figure 3.6. Common transcription factor binding sites within other evolutionary conserved regions at the *Atoh1* locus. 127
Figure 3.7. Common transcription factor binding sites predicted within *Atoh1* enhancer A of mouse and human 129
Figure 3.8. Common transcription factor binding sites predicted within putative enhancer C of chick and zebra finch 130

Figure 3.9. Location of the YY1, NF-κB and ATOH1 predicted binding sites within the *Atoh1* conserved regions 135
Figure 3.10. Predicted E2F binding sites within mouse and chick *Atoh1* conserved regions. 137
Figure 4.1. Binding of YY1 to *Atoh1* enhancer A binding site. 146
Figure 4.2. Binding of NF-κB to putative enhancer C. 148
Figure 4.3. Effect of the YY1 transcription factor on the activity of the mouse and chick *Atoh1* enhancers and putative enhancer C. 151
Figure 4.4. Effect of the NF-κB transcription factor on the mouse and chick *Atoh1* enhancers and putative enhancer C 153
Figure 4.5. Dose-response effect of *ATOH1* on the *Atoh1* conserved elements. 156
Figure 4.6. Effect of ATOH1 on the *Atoh1* non-coding conserved elements 158
Figure 4.7. Effect of ATOH1 and E47 on the regulation of E-box sites 160
Figure 4.8. Effect of ATOH1 and E47 on the *Atoh1* evolutionary conserved regions. 162
Figure 5.1. The E2F family 170
Figure 5.2. Schematic representation of the role of the E2F/Rb complex in the control of the cell cycle.. 172
Figure 5.3. Dose-response effect of the E2F1 transcription factor on the *Atoh1* conserved regions. 180
Figure 5.4. Endogenous expression of E2F1 in UB/OC2 cells. 182
Figure 5.5. RT-PCR for E2F1. 183
Figure 5.6. Comparison between E2F1 transfected and non-transfected UB/OC2 cells 184
Figure 5.7. Comparison of the binding of a known E2F1 binding site incubated with nuclear protein extracts from non-transfected UB/OC2 cells or nuclear protein extracts from UB/OC2 cells transfected with E2F1 and DP1 188
Figure 5.8. Location of the predicted E2F binding sites in the chick *Atoh1* enhancers and putative enhancer C. 190
Figure 5.9. EMSA analysis of the predicted E2F sites in the chick *Atoh1* conserved regions 192
Figure 5.10. Competition assay to test specificity of Probe 2. 195
Figure 5.12. Comparison between the consensus E2F1 binding site and the predicted site 2 and site 6 200
Figure 5.13. Verification of the nucleotide substitutions by Site-directed mutagenesis. 202

Figure 5.14. Response of the *Atoh1* regulatory regions to E2F1 when the putative E2F sites are mutated 204
Figure 5.15. Effect of E2F2, E2F3 and E2F4 on the *Atoh1* conserved regions 207
Figure 5.16. Immunolabeling of E2F1 in E7 chick crista. 211
Figure 5.17. Immunolabeling of E2F1 in E10 chick crista. 212
Figure 5.18. E2F1 expression in chick retina assessed by *in situ* hybridization and by immunolabeling 214
Figure 5.19. E2F1 expression in the chick inner ear by *in situ* hybridization (ISH) 215
Figure 5.20. Expression of E2F1 in P0 cochlear explants 217
Figure 5.21. Expression of E2F1 in the mouse organ of Corti. 219
Figure 5.22. Cellular localization of E2F1 expression at P21 220
Figure 6.1. Constitutive expression of Tol2 reporters via *in ovo* electroporation 230
Figure 6.2. Activity of the *Atoh1*-ChickAB-down::nEGFP-mCherry 233
Figure 6.3. Activity of the *Atoh1*-ChickC-down::nEGFP-mCherry at E7 234
Figure 6.4. Activity of the *Atoh1*-ChickC-down::nEGFP-mCherry at E9 235
Figure 6.5. Activity of the chick *Atoh1*-ChickABC-down::nEGFP-mCherry at E9. 236
Figure 6.6. Activity of the base Tol2 vector at E7. 237
Figure 6.7. Activity of the *Atoh1*-ChickAB-up::nEGFP-mCherry at E7 240
Figure 6.8. Activity of the *Atoh1*-ChickC-up::nEGFP-mCherry at E7.. 241
Figure 6.9. Gene transfer by *in ovo* electroporation. 242
Figure 6.10. E4 chick otocyst electroporated with E2F1. 243
Figure 6.11. ATOH1 expression in the E4 chick hindbrain.. 245
Figure 7.1. Updated comparative analysis of the *Atoh1* 3' sequence in mammalian and avian species. 251
Figure 7.2. Hypothesis of the role of the E2F1-4 on the control of *Atoh1* expression 255
Figure 7.3. Changes in ATOH1, E2F1, E2F7 and E2F8 during hair cell regeneration 257

Appendix Figure 1. Attempt to show binding of UB/OC2 cell nuclear protein extract to a consensus E2F binding site 262
Appendix Figure 2. EMSA with *in vitro* translated proteins. 265

List of Tables

Table 2.1. Summary of the primers used in this study.. 74
Table 2.2. Summary of the antibodies selected in this study.....103
Table 3.1. MatInspector analysis of candidate genes.....136
Table 3.2. Predicted E2F binding sites within chick *Atoh1* enhancer region 139
Table 3.3. Predicted E2F binding sites within chick *Atoh1* putative enhancer C.. 140
Table 3.4. Predicted E2F binding sites within mouse *Atoh1* enhancer region.....141
Table 4.1. Oligonucleotides for YY1 and NF-κB EMSA analysis.....145
Table 5.1. Consensus oligonucleotides for EMSA experiments 185
Table 5.2. EMSA oligonucleotides containing the putative E2F sites in the *Atoh1* regulatory region.....189
Table 5.3. Primers used for EMSA experiments containing point mutations in Probe 2 and Probe 6.....194

Dedication

To my family who supported me every step along the way

Acknowledgements

I would like to thank the people who provided me the opportunity to carry out the work conducted in this thesis and supported me throughout. First of all, I would like to express my gratitude to my supervisors Dr Sally Dawson, Dr Jonathan Gale and Dr Nicolas Daudet at the Ear Institute for providing me the opportunity to conduct this research work and guiding me over the past years. This work could have never been possible without their support, advice and guidance.

I wish to thank Dr Wayne Clark and Dr Peter Bolton from Richmond University for providing me advice and help during the first steps of my scientific career. I will always remember the enthusiasm delivered during your lectures and lab sessions which have been a great inspiration for many students including myself.

Thanks must also go to the current and past students/postdocs/lab members of the department: Claudia, Naila, Sara, Steph, Katie, Hassan, Jimena, Roberta, Ghada, Zoe, Mike, Camille, Fitim, Elena, Steve, John, Emily, Greg, Valentina, Piotr, Hector, David, for the many hours of mutual support, and specially to Lisa for the training provided in various techniques used in this research and the endless support received, not only as scientist but also as friend.

Finally, but not least, I would like to thank to my dear friends Laura, Cristina, Oscar and Jose x2 for being always there, even in the distance. To Ivan and Leticia for the many moments, unforgettable trips around Europe, laughs and tears shared here in London. I feel very lucky for having you all. And finally, many thanks to my family for supporting me in everything I have chosen to do.

Abbreviations

ABR	Auditory brainstem response
Ad	Adenovirus
A-P	Anterior-Posterior
ARHL	Age-related hearing loss
Atoh1	Atonal homolog 1
BDNF	Brain derived neurotrophic factor
bHLH	Basic helix-loop-helix
BLAST	Basic local alignment search tool
BMP	Bone morphogenetic protein
bp	Base pair
BrdU	5-bromo-2'-deoxyuridine
BREu	Upstream TFIIB Recognition Element
cD1	Cyclin D1
Cdk	Cyclin-dependent kinase
cDNA	Complementary DNA
CMV	Cytomegalovirus
CNS	Central nervous system
Cre	Cre-recombinase
CVG	Cochleovestibular ganglion
DCE	Downstream Core Element
DNA	Deoxyribonucleic acid
DP	Dimerization protein
DPE	Downstream Promoter Element
D-V	Dorsal-Ventral
E	Embryonic day
E2F	E2 promoter binding Factor
EMSA	Electrophoretic mobility shift assay
ECR	Evolutionary conserved region
FACS	Fluorescence-activated cell sorting
FGF	Fibroblast growth factor

GER	Greater epithelial ridge
GFP	Green fluorescent protein
h	Hour
HBS	Hank's buffered saline
IHC	Inner hair cell
InR	Initiator
kb	Kilobase(s)
M-L	Medial-Lateral
min	Minute
mRNA	Messenger ribonucleic acid
MTE	Motif Ten Element
NLS	Nuclear localization signal
OHC	Outer hair cell
P	Post-natal day
PBS	Phosphate buffered saline
PCNA	Proliferating cell nuclear antigen
PCR	Polymerase chain reaction
PFA	Paraformaldehyde
q-PCR	Quantitative polymerase chain reaction
PIC	Pre-initiation complex
Rb	Retinoblastoma
RNA	Ribonucleic acid
rpm	Revolution per minute
rRNA	Ribosomic RNA
RT-PCR	Reverse transcriptase polymerase chain reaction
s	Seconds
SDM	Site-directed mutagenesis
Shh	Sonic Hedgehog
SNP	Single nucleotide polymorphisms
S-phase	DNA synthesis -phase
TEMED	Tetramethylethylenediamine
TSS	Transcription start site
UB/OC2	University of Bristol/Organ of Corti cell line 2

UTR	Untranslated region
WHO	World Health Organization
XCPE1	X Core Promoter Element 1
ZNPC	Zone of non-proliferating cells

Notes to Reader

- Human gene names are in upper case and italicised
- Non-human gene names are italicised with capitalised letters only
- Non-human gene names are used if referring to both human and non-human genes
- All protein names are fully upper case and not italicised
- Mouse AB refers to the mouse *Atoh1* enhancers
- Chick AB refers to the chick *Atoh1* enhancers
- Chick ABC or chick conserved elements refers to the chick *Atoh1* enhancers and chick putative enhancer C

Chapter 1

1 General Introduction

1.1 The study of the inner ear and hearing loss

Hearing loss is the most common form of sensory impairment in humans. According to the World Health Organization (WHO), 360 million people worldwide have a moderate to profound hearing loss and 1 in 500 children are born with impaired hearing (Thompson et al. 2001). In addition to congenital hearing loss, the problem is increasing due to additional environmental and lifestyle factors. The unsafe use of personal audio devices, such as smartphones, and the exposure to noisy environments like entertainment venues, could bring negative consequences. It has been estimated that over 1 billion teenagers and young adults are at risk of hearing loss (WHO data from February 2015).

Noise-induced hearing loss however, is not the only cause of deafness. Other conditions such as age related hearing loss (ARHL), genetic disorders, certain infectious diseases as well as the use of particular drugs are also very important factors that contribute to hearing loss (Liu and Yan 2007; Uchida et al. 2011; Van Eyken et al. 2007; Brown 1981).

Identifying and addressing hearing loss early will bring many benefits to enhance quality of life of those affected by a deafness condition. However, to achieve this, it is crucial to understand how the hearing system works in order to develop new therapies and approaches that can contribute to improve patient lives. Of course, this is not an easy achievement. The inner ear is a small and fragile structure which can easily be damaged. In addition, the location of the inner ear within the temporal bone makes access to the different ear structures a very challenging task. New technologies based on regenerative medicine and gene therapy are being developed and it is hoped that these could be alternative routes for restoring lost auditory function and overcome some of the obstacles to the study of the hearing system.

1.2 General anatomy and function of the mammalian ear

The ear anatomy is possibly the most complex sensory system in the human body. The mammalian ear is formed by a three-dimensional structure responsible for balance and sound detection located inside the temporal bone. Anatomically and functionally the mammalian ear is divided in three interconnected structures: the outer, the middle and the inner ear.

1.2.1 The outer ear

The outer ear consists of an external cartilaginous structure called the pinna followed by the ear canal or external auditory meatus which leads to the eardrum or tympanic membrane (Haines 2013; Purves et al. 2008) (Figure 1.1). The function of the external part of the ear is mainly focused on the collection of the sound waves over the area of the pinna structure (Faddis 2008). As the outer ear narrows into the ear canal, the pressure gained at the tympanic membrane increases the energy to be transferred into the middle ear. The increase in sound pressure in humans at the tympanic membrane produces a broad peak of 15-20dB at 2.5Hz (Wiener and Ross 1946). Another important function of the outer ear is sound localization (Pickles 1998). As the ear pinna and concha (funnel-like opening to the outer ear canal) are shaped in folded cartilage, this structure reflects and attenuates the sound waves and helps the brain to determine the location of the sound. As we have two ears, the difference in the sound waves travelling along the ear canal and consequently the movements of the eardrum in both ears followed by mechanotransduction and neural processing will be interpreted by the brain to locate the sound (Pickles 1998).

1.2.2 The middle ear

The middle ear is formed by the internal part of the tympanic membrane, the auditory ossicles and the oval window (Figure 1.1). As the sound waves travel into the ear canal, the pressure gained produces the vibration of the tympanic membrane which subsequently is transformed as mechanical pressure into the cochlear fluids. In this process, the three ossicle bones, the malleus, incus and the stapes, amplify the pressure wave in to the cochlea (Haines 2013; Purves et al. 2008). The tip of the malleus is

Picture removed for copyright purposes

Figure 1.1. Anatomy of the mammalian ear. The ear is divided into the outer, middle and inner ear. In the outer ear are found the pinna, the external auditory meatus or ear canal and the tympanic membrane that separates the outer and middle ear. The three ossicle bones, the malleus, incus and the stapes comprise the middle ear. The cochlea, the vestibular system and the auditory nerve form the main structures of the inner ear (Figure reproduced from Kelley, 2006).

pushed by the tympanic membrane and the mechanical movement is transferred to the incus and then to the stapes, the smallest bone in the human body. The stapes is attached to an aperture in the wall of the cochlea, known as the oval window. The main function of the middle ear is to reduce the magnitude of movements between the air environment in the outer ear while increasing the force in the fluid environment of the inner ear, a function known as the impedance matching (Pickles 1998). Since the area of the tympanic membrane is larger than the stapes footplate in the cochlea, the force collected over the tympanic membrane is concentrated and transferred to the cochlea with a higher pressure. In addition, the arm of the incus is shorter than that of the malleus, which increases the force, reduces the velocity at the stapes and contributes to the impedance match (Pickles 1998).

1.2.3 The inner ear

The mammalian inner ear consists of two sensory organs, the cochlea and the vestibular system, interconnected by a series of canals and enclosed in the temporal bone, the hardest bone in the human body (Frisch et al. 1998).

1.2.3.1 The cochlea

The human cochlea is formed by a coiled structure with approximately $2^{1/2}$ to $2^{3/4}$ turns from base to apex (Hardy 1938). The cochlea is bisected from its basal end to almost the apical end (Purves et al. 2008) by three different compartments: the scala media (also known as the cochlear duct), the scala vestibuli and the scala tympani (Figure 1.2a). In cross section, the scala media is bounded by the basilar membrane, the Reissner's membrane and the stria vascularis in the external part. This compartment is filled by the endolymph, a fluid rich in potassium and with different chemical properties in comparison to the perilymph, the fluid that fills the scala vestibuli and scala tympani which contains a high concentration of sodium (Forge and Wright 2002). It is essential for the correct function of the ear that these two fluids remain in separate compartments. Resting on the basilar membrane is the organ of Corti, the sensory epithelium for hearing (Figure 1.2b). The organ of Corti is composed of inner hair cells (IHC) and outer hair cells (OHC) separated by supporting cells (the pillar cells). The inner and outer hair cells are separated by the tunnel of Corti which is formed by filamentous arches of inner and outer pillar cells. In most mammals, a single row of IHC and three rows of OHC are found. Other supporting cells are also found in the epithelium of the organ of Corti such as the Deiters' cells which are found between the OHC providing mechanical support and the Hensen cells which are located on the outside of the OHC providing mechanical loading to the cells of the organ of Corti in response to sound stimulation (Forge and Wright 2002). The remaining cells resting on the floor of the basilar membrane are the inner sulcus cells, inner phalangeal, Claudius and Boettcher cells whose functions have been less studied but are possibly involved in ion transport processes.

The tectorial membrane is the gel-like tissue that extends outwards over the sensory epithelium from the limbus of the spiral lamina (Haines 2013). Since the tectorial membrane is in contact with the taller stereocilia of the OHC, the displacement of the basilar membrane in response to sound-induced motion produces deflections of the

stereocilia and therefore the depolarization of the OHC (Dallos 1992). The IHC are also in contact with the tectorial membrane via a ridge located along the middle and inner part of the tectorial membrane. The matrix and the small fibres found in the tectorial membrane are formed by collagen type II, V and IX (Richardson et al. 1987; Slepecky et al. 1992) and different glycoproteins which are unique to the inner ear and not found anywhere else in the human body. These glycoproteins are otogelin (Cohen-Salmon et al. 1997) and α- and β-tectorin (Legan et al. 1997; Legan et al. 2000) which are detected during the development of the cochlea and that upon damage are not replaced. Another important structure of the cochlea is the stria vascularis. The stria vascularis is located in the lateral wall of the scala media (Figure 1.2) and is responsible for the production and maintenance of the potassium concentration of the endolymphatic fluid (Forge and Wright 2002).

The cochlear duct spirals around the modiolus, a spongy bone structure that houses the spiral ganglion, the group cochlea-vestibular nerves and fibres involved in sending the electrical signals to the brain.

Picture removed for copyright purposes

Figure 1.2. General anatomy of the cochlea. a) Cross section of the cochlea showing the three main compartments of the cochlear duct: the scala vestibuli, the cochlear duct or scala media and the scala tympani. The organ of Corti is located between the tectorial membrane and the basilar membrane (figure reproduced from OpenStax College CCBY 3.0). **b)** Diagram showing the different cell types and structures of the organ of Corti (figure reproduced from Anatomy of the auditory system. Clinical Gate, http://clinicalgate.com/anatomy-of-the-auditory-system/).

1.2.3.2 The vestibular system

The vestibular system is formed by a network of interconnected chambers, also known as the labyrinth which comprises the otolith organs (the utricle and the saccule) and three semicircular canals (Figure 1.3). The utricle and saccule are the main components to respond to linear acceleration of the head and static head position, whereas the semicircular canals respond to the rotational accelerations of the head (Purves et al. 2008). The labyrinth, as the cochlear duct, is filled with endolymph, a solution high in potassium and low in sodium. At the base of the labyrinth, enlarged structures are found, denominated as ampullae or cristae (crista ampullaris). These structures, as well as the saccule and utricle contain vestibular hair cells. The vestibular hair cells are

Picture removed for copyright purposes

Figure 1.3. Anatomy of the mammalian vestibular system. a) The vestibular system in mammals consists of two otolith organs, the utricle and saccule, and three semicircular canals. Vestibular hair cells are found in the utricle, saccule and in three enlarged structures at the base of the semicircular canals called ampullae or cristae. The vestibular organ is innervated by primary afferent nerves that join with those in the cochlear system to the vestibulocochlear VIII cranial nerve. (Figure reproduced from Purves, 4th Edition) **b)** Orientation of the vestibular hair cells. In the cristae (ampulla) hair cell bundles are orientated in the same direction whereas in the saccule and utricle, the striola separates hair cells with opposing hair cell bundle polarities. (Image reproduced from Peripheral Vestibular Apparatus, Encyclopedia of Neuroscience, J. David Dickman).

similar in structure and function to the cochlear hair cells. However, the hair cell bundles of the vestibular hair cells have a specific orientation and therefore they can respond to displacements in all directions. For example, the hair cells in the cristae are all polarized in the same direction whereas the hair cells in the saccule and utricle are separated by the striola, a curved dividing ridge that separates hair cells with opposite polarities (Figure 1.3b). The directional polarization of the vestibular hair cells enables the linear and rotational acceleration function of this organ.

1.3 Hair cells and mechanoelectrical transduction

Hair cells are responsible for converting mechanical stimulus into an electrical signal. (Purves et al. 2008). The hair cells are flask-shaped epithelia cells with a bundle of hair-like stereocilia. Each hair cell contains from 30 to a few hundred stereocilia and a single and taller kinocilium which is only present during the hair cell development and in the mouse, which disappears shortly after birth (Purves et al. 2008). At the top of the stereocilia, an individual hair bundle is connected by an extracellular structure denominated "tip-link" (Pickles 1993). When sound waves are transmitted into the cochlea, the displacement of the basilar membrane in response to fluid movements in the scala tympani bends the taller stereocilia of the hair cells in the organ of Corti against the tectorial membrane. This causes the opening of the K^+ channels, allowing the entry of K^+ flow into the hair cells body. This event results in the depolarization of the hair cell and consequently the opening of the voltage-gated Ca^{2+} channels at the base of the hair cell membrane. The resultant intake of Ca^{2+} into the hair cell body causes synaptic vesicles to fuse to the hair cell membrane and the release of a neurotransmitter from the basal end of the hair cell onto the auditory nerve ending. The neurotransmitter will produce the depolarization of the afferent nerve fibre and an action potential will be transmitted along the cochlear nerve to the brain. As the movement toward the tallest stereocilia depolarizes the hair cell, the movement in the opposite direction leads to the closing of the K^+ channels and therefore to the hyperpolarization of the cell (Haines 2013).

The ion transfer is possible because of the electrical gradient across the membrane of the stereocilia. The endolymph fluid (high in K^+) in the scala media and the perilymph fluid (high in Na^+) creates a potential difference of +80mV between both compartments whereas inside of the hair cell is about 45mV more negative than in the perilymph and

about 150mV more negative than in the endolymph. The large potential difference between the endolymph and the hair cell body is therefore the driving force responsible for the mechanoelectrical transduction of the cochlea. This is known as the endocochlear potential.

Signals from the auditory system travel to the auditory cortex via sensory neurons which have their cell body in the spiral ganglion. The central axons innervating the cochlea and vestibular system form the vestibulocochlear nerve (VIII cranial nerve) and is responsible for transmitting the sound and balance sensation to the brain (Kingsley 1999).

1.4 Inner ear development

The formation of the organ responsible for hearing and balance occurs under a series of events and signals that transforms a very simple cellular epithelium in a complex three dimensional structure.

1.4.1 Early inner ear development

In vertebrates, the inner ear arises from the otic placode, a thickened primordium of the embryonic ectoderm located close to the hindbrain (Torres and Giráldez 1998). The first morphological event during the early development of the inner ear is the otic placode induction. The process of placode induction was reviewed by Ohyama et al. 2007, and proposed to occur in several different steps (Figure 1.4a). The first step is the formation of a "pre-placodal domain" followed by a second step based on the induction of the "pre-otic field" within the pre-placodal domain which will be refined into the otic placode (Ohyama et al. 2007). The different craniofacial organs, including ear, nose, lens, trigeminal and epibranchial ganglia arise from this initial pre-placodal domain.

The otic placode is defined by the expression of early specific molecular markers including the transcription factors PAX8 (Pfeffer et al. 1998; Heller and Brändli 1999) and PAX2 (Nornes et al. 1990; Krauss et al. 1991; Groves and Bronner-Fraser 2000), FOXI1 (Nissen et al. 2003; Solomon et al. 2003) and SOX9 (Wright et al. 1995; Saint-Germain et al. 2004). A few other signalling molecules and additional transcription factors markers were also examined in the otic placode in different vertebrate species and included EYA1, GATA3, NKX5.1/HMX3, GBX2, SOX3, DLX, BMP4 and BMP7

(Kelley et al. 2005). During the early induction of the otic placode a number of fibroblast growth factors (FGFs) have also been described for being necessary during the early development of the inner ear in fish, chick and mouse. Different members of the FGF family such as FGF10, FGF19 and FGF15 are produced from the underlying mesenchyme of the otic placode to contribute to the otic induction (Maroon et al. 2002; Léger and Brand 2002).

As the embryonic development progresses the otic placode invaginates to form the otic cup, a structure that soon closes to form the otic vesicle or otocyst (Alvarez and Navascués 1990; Bancroft and Bellairs 1977; Torres and Giráldez 1998). At this stage, the otic vesicle undergoes an intensive proliferative growth before cellular differentiation begins.

Picture removed for copyright purposes

Figure 1.4. Development of the inner ear. a) Cranial placode development. The first step during the early inner development is otic placode induction. According to the model reviewed by Ohyama, the first step is the formation of a "pre-placodal domain", a narrow band of ectoderm in the neural plate. The second step is based on the induction of the "pre-otic field" within the pre-placodal domain which will be refined into the different craniofacial placodes including the otic placode. Figure adapted from Ohyama et. al, 2007. **b)** Summary of the chick inner development. The otic placode invaginates after its induction to form the otic cup at E2.5 which in turn pinches off to form the otic vesicle or otocyst (E3.5). By E10 the different structures of the mature inner ear are already formed. Adapted from Daudet et. al, 2005.

1.4.2 From the otic placode to the otocyst

Following the induction of the otic placode, the otocyst also known as the otic vesicle is formed. This process occurs in a similar pattern in amphibians, birds and mammals. However, the process of morphogenesis has been well studied in chick since it provides a good insight of the mechanism of morphogenesis in vertebrates. Also because the chick otic epithelium can be easily manipulated both *in ovo* and *in vitro*, the chick has been used as a model to study the morphogenesis of the inner ear.

The major event of the transformation of the otic placode consists in the bending of the placode epithelium to form an otic cup first, followed by the fusion of the rim cells, closing the pit which results in the formation of the otocyst (Kelley 2006) (Figure 1.4b).
The formation of the otic vesicle undergoes a process of rapid cell proliferation which is controlled by different growth-factors. Among all of growth-factors, the insulin growth-factors (IGF) were studied for playing important roles during the formation of the otic vesicle. For instance IGF-I was described for inducing DNA synthesis to increase the number of mitotic cells of the cochlea-vestibular ganglion (León et al. 1995b). In addition, IGF-II also was seen to induce the cellular growth of the otic vesicle although with a lower potency. The action of the IGFs promotes the rapid induction of the *c-fos* gene which was suggested to contribute the pattern proliferative growth of the otic vesicle (Represa et al. 1990; León et al. 1995a).
As the morphogenesis continues, the otic epithelium diversifies and differentiates into the different patches that will later form the sensory organs. One of the first events that occur during the differentiation process is the production of retinoic acid in the otocyst. The retinoic acid downregulates the production of growth factors produced during the process of cell proliferation and stimulates the differentiation of the sensory epithelium (Represa et al. 1990). In addition, the retinoic acid is also able to downregulate the *c-fos* genes in parallel to the inhibition of cell proliferation (León et al. 1995a). Following the inhibition of the cell proliferation process is the differentiation of the cells of the otocyst into the three major cell lineages: proneural cells (the future neuronal cells), prosensory (future hair and supporting cells) and nonsensory cells (formed by other cells derived from the otocyst).

Figure 1.5. Morphogenesis of the inner ear. a) Compartment-boundary model. In this model, the otocyst is compartmentalized in three different boundaries, A-P (anterior-posterior), M-L (medial-lateral) and D-V (dorsal-ventral), dividing the otocyst in eight compartments. Several genes are expressed in the different parts of the otocyst which will define the predicted fate map and the different sensory organ regions arisen from the early markers. Adapted from Fekete and Wu, 2002. **b)** Sensory organ formation of the mouse inner ear and the main genes expressed in the different sensory patches. Adapted from Bok et. al, 2007. **c)** Development time series of the chick and mouse inner ear development. Lateral views of paint-filled inner ears. Adapted from Brigande et. al, 2000 (scale bar=1mm) and Cantos et. al, 2000 (scale bar=100μm). Arrowheads identify the proximal region of the cochlea. Abbreviations: aa, anterior ampulla; AC, anterior crista; asc, anterior semicircular canal; co, cochlea; cds, cochleosaccular duct; ed, endolymphatic duct; es endolymphatic sac; la, lateral ampulla; LC, lateral crista; lsc, lateral semicircular canal; oC/BP, organ of Corti/basilar papilla; pa, posterior ampulla; psc, posterior semicircular canal; s, saccule; SM, saccular macula; u, utricle; UM, utricular macula; usd, utriculosaccular duct. Orientation: D, dorsal; A, anterior.

The model proposed by Fekete and Wu defined the regional compartmentalization to establish a fate map of the different cell types in the inner ear (Figure 1.5a). According to this model, the axial identity of the otocyst is defined by the formation of three main boundaries: the anterior-posterior (A-P), the medial- lateral (M-L) and the dorsal-ventral boundary (D-V) (Fekete and Wu 2002).

The definition of the A-P axis was suggested as being marked by the expression of several neural/sensory markers such as *Fgf10*, *Lunatic fringe* (*Lfng*), *Delta1*, *Neurogenin1* (*Ngn1*) and *NeuroD* in the anterior region whereas the posterior axis is defined by the formation of the posterior-cochleovestibular ganglion and the expression of *Irx1*, *Lmx1b*, *HNK-1* and *Hairy 1* (Myat et al. 1996; Morsli et al. 1998; Cole et al. 2000; Alsina et al. 2004; Alsina 2007). However, transplantation studies conducted in chick demonstrate that the formation of the A-P boundary and the expression of the specific markers occurs gradually until the otic cup is half-closed (Wu et al. 1998; Bok et al. 2005). Signals from the hindbrain are also thought to contribute to the formation of the A-P axis since each rhombomere in the hindbrain expresses a unique profile of genes that will coordinate the location of the sensory ganglia along the A-P axis (Trainor and Krumlauf 2000; Graham et al. 2004). In mouse, the *Tbx1* gene is expressed in the posterior half of the otic cup and therefore is also considered for being an important factor to contribute to the identity of the A-P axis (Vitelli et al. 2003; Raft et al. 2004; Arnold et al. 2006).

The D-V axis is also defined by different genetic markers. The dorsal vestibular region is characterized by the expression of *Dlx5, Dlx6, Hmx2, Hmx3* and *Gbx2* whereas the ventral auditory and neurosensory region expresses among other the *Lfng, Ngn1, NeuroD1, Sox2* and *Six1* genes (Fekete and Wu 2002). As with the A-P patterning, the development of the D-V axis is also influenced by different signal molecules produced by the adjacent tissues. Wnts signalling molecules secreted by the dorsal neural tube and Sonic hedgehog (Shh) produced by the floor plate and notochord are known for contributing to establish the D-V axis (Liu et al. 2002; Riccomagno et al. 2002; Bok et al. 2005; Riccomagno et al. 2005).

The M-L is the last axis to be defined since the lateral region does not exist until the otic cup closes (Bok J. 2007). However, the signals and markers expressed in the M-L axis are not that well defined. The *Gbx2* and *Pax2* genes are associated with this medial

patterning (Groves and Bronner-Fraser 2000; Hidalgo-Sánchez et al. 2000; Burton et al. 2004; Lin et al. 2005).

It is possible that the hindbrain also plays a role in the development of the M-L axis since hindbrain mutants lacked the mature medial structures as well as the endolymphatic duct (Deol 1964; Mansour et al. 1993; Mark et al. 1993; Choo et al. 2006).

The model proposed by Fekete and Wu contributed to the understanding of how the different boundaries are formed during the inner ear development. Many of the compartmentalisations described in this model are observed during the inner ear formation in chick. However, how boundaries are specifically formed and maintained throughout development is still debated in the field.

1.4.3 Late morphogenesis and sensory development of the inner ear

The late morphogenesis of the inner ear is characterized by the formation of the six sensory organs: utricle, saccule, three cristae and the auditory organ. The molecular mechanisms to define the sensory organs are thought to involve *Sox2, Six1* and the Notch signalling pathway (Kelley 2006).

1.4.3.1 Crista and semicircular canal formation

The structure that forms the cristae and semicircular canals derive from the vertical and horizontal pouches of the developing otocyst (Bok J. 2007). As a result of the formation of different morphological changes in the otic epithelium, the development of a tube-shaped canal will define the formation of the semicircular canals. Wnt signalling molecules from the hindbrain are thought to regulate expression of different genes such as *Gbx2, Dlx5* and *Dlx6* which participate in the development of the semicircular canals and cristae (Riccomagno et al. 2005). Studies with knockout mice for these genes revealed structural malformations in the semicircular canals and cristae (Merlo et al. 2002; Lin et al. 2005; Robledo and Lufkin 2006). In addition, the expression of *Bmp4* in the cristae of different species linked this gene to the formation of semicircular canals and crista (Chang et al. 2008; Gerlach et al. 2000) but other genes including *Sox2, Jagged1* and *Fgf10* were also considered to be important in this process (Pauley et al. 2003; Kiernan et al. 2005; Brooker et al. 2006; Kiernan et al. 2006).

1.4.3.2 Utricle and saccule formation

The formation of the utricle and saccule share a common origin with the neural cells of the cochleovestibular ganglion (Bok J. 2007). After the formation of the otocyst, the neurosensory region expressing *Lfng* in the prosensory domain segregates to form the utricular macula, the saccular macula and the organ of Corti. This event occurs around E12 in mouse, and by E13 the utricle and saccule are completely separated to each other (Morsli et al. 1998) (Figure 1.5b). It is not clear how this segregation occurs but studies in mice with double knockout for *Hmx2* and *Hmx3* (Wang et al. 2004) and for *Otx1* and *Otx2* (Morsli et al. 1999) failed to form a complete separation of these organs linking therefore these genes with the segregation process of these sensory patches. *Gata3* is the only known gene that is expressed in the utricle and not in the saccule (Bok J. 2007).

1.4.3.3 Cochlear patterning

In mice, the development of the cochlea begins with the formation of the cochlear duct from the postero-lateral region of the otocyst (Bok J. 2007) (Figure 1.5b). By embryonic day 12, the cochlear duct descend to the ventral-medial position to form the L-shaped duct characteristic of mammalian species (Bok J. 2007). On the contrary, in birds, the cochlear duct remains relatively straight (Dooling and Fay 2000) (Figure 1.5c).

In mouse, between E12-E14, the nascent cells that will form the organ of Corti, exit the cell cycle and minimal cell proliferation is conducted in the cochlear epithelium (Jones and Chen 2007; Ruben J, 1967). The elongation of the cochlear duct continues until approximately one and three quarters turns in the mature mouse (Bok J. 2007). In cross sections, the cochlear duct is a triangular shaped structure defined by three walls: the basilar membrane where the organ of Corti is located, the thin medial wall denominated Reissner's membrane and the lateral wall which consists of the stria vascularis and the spiral ligament (Bok J. 2007). Among all the genes expressed in the developing cochlear duct, *Otx2* is known for being expressed in the Reissner's membrane (Morsli et al. 1999), *Pax2* in the stria vascularis (Burton et al. 2004) and *Atoh1* in the developing hair cell epithelium of the organ of Corti (Bermingham et al. 1999).

1.4.4 Summary of inner ear development

The formation of the inner ear is a complex process defined and controlled by multiple genes and signalling pathways. Some of these signals and genes are well studied,

especially in chick, a species that has served as a model to describe the inner ear patterning (reviewed in Fekete and Wu, 2002). However, it is still not clear how the different signals regulate the regional identity and whether the modification of these pathways can alter the normal development of the inner ear. Solving all these questions could have a big impact and contribute to the understanding of the formation of this system but also would help in the design of future regenerative strategies in the inner ear epithelium.

1.5 Development of auditory hair cells

During the formation of the inner ear, different developmental processes take place in the cochlea and vestibular system to give rise to the hair cells. There are four types of hair cells in mammals: inner hair cells (IHCs) and outer hair cells (OHCs) which are located in the cochlea to perform the auditory transduction and the vestibular hair cells Type I and Type II which are required for balance sensation (Kingsley 1999).

1.5.1 Early cellular differentiation of the primordium cochlear epithelium

The early formation of the cochlear epithelium begins from the ventromedial axis of the otocyst before E12 in the mouse inner ear (Morsli et al. 1998). Between E12 and E14, the cells located in the primordial epithelium that will form the organ of Corti, exit the cell cycle (Ruben 1967) and therefore at this point of the development, the progenitor cells undergo the last mitosis. The exit of the cell cycle requires $p27^{Kip1}$, a cyclin-dependent kinase inhibitor that functions as an inhibitor of cell cycle progression (Chen and Segil 1999). Immunohistochemistry experiments identified a zone of non-proliferating cells (ZNPC) in the sensory primordium epithelium which failed to incorporate BrdU and that correlated with the onset of $p27^{Kip1}$ expression (Figure 1.6a) (Chen et al. 2002). In addition, the experiments conducted by Chen and Segil also concluded that the deletion of $p27^{Kip1}$ prolonged the division of cells of the developing neuroepithelium in the mutant mice in comparison to their wild type littermates. Therefore $p27^{Kip1}$ was suggested to be involved in determining the size of progenitor population by controlling exit from the cell cycle (Chen and Segil 1999) but not necessarily required for the formation of hair cells. However, homozygous $p27^{Kip1}$ mutant mice have a severe hearing impairment suggesting that $p27^{Kip1}$ could be involved

in the correct control of the cell cycle during development to produce functional hair cells.

At later stages, in differentiated hair cells, $p27^{Kip1}$ is rapidly downregulated although its expression continues in the supporting cells (Figure 1.6b) (Chen and Segil 1999). Based on these observations, $p27^{Kip1}$ is considered as the cellular marker of terminal mitosis and possibly necessary for controlling the cell cycle during the differentiation of hair cells.

As the development of the cochlea continues, it is thought that cells in the ZNPC will develop into either hair cells or supporting cells (Kelley 2007). The earliest hair cell marker expressed in the ZNPC is the basic helix-loop-helix transcription factor *Atoh1* (formerly known as *Math1* in mammals) (Chen et al. 2002). Within the ZNPC region, the first cells expressing *Atoh1* are located in the epithelium close to the base of the cochlear duct and near the medial border of the ZNPC (Figure 1.6c). Since ATOH1 was observed within the borders of the ZNPC, it was suggested that only cells that have exited the cell cycle express ATOH1. Experiments where pregnant mice were injected with the cell division marker BrdU showed that cells in the primordium epithelium fail to incorporate BrdU in this region and therefore become postmitotic between E12.5 and E13.5 before expressing ATOH1 (Chen et al. 2002). Later in development, at about E15.5, the early hair cell-specific marker MyosinVIIa was detected near the base of the cochlea (Chen et al. 2002). From this point the differentiation of the hair cells spreads longitudinally towards the apex and also to the base (hook region) of the cochlea.

By E16, the cochlear cells that express *Atoh1* are committed to developing as hair cells, whereas *Atoh1* negative cells will develop as supporting cells (Kelley 2007).

Picture removed for copyright purposes

Figure 1.6. Early cellular differentiation of the primordium cochlear epithelium. a) Onset of the cyclin-dependent kinase inhibitor p27Kip[1] expression. A zone of non-proliferating cells (ZNPC) was identified in the sensory primordium of the cochlea. Between E12.5 and E14.5, the ZNPC region is marked by the lack of BrdU incorporation (in green) and the upregulation of p27Kip[1] expression (in red). Adapted from Chen et.al, 2002. Scale bar: 50μm. **b)** p27Kip[1] (in red) and myosin VIIa expression (in green) through the basal (right) and apical (left) turns of the E15.5 cochlea. As hair cells differentiate, p27Kip[1] is downregulated and myosin VIIa is upregulated along the basal-to-apical axis of the cochlea. Adapted from Chen et al. 1999. Scale bar: 50μm. **c)** Model of organ of Corti development. Between E12.5 and E13.5, a zone of non-proliferating cells (ZNPC) (in yellow) in the prosensory domain can be observed which lacks BrdU incorporation (in blue) and an upregulation of the CDK inhibitor p27Kip[1] (in green) is observed. Between E13.5 and E14.5, ATOH1 expression (Math1 in the figure) begins in the base of the cochlea (in red) within the ZNPC. As cellular differentiation progresses between E14.5 and E15.5, myosin VIIa (in red) was seen as an early marker of hair cell differentiation in the base of the cochlea. Adapted from Chen et. al, 2002.

1.5.2 Specification of hair cells and supporting cells: Id proteins and Notch signalling

The Id proteins and the Notch signalling pathway play a major role to limit *Atoh1* expression to hair cells and not to supporting cells. Id proteins (inhibitors of differentiation and DNA binding) are, like *Atoh1*, bHLH molecules. However, the proteins lack the basic DNA binding domain in their sequence and consequently form an heterodimer with other factors, the E-proteins (E47, E12, E2-2, HEP) in order to bind DNA and to become functionally active (Kelley 2007). In the cochlea there are four types of Id genes: Id1, Id2 and Id3 are expressed between E12 and E14 in the epithelium of the otic vesicle and Id4 is detected in the otic vesicle and in part of the VIIIth ganglion (Jen et al. 1997) (Jones et al. 2006). The downregulation of the Id proteins correlates with the upregulation of *Atoh1* which suggest that the loss of Id proteins could influence the onset of *Atoh1* expression (Kelley 2007).

The Notch signalling pathway has been suggested as the primary mechanism specifying hair cells versus supporting cells although this event has been questioned in the past decade. The classical Notch signalling has been associated with inhibitory interactions to determine cell fate (Fekete 1996). In this model, cells that commit to a primary cell fate, in this case developing hair cells, express two of the Notch ligands, Jag2 and Delta-like1 (Dll1) (Kelley 2006). These ligands mediate the process of lateral inhibition right after the exit of cell cycle (Fekete 1996) by acting on the Notch1 receptor of their adjacent cells. The activation of the Notch1 receptor initiates the expression of the Notch target genes *Hes1* and *Hes5* (Lanford et al. 2000). *Hes1* and *Hes5* are inhibitors of *Atoh1* expression leading to the inhibition of the hair cell fate and subsequently these cells will develop as supporting cells (Figure 1.7). The Notch signalling interactions have therefore been associated with the cellular mosaic of hair cells and supporting cells of the developing inner ear epithelium.

Picture removed for copyright purposes

Figure 1.7. The Notch signalling pathway. Interactions between individual cells determine whether they will commit to a hair cell or supporting cell fate. The developing hair cells express the Jagged2 (JAG2) and delta 1 (DLL1) ligands which bind to the Notch1 ligand in adjacent cells. This binding mediates the activation of the Notch1 intracellular domain (N1-ICD) which upregulates the expression of hairy and enhancer of split (HES1) and HES5 proteins. Consequently, the HES genes block the expression of the prosensory gene *Atoh1*, leading to the inhibition of hair cell fate. Therefore inhibited cells will develop as supporting cells. Figure adapted from Kelley et al. 2006.

1.5.3 Hair cell differentiation

Each hair cell is separated from its neighbours by surrounding supporting cells in a way that hair cells do not contact each other (Bryant et al. 2002). In the vestibular system of both mammals and birds two types of hair cells are formed: Type I and Type II (Bergström 1973). Type I hair cells are pear shaped and are connected in the basolateral portion by a single afferent nerve ending. Type II hair cells, on the other hand, have a cylindrical shape and contact both afferent and efferent nerve endings (Kelley et al. 2005).

In the organ of Corti, there are also two types of hair cells: a single row of flask-shaped inner hair cells (IHC) containing mainly afferent innervation and three rows (in some cases four) of outer hair cells (OHC) with a cylindrical shaped with mainly efferent innervation (Kelley et al. 2005).

It is possible that all factors that are required for the differentiation of hair cells reside in the sensory epithelium. Once the sensory epithelium is specified, the differentiation process requires the activation of the transcription factor POU4F3 (also known as Brn3c/Brn3.1) (Fekete and Wu 2002). In mouse, *Pou4f3* was shown to be uniquely expressed in both cochlear and vestibular hair cells of the inner ear (Erkman et al. 1996; Xiang et al. 1997). If *Pou4f3* is not activated, developing hair cells die followed by supporting cells and neurons (Erkman et al. 1996; Xiang et al. 1998). Studies using *Pou4f3* null mutant mice concluded that although some of the early hair cell markers were still expressed in these cells, no hair cell bundles were seen on the apical surface of the sensory epithelia (Xiang et al. 1998). Moreover, the loss of hair cell bundles seems complete in post-natal and adult stages (Erkman et al. 1996). In addition, an increase of cell death was observed in *Pou4f3* null mutant mice in the vestibular sensory epithelium (Xiang et al. 1998). In humans, *POU4F3* was also suggested to play roles in maintaining hair cells and promoting their survival (Ryan 1997). Studies conducted in three human families with mutations in the *POU4F3* coding sequence showed an autosomal dominant late-onset hearing loss (Collin et al. 2008; Vahara et al. 1998; Weiss et al. 2003). The mutations were shown to be caused by an amino acid substitution or protein truncation in the POU domain of *POU4F3* that confers the nuclear localization signal of this transcription factor (Collin et al. 2008; Vahava et al. 1998; Weiss et al. 2003). A more recent study which combines linkage analysis and whole-exome sequencing in a Korean family identified a novel *POU4F3* mutation in the POU homeodomain of the *POU4F3* gene (Kim et al. 2013). Different hypothesis have been proposed to explain the deafness due to *POU4F3* mutations, however haploinsufficiency, a condition where a single copy of the gene is not sufficient to maintain the wild type phenotype, seems to be the most probable explanation. Altogether, and based on this evidence, *POU4F3* seems to be critical for the maturation of hair cells in humans.

Downstream targets of POU4F3 are also known for playing roles in hair cell development and survival. To date, there is evidence that POU4F3 regulates brain

derived neurotrophic factor (BDNF) and neurotrophin 3 (Clough et al. 2004), *Gfi1* (Hertzano et al. 2004), *Lhx3* (Hertzano et al. 2007), *Caprin-1* (Towers et al. 2011) and *Nr2f2* (Tornari et al. 2014). *In vitro* and *in vivo* analysis showed that POU4F3 binds to specific elements within the promoters of these genes. However, the identification of downstream targets of POU4F3 in the inner ear has limitations since the ongoing hair cell death makes the comparison of gene expression in wild type cochlear tissue and mutant *Pou4f3* mice a difficult task to identify downstream genes. However, POU4F3 and its target genes are possibly only one of the mechanisms involved in determining and maintaining hair cell fate (see section 1.7.4).

In addition to POU4F3, BARHL1 is another transcription factor essential for the survival and maintenance of hair cells since its loss in mouse causes the degeneration of hair cells and consequently profound deafness (Li et al. 2002). Expression of BARHL1 in mouse hair cells was observed at a later stage in comparison to the expression of POU4F3 (Li et al. 2002; Xiang et al. 1998). Therefore, it has been suggested that BARHL1 could play a role in long-term maintenance of cochlear hair cells. Studies conducted in cell lines derived from the organ of Corti (OC-1 and OC-2) found that BARHL1 acts as a repressor of transcription (Sud et al. 2005).

GFI1 is also a critical transcription factor for the correct development of cochlear hair cells (reviewed by Jafar-Nejad and Bellen, 2004; Möröy et al. 2005; Kazanjian et al., 2006). In mouse, *Gfi1* is expressed in the developing cochlear and vestibular hair cells and if absent, outer hair cells are lost (Wallis et al. 2003; Hertzano et al. 2004). In humans, the mutation of *GFI1* causes severe congenital neutropenia linking this gene to deficiencies in pathways involved in myeloid differentiation (Person et al. 2003). However, patients with dominant negative mutations in the *GFI1* gene have not been found to have a hearing loss (Möröy 2005).

The upstream control of *Pou4f3*, *Barhl1* and *Gfi1* expression is suggested to be conducted by direct and/or indirect interactions with ATOH1 to regulate the hair cell phenotype (Masuda et al. 2011; Ikeda et al. 2014; Chellappa et al. 2008; Wallis et al. 2003; Shroyer et al. 2005). Co-transfection in HEK293 and VOT-E36 cells, in addition to chromatin immunoprecipitation experiments demonstrated that ATOH1 regulates *Pou4f3* through direct binding at the distal enhancer in the 3' region of *Pou4f3* (Masuda, 2011). The spatial and temporal regulation of *Barhl1* is also crucial for its normal

function which was suggested to be controlled by BARHL1 itself but also by ATOH1. Studies with *Atoh1*-lacZ null mice showed that *Barhl1* expression was absent in cochlear hair cells in comparison to wild-type mice where *Barhl1* expression followed that of *Atoh1* expression in hair cells (Chellappa et al. 2008). These data suggest the possibility of a direct and/or indirect activation of *Barhl1* expression by ATOH1 in cochlear hair cells. A similar pattern was observed for *Gfi1* expression. The expression of *Gfi1* in the inner ear was drastically reduced in *Atoh1* mutant mice after E14.5 suggesting that ATOH1 is possibly required for the maintenance of *Gfi1* expression (Wallis et al. 2003).

Another gene associated with hearing loss in humans is the transcription factor *LHX3*. Recessive mutations were found in the human *LHX3* and linked to sensorineural hearing loss (Rajab et al. 2008). *LHX3* expression was observed in the sensory epithelium of human embryonic and fetal tissues overlapping with the expression of *SOX2* (Rajab et al. 2008). A more recent study conducted on a child revealed a novel mutation in *LHX3* also associated with sensorineural hearing loss and pituitary hormone deficiencies (Bonfig et al. 2011).

GATA3 may be also involved in hair cell differentiation. Epithelial cells in the dorsal part of the cochlear duct express GATA3, however its expression is specifically downregulated in both hair cells and supporting cell as they differentiate (Rivolta et al. 1998). In humans, haploinsufficiency of *GATA3* is associated with hearing loss (Bilous et al. 1992; Van Esch et al. 2000).

Besides the need for these transcription factors, as development progresses, myosinVIIa (an actin binding motor protein) begins to be expressed at the base of the cochlea at E15.5 whereas $p27^{Kip1}$ is downregulated at the same time (Chen et al. 2002). This event indicates the initiation of hair cell differentiation in a base-apical gradient. By E17, the entire length of the cochlear organ is patterned with one row of IHCs and three rows of OHCs. Between E14-18 a bilayer of hair cells and supporting cells is observed, characteristic of the mature organ of Corti (Chen et al. 2002). Other proteins expressed in the sensory epithelium that are specific to hair cells are calmodulin and calretinin (Zheng and Gao 1997).

As discussed in section 1.4.2, retinoic acid is secreted during the early development of the otocyst and contributes to its differentiation. It is expressed in the developing

cochlea and is known for playing roles during hair cell development (Bryant et al. 2002). Studies with cochlear cultures produced the extra rows of IHC and OHC after the addition of retinoic acid (Kelley et al. 1993). Thyroid hormone receptors are also expressed in the inner ear at early stages and some members become restricted to the cochlear epithelium once differentiated (Bradley et al. 1994). Chemically induced hypothyroidism has been linked with a delay in the maturation of most of the cochlear cells (Rüsch et al. 2001).

1.5.4 Maturation of the hair cells

The development of the hair cell bundle is considered a characteristic of its maturation (Gowri et al. 2007). As described in section 1.3, hair cell bundles are required for the mechanoelectrical transduction process (Pickles 1998). The formation of the hair cell bundle begins with the formation of small stereocilia over the apical surface, clustered around the kinocilium to form a short bundle. Between P0 and P4, the kinocilium migrates to one side of the cell and the stereocilia begin to elongate in a staircase pattern with adjacent rows of stereocilia organized by increasing heights. At this point the kinocilium is eccentrically located with the tallest rows of stereocilia. The position of the kinocilium marks the polarity of the hair cell bundle. By P4-P6, the stereocilia grow to their final height and width and the bundle acquire the characteristic W-shape found in OHC and the relatively straight shape found in IHC (Goodyear et al. 2005). Later on in the development, at about P6, the kinocilium is lost (Lelli et al. 2009). Functional maturation occurs at around P10-12 for IHCs and at P8 for OHCs, with the apical hair cell stereocilia longer than the ones at the base due to the faster growth rate at that end (Kelley et al. 2005; Lelli et al. 2009; Goodyear et al. 2005).

Little is known about the molecular mechanisms that control the formation of the hair cell bundle although the actin cytoskeleton is thought to be involved (Bryant et al. 2002).

1.6 *Atoh1*

The discovery of *Atoh1* as a gene required for the formation of hair cells led to numerous investigations focused on the study of this gene, not only for its essential requirement during hair cell development but also because its potential capacity to restore hearing.

1.6.1 Initial studies

The study of *Atoh1* began with the work conducted in *Drosophila* in the early 1990s. During development in *Drosophila*, a number of proneural genes encoding basic-helix-loop-helix transcription factors (bHLH) denoted as the Aschaete-Scute complex (ASC), were shown to be required for the normal development of the nervous system. *Atoh1*, named *atonal* (*ato*) in *Drosophila*, was originally identified as a new ASC gene, for sharing many of the structural features of the bHLH proteins. Experiments conducted with *ato* mutants showed that the majority of the external sense organs in *Drosophila* were missing which demonstrated the importance of *atonal* during neurogenesis (Jarman et al. 1993; Jarman et al. 1994). Based on these initial studies, this new candidate was defined as a proneural gene necessary and sufficient for the formation of the mechanoreceptor neurons and photoreceptor cells.

Following the studies in *Drosophila*, a screen using mouse embryonic tissue was conducted in order to characterize the murine *Atoh1*, formerly known as *Math1*. One clone obtained from this screen showed a high homology with the amino acid sequence of the *atonal* product in *Drosophila* confirming therefore the identification of the mouse *Atoh1* (Akazawa et al. 1995). The mouse *Atoh1* (atonal bHLH transcription factor 1) is a member of the bHLH family located on chromosome 6 (6:64,729,125-64,731,245 forward strand- Ensembl release 86). A typical bHLH member contains a basic domain at the amino-terminal which mediates the binding to DNA and a HLH domain, consisting of two α-helices separated by a variable loop region, at the carboxyl-terminal end which facilitates interactions with other protein subunits (Jones, 2004). The mouse *Atoh1* open frame consists of a single exon of 1053 bp that produces a protein of 351 amino acids long and 37 kDa in size (Akazawa et al. 1995).

Four years after characterizing the mouse *Atoh1*, studies conducted by Bermingham's group confirmed the importance of this gene for the formation of hair cells (Bermingham et al. 1999). A transgenic mouse was generated by replacing the *Atoh1* coding region with the *lacZ* reporter gene in order to study the expression of *Atoh1*, in heterozygous *Atoh1* mice (*Atoh1*$^{+/\beta\text{-Gal}}$) and the homozygous mutants (*Atoh1* $^{\beta\text{-Gal}/\beta\text{-Gal}}$). The heterozygous mice appeared normal and the expression of the β-Gal reproduced the pattern observed in the *Atoh1* wild-type mice. However, the homozygous mutant mice die shortly after birth and lack cerebellar granule neurons (Bermingham et al. 1999). In

the sensory epithelium at early stages in development (E12.5), both heterozygous and homozygous mice showed β-Gal staining before the differentiation of hair cells (Figure 1.8a). However by E18.5 when hair cells are formed, β-Gal was restricted to hair cells in the heterozygous *Atoh1*$^{+/\beta\text{-Gal}}$ mice whereas no specific staining was found in the homozygous *Atoh1* $^{\beta\text{-Gal}/\beta\text{-Gal}}$ mutant mice (Figure 1.8a). When the sensory epithelium was analysed in detail at the same stage (E18.5) by electron microscopy, it was confirmed that the *Atoh1* $^{\beta\text{-Gal}/\beta\text{-Gal}}$ mutants lacked hair cells and only non-specialized epithelial cells were present. However, supporting cells appeared normal. In the vestibular system of the *Atoh1* $^{\beta\text{-Gal}/\beta\text{-Gal}}$ mutants, the crista and utricle were smaller in comparison to wild types and as in the cochlear epithelium, hair cells were absent. In addition, immunohistochemistry results with specific hair cell markers such as MyosinVI and Calretinin demonstrated that these markers were absent in the *Atoh1* $^{\beta\text{-Gal}/\beta\text{-Gal}}$ mutants confirming that hair cells did not develop in the sensory epithelium (Figure 1.8b).

In summary, the studies of Bermingham et al. demonstrated for the first time that *Atoh1* is an essential gene necessary for the formation of hair cells.

Figure 1.8. *Atoh1* is required for the formation of hair cells. a) Inner ear β-Gal staining (blue) before and after hair cell fate in heterozygous transgenic mice (*Atoh1*$^{+/\beta\text{-Gal}}$) and homozygous mutants (*Atoh1* $^{\beta\text{-Gal}/\beta\text{-Gal}}$). At E12.5, before the formation of hair cells, β-Gal staining was observed in both heterozygous and homozygous mutants. However, once the sensory epithelium differentiates, β-Gal staining is restricted to hair cells in heterozygous mice and no specific β-Gal staining was found in homozygous mutants. Original magnification at E12.5 is x100, at E18.5 is x630 and insets at E18.5 is x160. **b)** Myosin VI and Calretinin were used as specific hair cell markers for immunohistochemistry studies in wild type and *Atoh1* $^{\beta\text{-Gal}/\beta\text{-Gal}}$ mutants. At E13.5, Myosin VI was found in wild type embryos but not in *Atoh1* $^{\beta\text{-Gal}/\beta\text{-Gal}}$ mutants. At E16.5, similar results were obtained with Calretinin staining only visible in wild type animals but absent in *Atoh1* $^{\beta\text{-Gal}/\beta\text{-Gal}}$ mutants. Figures adapted from Bermingham et al. 1999. Scale bars for MyosinVI and Calretinin expression are 50μm and 100μm respectively.

1.6.2 Expression of *Atoh1* in the developing inner ear

The spatial and temporal expression of *Atoh1* has been described using four different techniques: *in situ* hybridization (ISH), immunohistochemistry, reporter gene studies and more recently by q-PCR. The use of these four different approaches to study *Atoh1* expression could explain the discrepancies among different studies which are influenced by the limitations of the technique used.

Based on the initial experimental data conducted by Jarman et al., *atonal* expression was analysed by *in situ* hybridization and showed that *atonal* was expressed in the epidermal and subepidermal epithelium of *Drosophila*. The ectodermal patches where *atonal* was expressed were therefore defined as putative proneural clusters (Jarman et al. 1993).

Following this work, the expression of *Atoh1* was analysed in embryonic mice. At early stages of the mouse development (E9.5), *Atoh1* mRNA was detected by *in situ* hybridization in the cranial ganglions as well as the dorsal wall of the neural tube. By E10.5, *Atoh1* was strongly expressed in the central neural systems and later on by E13, was notably detected in the dorsal part of the hindbrain and neural tube. However by E18 expression was restricted to the cerebellum and was downregulated in the spinal cord. On post-natal day 3 (P3), mRNA expression was decreased and only seen in the external granular layer of the cerebellum and by P28, *Atoh1* mRNA is no longer detected in the nervous system (Akazawa et al. 1995).

In the mammalian inner ear, *Atoh1* expression was first described by the studies conducted by Bermingham et. al. 1999 where the β-galactosidase reporter marker was used in order to show *Atoh1* expression patterns along different stages (see section 1.6.1). The findings of these studies showed that *Atoh1* was first expressed in the otic vesicle at E12.5 before cochlear hair cells are formed and that its expression was seen throughout the sensory epithelium of vestibular organs and cochlea at E14.5. At later stages, approximately by E18.5, *Atoh1* expression was restricted to hair cells (Figure 1.9a) (Bermingham et al. 1999).

Using *in situ* hybridization *Atoh1* mRNA expression was observed in the cochlea between E12.5 and E13 (Lanford et al. 2000) (Figure 1.9a). By E15, *Atoh1* transcript was detected along the cochlear duct and by E17, *Atoh1* expression was restricted to one

single row of inner hair cells and the three rows of outer hair cells. A more recent study detected *Atoh1* mRNA in the cochlea later than E13.5 and its downregulation was observed between E17-E18.5 showing a basal-apical gradient (Pan et al. 2012). In post-natal stages, *Atoh1* mRNA expression was still detected at P4 (Pan et al. 2012) and shortly after expression was no longer seen. Similar results were described using the same approach by Woods et al., where expression of *Atoh1* mRNA was first detected in the developing cochlea at E13.5 (Woods et al. 2004).

ATOH1 protein expression has also been assessed by immunohistochemistry. Studies conducted with anti-ATOH1 antibodies showed that ATOH1 expression begins in vestibular hair cells by E12.5 and in the cochlear hair cells, ATOH1 expression was not observed before E13.5 (Chen et al. 2002) (Figure 1.9b). Additional immunohistochemistry studies also showed ATOH1 expression in inner and outer hair cells at E16 and its expression was still observed at P0 (Driver et al. 2013) (Figure 1.9b). The differences found between *Atoh1* mRNA and protein expression may be due to the delay in the translation process or conditioned by the specificity of the anti-ATOH1 antibody. Data collected by *in situ* hybridization suggested that *Atoh1* mRNA was expressed in a greater population of cells than the cells that were fated to differentiate into hair cells.

Other studies conducted with a reporter mouse line where GFP was driven by the *Atoh1* enhancer (Helms et al. 2000) reproduced *Atoh1* mRNA expression although with a delay in expression in the cochlear system. *Atoh1* expression from the reporter in the vestibular system was seen at the same stages observed using *in situ* hybridization (Matei et al. 2005) (Figure 1.9c). However, in the cochlea *Atoh1*-GFP expression was not observed at E13.5, suggesting that the *Atoh1*-GFP reporter was not able to reproduce the onset of endogenous *Atoh1* expression (Matei et al. 2005). In fact, *Atoh1*-GFP expression from the reporter did not begin until E14.5 in the mid-basal region of the developing cochlea. Later in development and using the same reporter, *Atoh1* activity was detected in the single row of IHC and in the three rows of OHCs at E15.5 matching *Atoh1* mRNA and protein expression observed using *in situ* hybridization and immunohistochemistry (Chen et al. 2002). Therefore, the activity of the mouse *Atoh1*-GFP reporter recapitulated endogenous *Atoh1* expression only after E14.5 (Figure 1.9c).

More recently, *Atoh1* mRNA levels were quantified by q-PCR from mouse cochleae (Stojanova et al. 2015). This study revealed that *Atoh1* mRNA in the developing mouse

cochlea starts at E13.5 and levels were found to peak at around E17.5. After that, *Atoh1* mRNA levels decreased until P6 the latest stage analysed in this study.

In non-mammalian vertebrates, such as chicken and zebrafish, ATOH1 expression has also been described in the embryonic inner ear and lateral line respectively.
In zebrafish, *Atoh1* expression was detected by *in situ* hybridization in the posterior lateral line primordium which contains sensory hair cells surrounded by supporting hair cells (Itoh and Chitnis 2001).
As in zebrafish, *Atoh1* expression in the chick embryo was also detected by *in situ* hybridization at early stages of ear development (Figure 1.9d). At E4, *Atoh1* can be detected in the nascent anterior and posterior cristae of the otocyst (Pujades et al. 2006), showing the typical expression mosaic of hair cells and supporting cells that results from lateral inhibition (see section 1.5.2). ATOH1 protein was also detected by immunohistochemistry at a similar stage in the superior crista of chick, reproducing the expression observed by *in situ* hybridization (stage 23; 3.5-4 days of development) (Stone et al. 2003) (Figure 1.9d).

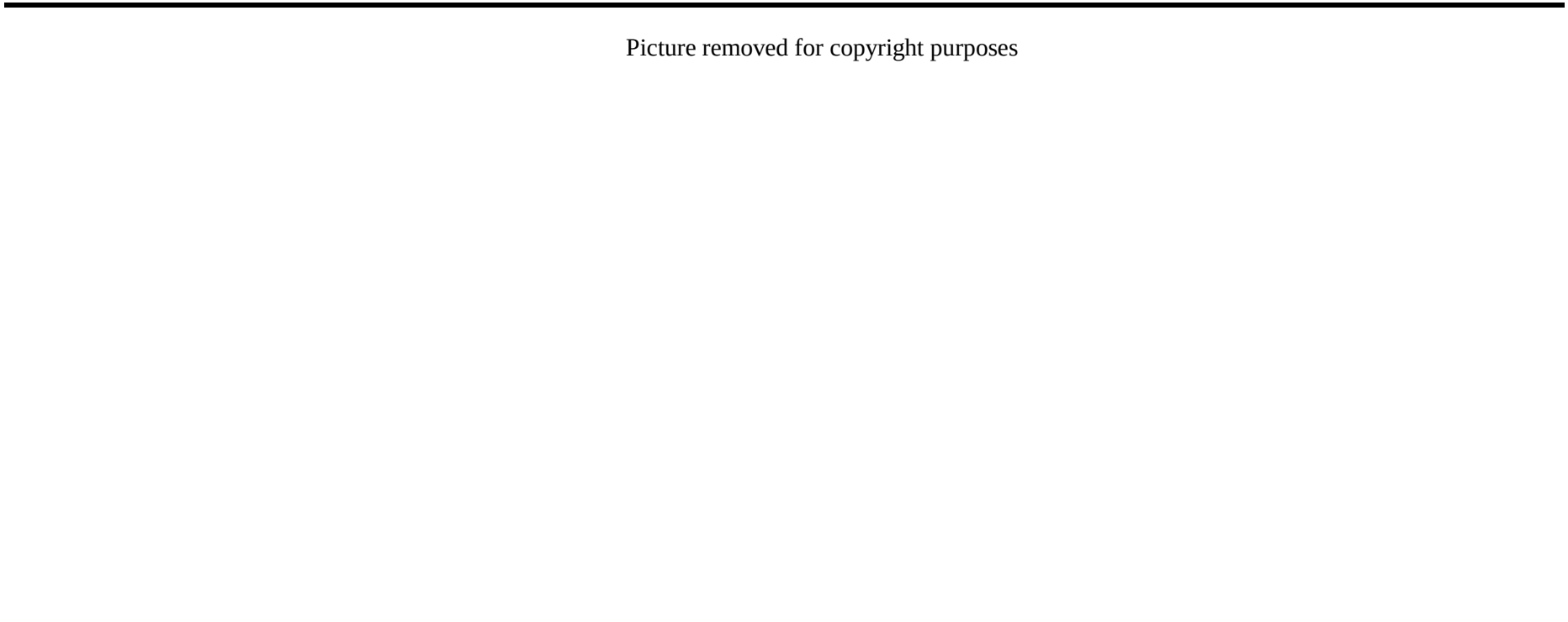

Figure 1.9. *Atoh1* expression in mouse and chick. a) mRNA *Atoh1* expression shown by *in situ* hybridization in mouse. *Atoh1* mRNA is detected in the developing cochlea by E13 whereas other studies detected mRNA expression at E13.5 only on the vestibular system (adapted from Landford et al., 2000 and Pan et al. 2010). Arrowheads mark *Atoh1* mRNA expression. Scale bar = 250μm and 100μm respectively. **b)** ATOH1 protein expression detected by immunohistochemistry in mouse is observed in the vestibular system at E12.5 and its expression is detected in the cochlea later at around E13.5. In post-natal stages, ATOH1 is still observed at P0, matching mRNA expression. By P5, ATOH1 expression was no longer detected (adapted from Chen et al., 2002 and Driver et al. 2013). Scale bars = 50μm. Arrowheads mark ATOH1 protein expression **c)** Studies with a reporter mouse line where GFP was driven by the *Atoh1* enhancer reproduced *Atoh1* mRNA expression in the vestibular system and in some delaminating cells (arrows in A). However, in the cochlea *Atoh1*-GFP activity was not observed until E14.5 (adapted from Matei et al. 2005 and Chen et al. 2002). Scale bars = 100μm. **d)** In chick, *Cath1* (chick *Atoh1* homologue) mRNA was detected in the otic vesicle at E3 and by E4 the hair cell/supporting cell mosaic was visible (adapted from Pujades et al., 2006) Scale bar= 100μm. ATOH1 protein was also examined by immunohistochemistry and observed in the superior crista at E4 (arrowheads) (adapted from Stone et al., 2003). Abbreviations: AC, anterior crista; HC, horizontal crista; PC, posterior crista; S, saccule; U, utricle; cvg, cochleo-vestibular ganglion; cg, cochlear.

1.6.3 The role of *Atoh1* in the inner ear

Atoh1 expression has been shown to be necessary for the formation and development of hair cells, hence homozygous *Atoh1* mutant mice do not develop differentiated hair cells (Bermingham et al. 1999). However, the precise role of *Atoh1* in hair cell development has been discussed in several publications and four different roles have been proposed:

The first is *Atoh1* as a proneural gene. *Atoh1* is involved in the development of different neuronal subtypes such as cerebellar granules, brainstem neurons, neural tube and inner ear hair cells. (Helms et al. 1998; Bermingham et al. 2001; Machold et al. 2005; Ben-Arie et al. 1997). Studies conducted in mouse concluded that the lack of *Atoh1* produces the loss of granule cells and germinal cells in the cerebellum (Ben-Arie et al. 1997) as well as the loss of hair cells in the inner ear (Bermingham et al. 1999). Other studies conducted in Drosophila with the homolog *Atoh1* (*atonal*) demonstrated that the absence of *atonal* leads to the entire loss of the lineage associated with mechanosensory organs (Jarman AP 1998).

In the inner ear, since the development of the prosensory epithelium is part of the process of neurogenesis, *Atoh1* is also defined as a prosensory gene. This second role suggests that although *Atoh1* is required for the specification of hair cells, as it is expressed before hair cells are formed it could have a prosensory function defining the group of cells that will form the prosensory epithelia that contains both mechanosensory hair cells and non-sensory supporting cells. In *Drosophila atonal* is also expressed before cell fate specification (Jarman et al. 1995), supporting also the prosensory role of *atonal*. Some parallels were also found in zebrafish, where the *Atoh1* genes, *Atoh1*a and *Atoh1*b, are involved in establishing the prosensory domain that triggers the fate specification in the preotic placode (Millimaki et al. 2007).

The third proposed role of *Atoh1* suggests that it could operate as a commitment factor for hair cells. To support this hypothesis, *in vitro* studies with cochlear epithelium demonstrated that although *Atoh1* is expressed in prosensory domain it is not directly required for generating supporting cells (Woods et al. 2004). Supporters of this model suggest that the absence of *Atoh1* causes the complete loss of both hair cells and supporting cells. However the loss of supporting cells in *Atoh1* mutants is thought to be

a consequence of the loss of hair cells, which may generate inductive signals that are required for supporting cell formation (Woods et al. 2004). The absence of *Atoh1* and the loss of supporting cells could therefore be an indirect consequence of the disruption of the Notch signalling pathway (described in section 1.5.2).

The final hypothesis proposes *Atoh1* as a differentiation factor of hair cells. As previously discussed, *in vitro* studies with mouse tissue concluded that *Atoh1* was not directly involved in the specification of the sensory primordium within the cochlea (see section 1.5.1). *Atoh1* is not expressed until shortly after, in a non-proliferation zone in which cells have exited the cell cycle. Moreover, the expression of ATOH1 is observed in a subpopulation of cells that go on to differentiate exclusively into hair cells.
In support of this model, *Atoh1*-null mutant mice were analysed and it was observed that the prosensory domain developed normally even though hair cells fail to differentiate (Chen et al. 2002). Therefore it is possible that *Atoh1* is only necessary for the differentiation of hair cells. Moreover, the same study showed using a EGFP-reporter mouse that *Atoh1* is only expressed in cells that go on to differentiate into hair cells.
The experimental data collected to investigate the role of *Atoh1,* are based on different approaches and therefore depending on the technique used, the data were consistent with one of these four hypotheses (Kelley 2006). For instance, ATOH1 protein expression was detected in progenitor cells that have exited the cell cycle and therefore expressed in cells that have differentiated into hair cells (Chen et al. 2002). However, mRNA expression data demonstrated that *Atoh1* transcripts were expressed a bit earlier in the cochlear developing epithelium suggesting a prosensory role for *Atoh1* (Lanford et al. 2000). It remains unexplored whether *Atoh1* is the only factor capable of generating hair cells or whether other mechanisms can also contribute to this process. *Atoh1* upstream regulatory factors presumably play important roles in the regulation of the expression of *Atoh1* and consequently in the formation of hair cells.

1.6.4 *Atoh1* function in other tissues

Atoh1 is expressed in various other tissues (Table 1.1) and *Atoh1* tissue-specific regulatory targets are still being investigated. In addition to the nervous system, one the best characterized systems where *Atoh1* is expressed is the intestine. *Atoh1* mutant mice lack goblet cells and epithelial cells are maintained in a proliferative state (Yang et al.

2001). Furthermore, *Atoh1* is described as having roles in cell fate by specifying the subgroup of secretory cells that form paneth cells, goblet cells and enteroendocrine cells. This mechanism was suggested to occur through the induction of *Neurogenin 3* and *Gfi1* (Yang et al. 2001; Shroyer et al. 2005; Bjerknes and Cheng 2006). Ectopic *Atoh1* expression in the intestine results in additional secretory cells (VanDussen and Samuelson 2010). In addition, *Atoh1* can arrest cell cycle during the development of the intestine by repressing the transcription factor RBP-Jκ but also can regulate genes involved in the progression of the cell cycle such as $p57^{kip}$ and $p27^{kip}$ (Kazanjian et al. 2010; Kim and Shivdasani 2011; Peignon et al. 2011). One of the main conclusions from studies in different systems is that *Atoh1* activity can vary depending on the tissue. In the developing cerebellum, *Atoh1* maintains cells in a proliferative state whereas in the intestine causes cell cycle arrests and differentiation (reviewed in Mulvaney, 2012). *Atoh1* has also been suggested to act as an oncogene in medulloblastoma arising from the external granular layer (Briggs et al. 2008; Zhao et al. 2008; Ayrault et al. 2010). By contrast in other tissues such as the intestine, *Atoh1* can function as a tumor suppressor gene inhibiting the proliferation of colon cancer cells (Leow et al. 2004; Bossuyt et al. 2009). The apoptotic role of *Atoh1* in the intestine was suggested to be conducted through the JNK/MAPK pathway (Bossuyt et al. 2009; VanDussen and Samuelson 2010).

Table 1.1. Summary of *Atoh1* expression. *Atoh1* mRNA expression in normal human tissues detected by microarray, RNA sequencing or SAGE (Serial Analysis of Gene Expression). Adapted from GeneCardsSuite (http://www.genecards.org/cgi-bin/carddisp.pl?gene=ATOH1).

Picture removed for copyright purposes

In summary, *Atoh1* has diverse biological functions which are dependent on both the cell type and the developmental stage. Some targets of ATOH1 are suggested to be common to various tissues whereas others are restricted to specific cells. In the nervous system, *Atoh1* directs the specification of different neural subtypes including the granule layer of the cerebellum (Ben-Arie el al. 1997), hindbrain neurons (Ben-Arie et al., 1997; Machold and Fishell, 2005; Wang et al., 2005; Maricich et al., 2009b; Rose et al., 2009), sensory hair cells (Bermingham et al., 1999; Zheng and Gao, 2000; Izumikawa et al., 2005; Raft et al., 2007) and Merkel cells in the skin and vibrissae (Ben-Arie et al., 2000; Maricich et al., 2009; Morrison et al., 2009; Van Keymeulen et al., 2009). Some neuronal subtype-specific targets of *Atoh1* are *Rassf4, Selm, Atoh1* and *Grem2,* those enhancers are bound by ATOH1 in the cerebellar tissue but not in the dorsal neural tube (Lai, et al. 2011). However, other targets of *Atoh1* such as *Rab5* and *Selm* are transcribed in the neural tube but not in other developmental tissues (Lai, et al. 2011).

1.7 Transcription factors and regulatory mechanisms of gene expression

The control of gene expression is critical for the correct control of biological mechanisms in both prokaryotic and eukaryotic organisms. According to the central dogma of biology which states that genetic information is processed from DNA to RNA and then to proteins, the regulation of gene expression can be controlled at different levels but the predominant mechanism is that of transcriptional regulation (reviewed in Kornberg 1999).

The mechanism that regulates the basal gene expression at the transcription level occurs by the action of transcription factors and additional regulatory proteins on core promoters, *cis*-regulatory elements or other enhancer elements that control the rate of transcription and hence expression of specific genes (see section 1.7.1). However, epigenetic regulation can also control gene expression by several different mechanisms including nucleosome occupancy, post-transcriptional modifications of histones, DNA methylation and nuclear regulatory non-coding RNAs (reviewed in Doetzlhofer and Avraham 2016).

The organization of the chromatin allows DNA to be tightly packed within eukaryotic nuclei. Heterochromatin, the highly condensed form of chromatin, is in general

inaccessible to DNA binding proteins and can lead to transcriptional silencing (Grewal and Moazed 2003). By contrast, euchromatin is more accessible to the different transcriptional apparatus. Nucleosome, are the basic units of chromatin packing. Nucleosomes cores are composed of 145-147 bps of DNA, assembled into an octamer of two copies of histone proteins H2A, H2B, H3 and H4 (Luger et al. 1997). Nucleosomes repress transcription by different mechanisms. For instance, they can occlude protein binding to DNA and consequently interfere in the binding of transcription factors, polymerases and other DNA-modifying enzymes (Workman and Kingston 1998). Interactions of nucleosomes with additional chromosomal proteins within heterochromatin have also been suggested to repress gene expression (Grunstein 1998).

Histone modifications also control gene expression. The core histones present in nucleosomes undergo modifications at different positions across their N-terminal ends. These include acetylation, methylation, phosphorylation and ubiquitination (reviewed in Doetzlhofer and Avraham 2016). One of the best characterized systems of histone modifications is DNA methylation at CpG dinucleotides which is associated with gene silencing (Bird 2002). DNA methylation occurs during the replication of the DNA and it is based on a covalent chemical modification caused by the addition of a methyl group at the 5' position of the cytosine ring by DNA methyltransferases (Das and Singal 2004). This modification occurs more frequently at CpG sites, where a guanine nucleotide follows a cytosine nucleotide (Cedar 1988). It has been suggested that this DNA methylation inhibits gene expression by affecting protein-DNA interactions that are required for transcription (Siegfried and Simon 2010).

RNA also can participate in the regulation of gene expression. Small RNAs and non-coding RNAs have recently emerged as regulators of gene expression by controlling genome stability and for participating in the recruitment of histone and chromatin-modifying complexes (Holoch and Moazed 2015).

In eukaryotic cells, mRNAs carry a 5' 7-methylguanosine cap and a 3' poly (A) tail which protect the RNA chain from degradation (reviewed by Day and Tuite 1998) and therefore influence the intrinsic stability of the RNA transcript. In mammals, microRNAs (miRNAs) can target the 3' untranslated region (UTR) which leads to a reduction in gene expression by translational suppression and mRNA destabilization (Guo et al. 2010). In addition, alternative splicing can lead to the production of various

mRNA isoforms and therefore can play an important role in regulating gene expression (Chen and Manley 2009).

Furthermore, expressed proteins can be regulated by post-translational modifications as well as by the rate of protein degradation. For instance, changes in the amino acid properties, such as the addition of a phosphate group, can alter the function and activity of a protein (Prabakaran et al. 2012).

1.7.1 Transcriptional control of gene expression

The core promoter is defined as the centre of the basal transcriptional machinery (Juven-Gershon and Kadonaga 2010) and it is a determining factor in the transcription of any gene (reviewed by Heintzman and Ren 2006). The DNA region containing the core promoter is typically located ~40 bp upstream and/or downstream of the transcription start site (TSS) of specific genes. The majority of the transcription factors that are required for the basal transcriptional machinery interact directly or indirectly with the core promoter to initiate gene transcription. The study of core promoters has led to the discovery of various sequence motifs which play a role in basal transcription. Among others, these include: the TATA box sequence (also named the Goldberg-Hogness box after its discoverers) which is present in approximately 24% of human genes (Yang et al. 2007), BREu (upstream TFIIB Recognition Element), InR (Initiator), MTE (Motif Ten Element), DPE (Downstream Promoter Element), DCE (Downstream Core Element) and XCPE1 (X Core Promoter Element 1) (Juven-Gershon and Kadonaga 2010). To prepare the promoter for the initiation of the transcription, sequence specific transcription factors bind to these regions in the promoter to form the pre-initiation complex (PIC) (Sainsbury et al. 2015). This process requires factors such as TFIIA, TFIIB, TFIID, TFIIE, TFIIF and TFIIH which are known as “general” or “basal” transcription factors (Figure 1.10) (Juven-Gershon and Kadonaga 2010). The initial step for the assembly of the PIC is the binding of TFIID (Sainsbury et al. 2015). Following this, a series of different steps occur including promoter melting and clearance before functional RNA polymerase II elongation is achieved. Once RNA polymerase II has been tethered to the promoter, it must be released from the complex to initiate the transcription (Alberts et al. 2002). After RNA polymerase II escapes from the promoter, TFIID, TFIIE, TFIIH remain on the core promoter sequence and subsequent re-initiation only requires *de novo* recruitment of the complex containing RNA polymerase II- TFIIF and TFIIB (reviewed in Maston et al. 2006).

Picture removed for copyright purposes

Figure 1.10. Initiation of transcription. In eukaryotic genes, the assembly of the RNA polymerase II requires the presence of "basal" or "general" transcription factors (TFIIA, TFIIB, TFIID, TFIIE, TFIIF and TFIIH) that recognize specific DNA sequence motif such as the TATA box in the promoter to initiate the transcriptional machinery as part of the pre-initiation complex. Additional transcription factors bind to distal regions of the promoter such as enhancers that contribute to the regulation of gene expression. This mechanism is conducted by the Mediator complex which adopts distinct functions at the appropriate stages of the transcription. Interactions between transcription factors and the Mediator complex generate structural changes in the genomic DNA sequence to facilitate interactions between the enhancer and the promoter region. Figure adapted from Web textbook CSLS. University of Tokyo (http://csls-text3.c.u-tokyo.ac.jp/active/10_03.html).

The effect of the basal transcription factors is complemented by other transcription factors, co-factors and protein complexes which have the ability to bring distal regulatory regions in the surrounding DNA sequence, such as enhancer elements, into close proximity to the promoter region to influence the rate of transcription. Enhancers and promoters can be separated from a few kb to over 1000 kb however, it is still unclear which molecules are involved in the communication of these two regulatory elements, when it takes place and whether this is the same for all classes of enhancers (reviewed in Vernimmen and Bickmore 2015).

Transcription factors are classified based on their sequence similarity and their DNA binding domains (Stegmaier et al. 2004). The helix-turn helix, zinc finger, leucine zipper, winged helix and helix-loop-helix domains are some of the most commonly

known (reviewed in Guasconi et al. 2003). The function of these transcription factors is to bind to specific sites in DNA regulatory regions to activate or repress transcription and consequently regulate gene expression. In addition to their DNA binding domains, transcription factors can also contain separate conserved domains that confer activation or repression often via interactions with other regulatory proteins. This includes the Mediator, a complex of 26 subunits in mammals that communicates regulatory signals from DNA-bound transcription factors to the RNA polymerase II (Allen and Taatjes 2015). The Mediator is crucial for the organization of different regulatory elements such as enhancers in the genomic DNA to generate gene loops that enable coordinated regulation of transcription (Plank and Dean 2014).

1.7.2 Regulation of *Atoh1*

Transcription factors, as well as being regulators of gene expression are also themselves subject to tightly controlled mechanisms of gene regulation. *Atoh1* is involved in the differentiation of auditory hair cells, neurons and secretory cells in the intestine (Mulvaney and Dabdoub 2012). Therefore, *Atoh1* expression must be tightly regulated since aberrant *Atoh1* activity results in several deficiencies during neurosensory development.

The transcriptional regulation of *Atoh1* has been studied in different organisms over the past twenty years. Investigations of how *Atoh1* is regulated began with the studies conducted in *Drosophila* where enhancer elements located, both up and downstream of the *atonal* coding sequence were identified that control *atonal* expression in several tissues (Sun et al. 1998). Regulation of *atonal* expression via the upstream region of the *atonal* sequence was shown to be tissue-specific, controlling the expression of chordotonal precursors such as the leg, wing and antennal discs, among others. Meanwhile, the downstream enhancer of the *atonal* region was shown to contribute to the initial phase of *atonal* expression in the leg and disc wing and partially the expression in the antennal and eye disc (Sun et al. 1998).

The evolutionary conservation of the *Drosophila atonal* sequence across different species, including mouse (Ben-Arie et al. 1996) suggested that similar regulatory mechanisms could control the expression of *Atoh1* in mammals.

The first study conducted in mouse identified a 21 kb region, flanking the *Atoh1* coding sequence shown to be sufficient to drive a *lacZ* reporter gene in some but not all, *Atoh1* expressing regions in the developing nervous system (Helms and Johnson 1998). These

studies utilized a transgenic mouse in which the *Atoh1* coding sequence was replaced by the *lacZ* reporter sequence, flanked by the 15 kb and 6 kb sequence upstream and downstream of the mouse *Atoh1* coding region respectively. This transgenic mouse showed similar expression to endogenous ATOH1 in the neural tube between E9.5 to E11.5, the external germinal layer of the cerebellum at E13-E15 and in developing hair cells and the semicircular canal. The correlation between the expression of endogenous ATOH1 and the l*acZ* transgene in different regions, confirmed the importance of the *Atoh1* flanking regions in the control *Atoh1* expression.

However, there are other *Atoh1* tissue specific regions where the *Atoh1*/*lacZ* transgene expression does not reflect endogenous ATOH1 protein expression detected by immunohistochemistry. That includes the Merkel cells of the hairy skin and the cranial ganglia, the first region expressing ATOH1 at E9-E9.5 (Akazawa et al. 1995). The absence of *lacZ* expression in these regions suggested the existence of additional regulatory regions outside the 15 kb upstream and 6 kb downstream flanking sequences of the mouse *Atoh1* gene. In addition, expression of the *lacZ* transgene was seen in differentiated neurons in the neural tube at E11.5. At this stage (E11.5), endogenous ATOH1 expression is not expected in the differentiated neurons derived from *Atoh1* progenitor cells in the neural tube which suggests that negative regulatory regions are also missing from the *Atoh1*/*lacZ* transgene (Helms and Johnson 1998). However, Helms et al., also suggested that the stability of the *lacZ* mRNA or the β-Gal protein in the *Atoh1*/*lacZ* transgenic mouse could be responsible for these discrepancies. To investigate this possibility, a new transgenic line was generated where the *lacZ* gene was replaced with an epitope-tagged ATOH1 protein (Helms et al. 2000) with the *Atoh1* flanking regions still maintained. The stability of this new transgenic mouse was intended to be similar to the stability of endogenous ATOH1 protein. Expression of the transgene re-capitulated endogenous ATOH1 protein expression in the dorsal region of the neural tube (Helms et al. 2000). However, expression of this reporter was also found outside the *Atoh1* expressing regions further suggesting that additional regulatory elements exist outside the 15 kb and 6 kb sequences flanking the mouse *Atoh1*.

Additional experiments conducted by Helms et al., with a *lacZ* transgene line containing only the 6 kb downstream region of the mouse *Atoh1* coding sequence (without the 15 kb upstream region) were sufficient to re-capitulate endogenous *Atoh1* expression in

the neural tube at E10.5 (the only *Atoh1* expressing region analysed in these experiments). In contrast, a similar reporter gene incorporating the 15 kb upstream sequence alone failed to show reporter activity.

The 6 kb 3' region flanking sequence has been refined further. An additional transgene generated with a 1.7 kb fragment located 3.4 kb downstream of the *Atoh1* mouse sequence was found to reproduce endogenous mouse *Atoh1* expression in the neural tube. This 1.7 kb sequence was found to contain two shorter conserved regulatory elements that regulate *Atoh1* expression in multiple tissues and were defined as mouse *Atoh1* enhancer A and enhancer B (Helms et al. 2000).

Enhancer A is sufficient on its own to drive expression in multiple *Atoh1* tissue-specific regions, including the ear epithelium, but not in the neural tube. In contrast, enhancer B on its own showed *lacZ* activity in all the *Atoh1* expressing regions but also in other tissues where *Atoh1* is not expressed.

The sequence of the two mouse *Atoh1* enhancers were investigated by the same group and sequence homology was not found between both enhancers in spite of having some redundant functions. As a result of this analysis, an E-box site located in the enhancer B (Figure 1.11) was demonstrated to be necessary for the expression of the *lacZ* transgene in the neural tube. In addition, this E-box sequence was shown to bind ATOH1 and its co-factor, E12/E47 (Akazawa et al. 1995), in electrophoretic mobility shift assays (EMSAs).

Subsequent experiments by Helms et. al. 2000, on an ATOH1 mutant background confirmed that ATOH1 is required for *Atoh1*/*lacZ* transgene expression in an auto-regulatory feedback loop controlling its own expression.

The requirement of ATOH1 for the expression of *Atoh1* in the mouse inner ear was also demonstrated by studies conducted with an *Atoh1*-GFP BAC transgenic mouse. This transgenic mouse expressing GFP under the control of the *Atoh1* enhancers matched the endogenous *Atoh1* mRNA expression in wild type animals but failed to express GFP in mutant animals lacking endogenous ATOH1 at stages E13.5 through E15.5. This confirms the need for ATOH1 to initiate *Atoh1* enhancer activity (Raft et al. 2007). However, GFP expression was persistent in the hindbrain in *Atoh1* mutant animals supporting the hypothesis that additional regulatory elements lie outside the *Atoh1* A and B enhancers necessary for endogenous regulation of mouse *Atoh1*.

Little is known about the mechanisms controlling the basal transcription of *Atoh1*. According to experiments conducted by Helms et al., the activity of the *Atoh1* enhancers is independent from the *Atoh1* promoter sequences immediately 5' of the start of transcription since 3' enhancer activity is observed when using other promoters such as the β-globin basal promoter (Helms et al. 2000). However, these experiments were limited to the spiral neural tube and hindbrain. The murine *Atoh1* promoter containing the 226 bp upstream region of the *Atoh1* transcription start site has recently been tested in cells within the prosensory domain of the developing cochlea (Abdolazimi, 2016). In this study it was suggested that the *Atoh1* promoter contains Hes/Hey binding sites that are required for timely repression of *Atoh1* within the cells of the prosensory domain that will form supporting cells. Therefore, based on these recent results, it is possible that the mouse *Atoh1* promoter does contribute to the temporal and spatial control of *Atoh1* expression in prosensory progenitors of the inner ear.

In summary, evidence to date suggests that murine *Atoh1* expression is strongly controlled by the presence of two 3' enhancers, enhancer A and enhancer B, which are sufficient to drive *Atoh1* expression in several *Atoh1* tissue-specific regions. However, very recent investigations raise the possibility that the *Atoh1* proximal promoter could have roles in *Atoh1* expression to select the hair cell and supporting cell fate (Abdolazimi, 2016). It has also been suggested that additional regulatory elements, not explored in previous studies, might also be involved in the regulation of *Atoh1* (Helms et al. 1998; Helms et al. 2000). ATOH1 appears to play a role in regulating its own expression via enhancer B (Helms et al. 2000). However, little is known about the mechanisms initiating *Atoh1* enhancer activity before ATOH1 is produced.

1.7.3 Transcription factors binding *Atoh1* enhancers

As described previously, the heterodimer formed by ATOH1/E47 binds to an E-box site located in the mouse *Atoh1* enhancer to control its own expression (Akazawa et al. 1995) (Helms et al. 2000). However, ATOH1 is not the only transcription factor binding to the *Atoh1* enhancers. A number of other transcription factors have also been shown to activate or repress ATOH1 expression by binding to the 3' enhancers.

In a screen to identify transcription factors involved in the regulation of *Atoh1*, the zinc-finger transcription factor ZIC1 was shown to downregulate the activity of the mouse *Atoh1* enhancer in the neural tube (Ebert et al. 2003). EMSA analysis demonstrated that ZIC1 binds to the mouse *Atoh1* enhancer B at a site 30 bp from the previously identified E-box site (Figure 1.11). Moreover, EMSA probes designed to the homologous sites within the human and chick *Atoh1* enhancers confirmed that the binding of ZIC1 is conserved among these species. In chick, electroporated ZIC1 also represses the expression of endogenous chick ATOH1 in neural tubes. In addition, Ebert et al. showed that the mutation or deletion of the ZIC1 binding site in the mouse *Atoh1* enhancer produced the loss of the enhancer activity.

A number of other transcription factors have been linked to regulation of *Atoh1* though with less experimental evidence than that for ZIC1 and ATOH1 itself and largely in non-auditory tissues. Hypermethylated in cancer-1 (HIC-1), a zinc-finger transcriptional repressor that is hypermethylated in various human cancers has been shown to be a specific repressor of *Atoh1* (Briggs et al. 2008). The upregulation of *Atoh1* commonly found in medulloblastoma cancers was suggested to be modulated by HIC-1 via epigenetic silencing.

CDX2 is a caudal-related homeobox transcription factor expressed in the nuclei of embryonic and adult mucosal epithelial cells of the intestine (Meyer and Gruss 1993). Reporter gene assays in IEC-6 intestinal epithelial cells demonstrated that CDX2 activates the transcriptional activity of *Atoh1*. The site of CDX2 binding was in the mouse *Atoh1* enhancer B downstream of the E-box sequence (Mutoh et al. 2006b) (Figure 1.11). Also in the intestinal epithelium, the hepatocyte nuclear factors Hnf1α and β, have been implicated in the regulation of *Atoh1* expression (D'Angelo et al. 2010). β-catenin, a key mediator of the Wnt signalling pathway, was also found to activate the expression of *Atoh1* in mouse neuroblastoma cells and neural progenitor cells (Shi et al. 2010). The interaction between β-catenin and *Atoh1* was through Tcf-Lef binding sites located in the mouse *Atoh1* 3' enhancers (Figure 1.11) as demonstrated by ChIP assays. Moreover, the mutation of the Tcf-Lef binding sites reduced the transcriptional activation of the mouse 3' *Atoh1* enhancers confirming the direct interaction.

Picture removed for copyright purposes

Figure 1.11. Schematic representation of the mouse *Atoh1* locus on chromosome 6. Location of the two conserved regulatory regions, enhancer A and enhancer B, (in blue) downstream of the *Atoh1* coding sequence (in red). The *Atoh1* enhancers A and B were demonstrated to be sufficient to control *Atoh1* expression (Helms et al. 2000). The position of known transcription factors within the 3' enhancer sequences are indicated within the boxed panels. An E-box sequence (CATATG) located in the enhancer B is required for the binding of ATOH1 to control its own expression. The binding sites of other transcription factors demonstrated to bind the *Atoh1* enhancers such as SOX2 and β-catenin in the enhancer A and SIX1, ZIC1, HIC1 and CDX2 in the enhancer B are marked in colours. Figure reproduced from Groves et al. 2013.

In addition, silencing β-catenin expression produced a decrease of mouse *Atoh1* mRNA levels in Neuro2a cells and neural progenitor cells based on RT-PCR results. Since the expression of bHLH genes, including *Atoh1* is partly regulated by the Notch pathway, the authors of this study proposed that β-catenin could potentially contribute to the initial up-regulation of *Atoh1* after Notch signalling inhibition.

Within the inner ear, the expression of *Atoh1* has recently been demonstrated to be dependent on the co-operation of three transcription factors: SOX2, EYA1 and SIX1 (Ahmed et al. 2012). EYA1 is a transcriptional co-activator that along with its co-factor, the homeodomain protein SIX1 plays essential roles during sensory development (Xu et al. 1999) (Zheng et al. 2003), whereas SOX2 is required for specifying precursors within the prosensory domain (Kiernan et al. 2005). The expression of SIX1 in the organ of Corti transiently increased in parallel with hair cell differentiation with an onset of expression slightly earlier than that of *Atoh1* (at E13.25). SOX2 expression is observed in the GER epithelium by E13.5 in post-mitotic cells but by E16.5 has becomes restricted to supporting cells. Finally, EYA1 expression was observed in the cochlear epithelium between 12.5-13.5 overlapping with SOX2 expression, although later on EYA1 becomes restricted to differentiated hair cells.

In order to determine whether these transcription factors were required for murine *Atoh1* expression, mouse cochlear explants were electroporated with an *Atoh1*-GFP construct and different combinations of SOX2, EYA1 and SIX1 expression constructs. The 3' *Atoh1* enhancer AB construct was activated by both SOX2 and SIX1. Moreover, electroporation with the individual *Atoh1* enhancer A or enhancer B constructs showed that SOX2 activates the mouse *Atoh1* enhancer A, whereas SIX1 activates the mouse *Atoh1* enhancer B. Using SOX2 and SIX1 antibodies in ChIP analysis confirmed the presence of SOX2 and SIX1 binding sites in enhancer A and B respectively *in vivo*. Overall, the work conducted by Ahmed et. al., suggested that the synergistic co-operation of SOX2, EYA1 and SIX1 is required to activate the transcription of mouse *Atoh1* both *in vitro* and *in vivo*.

Confirming the results from the previous study, Neves et. al., also found that the transcription factor SOX2 induces *Atoh1* transcription. Overexpression of SOX2 in HEK293T cells and in chick otic vesicles was seen to activate mouse *Atoh1* enhancer activity (Neves et al. 2012).

1.7.4 Signalling pathways, ATOH1 expression and sensory cell fate in the inner ear

The development of the inner ear is a complex process regulated by multiple genes and signalling pathways. The Notch signalling pathway (see section 1.5.2), transcription factors such as ATOH1, SOX2, POU4F3 and GFI1 (discussed in sections 1.5.3 and 1.7.3) as well as other proteins combine to regulate supporting cell/hair cell fate during inner ear development. In addition to these, the BMP, SHH, FGF and WNT signalling have been linked to the activation of *Atoh1* expression and therefore participate in the determination of hair cells and supporting cells.

The role of the bone morphogenetic protein (BMP) signalling pathway on the control of *Atoh1* expression is still unclear. The BMP signalling pathway induces *Atoh1* expression in early stages of cell differentiation in dorsal neurons (Alder et al. 1999; Lee et al. 2000) and rhombic lips (Krizhanovsky and Ben-Arie, 2006). However, in contrast the BMP signalling pathway reduces ATOH1 protein expression during the developing of cerebellum (Zhao et al. 2008) and in medulloblastoma (Grimmer and Weiss 2008). One of the mechanisms proposed for ATOH1 downregulation in the inner ear was suggested to be mediated by BMP4 and BMP7. These molecules may induce the phosphorylation of SMAD1,5,7, leading to the induction of the inhibitor of DNA-binding proteins Id1-3 to consequently reduce ATOH1 expression in hair cells (Kamaid et al. 2010; Zhao et al. 2008).

The Sonic Hedgehog (Shh) and WNT signalling pathways have also been suggested to play a role on hair cell fate by regulating *Atoh1* expression. Data suggests that SHH contributes to the differentiation of cochlear neural progenitors by activating *Atoh1* expression and *Pou4f3* activity to promote hair cell differentiation (Hu et al. 2010).

WNT signalling pathway induces *Atoh1* expression during embryonic development (Landsberg et al. 2005). As discussed in section 1.7.3, β-catenin, a key mediator of the canonical WNT pathway, binds to the mouse *Atoh1* 3' enhancers to activate ATOH1 expression in neural progenitor cells (Shi et al. 2010).

In zebrafish, *Fgf3* and *Fgf8* signals have also been proposed to activate ATOH1 expression during the development of the pre-otic placode and later during the development of the otic vesicle (Millimaki et al. 2007). In mouse, FGF20 was also suggested to activate ATOH1 expression since its expression overlaps with SOX2

expression in the otic vesicle (Hayashi et al. 2008). FGF20 signals activate downstream members of the Ets-domain transcription factor family, PEA3 and ERM, and thereby activate ATOH1 expression.

In summary, the interaction of different signalling pathways is thought to have diverse effects on the expression of genes, like *Atoh1*, to control hair cell fate in the inner ear.

In addition, other regulatory mechanisms such as epigenetic regulation (discussed in section 1.7) are likely to contribute to the complex network which regulates ATOH1 involvement in the proliferation and differentiation of sensory cells in the inner ear.

1.7.5 Can *Atoh1* restore hearing?

Beyond its developmental role as a gene required for the formation of hair cells, *Atoh1* was chosen as a potential candidate for regenerating hair cells and thereby restoring hearing (Zheng and Gao 2000; Woods et al. 2004; Gubbels et al. 2008; Shou et al. 2003). Hair cells are delicate structures, susceptible to ototoxic drugs and chronic noise exposure. In addition, in ageing animals, hair cell numbers decline leading to age-related hearing loss. The identification of mechanisms that can restore hearing by stimulating regeneration of functional hair cells is one of the most difficult challenge that faces inner ear biology but one of immense clinical potential.

Non-mammalian vertebrates, including birds, can produce new hair cells through direct or indirect transdifferentiation of surviving supporting cells into hair cells. (Cotanche 1987; Corwin 1989; Ryals 1988; Stone 1998; Adler and Raphael 1996; Taylor and Forge 2005). As in mammals, ATOH1 expression is not seen in the basilar papilla of post-hatch birds in which no new hair cells are formed. However, upon hair cell damage, ATOH1 expression is re-activated in the chick auditory epithelium (Cafaro et al. 2007; Daudet et al. 2009) and as a consequence hair cells are spontaneously regenerated. This was shown in experiments using immunofluorescence in chick after ototoxic drug exposure where ATOH1 expression was observed in regenerated hair cells in comparison to untreated animals where ATOH1 was not detected. Moreover, this re-activation was observed in both direct and indirect mechanisms of trans-differentiation of supporting cells into hair cells. In addition, ongoing production of vestibular hair cells has also been observed in birds (Jorgensen et al. 1988).

In contrast, in mammals hair cell regeneration is very limited. To date, only vestibular hair cells have been demonstrated to have some potential to regenerate (Forge et al. 1993; Rubel et al. 1995; Lopez et al. 1998; Kawamoto et al. 2009).

Therefore, due to the different regenerative capabilities found in mammals and avians, one of the main questions that remain unsolved is elucidating the mechanisms that differentiate the regenerative capabilities of avian and mammalian hair cells. The upregulation of *Atoh1* was suggested to be, at least in part, responsible for the spontaneous regeneration of hair cells after injury in birds as a recapitulation of the events that occur during the embryonic development of hair cells in which ATOH1 is expressed (reviewed in Groves, 2010). Based on this hypothesis, several groups studied the ability of ectopic ATOH1 to generate new hair cells mainly by the use of three different techniques: ectopic transfection of an *Atoh1* expression construct, *in utero* electroporation of *Atoh1* or adenovirus-mediated expression of *Atoh1*.

In *Drosophila*, ectopic expression of *atonal* was observed to promote extra sense organs such as scolopales, the fundamental units of the mechanoreceptor organs in insects (Jarman et al. 1993). In mammals, the overexpression of *Atoh1* resulted in the production of extra hair cells in the greater epithelial ridge of P0 rat cochlear explants (Zheng and Gao 2000). Ultrastructural analysis and immunohistochemistry of post-natal cultures electroporated with a mouse *Atoh1* construct suggested the presence of ectopically induced hair cells in the greater epithelial ridge. *In utero* electroporation of *Atoh1* into an embryonic mouse otocyst was also suggested to generate ectopic hair cells in the organ of Corti showing the electrophysiological properties of normal hair cells (Gubbels et al. 2008)

The conversion of non-sensory cochlear cells into sensory hair cells after adenovirus induction of *Atoh1* was also investigated in young adult guinea pigs. Different studies conducted by Raphael's group attempted to induce hair cell regeneration by the inoculation of an *Atoh1* expressing adenovirus into the cochlear endolymph (Kawamoto et al. 2003; Izumikawa et al. 2005; Izumikawa et al. 2008). In the first study conducted by this group, it was assumed that the injected volume of virus into the endolymph was sufficient to generate a mechanical trauma that caused degeneration of the majority of the hair cells (Kawamoto et al. 2003). It was not clear whether the *Atoh1* positive cells shown by immunohistochemistry or scanning microscopy after the inoculation of the virus were new hair cells or surviving hair cells after the mechanical trauma. Following

this work, a subsequent study by the same group performed *Atoh1* adenovirus inoculation into the cochlea of young adult guinea pigs that had been deafened by the administration of kanamycin (Izumikawa et al. 2005). Kanamycin is an aminoglycoside antibiotic that causes permanent damage to sensory cells (Erol 2007). Some deafened animals showed a recovery in hearing with *Atoh1* inoculation according to auditory brain-stem responses (ABRs). However, the lack of controls showing that cochlear hair cells were completely eliminated after the ototoxic insult, and the fact that the study did not show whether or not ATOH1 positive cells were found in the cochleae inoculated with an empty adenovirus means these data should be interpreted with caution. Additional studies also conducted in guinea pig were unable to detect new hair cells in the flat cochlear epithelium after neomycin treatment and *Atoh1* virus inoculation which suggests that differentiated supporting cells are required for transdifferentiation to occur (Izumikawa et al. 2008).

Although these results suggest potential for an *Atoh1* therapeutic approach in restoring hearing, they remain controversial. The main concern with these studies is that some deafened animals still show normal patterning of IHC, OHC and supporting cells in the cochlear epithelium right after the ototoxic treatment to differing extents. Therefore the cochlear epithelium in these animals could have retained some of the features that are required for the recovery of hair cells which might explain the hearing recovery rather than *Atoh1* induced regeneration. The plasticity of cochlear cells to respond to *Atoh1* and the ability of hair cells to recover after injury could also change as the organ of Corti matures (Groves 2010). Embryonic and neonatal animals both birds and mammals, showed a greater capability to transdifferentiate supporting cells into hair cells in comparison to mature animals. It is also possible that there is a short time frame after hair cell damage in which *Atoh1* can be introduced before the supporting cells degenerate and a flat and non-regenerative epithelium is formed which may influence these results. Other factors in addition to *Atoh1* could also be required to transdifferentiate supporting cells into hair cells. All these considerations might limit the therapeutic potential of this regenerative approach to correct hearing loss in humans.

Atoh1 therapy as a method to regenerate hair cells is still being investigated by many groups as an approach toward the recovery of hearing. Currently, a clinical trial based on *Atoh1* gene therapy is being conducted on human volunteers with hearing loss by University of Kansas Medical Center in collaboration with the pharmaceutical company

Novartis. A group of 45 volunteers will have the *Atoh1* adenovirus injected into their cochleae and the study will test whether the hearing is improved after the inoculation of the *Atoh1* virus. The trial results are expected in 2017 (Information found at the Novartis website: https://www.novartis.com/stories/discovery/can-we-unlock-bodys-ability-regenerate-lost-hearing).

1.8 New perspectives and treatments for hearing loss

There are several advantages to the use of gene therapy approach described above to treating hearing. Gene therapy offers the possibility of introducing a transgene to specific cells via cell specific promoters to produce the desired protein in the correct location for long periods. However, as discussed above there are major challenges to be overcome. First, the injection of an adenovirus can damage the delicate cochlear epithelium. In addition, there is a short time frame of approximately one week after severe ototoxic injury at which the efficacy of the gene therapy starts to decrease (reviewed in Groves 2010).

In addition to gene therapy, a regenerative approach is currently being investigated by the introduction of stem cells into the damaged ear with the aim of differentiating them into functional hair cells. Promising protocols have been established to demonstrate that mouse embryonic stem cells can be directed toward the formation of an ectodermic epithelium which is able to respond to otic-inducing growth factors to form hair cell-like cells (Oshima et al. 2010; Rivolta 2012).

A more recent study also showed that mouse embryonic stem cells can be differentiated into a three-dimensional inner ear-like epithelium (Koehler et al. 2013). It is hoped that the use of these protocols that can be applied to human stem cells. *In vitro* studies conducted with human stem cells, isolated mainly from bone marrow-derived mesenchymal stem cells or adipose-derived stem cells can be induced to express different otic markers including *ATOH1, POU4F3, SOX2, PAX2, PAX8, GATA3* and *MYOSIN7a* (Boddy et al. 2012; Durán Alonso et al. 2012). A key factor of the stem cell approach is the delivery of the correct signals in order to mimic the normal inner ear environment during development. Therefore to achieve this, a combination of different factors in an embryonic or stem cell environment must be added to achieve the correct

re-programming of stem cells into the hair cells. Recent studies have shown that the combination of the transcription factors ATOH1, GFI1 and POU4F3 can have the potential to re-programme mouse stem cells into sensory hair cell-like cells (Costa et al. 2015). However, isolating human stem cells is challenging, as is re-programming them *in vivo* or re-introducing *in vitro* re-programmed stem cells to the inner ear which makes this approach very difficult in a clinical scenario (Chen et al. 2009; Hu et al. 2012).

Regardless of the approach, a major challenge is the delivery of stem cells or genetic material into the inner ear. Transplanted cells might not be integrated into the organ of Corti or may die in the process (Muller and Barr-Gillespie 2015). The therapeutic approach also needs to consider the different forms and degrees of hearing loss. Many forms of hearing loss are not just a result of hair cell defect but also due to defects in other structures in the cochlear epithelium, such as the stria vascularis or the auditory nerve (Yamasoba et al. 2013; Fetoni et al. 2011).
The use of pharmacological drugs as a treatment for some forms of hearing loss is also being studied. Over a thousand compounds have already been tested in a screen conducted in zebrafish to identify biological and chemically designed drugs that can modulate hair cell regeneration (Namdaran et al. 2012).
Finally, cochlear implants and 3D printing will bring together functional electronic devices with the use of reconstructed/bionic ears (Mannoor et al. 2013) and may also provide a mechanism in which to deliver therapeutic agents to the inner ear.

There is no doubt that the market for therapeutics toward the cure for hearing loss will bring new exciting and novel approaches. The combination of science and technology will be highly important, which will be expanded over the next coming years.

1.9 Investigation of inner ear biology

1.9.1 The challenge of studying the inner ear

The study of the auditory and vestibular system is necessary for understanding inner ear dysfunctions. However, the inner ear is located deep inside in the temporal bone and therefore its accessibility is complex. Accessing the inner ear requires extensive training and advance dissecting skills in order to reach such a small structure. Moreover, the inner ear epithelium is composed of different cell types including hair cells and

supporting cells formed by extremely fragile structures which can be permanently damaged under mechanical and environmental changes. The use of animal models, usually mouse, rat or guinea pig, is a common approach in the study of biomedical research. Depending on the animal model used, many inner ears would be required for experimentation based on the low number of hair cells per ear (approximately 20,000 depending on species) (Slepecky 1996). The use of cell lines overcomes some of these problems and disadvantages.

1.9.2 The use of cell lines as a model to study gene regulation

To overcome the difficulties outlined above on the study of the inner ear, cell lines were used in molecular experimentation. Cell lines have proven to be a valuable source in many research areas including studies on visual (Seigel 1999) and olfactory (Barber and Ronnett 2000) systems. The use of cell lines generates many advantages in comparison to animal experimentation. For instance, they require minimal care in comparison to animal work, decreasing the cost invested on their maintenance and can also provide a higher cell population in comparison to the number of cells obtained from dissected inner ears. However, as any other approach, the use of cell lines also has some limitations. Cell lines are *in vitro* preparations, isolated from specific cell populations at a precise developmental stage. Therefore, all the surrounding epithelium, intercellular factors and connective tissue that they would normally experience *in vivo,* are absent in these cellular preparations. In spite of these disadvantages, cell lines retain many of the characteristics and gene expression profiles possessed at the time they were established. Therefore, cell lines are useful tools on the study of gene regulation since they express many of the genes, transcription factors and other protein molecules that are required for the study of a precise stage of development (Rivolta and Holley 2002). The use of inner ear cell lines commenced in the late nineties with the development of immortalized cell lines (Rivolta and Holley 2002). UB/OC1 and UB/OC2 cell lines, named after University of Bristol, are conditional immortalized cell lines derived from E13 primary cultures of the developing organ of Corti (Rivolta et al. 1998). They are derived from a transgenic mouse (H-2K^{b}-*ts*A58) which carries a temperature-sensitive oncogene which regulates the differentiation of the cells based on temperature changes (Jat et al. 1991). Therefore, when these cells are cultured at 33^{o}C in the presence of a γ-interferon, the proliferative state of these cells is maintained, but if the temperature is increased to

39^{o}C and the γ-interferon is removed the cells stop proliferating and start to differentiate (Rivolta and Holley 2002). This generates a specific time window that retains some of the *in vivo* characteristics possessed after the last mitosis of hair cells and before they start to differentiate. UB/OC2 cells were used for some experimental procedures conducted in this thesis. The expression of different hair cell markers such as POU4F3, α9AChR, Myo7a and Myo6 were detected by RT-PCR (Rivolta and Holley 2002) which makes this cell line a valuable source for the study of hair cell gene regulation and physiological studies (Jagger et al. 1999).

1.10 Project aims

Over 5% of the world's population (360 million people) are affected with a moderate degree of hearing loss (WHO-March 2015), with the loss of cochlear hair cells as one of the major causes of deafness. Understanding how hair cells are formed and the mechanisms required for its differentiation and regeneration is therefore critical to find a cure for deafness. The general aim of this project is to identify transcription factors involved in the regulation of *Atoh1*, the pro-hair cell master gene required for the formation of hair cells in the inner ear (Bermingham et al. 1999). Though a few candidates have been identified for controlling *Atoh1* expression in different tissues (Helms et al. 2000; Ebert et al. 2003; Briggs et al. 2008; Mutoh et al. 2006; Shi et al. 2010), very little is known about the regulation of *Atoh1* expression in the inner ear (Neves et al. 2012; Ahmed et al. 2012). There are clearly some differences in the regenerative capabilities of hair cells in mammalian and avian species. This condition appears to be linked to the re-activation of the expression of *Atoh1*, a mechanism that spontaneously occurs in avians (Cafaro et al. 2007; Daudet et al. 2009) but that is extremely limited in mammals including humans (Wang et al. 2010). It was hypothesized that these differences may be found in the regulatory mechanisms that govern its expression. To test this hypothesis, the investigation was sub-divided in to three different objectives:

- **To compare and identify common and distinct regulatory elements and putative transcription factor binding sites in the *Atoh1* gene locus in avians and mammals** (Chapter 3).

- **To investigate whether four of these candidates YY1, NF-κB, ATOH1 and E2F transcription factors are involved in the regulation of *Atoh1* expression** (Chapter 4 and 5).

- **To investigate the role of a novel avian conserved region, putative enhancer C and the effect of E2F1 on *Atoh1* regulation in the chick inner ear *in vivo*** (Chapter 6).

Chapter 2

2 Material and Methods

2.1 Material

General equipment and stock solutions are described in the following sections. Specific equipment used to conduct some of the techniques performed for this project, are stated in the corresponding section. All water used is type III ultrapure purified water unless otherwise stated. Restriction endonucleases were purchased from Promega® or Sigma-Aldrich unless otherwise stated.

2.1.1 General Equipment

Autoclaves: Prioclave PS/MVA/C60 and PS/QVA/EH150

Bench-Top microbiological Incubator: Genlab MINI/100/CLAD

C25 Incubator Shaker: New Brunswick Scientific

Centrifuges: Eppendorf 5417C, 5417R and 5804R. SORVALL® RC 5Cplus centrifuge

Concentrator: Eppendorf 5301

Cryostat CM1850: Leica

Ice Maker: Porkka KF 165

Mini- Plus horizontal Gel Electrophoresis: Jencons

R100 rotatest shaker: Luckham

Nanodrop® 1000 spectrophotometer: Thermo Scientific

Thermal cyclers: Eppendorf Mastercycler gradient and Mastercycler personal

Upright -80C Freezer uLT2586-9W ultima II Series: Revco

Dishwasher: Miele G7883CD

3UV^{TM} Transilluminator GelDoc-It Imaging System: UVP

Dri-Block ® DB-2D heat block: Techne

Elix and Milli-Q® water purification System: Millipore

2.1.2 Stock solutions

Luria-Bertani Broth (LB)

1% Bacto-tryptone

0.5% yeast extract

0.17M NaCl

pH 7.5

LB-Agar

98.5% LB

1.5% Micro Agar

Phosphate-Buffered Saline (PBS)

10 mM Na_2HPO_4

2.7 mM KCl

137 mM NaCl

2 mM KH_2PO_4

pH 7.4

50x TAE

2M Tris base

1M Glacial acetic acid

50mM EDTA pH 8.0

2.1.3 Safety

All procedures were carried out according to UCL safety regulations.

2.1.4 Primers

Primers used for plasmid construction, quick change site-directed mutagenesis and sequencing are listed in Table 2.1

Table 2.1. Summary of the primers used in this study. Primers containing a SalI restriction enzyme sites are marked in red. Primers containing SacI overhangs are marked in green. Primers where mutations were introduced are underlined.

Oligo	Primer Sequence (5' to 3')	Location	Length (bp)	Tm (°C)
1	TAAGCGTCGACAGATCTCAATGAAGTTTGCATAACAA	*Atoh1* Mouse AB	37	60.1
2	ATTCGTGTCGACGCTAGCCCGGGCGAATG	*Atoh1* Mouse AB	29	59.8
3	TAGAAGTCGACGCAGCGCATTTCCATGTTGAG	*Atoh1* Chick AB	32	61.2
4	ATTCGTGTCGACCATGGGAGCACGCACACG	*Atoh1* Chick AB	30	60.8
5	TAAGCAGTCGACTGTCCTCTCGCCCGCCCTG	*Atoh1* Chick C	31	66.1
6	ATTCGTGTCGACGGTTACAGTGTCGGTGAGCTGC	*Atoh1* Chick C	34	65.8
7	GCGGAGCAAATCGCACCCACTTAC	*Atoh1* Chick C	24	66.1
8	CGTTGGCATGGGCGGTTCTAAGC	*Atoh1* Chick C	23	66
9	TCGACCAGCTGTACGACAGCTGCATCTCAGCTGG	Non-coding	34	79
10	TCGACCAGCTGAGATGCAGCTGTCGTACAGCTGG	Non-coding	34	79
11	TCGAC**ATT**CTGTACGA**ATT**CTGCATCT**ATT**CTGG	Non-coding	34	71.6
12	TCGACCAG**AAT**AGATGCAG**AAT**TCGTACA**GAAT**G	Non-coding	34	71.6
13	TCGACTAGAGGGTATATAATGGAAGCTCGACTTCCGGTCGAC GAGCT	Minimal promoter	47	82.4
14	CGTCGACCGGAAGTCGAGCTTCCATTATATACCCTCTAG	Minimal promoter	39	78.8
15	ATTCGTGTCGACGGAAGTCGAGCTTCCATTATATACCCT	Non-coding	39	76.7
16	TCCCGCGCCCAACTTGGGACAGCGACGC	Non-coding	28	78.7
17	GCGTCGCTGTCCCAAGTTGGGCGCGGGA	Non-coding	28	78.7
18	CGCTTTAAAGAAATGCCTCAAAAAAAGATAAAAAATGGCACA AAGCAAAGC	Non-coding	51	76.4
19	GCTTTGCTTTGTGCCATTTTTTATCTTTTTTTGAGGCATTTCTTT AAAGCG	Non-coding	51	76.4
20	ACAATTGCATTCATTTTATGTTTCAGGT	*Atoh1* Mouse AB	28	60.5
21	ATATGGGGAATGAGCGCTCCGA	*Atoh1* Chick AB	22	64.2
22	TTCTTCTGCGCCTTAGTC	Minimal promoter	18	53.8
23	CAACTCTGCGGTGCAAGCTAAG	Non-coding	22	64.5
24	TGCGTATGAAATGATGGTAAAT	Non-coding	22	54.7
25	ATCTATGACATCACCAACGTCCTT	E2F1 coding sequence	24	62
26	TCCGAAGAGTCCACGGCTTG	E2F1 coding sequence	20	62.5
27	AACGGGAAGCCCATCACC	GAPDH coding sequence	18	58.4
28	CAGCCTTGGCAGCACCAG	GAPDH coding sequence	18	60.8

2.2 Methods

2.2.1 DNA purification

Different procedures were followed according to the amount and type of genetic material to be prepared.

2.2.1.1 Genomic DNA preparation from animal tissue

Brain tissue from chicken was cut into small pieces and placed in a 1.5ml eppendorf tube. 20µl of proteinase K was added to the tissue, homogenised by vortexing and incubated at 56 ^{o}C until the tissue was completely lysed. The mixture was then vortexed for 15s and 200µl of Buffer AL from the QIAGEN DNeasy Blood and Tissue Kit was added. The sample was mixed again by vortexing and 200µl of 100% ethanol was added to the mixture. The tissue mixture was then transferred into a DNeasy Mini spin column with a collection tube and was centrifuged at 6,000 x g for 1 min. The flow-through in the collection tubes was discarded and the DNeasy Mini spin column was placed in a new collection tube. 500µl of Buffer AW1 were added onto the column and centrifugation was conducted for 1min at 6,000 x g. The flow-through was again discarded and the DNeasy Mini spin column was placed onto a new collection tube. 500µl of Buffer AW2 was added and centrifugation was conducted for 3min at 20,000 x g in order to dry the DNeasy membrane in the column. The flow-through was discarded and the column was dried at 55 ^{o}C in a hot block for 2min. The DNeasy Mini spin column was placed in a clean 1.5 eppendorf tube and 200µl of Buffer AE was added in the centre of the column. The sample was centrifuged for 1min at 6,000 x g to collect the genomic DNA.

2.2.1.2 Small scale plasmid DNA purification from transformed E. Coli

Approximately 1ml of an 8h or overnight bacterial starter culture was harvested and centrifuged at 6000 x g for 15 min at 4 ^{o}C. The supernatant containing the growth medium was discarded and the bacterial pellet was re-suspended in 250µl of Buffer P1 according to the QIAGEN plasmid purification protocol. After a complete re-suspension of the bacterial pellet by vortexing or pipetting, 250µl of Buffer P2 was added and vigorously mixed by inverting the tube 4-6 times. The mixture was then incubated at room temperature for 5 min. 350µl of chilled N3 buffer were then added and mixed by vigorously inverting the tube 4-6 times and incubated on ice for 5 min. The bacterial mixture was then centrifuged at 13000 rpm for 10 min. The supernatant containing the plasmid DNA was collected and placed in QIAprep spin column and centrifuged for 1 min. The flow-through was discarded and the spin column where the DNA is retained was washed by adding 500µl of Buffer PB and centrifuged for 1 min. The QIAprep spin column was then washed with 750µl of Buffer PE and centrifuged for 1 min. The flow-

through was again discarded and the column was spun for an additional minute to remove any residual trace of Buffer PE. The QIAprep column was then placed in a fresh 1.5ml eppendorf tube and incubated at 55 ^{o}C for 2 min in order to remove any traces of ethanol contained in the Buffer PE. 50µl of Nuclease-free water was then added to the centre of the QIAprep column and centrifuged for 1min. After centrifugation, the QIAprep column was discarded and the flow-through containing the bacterial DNA was collected and stored at -20 ^{o}C.

2.2.1.3 Medium scale plasmid DNA purification from transformed E. Coli

Approximately 50ml of the 8h or overnight bacterial starter culture was harvested and centrifuged at 6000 x g for 15 min at 4 ^{o}C. After removing the supernatant, the pellet was re-suspended in 4ml of Buffer P1 supplied by the Plasmid MIDI Kit from QIAGEN. The complete re-suspension of the bacterial pellet was carried out before adding 4ml of Buffer P2. The tube was vigorously inverted 4-6 times, sealed and kept at room temperature for 5 min. After this incubation, 4ml of chilled Buffer P3 was added to the mixture and mixed by inverting the tube 4-6 times and placed on ice for 10 min. The mixture was then centrifuged at 13,000 rpm for 30 min at 4 ^{o}C in a SORVALL® RC 5Cplus centrifuge. The supernatant was then filtered through a membrane cloth in order to remove any trace of lysed bacterial components. The filtered mixture was loaded onto a QIAGEN-tip column which was previously equilibrated with 4ml of QBT Buffer. After leaving the filtered mixture in the resin of the column to be filtered by gravity flow, column was washed twice with 10ml of Buffer QC. The QIAGEN-tip columns were transferred to a new tube and 5ml of Buffer QF was added in order to elute the DNA. The DNA was then precipitated by adding 3.5ml of isopropanol and the tube was sealed with parafilm. The tube was then centrifuged at 15,000 x g for 30 min at 4 ^{o}C. The supernatant was carefully removed without disturbing the DNA pellet. The pellet was then washed with 2ml of 70% ethanol and centrifuged at 15,000 x g for 10 min at room temperature. After centrifugation, ethanol was removed and the pellet was air-dried for 10 min. The DNA pellet was then re-dissolved with 200µl of TE buffer, pH 8 and the tube was labelled accordingly.

2.2.1.4 DNA clean up

2.2.1.4.1 From PCR product

When using DNA fragments from PCR products, the QIAquick® PCR purification Kit from QIAGEN was used. To the final volume of the PCR mixture, 5 volumes of Buffer PB was added. The mixture was then placed in a QIAquick® spin column and centrifuged for 1 min. The flow-through was discarded and the column was washed with 750µl of Buffer PE and centrifuged for 1 min. Flow-through was discarded again and column was dried in a heating block for 2 min at 55 ^{o}C. The column was then placed in a clean 1.5ml eppendorf tube and the DNA retained in the column was eluted by adding 50µl of nuclease free water in the center of the column before centrifuging for 1min. Purified DNA was quantified by a Nanodrop or analysed on an agarose gel.

2.2.1.4.2 From Agarose Gel

DNA bands were excised from the gel with a clean sharp scalpel. The gel band was weighed in a 1.5 ml eppendorf tube and 3 volumes of Buffer QG were added following the MiniElute ® Gel Extraction Kit protocol from QIAGEN. The mixture was incubated at 50 ^{o}C for 10 min in order to completely dissolve the agarose gel. Then 1 volume of isopropanol was added to the sample and mixed by pipetting. The mixture was then placed in a MiniElute column for DNA fragments no bigger than 4 kb or in a QIAquick spin column for DNA samples up to 10 kb and centrifuged for 1 min. The flow-through was discarded and 500µl of Buffer QG was added to the column and centrifuged for 1 min. The flow-through was discarded again and 750µl of Buffer PE was added to the column and centrifuged for 1 min. The flow-through was discarded and column was placed in a heating block for 2 min at 55 ^{o}C. The column was then placed in a clean 1.5ml eppendorf tube and 10-30µl of nuclease free water was added to the center of the column before centrifuging for 1 min. The purified DNA was quantified by a Nanodrop or analysed on an agarose gel.

2.2.1.5 Quantification of prepared DNA material

DNA material was measured using a Nanodrop 1000 spectrophotometer. Typically, 2µl of water was used to obtain the baseline reading (blank) and then between 1 to 2µl of DNA were measured. The intensity of the light transmitted through the sample is recorded. The sample and the bank measurements were used to calculate sample

absorbance at a given wavelength. The concentration was then given by the Nanodrop based on Beer-Lambert equation:

$$c = (A \times e) / b$$

where **A** is the absorbance represented in absorbance units, **e** is the wavelength-dependent extinction coefficient in ng-cm/µl and **b** is the path length in cm.

2.2.2 Plasmid construction

Plasmids generated for this project were made by either TA cloning or restriction digest.

2.2.2.1 TA cloning

The pDrive vector from QIAGEN (Figure 2.1) or pGEM® T Easy Vector System from Promega (Figure 2.2) were used to insert PCR products. These are linearized plasmids containing either U or T-overhangs respectively at their 3' terminal ends which are capable of ligating with the A-overhangs produced at the end of PCR products generated by certain DNA polymerases.

Picture removed for copyright purposes

Figure 2.1: pDrive vector. Schematic representation of the pDrive cloning vector. Purchased from QIAGEN, the pDrive vector was used for the cloning of PCR products that has a single A overhang at each 3' end.

Picture removed for copyright purposes

Figure 2.2: pGEM®-T Easy Vector. Schematic representation of the pGEM®-T Easy PCR cloning vector with T-overhangs at the multiple cloning site.

Ligation of PCR products

Ligation using PCR products was performed according to the manufacturer's protocol with the following components:

- 1µl of cloning vector (pDrive or pGEM®T easy)
- 2µl of (5X) Ligation buffer
- 1-4µl of PCR product
- 1µl T4 ligase
- up to 10µl of water

The reaction was mixed by pipetting and incubated for 1h at room temperature. Bacterial transformation was then performed as described on section 2.2.2.3.

2.2.2.2 Restriction digest cloning

The general procedure for producing constructs generated by restriction digestion is described in the following sections.

Restriction endonuclease digest

DNA material was digested as follows:

- 1µg DNA material
- 1µl of 10x enzyme buffer
- 1unit of enzyme
- up to 10µl of water

The digestion mix was incubated for 1h at the optimal activity temperature for the enzyme, usually 37^{o}C.

DNA Polymerase I Large (Klenow) method to generate blunt ends

Depending on the cloning strategy used to generate new constructs, in some cases it was necessary to create blunt ends. After conducting restriction digest, the reaction was incubated for 10min at 65^{o}C in order to inactivate the enzyme. 2mM of deoxynucleotide triphosphates (dNTPs) from Promega were added to the reaction with 1 unit of DNA Polymerase I Large (Klenow). The reaction mix was incubated at room temperature for 30 min. After this, the reaction mix was kept for 10 min at 75 ^{o}C in order to inactivate the Klenow enzyme. The reaction was then subjected to agarose gel electrophoresis and the DNA band was purified as described in section 2.2.1.4.2.

Dephosphorylation of the vector

In order to prevent self-ligation of the digested plasmid dephosphorylation was conducted to remove the 5' phosphate group prior to ligation. By doing this, ligation will favour the incorporation of an insert as a result of the formation of a phosphodiester bond between the 3'-hydroxyl group in the plasmid and the 5'-phosphate group in the insert. Calf Intestinal Alkaline Phosphatase (CIAP) from Promega® was used in the following reaction:

- 1-5µg of DNA

- 3µl of CIAP (0.03units per 1µg of DNA)
- 3µl of 10x reaction buffer
- up to 30µl of water

Reaction was incubated for 1h at 55 ^{o}C.

Ligation

Typically, a 1:3 molar ratio of vector: insert DNA was used when cloning an insert into a vector. The following equation was used to convert molar ratio to mass ratio for kb of DNA:

$$\frac{\text{ng of vector x kb size of insert}}{\text{kb size of vector}} \times \text{molar ratio of } \frac{\text{insert}}{\text{vector}} = \text{ng of insert}$$

The following reaction was then set up:

- 1µl of ligase 10x buffer
- 1µl (1unit) of T4 DNA ligase from Promega
- 1-5µl vector
- 1-5µl insert
- up to 10µl water

The reaction was incubated overnight at 4 ^{o}C in order to improve ligation efficiency.

2.2.2.3 Bacterial Transformation

Alpha-selected chemically competent cells from Bioline were used to transform DNA material. Cells were removed from the -80 ^{o}C freezer and kept on ice. 50µl of competent cells and 5µl of DNA material were used per reaction in pre-chilled 17 x 100mm polypropylene tubes, (Falcon catalogue no. 2059). The cells were gently mixed and incubated on ice for 30 min. The cells were then incubated in a 42 ^{o}C in a water bath for 30s and then for 2min on ice. 500µl of pre-warmed SOC media was added to the reaction mix. The cells were incubated in a shaker at ~200rpm for 60 min at 37 ^{o}C. The culture mix was then plated by spreading the transformation mixture on LB agar plates containing the appropriate antibiotic. The plates were left at room temperature for 2min and then incubated overnight at 37 ^{o}C.

2.2.2.4 Bacterial culture

Single colonies were picked from transformed plates and inoculated in a 5ml culture tube containing LB medium with 5µl of a 1000x stock of the appropriate selective antibiotic. The culture was kept in a shaking incubator at 37 ^{o}C for a minimum of 8h to overnight with vigorous shaking (225rpm). After 8h, the bacterial cultures typically reach the exponential growth phase and can be used to prepare small scale plasmid DNA as described in section 2.2.1.2.

For the preparation of medium scale plasmid DNA, 1/500 to 1/1000 of the starter culture was transferred to 50 to 100ml selective LB medium in a flask and grown at 37 ^{o}C for 12-16h with vigorous shaking.

2.2.3 Screening of bacterial recombinants

Recombinant clones were screened using one or both of the following methods.

2.2.3.1 Blue-white selection of transformed colonies

Blue-white colour selection was used when the destination vector contained a *lacZα* gene, in the multiple cloning site (MCS). The *lacZα* peptide which encodes the N-terminal amino acid sequence of β-galactosidase, will function in *trans* to complement β-galactosidase activity in the *E. coli* host strain. The *E.coli* strain used to transform the ligated products carries a *lacZ* deletion mutant (*lacZΔM15*) but also an F' episome which provides the complementary element to the *lacZα* in the vector to produce a functional *lacZ* gene product, the β-galactosidase.

If the vector incorporates an insert in the MCS, the *lacZα* is disrupted and therefore it will fail to produce β-galactosidase. In contrast, if the vector fails to incorporate the insert, a functional β-galactosidase is produced. This will be visualized if using plates containing X-gal, a colourless analog of lactose that may be cleaved by the β-galactosidase to form 5-bromo-4-chloro-indoxyl, producing a blue colour. Isopropyl β-D-1 thiogalactopyranoside (IPTG) was also used on the bacterial plates in order to enhance the blue phenotype of the indicator by activating the promoter.
Using this method, colonies that incorporated the insert (white colonies) can be discriminated from colonies that failed to introduce the insert (blue colonies).

2.2.3.2 By Restriction digest

Restriction digest was conducted in order to verify the cloning of the desired insert in the destination vector as well as its orientation. The reaction was performed as described in section 2.2.2.2.

2.2.4 Sequencing of plasmid constructs

Plasmids generated for this project were sequenced by Source Bioscience. DNA sequences and chromatograms were analysed and aligned against the appropriate DNA regions in order to verify the presence of the desired region.

2.2.5 Reverse Transcriptase Polymerase Chain Reaction (RT-PCR)

2.2.5.1 RT-PCR primer oligonucleotide design

Primers used for RT-PCR were designed to be as sequence specific as possible, maintaining the optimal melting temperatures to avoid non-specific amplification. The optimal requirements for a successful RT- PCR are described below:

- Primer length between 20-35 nucleotides
- G/C content between 40-60%
- Salt-adjusted melting temperature (Tm) > 60 ^{o}C.
- Multiple runs of 3 or more G or C at the 3' end
- The use of complementarity of two or three bases at the ends of primer pairs was avoid to reduce primer–dimer formation
- Mismatches between the 3' end of the primer and the target-template sequence were avoided.
- Complementary sequences within a primer sequence and between the primer pair were avoid.

All these parameters were checked using the web based software Oligocalc (http://biotools.nubic.northwestern.edu/OligoCalc.html). In addition the primers were designed to cross exon boundaries to span an intron. Therefore any product amplified from genomic DNA (gDNA) will be much larger than the product amplified from the cDNA since the intron between the two exons will be spanned. The primers were also

designed to generate an amplicon large enough to be size-separated by agarose gel electrophoresis in order to distinguish it from any gDNA amplification.

2.2.5.2 Purification of RNA from animal cells

The RNeasy Mini kit from QIAGEN was used to purify RNA from UB/OC2 cells. UB/OC2 cells were grown in T75cm^2 flasks or 6 well plates until 80% confluent. The cells were then disrupted with Buffer RLT according to the manufacturer's instructions, collected and homogenized in a QIAshedder spin column at full speed for 2 min. To the homogenized lysate, 1 volume of 70% ethanol was added and mixed by pipetting. The mixture was then transferred to an RNeasy spin column and centrifuged for 15s at 10000 rpm. The flow-through was discarded and the column was washed with buffer RW1 and spun for another 15s at 10000 rpm. Two more additional washes with buffer RPE were conducted in order to remove any traces of ethanol from the column. Finally, the spin column was placed in a new microcentrifuge tube and was eluted with 30-50µl of RNase-free water.

2.2.5.3 Reverse transcription procedure

RNA was reverse transcribed into cDNA using the Omniscript Reverse Transcriptase kit from QIAGEN. The master mix reaction was prepared according to the manufacturer's instructions with the following reagents:

- 1x Buffer RT
- 0.5M of each dNTP
- 1uM Oli-dT primer
- 10 units of RNase inhibitor
- 4 units of Omnistript Reverse Transcriptase
- up to 20µl RNA
- water up to 20µl

The reaction was incubated for 1h at 37 ^{o}C.

2.2.5.4 PCR design and parameters

Typically PCR reactions were performed as follows:

- 10µl of 5x GoTaq® Flexi buffer
- 8µl (4mM) of $MgCl_2$
- 1µl dNTPs
- 1µl sense primer (10µM)
- 1µl antisense primer (10µM)
- 1µl of cDNA from UB/OC2 cells (approximately 500ng)
- 0.25µl GoTaq® polymerase
- 27.75µl of water

PCR parameters were set as follows:

1. Initial denaturation: 95 °C for 2 min
2. Denaturation: 95 °C for 1 min
3. Annealing: 62-65 °C for 30 sec
4. Extension: 72 °C for 1 min

Steps 2-4 were repeated for 30 cycles

5. Final extension 72 °C for 5 min
6. Hold 4 °C

2.2.6 Cell culture

Materials and procedures for cell culture experiments are described in the following sections.

2.2.6.1 Equipment for cell culture

Centrifuge: ALC PK 110

Galaxy 170S CO_2 incubators: New Brunswick

Hera safe KS15 fume hood: Kendro

Eclipse TS100 microscope: Nikon

2.2.6.2 Culture of UB/OC2 cells

The UB/OC2 cell line, derived from E13 Immortomouse organ of Corti (Rivolta and Holley 2002), obtained from University of Bristol, was cultured in Minimum Essential Medium (MEM-gibco®) supplemented with 10% Fetal Bovine Serum (heat inactivated; EU approved) and 50U/ml of gamma-interferon and incubated at 33°C and 5% CO_2.

Cells were trypsinized when 80% confluent with 10% Trypsin in Hanks' Balance Salts solution (supplemented with $CaCl_2$ and $MgCl_2$) for 5 min at room temperature. To the detached cells, an equal volume of growth medium was added before centrifuging at 1000g for 3min. Supernatant was removed and the cell pellet was re-suspended in fresh medium. Cells were divided between new culture flask at the desired seeding density, typically at 1:5 ratio.

2.2.6.3 Preparation of nuclear extracts

UB/OC-2 cells were grown in T175 flasks until 90% confluent. Flasks were placed on ice and the cells were washed with 15ml of PBS (calcium magnesium free). After removing the PBS, 3ml of cold cytoplasmic lysis buffer (section 2.2.8.2) was added to each flask and incubated on ice for 5 min. The cells were then collected using a cell scraper and transferred to eppendorf tubes. While keeping eppendorf tubes on ice, 0.6% of NP-40 was added to the cell-lysis buffer mixture and vortexed for a few seconds. The cells were subjected to centrifugation at 4 °C for 30 seconds. The supernatant containing the cytoplasmic proteins was removed from nuclear pellet before adding a 1:1 volume of nuclear lysis buffer (2.2.8.2). The amount of nuclear lysis buffer differed depending on the size of the pellet but was typically 40-50µl. The tubes were then flicked gently to dislodge the pellet and to ensure that the pellet was surrounded by the nuclear lysis buffer. Proteins were extracted from the pellets by conducting three freeze-thaw cycles using an ethanol-dry ice bath and a 37 °C water bath. After this, samples were subject to centrifugation for 10min at 4 °C. The supernatants containing nuclear proteins were pooled in a single eppendorf tube and protein concentration was estimated using the following formula:

$$\text{Concentration } (\mu g/\mu l) = (1.55 \times A_{280}) - (0.76 \times A_{260})$$

The nuclear extracts were then aliquoted into pre-chilled eppendorfs, snap frozen in liquid nitrogen and stored at -80 ^{o}C.

2.2.7 *In vitro* transcription and translation procedure

The TNT Quick-coupled Transcription/Translation System from Promega was used in order to make *in vitro* translated protein from plasmid DNA. Components supplied in the TNT System were thawed out at room temperature and then placed on ice. For the reaction, 40µl of the TNT Quick Master Mix was combined with 1mM of Methionine, 1µg of the plasmid DNA and up to 50µl of Nuclease-Free water according the manufacturer's protocol. After mixing, the reaction was incubated at 30 ^{o}C for 90 min. The translated protein was then used in EMSA experiments.

2.2.7.1 DP1_pcDNA3 constructs generated to make *in vitro* translated protein

The DP1_pcDNA3 contains the human DP1 cloned into the expression construct pcDNA3 described in Figure 2.5 under the control of the T7 promoter. This construct was produced as follows: the pCMV-Neo-Bam1 (kindly provided by Dr Tony Kouzarides, University of Cambridge, UK) containing the human DP1 was digested with EcoRI in order to isolate the DP1 fragment (accession number L23959). The fragment was inserted into pcDNA3 by restriction digest cloning as described in section 2.2.2.2.

2.2.8 The electrophoretic mobility shift assay (EMSA)

2.2.8.1 Equipment for EMSA assays

Protean IIxI cell for PAGE (20cm glass plates, 3mm spacers): Bio-Rad Protean II

Gel Dryer: Scie-Plas (GD4534)

Gel Master Dyer Vacuum System (1428): Rietschle Thomas

Mini 900 Ratemeter: Thermo

Micro G-25 spin columns (sc 202390): Santa Cruz

2.2.8.2 Solutions for EMSA assays

Cytoplasmic lysis buffer

10mM HEPES pH 7.6
1mM EDTA
0.1mM EGTA
10mM KCl
1mM DTT
1mM Na pyrophosphate
1mg/ml vanidate
ddH_2O

10x Maniatis Medium Salt Buffer

0.5M NaCl
0.1M Tris-HCl pH7.5
0.1M MgCl 2
0.01M DTT

2x Parker buffer

16% Ficoll
40mM HEPES pH7.9
100mM KCl
2mM EDTA
1mM DTT
4mM MgCl2

Nuclear lysis buffer

20mM HEPES pH7.6
0.2mM EDTA
0.1mM EGTA
25% Glycerol
0.42M NaCl2
1mM DTT
1mM Na pyrophosphate
1mg/ml SP1
1mM vanidate
ddH2O

10x TBE

0.89M Tris-borate
20mM EDTA pH 8.0

3µg/µl Poly(dI-dC)

10Units poly (deoxyinosinic-deoxycytidylic) acid sodium salt (15Units/mg)
222.2µl H2O

2.2.8.3 EMSA Probe design

Double stranded oligonucleotides were designed and synthetized by Eurofins MWG Operon (HPSF purified). Oligonucleotides were re-suspended in MilliQ water to a stock concentration of 1µg/µl.

2.2.8.4 Annealing EMSA probes

10µg of sense and antisense oligonucleotides were combined in 1x Maniatis Medium Salt buffer to a final volume of 22µl. The double stranded oligonucleotide mixture was incubated at 95^{o}C on a heating block for 10min. The reactions were allowed to cool down overnight to room temperature. To verify that sense-antisense oligonucleotides were annealed, 1µl of each double stranded oligonucleotide was run on a 3% agarose

gel alongside the single stranded oligonucleotides. The annealed probes were then diluted to 25ng/µl and stored at -20 ^{o}C.

2.2.8.5 EMSA probe labelling

50ng of the double stranded oligonucleotides (EMSA probes) were labelled with ɣ32 P-ATP (0.37MBq/µl, total of 1.11MBq) in the following reaction:

- 50ng of probe
- 2µl 10x T4 kinase buffer
- 3µl of ɣ32 P ATP
- 1µl T4 kinase enzyme (5-10U/µl)
- to 20µl of water

The reaction mix was incubated for 30 min at 37 ^{o}C in a heating block. The reaction was then diluted to 50µl, loaded onto a micro G-25 spin column and spun at 1500rpm for 2 min to separate the labelled probe from unincorporated nucleotides. The labelled probes were stored at -20 ^{o}C.

2.2.8.6 EMSA binding reaction

Each binding reaction contained:

- 10µl of 2x Parker buffer
- 1.5µg of poly dI/ dC
- 10µg of nuclear extract protein
- 0 to 500ng non-labelled competitor oligonucleotide
- water to 20µl

The binding reaction was incubated at room temperature for 10min.

For competition assays, an excess of 500ng of cold competitor was added to the reaction and incubated for 20min to 2h at room temperature. Following incubation with the competitor, 2µl (50ng) of labelled probe was added to the reaction and left for 30min at room temperature. For supershift assays, 1µl of antibody was added to the binding reaction either 1h before or 30min after the probe was added. Antibodies were

purchased from Santa Cruz Biotechnology, Inc: rabbit polyclonal anti-E2F1 (C-20 SC-193X) and rabbit polyclonal anti-SP1 antibody (H-225X).

The addition of glycerol to the gel produced, in some cases, an improvement in DNA-protein complexes (Sidorova et al. 2010). For EMSA experiments with E2F probes, a number of publications were found where glycerol was added to the poly-acrylamide gel to describe the binding affinities of E2F to putative binding sites (Pasteau Stephane 1995) (Tanaka et al. 2002) (Kherrouche et al. 2006) (Fontemaggi et al. 2009). Therefore, 10% glycerol was added to the poly-acrylamide gel in EMSAs performed to detect E2F-DNA binding. Other modifications were also introduced in the EMSA protocol such as the duration of the incubation between the nuclear protein extracts and the cold competitor in order to optimise the particular binding reaction.

2.2.8.7 EMSA poly-acrylamide gel electrophoresis

A 4% 0.25x TBE acrylamide gel (29:1) was made with the following mixture:

- 10ml of 40% acrylamide (29:1 bis ratio)
- 2.5ml of 10x TBE
- 700µl of 10% ammonium persulphate
- 37µl TEMED
- 10% glycerol
- water to 100ml

The mixture was poured to a 20cm Bio-Rad gel cast and allowed to set for 45min. The gel was then pre-run in a cold cabinet for 30min at 4°C in 0.25x cold TBE at 200 volts. Before loading samples, the wells were rinsed with TBE buffer to remove any non-polymerised acrylamide inside the wells. The samples were then loaded and the gel was subject to electrophoresis for 2.5-3 hours.

2.2.8.8 Gel drying and autoradiography

The EMSA gel was carefully removed from the glass plates, placed onto Whatman 3mm paper, covered with cling film and dried in a vacuum gel dryer (Scie-Plas) at 80 ^{o}C for 1-2 hours until dry. The dried gel was then placed into a X-ray film cassette and exposed to a X-ray film at -80 ^{o}C for between 10h to 5 days. Following exposure, films

were developed using Kodak film developing reagents according to the manufacturer's instructions.

2.2.9 Reporter Gene Assay

Reporter Gene Assays were used in order to quantify enhancer response. Procedure and material used are described in the following sections.

2.2.9.1 Equipment for Reporter Gene Assays

Turner TD-20e Luminometer

2.2.9.2 Stock solutions for Reporter Gene Assays

10x HEPES-Buffered Saline (HBS)

8.18% NaCl (w/v)

5.94% HEPES (w/v)

0.2% Na2HPO4 (w/v)

Solution was sterilised through a 0.2µN filter, diluted to 2xHBS and pH adjusted to 7.12.

1x Phosphate Buffered Saline (PBS)

137mM NaCl

2.7mM KCl

10mM Na_2HPO_4

1.8mM KH_2PO_4

pH adjusted to 7.4

2.2.9.3 Constructs for Reporter Gene Assays

A description of commercial plasmids and recombinant vectors generated for reporter gene assays are described in the following sections.

Commercial plasmids

pGL4.23[*luc2*/minP]

The pGL4.23[*luc2*/minP] vector (Promega®) encodes the luciferase reporter gene *luc2* (*Photinus pyralis*), a minimal promoter and contains a multiple cloning site to introduce the desired regulatory element. The pGL4.23[*luc2*/minP] vector also contains an ampicillin resistance gene to allow for selection in *E. coli*. Schematic representation of the pGL4.23[*luc2*/minP] vector map is represented in Figure 2.3.

Picture removed for copyright purposes

Figure 2.3: pGL4.23[*luc2*/minP]. Vector map of the pGL4.23[*luc2*/minP] luciferase vector used to insert the *Atoh1* enhancer elements. The pGL4.23[*luc2*/minP] vector contains a synthetic luciferase gene driven by a minimal promoter.

pSI Mammalian expression vector

The pSI vector (Promega®) is a mammalian expression vector that was used to generate the *Atoh1* expression construct described below and also to equilibrate the amount of DNA in some of the transfection experiments. The pSI vector was designed to produce constitutive expression of the cloned insert in mammalian cell lines. The vector contains the simian virus 40 (SV40) enhancer and an early promoter region to control the expression of the cloned insert. A schematic map of the pSI expression vector is represented in Figure 2.4.

Picture removed for copyright purposes

Figure 2.4. pSI Mammalian expression vector. Schematic representation of the pSI vector containing a multiple cloning site, a SV40 enhancer/early promoter region and an Ampicillin resistance gene to allow for selection in *E. coli*

pcDNA3 Mammalian expression vector

The pcDNA3 vector (Invitrogen^{TM}) is a mammalian expression vector designed for high level stable and transient expression in mammalian cell lines. The pcDNA3 is controlled by a human cytomegalovirus immediate-early (CMV) and T7 promoter and contains a multiple cloning site, neomycin and ampicillin resistance genes. The pcDNA3 vector was used to equilibrate the amount of DNA used in some of the transfection experiments.

Picture removed for copyright purposes

Figure 2.5. pcDNA3 expression construct. Schematic representation of the pcDNA3 expression vector. The pcDNA3 is controlled by CMV and T7 promoter and contains a multiple cloning site to facilitate cloning strategy.

Novel constructs generated for reporter gene assays

MouseAB_downstreamluciferase_pGL4.23 (MouseAB_down_luc)

The MouseAB_down_luc plasmid was generated by amplifying mouse genomic DNA (Promega) with the primers 1 and 2 listed in Table 2.1. The amplified PCR product was digested with SalI to generate a 1402 bp fragment corresponding to the mouse *Atoh1* AB enhancer and inserted into the SalI in the pGL4.23[luc2/minP] vector (Figure 2.3) as described in 2.2.2.2. Sequencing with the primer 20 (Table 2.1) confirmed the presence and orientation of the mouse *Atoh1* enhancer cloned downstream of the luciferase sequence.

ChickAB_downstreamluc_pGL4.23 (ChickAB_down_luc)

The ChickAB_down_luc was generated by amplifying chick genomic DNA as described in 2.2.1.1 with primers 3 and 4 (Table 2.1). The amplified product was digested with SalI to generate a linearized fragment of 957 bp which was cloned into the SalI site downstream of the luciferase sequence in the pGL4.23[luc2/minP] vector (Figure 2.3). Sequencing results confirmed the presence of the chick *Atoh1* enhancer downstream of the luciferase sequence.

ChickC_downstreamluc_pGL4.23 (ChickC_down_luc)

The vector containing the putative enhancer C was generated by amplifying chicken genomic DNA using primers 5 and 6 (Table 2.1) and inserted into the pDrive cloning vector (Figure 2.1). The putative enhancer C fragment was then isolated from pDrive by restriction digest with BamHI/SalI and subcloned into the SalI/BamHI sites in the pGL4.23[luc2/minP] vector (Figure 2.3).

ChickABC_downstreamluc_pGL4.23 (ChickABC_down_luc)

The ChickABC_down_luc was also generated by amplifying chick genomic DNA as described in section 2.2.1.1 with primers 3 and 6 listed in Table 2.1. After PCR amplification of the enhancer fragment ABC (1905 bp), the fragment was cloned into the SalI site downstream of the luciferase sequence in the pGL4.23[luc2/minP] vector. The cloning and orientation of the Chick ABC fragment downstream of the luciferase sequence was confirmed by sequencing.

MouseAB_upstreamluc_pGL4.23 (MouseAB_up_luc)

The MouseAB_up_luc contains the Mouse *Atoh1* enhancer upstream of the minimal promoter of the basic pGL4.23[*luc2*/minP] luciferase vector (Figure 2.3). This construct was produced as follows: A J2XnGFP vector kindly provided by Professor Jane Johnson (University of Texas Southwestern Medical School, USA) containing the mouse *Atoh1* enhancer was digested with SacI and XbaI (1408 bp) in order to isolate the enhancer region. The resultant fragment was cloned into the pGL4.23[*luc2*/minP] luciferase vector previously digested with SacI and NheI. Sequencing results with a T7 primer confirmed the cloning and orientation of the mouse *Atoh1* enhancer upstream of the basic pGL4.23[*luc2*/minP] luciferase vector.

ChickAB_upstreamluc_pGL4.23 (ChickAB_up_luc)

The ChickAB_up_luc vector contains the Chick *Atoh1* enhancer upstream of the minimal promoter of the basic pGL4.23[*luc2*/minP] luciferase vector (Figure 2.3). This construct was generated by digesting the PE1-chick homology-AB, kindly provided by Professor Jane Johnson (University of Texas Southwestern Medical School, USA), with SalI and EcoRI in order to isolate the chick *Atoh1* enhancer (1015 bp). The enhancer fragment was then sub-cloned into the XhoI/EcoRV located upstream of the luciferase sequence in the basic pGL4.23[*luc2*/minP] luciferase vector after the 3' end was blunted using Klenowed enzyme (see section 2.2.2.2). Sequencing results with the primer 21 (Table 2.1) confirmed the presence and orientation of the Chick AB enhancer upstream of the minimal promoter in the pGL4.23[*luc2*/minP] vector.

ChickC_upstreamluc_pGL4.23 (ChickC_up_luc)

The ChickC_up_luc vector contains the putative enhancer C fragment upstream of the minimal promoter of the basic pGL4.23[luc2/minP] luciferase vector. Putative enhancer C was generated by amplifying chicken genomic DNA using primers 5 and 6 (Table 2.1). Amplified PCR product was digested with SalI to isolate putative enhancer C (383 bp) and cloned into the basic pGL4.23[luc2/minP] luciferase vector digested with XhoI. Diagnostic digest with SmaI/EcoRV and also with HaeII confirmed the insertion and orientation of the putative enhancer C upstream of the minimal promoter.

ChickABC_upstreamluc_pGL4.23 (ChickABC_up_luc)

The ChickABC_up_luc vector was generated by amplifying chick genomic DNA with primers 3 and 6 listed in Table 2.1. After PCR amplification, restriction digest was conducted with SalI to isolate the ABC fragment (1905 bp) and then cloned into the basic pGL4.23[luc2/minP] luciferase vector digested with XhoI. Diagnostic digest with BamHI and also with BamHI/Bgl II confirmed the insertion and orientation of the region ABC upstream of the minimal promoter.

***Atoh1*_pSI**

The *Atoh1*_pSI construct contains the mouse *Atoh1* coding putative enhancer cloned into the pSI mammalian expression vector (Figure 2.4). In order to generate this construct, the pBlueScript II SK (+) vector containing mouse *Atoh1* (kindly provided by Dr. Aida Costa, Institute of Molecular Medicine, Lisbon University, Portugal) was digested with EcoRI and NotI to produce a fragment containing the mouse *Atoh1* coding region. The resulting fragment was cloned into the multiple cloning site of pSI digested with EcoRI/NotI. A diagnostic digest with EcoRI/NotI confirmed the insertion of the mouse *Atoh1* coding region.

***Atoh1*_3xBS_pSI and *Atoh1*_3xmutBS_pSI**

Double stranded oligonucleotides containing three *Atoh1* binding sites (primers 9 and 10) and the mutant version (primers 11 and 12) containing three mutated *Atoh1* binding sites are listed in Table 2.1 (Sal I restriction enzyme site are marked in red. The *Atoh1* binding sites are underlined and mutations in the *Atoh1* binding sites are marked in bold). These oligonucleotides containing SalI overhangs were ligated into the pGL4.23[luc2/minP] luciferase vector previously digested with SalI. Therefore, the *Atoh1* binding sites were cloned downstream of the luciferase cDNA sequence in the pGL4.23[luc2/minP] vector.

2.2.9.4 UB/OC2 transient transfection by calcium phosphate

UB/OC2 cells were grown in T75 flasks, trypsinized and re-suspended in fresh medium as described in section 2.2.6.2. Cells were plated at $2x10^5$ cells per well in 6-well plates and incubated overnight at 33^oC.

Following overnight incubation, the cell culture media was changed to DMEM + 10% FCS. These were incubated at 37 ^{o}C for at least 1h before transfecting with the DNA material. The DNA precipitate to be transfected was prepared as follows:

- Tube A: Purified DNA mixture, 49.6µl of 2M $CaCl_2$, up to 400 µl of water
- Tube B: 400 µl of 2x HBS

The reaction in tube A was mixed by pipetting up and down and then the content of tube B was added to tube A in a drop-wise manner. The combined tube A and tube B solution was mixed and 200µl was added to each reaction well. Plates were then gently swirled to mix with media before incubating at 37 ^{o}C overnight. The following day, cells were subjected to a glycerol shock. The media and precipitate was removed from the cells and replaced by 2ml of DMEM containing 15% glycerol for 2min and 30s. The cells were then washed twice with 2ml of HBSS in order to remove any traces of glycerol. Then 2ml of MEM complete media was added to each well and the plates were incubated overnight at 33 ^{o}C.

2.2.9.5 Luciferase Assay System

Following overnight incubation, the Dual-Luciferase® kit (Promega) was used to assess the luciferase activity according to the manufacturer's protocol. This dual system offers the advantage of sequential assays of both Firefly luciferase (the experimental reporter gene) and the Renilla luciferase (an internal control reporter) within a single sample (Bruce A. Sherf 1996). Briefly, the cells were harvested 24h after the glycerol shock. The culture medium was removed and cells were washed twice in PBS. Following washes, 100µl of 1x Passive Lysis Buffer (PLB) was added to each well and the cells were scrapped and collected in a 1.5ml eppendorf tube. The lysed cells were then frozen at -20 ^{o}C for 15min and then thawed at room temperature for 10min. The lysed mix was then centrifuged for 1min and the supernatant was collected.

Prior to taking luciferase readings, the Luminometer was adjusted to the following settings:

- Delay = 5s
- Read for 30s

20µl of lysed mix was added to 50µl of LARII from the Dual Luciferase® Reporter Assay System for each sample and the Firefly Luciferase readings were recorded by the luminometer. Following this, 20µl of Stop&Glo was added to the reaction and the Renilla Firefly readings were collected.

2.2.9.6 Statistics

Student's paired *t*-tests were conducted to compare data sets obtained in the transfection assays to determine the statistical difference. Analysis was determined by the group average values, sample size and the standard error of the mean. A p-value < 0.05 was considered to be statistically significant.

2.2.10 Quick Change Site-Directed Mutagenesis

The QuikChange II Site-Directed Mutagenesis Kit (Agilent Technologies) was used in order to introduce point mutations in a vector. Oligonucleotides for this technique were designed using the primer design tool provided on the manufacturer's website (http://www.genomics.agilent.com/primerDesignProgram.jsp). Oligonucleotides were synthesized by Eurofins MWG Operon as DNA cloning oligonucleotides for being this, the most optimised method for this application. The oligonucleotides used for this method are shown as 16 to 19 in Table 2.15.4.2. Sample reaction for the Site-Directed Mutagenesis was:

- 5µl of 10x reaction buffer
- 5-50ng of dsDNA template (construct to be mutated)
- 125ng of oligonucleotide primer 1
- 125ng of oligonucleotide primer 2
- 1µl of dNTP mix
- ddH_2O to a final volume of 50µl

Then, 1µl of *PfuTurbo* DNA polymerase (2.5U/µl) was added.
Cycling parameters were set as follows:

- Segment 1 (1 cycle): 95°C for 30sec
- Segment 2 (18 cycles): 95°C for 30sec
  60°C for 1min
  68°C for 1min/kb of plasmid length

Following temperature cycling, the reaction was placed on ice for 2min. Then 1µl of DpnI (10 U/µl) was added to the amplification reaction and mixed by pipetting. The mixture was then centrifuged for 1min and incubated at 37^{o}C for 1h to digest the parental methylated DNA. Following incubation, 5µl of reaction mixture was transformed in 50µl of competent cell as described in section 2.2.2.3. except that NZY^{+} broth rather than LB-broth was used in the transformation. After overnight incubation at 37 ^{o}C, colonies were grown and DNA was purified as described in section 2.2.1.3. The DNA material was then sequenced with primers 23 and 24 (Table 2.1) in order to verify whether the mutations were successfully introduced.

2.2.11 Dissections of animal material

Both mammalian and avian specimens were used for this project. All procedures were approved by University College London and by the UK Home Office (Scientific Procedures Act 1986). Dissections were conducted as described in the following sections.

2.2.11.1 Mouse tissue

The mouse inner ear dissections for cryosections were conducted by NH. Mouse specimens were sacrificed followed by decapitation. Using a scissors and a pair of curved forceps, the skull was cut along the top of the head in order to separate the left and right ear. The tissue containing the cochlea on each side was cut and brain was removed. The tissue was then transferred to a 35mm dish containing M199 Hanks media (Gibco®). The tissue around the auditory bulla was gradually removed in order to access the auditory and vestibular system. The tissue was then transferred to another dish with fresh and sterile M199 Hanks media. The cochlear wall was removed and the organ of Corti separated from the modiolus. Once the organ of Corti was isolated, the stria vascularis was removed and the tissue transferred to glass-bottomed dishes (MatTek®) with culture medium and incubated at 37ºC under 5% CO_2.

The ex-vivo mouse cochlear explants dissections were conducted by CG. Cochleae were isolated from post-natal day 0 (P0) from C57BL/6 mice. After isolating the organ of Corti, both modiolus and stria vascularis were removed. The hook and apex regions were cut for culture purposes. The cochlear explants were cultured in glass-bottomed dishes (MatTek®) coated with CellTak (BD Biosciences) and sodium bicarbonate. The

explant cultures were incubated in DMEM F-12 medium supplemented with 1% FBS at 37ºC under 5% CO_2 atmosphere, during 18-20h, before any treatments had been applied.

2.2.11.2 Chick tissue

Fertilized White Leghorn chicken (*Gallus gallus*) eggs were obtained from Henry Stewart UK and incubated at 37.8^{o}C. Embryonic stages were listed as embryonic days (E) with E1 corresponding to 24h of incubation. Samples older than E5 were sacrificed by decapitation. When ear dissections were conducted, decapitated chicken heads were cut in half to separate left and right hemispheres and the brain and eyes removed before fixation. Typically, tissue was fixed in PFA for 2h unless otherwise stated. The samples were then rinsed twice in PBS. Following this, all superficial tissue and cartilage around the inner ear area was carefully removed using a pair of fine tweezers. The cartilage surrounding the sensory organs was also removed to maximize tissue exposure to immunolabeling reagents.

2.2.12 Tissue processing for cryo-sections

Fixed tissue was rinsed three times in PBS and then kept in serial dilutions of 10% followed by 20% sucrose in PBS at room temperature with rotation. Once specimens were sunk at the bottom of the tube, samples were transferred into a 30% sucrose solution and left overnight at 4^{o}C. The samples were then embedded in 1% low melting point agarose with 18% sucrose using 15x15x5mm cryo-moulds (VWR). Embryonic heads were orientated, usually with heads facing down (for chick specimens) and samples were kept at room temperature until the agarose was set. Samples blocks were then frozen in isopentene and stored at -80^{o}C. Before proceeding to cryo-sectioning, the specimens were left in the cryostat (Leica CM1850) for 1h to equilibrate. The moulds were then removed and the frozen blocks were attached to cryostat chucks using OCT embedding gel (VWR). Sections of 20µm thickness were then collected onto Superfrost® plus slides (VWR). Slides were dried at room temperature for 30 min and then stored at -80^{o}C until used.

2.2.13 Immunohistochemistry

2.2.13.1 Equipment for immunohistochemistry

LSM 510 META inverted laser scanning confocal microscope and laser module: Carl Zeiss

Dissecting microscopes: Leica MZ125 & MZ75

2.2.13.2 Reagents for immunohistochemistry

Blocking solution

0.8% Goat or horse serum (Invitrogen)

0.4% Triton X-100 solution (Sigma-Aldrich)

2% Albumin from Bovine Serum (Sigma-Aldrich)

96.8% PBS solution

Antibodies

(see Table 2.2)

2.2.13.1 Immunohistochemistry in UB/OC2 cells

UB/OC2 cells were seeded in 6 well plates containing 13mm diameter uncoated glass coverslips (VWR) and cultured as described in section 2.2.6.2. The cells were grown on coverslips until 80% confluency and fixed in 4% PFA for 15-20min. Following fixation, cells were washed three times in PBS for 5 min to eliminate any traces of fixative reagent. Cover slips containing adherent cells were then transferred onto a petri dish covered with parafilm. Cells were incubated in blocking solution for 1h at 28^{o}C to prevent non-specific binding of immunoglobulins. Following this, primary antibodies were added to the cells at the appropriate concentration and incubated for 1h at 28^{o}C. After incubation with the primary antibodies, coverslips were rinsed three times in PBS. Secondary antibodies were then added to the cells and incubated overnight at 4^{o}C. Following incubation, coverslips were rinsed three times in PBS and then mounted onto glass slides using Fluoromount G (Cambridge Bioscience).

Table 2.2: Summary of the antibodies selected in this study.

Antibody	Host species	Isotype	Immunogen	Clonality	Dilutions	Provider
E2F1	Rabbit	IgG	Peptide mapping at the C-terminus of E2F-1 of human origin	Polyclonal	For immunohistochemistry: 1:400 For gel supershifts: 1ug	Santa Cruz: E2F-1 (C-20): sc-193
MyosinVIIa	Mouse	MIgG1, kappa light chain	amino acids 927-1203 of human myosin-VIIa	Monoclonal	1:250	Developmental Studies Hybridoma Bank (Soni et al. 2005)
Atoh1	Chick	chicken anti-peptide antibody	amino acids 330– 351 of mouse ATOH1	Polyclonal	1:5000	Kindly provided by Matthew Kelley (Driver et al. 2013)

2.2.13.2 Immunohistochemistry in animal tissues

Cryo-sections

Cryosectioned tissue was taken from the -80^{o}C freezer and equilibrated at room temperature for 30 min. An hydrophobic pen was used to draw around the tissue sections in order to keep the tissue immersed in the immunohistochemistry reagents. Sections were incubated in blocking solution for 1h at room temperature. After incubation, the blocking solution was removed and the primary antibody was added at the desired concentration and incubated overnight at 4^{o}C. Following this, three rinses of 30min in PBS were conducted before adding the secondary antibody for 2h at room temperature. After incubation, tissue was rinsed three times in PBS before mounting in Fluoromount G under a coverslip (N° 0 thickness 22mmx50mm from VWR).

Whole mounts

Dissected tissue samples were kept in eppendorf tubes or MatTek dishes for immunohistochemistry. The incubation procedure with blocking solution and antibodies was as described in section 2.2.13.1. Following immunohistochemistry, samples were mounted by placing a drop of Fluoromount G in the middle of a 76mmx26mm slide (Thermo Scientific) surrounded by silicone lubricant for glass (Dow Corning Co.).

Tissue was then placed in the right position and orientation inside the Fluoromount G solution and covered by a N° 0 thickness 22mmx50mm coverslip.

2.2.14 *In ovo* electroporation

All procedures and material used for electroporation experiments are described in the following sections.

2.2.14.1 Equipment for electroporations

Egg incubator set at 37.8°C

Electrodes
Cathode = Tungsten needle
Anode = Gold-coated platinum electrode

Electro Square Porator™ ECM830: Harvard Apparatus

Electrodes: Series CUY611 and CUY613: Sonidel

Glass capillary tubes 1.2mm x 0.94mm: Harvard Apparatus

Hera guard fume hood: Heraeus

Magnetic base x2: RS

Microloader tips (0.5-20µl): Eppendorf

Microinjection Electrode Holder: Harvard Apparatus

Microscope MZ16F: Leica

One-port holder: MP series

Sellotape
Cellulose 48mm x 66mm

Small handheld lens

Standard three-dimensional manipulators

Stereomicroscope (40×): WPI

2.2.14.2 Solutions for electroporations

Injection solution 10X	**PBS**
Distilled water containing 20% sucrose	Phosphate Buffered Saline
1–2% Fast Green.	

2.2.14.3 Plasmid construction for electroporation experiments

Empty pT2K-MinProm-bicolor (Empty pT2K-bicolor)

The empty pT2K-bicolor vector was generated as a modified construct of the Tol2-Hes5: H2B-mCherry-2A-nD2EGFP (generated by ND). To generate the empty pT2K-MinProm-bicolor, the following procedure was conducted: SalI restriction digest of the Tol2-Hes5:H2B-mCherry-2A-nD2EGFP and subsequent SacI digestion to remove the Hes5 promoter (772 bp) from the parental construct. A minimal promoter sequence was inserted as a manufactured double stranded oligonucleotide to produce the Empty pT2K-bicolor (primers 13 and 14 in Table 2.1; Eurofins MWG Operon). Sequencing with the primer 22 (Table 2.1) confirmed the substitution of the Hes5 promoter by the minimal promoter.

***Atoh1*-ChickAB-down::nEGFP-mCherry**

The Chick AB *Atoh1* enhancer was cloned into the empty pT2K-bicolor vector by PCR amplification of chick genomic DNA with primers 3 and 4 (Table 2.1). The amplified product was digested with SalI to isolate the 957 bp fragment containing the chick *Atoh1* enhancer and ligated into the XhoI site in the empty pT2K-bicolor vector. The purified DNA was sequenced to confirm the cloning and orientation of the chick *Atoh1* enhancer.

***Atoh1*-ChickC-down::nEGFP-mCherry**

The Chick C *Atoh1* region was cloned into the empty pT2K-MinProm-bicolor by amplifying chick genomic DNA with the primers 5 and 6 against chick *Atoh1* enhancer C containing SalI overhangs as described in Table 2.1. Purified DNA was sequenced to confirm the cloning and orientation of the Chick C region.

***Atoh1*-ChickABC-down::nEGFP-mCherry**

The Chick ABC *Atoh1* enhancer was cloned into the empty pT2K-MinProm-bicolor by amplifying chick genomic DNA with the primers 3 and 6 as listed in Table 2.1. Sequencing confirmed the cloning and orientation of the chick ABC enhancer.

***Atoh1*-ChickAB-up::nEGFP-mCherry**

The Chick AB enhancer plus minimal promoter sequence was amplified from the ChickAB_upstreamluc_pGL4.23 construct using primers 3 and 15 listed in Table 2.1. Amplified DNA product was digested with SalI to produce a fragment of 1048 bp containing Chick AB and Minimal promoter sequences together and then cloned into the Empty pT2K-MinProm-bicolor where minimal promoter was removed by SalI digestion. Sequencing confirmed the insertion and orientation of the Chick AB plus minimal promoter fragment.

***Atoh1*-ChickC-up::nEGFP-mCherry**

The Chick C region plus minimal promoter sequence was amplified from the ChickC_upstreamluc_pGL4.23 construct using primers 5 and 15 listed in Table 2.1. Amplified DNA product was digested with SalI to produce a fragment of 457 bp containing Chick C and minimal promoter sequences together and then cloned into the Empty pT2K-MinProm-bicolor where minimal promoter was removed by SalI digestion. Sequencing confirmed the insertion and orientation of the Chick C plus minimal promoter fragment.

2.2.14.4 *In ovo* electroporation in the otic cup

Procedure for electroporation was performed as described by Freeman et al. (2012). Fertilized White Leghorn chicken (*Gallus gallus*) eggs were obtained from Henry Stewart UK and incubated at 37.8^{o}C in a humidified incubator for approximately 48h (control) corresponding to stage 12-15 Hamburger–Hamilton. The eggs were removed from the incubator, sprayed with 70% ethanol and kept horizontally for 5-10 min. While keeping the eggs in horizontal position, a band of 15 mm wide of Sellotape tape was put on the surface of the eggs. Using a pair of forceps, two holes were made through the tape and eggshell, one in the middle part of the egg and one at the more rounded end of the egg. Through the hole made in the round end of the egg, 3-4 ml of

albumen was removed using a 20ml syringe and an 18G needle. The eggs were then left for 10min. Using the hole made in the middle part of the egg, a window of about 15x 30 mm was opened using a pair of fine scissors to perform the electroporation. 8µg of a Tol2-transposase vector containing the *Atoh1* conserved elements was co-electroporated with 8µg of a vector expressing membrane GFP (in order to label the plasma membrane of electroporated cells). Plasmid DNA used for electroporation was purified as described in section 2.2.1.3 to a final concentration of 1–3 µg/µl.

Briefly, 10µl of the DNA solution was mixed with 1µl of the 10×Fast Green solution for easy visualization of the DNA mix during electroporation. Approximately, 5µl of the DNA solution was pipetted using a Microloader tip into the glass needle in the electroporation rig. The tip of the glass needle was gently cut with a fine tweezers and the tungsten needle was adjusted to a posterior position to the glass needle. During the electroporation, the opened egg was placed under the stereomicroscope and lighting adjusted to clearly visualize the otic cup. The vitelline membrane was excised by using a 25G needle and a few drops of PBS were added. Following this, the vitelline membrane was removed from the otic cup and surrounding areas for better visualization of the right otic cup. Once the otic cup was well visualized, the injection glass needle and the tungsten needle (cathode) were placed on top of the right otic cup whereas the left electrode (anode) was placed in the left side of the embryo. The DNA mixture was then injected by air-blowing into the right otic cup and subjected to three electric pulses of 10V of 100ms with 500ms interval between each pulse. The electrodes were then carefully removed from the embryo, a few drops of PBS were added, the egg was sealed with the tape and finally returned to the incubator. Eggs were kept in the incubator at 37.8^{o}C until reaching the desired development stage and examined by microscopy.

2.2.15 *In situ* hybridization (ISH)

2.2.15.1 Solutions for *in situ* hybridization

AP Buffer

100mM Tris-HCl pH9.5

50mM $MgCl_2$

100mM $NaCl_2$

0.1% Tween or Triton

PBT

PBS + 0.1% Tween20

ISH buffer	**TBST**
50% Deionized Formamide	50mM Tris-HCl
5% Sodium Saline Citrate buffer (Giese et al. 1995)	150mM NaCl
2% Boehringer Blocking powder	0.1% Tween
0.2% Triton x100	pH 7.6
50µg/ml Heparin	
50µg/ml Yeast t-RNA	
5mM EDTA	

2.2.15.2 DIG-labelled RNA probe synthesis

Digoxigenin-labelled RNA probe (Halaban et al. 1998) were from plasmid DNA containing partial cDNA sequences of the chick E2F1 gene (a gift from Dr. Matthew Towers, University of Sheffield, UK). The plasmid was digested with NotI and DNA was purified as described in section 2.2.1.4. The linearized plasmid was then used for transcription of DIG-ribo-probe in the following reaction:

- 1µg of linearized E2F1 plasmid
- 4µl of 5x transcription buffer (Promega)
- 1µl of DIG nucleotide mix (Roche)
- 2µl of 10x DTT (Promega)
- 1µl of RNasin
- 1µl of T3 RNA polymerase (Promega)
- up to 20µl of water

The transcription reaction was incubated for 2h at 37^{o}C. The DIG-ribo-probe was then diluted in ISH buffer to a final concentration of 1µg/ml and stored at -20^{o}C until used.

2.2.15.3 *In situ* hybridization on cryo-sections

Sections were removed from the -80^{o}C freezer and dried for 30min onto a microscope slide box containing Whatman paper soaked in 50% formamide + 2x SSC solution. The box had previously been rinsed with 5% hydrogen peroxide water and RNase free water in order to prevent RNase contamination of the tissue. The diluted DIG-ribo-probe was

denaturated by incubating at 70°C for 10min. About 100-200µl of DIG-ribo-probe was applied to each slide and incubated overnight at 70°C. Following the overnight incubation, slides were immersed in rinse buffer (1XSSC, 50% formamide, 0.1% tween, pre-heated to 70°C) in a coplin jar. The slides were rinsed twice by gently rocking at 65°C for 30min with 2XSSC + 0.1% Triton and then rinsed two more times with 0.2XSSC + 0.1% Triton. Following this, the slides were rinsed twice in TBST solution at room temperature for 10min. The slides were then incubated in blocking solution (TBST + 10% goat serum) for 1h at room temperature followed by overnight incubation in mouse anti-DIG (1:2000, Roche) at 4°C. After incubation, slides were rinsed at least 4 times in PBT for 20min at room temperature, incubated twice in AP buffer for 10min at room temperature and then incubated in AP buffer containing 4.5µl/ml of NBT (nitroblue tetrazolium, 75mg/ml in 70% dimethylformamide) and 3.5µl/ml of BCIP (5-bromo-4-chloro-3-indolyl-phosphate, 50mg/ml in 100% dimethylformamide). Colour development was carried out in the dark and monitored periodically under the microscope. The colour reaction was stopped by several rinses in TBST and in some cases with washes in acetone to remove any remaining traces of developing reagents. The slides were then mounted in Fluoromount G solution under a N° 0 thickness 22mmx50mm coverslip and stored at -20°C until imaged.

2.2.15.4 *In situ* hybridization on whole mounts

Tissue was dissected and fixed in 4% of PFA for between 2h to overnight and rinsed twice in PBT for 5min. For inner ear specimens, dissection of the membranous and cartilaginous caps was performed. Tissue was then either dehydrated in 50%, 75% and 100% methanol for storage at -20°C or immediately used for *in situ* hybridization following the protocol described in section 2.2.15.3.

Chapter 3

3 Bioinformatic analysis

3.1 Strategy of the investigation

The spatial and temporal expression of a gene relies on regulatory mechanisms which are conducted at many different levels to ensure that the correct protein is delivered at the appropriate time and in the right location. Understanding how gene expression is controlled under physiological conditions has been an intensive focus of research. Over the past decade, the rapid development of bioinformatic tools has helped in the study of the mechanisms that control gene expression in different biological systems. Based on the use of various computational analysis combined with functional experimentation, my investigation aimed to identify evolutionary conserved regions (ECRs) in the *Atoh1* gene locus and transcription factor binding sites that could potentially contribute to the species-specific regulation of *Atoh1* expression. As described in section 1.6, *Atoh1*, the pro-hair cell master gene, is required and sufficient for hair cell formation (Bermingham et al. 1999). Significantly, there is also correlation between re-activation of ATOH1 expression when hair cell damage occurs and the generation of new hair cells right after damage. The mechanism that re-activates the expression of ATOH1, leading to the formation of new hair cells and consequently restoration of hearing occurs spontaneously in lower vertebrates including avians (Cafaro et al. 2007; Daudet et al. 2009). However, the re-activation of ATOH1 (Wang et al. 2010) and consequently the formation of new hair cells after damage is limited in mammalian species (Forge et al. 1993; Rubel et al. 1995; Kelley et al. 1995; Lopez et al. 1998; Kawamoto et al. 2009). The molecular mechanisms and the potential differences between avian and mammals that mediate re-activation of ATOH1 expression to produce new hair cells in avians but not in mammals are poorly understood. Therefore, in order to gain a better understanding of the regulation of *Atoh1*, a combination of bioinformatic analysis, EMSA (electrophoretic mobility shift assay) and reporter gene assays were used to identify the different *Atoh1* regulatory networks in mammalian and avian species.

3.2 Identification of conserved elements by comparative genome analysis

Cross-species sequence alignment has been widely used to identify evolutionary conserved regions that may be enriched with regulatory elements since essential functional information is contained in their sequences to control the spatial and temporal the expression of nearby genes (Chinwalla et al. 2002; Chiaromonte et al. 2003). ECRs outside protein coding regions therefore often contain high affinity binding sites for transcription factors which are essential components in gene regulation. Since there are well-stablished differences in the capacities of mammalian and avian species to reactivate ATOH1 expression after hair cell injury, the differences and homologies in the ECRs of *Atoh1* within and between these two groups were investigated.

3.2.1 Comparative alignment of the human and mouse *Atoh1* locus

Previous work has shown that the regulation of mammalian ATOH1 expression is largely dependent on two ECRs downstream of the *Atoh1* locus which are sufficient to drive the expression of an *Atoh1*/*lacZ* reporter in most of the ATOH1 tissue-specific regions (Helms et al. 2000). As expected, these two regions, known as the *Atoh1* enhancer A and enhancer B (or the *Atoh1* promoter in some publications) are highly conserved between mouse and human genomes (Helms et al. 2000). Based on these findings, the region downstream of the *Atoh1* coding sequence was suggested to be a major component in the control of ATOH1 expression. In contrast, the region immediately upstream of the *Atoh1* coding region has not been shown to drive expression of a *Atoh1*/*lacZ* reporter (Helms et al. 2000).

In order to investigate whether any additional conserved elements are located within the mammalian *Atoh1*, a comparative alignment was performed between the mouse and human *Atoh1* locus (Ensembl version 63, June 2011). As shown in Figure 3.1, the comparison of the human *Atoh1* genomic sequence to ~22 kb to the mouse *Atoh1* gene locus identified two regions with high homology. These regions corresponded to the previously reported *Atoh1* enhancers A and B. The sequence homology between the human and mouse sequences is 90.73% and 88.79% for enhancer A and B, respectively.

It is notable that this degree of enhancer sequence homology is even higher than the homology found in the *Atoh1* coding region which is 83.19% between human and mouse (Figure 3.1b). Other less well conserved ECRs were found in the mouse and human *Atoh1* locus (see asterisks in Figure 3.1a). For example, approximately 2 kb and 4 kb downstream of enhancer B two more conserved regions were found of about 100 bp in length and with ~70% homology between mouse and human. However, because these regions are shorter in length and since the degree of homology is not as high as the one found in the A and B enhancers, further investigations were not conducted to test the functionality of these regions. The 20 kb sequence 5' of the *Atoh1* coding region appears to have several short regions with a limited degree of homology between mouse and human but these are shorter and less well conserved than the 3' regions (regions marked with asterisks in Figure 3.1a). Since the region upstream of the *Atoh1* sequence did not show *Atoh1/lacZ* expression in the transgenic line investigated by Helms et al. 2000, my investigation and consequent analysis focused on the study of the 3' region of the *Atoh1* locus.

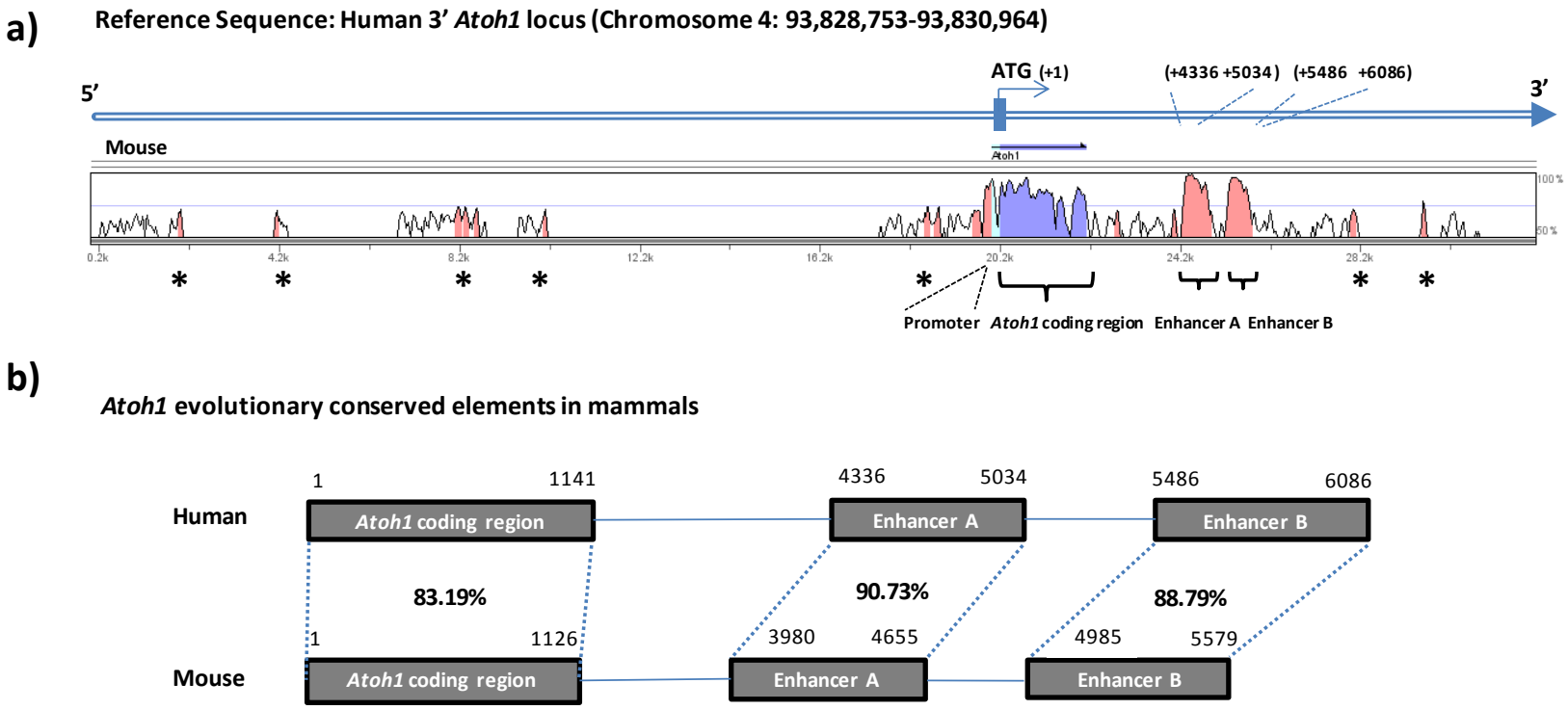

Figure 3.1. Alignment comparison between the human and mouse *Atoh1* genome sequences. a) Sequence conservation analysis showing the degree of homology of the *Atoh1* human and mouse genome sequences including the promoter region (chromosome 6: 64,729,085-64,729,333 in mouse), the *Atoh1* coding region (marked in purple- chromosome 6:64,729,125-64,731,245 in mouse and chromosome 4: 93,828,753-93,830,964 in human), UTR (untranslated region; marked in pale blue) and non-coding evolutionary conserved regions (marked in pink). The schematic extracted from mVista (Mayor et al. 2000) shows that among all the non-coding evolutionary conserved regions, the *Atoh1* enhancer A and B (chromosome 6: 65,155,797-65,156,046 in mouse) share the highest degree of homology when comparing the mouse and human *Atoh1* locus. Other non-coding regions with a lower degree of homology are shown either upstream or downstream of the *Atoh1* enhancers (marked with an asterisk). Parameters for mVista show conservation level in the y axis (in percentages) and length of the conserved regions in the x axis (minimum length 100 bp). **b)** Schematic representation (not scaled) of the position of the *Atoh1* coding region and *Atoh1* enhancers showing the percentages of homologies using Clustal2.1.

3.2.2 Comparative alignment of the chick and zebra finch *Atoh1* locus

A comparative analysis was performed to assess the degree of conservation of the *Atoh1* locus in avian species. The *Atoh1* coding sequence in chick has recently been characterized (Mulvaney et al. 2015) and the studies conducted by Ebert et al., 2003 identified and cloned the genomic 3' sequence corresponding to the chick *Atoh1* enhancers (accession number, AF467292). Therefore, a 7.5 kb of the chick genomic sequence was aligned to other avian species. At the time this investigation was initiated, only the zebra finch and turkey sequences were available. However, the turkey genome sequence was incomplete and therefore initially, only the zebra finch sequence was compared against the chick sequence (extended analysis was conducted later on and is described in the discussion). Outside the coding sequence there are regions of high conservation between the chick and zebra finch *Atoh1* genomic loci (Figure 3.2a). The length and relative position of these two regions in the zebra finch sequence was very similar to the location of the chick *Atoh1* enhancers as shown in Figure 3.2b. Also, the degree of homology shared between the chick *Atoh1* and zebra finch ECRs (89.6% and 88.36%) suggests that these conserved regions represent enhancer A and B and are therefore conserved across mammals and avians. In addition, a third highly conserved region of almost 400 bp is present which shares a 79.61% homology between the chick and zebra finch genome. This conservation is of a similar level to the chick *Atoh1* enhancer A and B annotated by Ebert et al. 2003 and was designated putative enhancer C (genomic location chromosome 4:36496979-36497355 in chick). This region is located 705 bp downstream of the enhancer B in chick and about 1.5 kb downstream in zebra finch. Four other much smaller regions of conservation were identified, less than 100 bp, two downstream of the *Atoh1* enhancers and two regions upstream, in close proximity to the *Atoh1* coding sequence (see asterisks in Figure 3.2). Based on these findings, my investigation primarily focussed on whether putative enhancer C plays a role in the regulation of *Atoh1*.

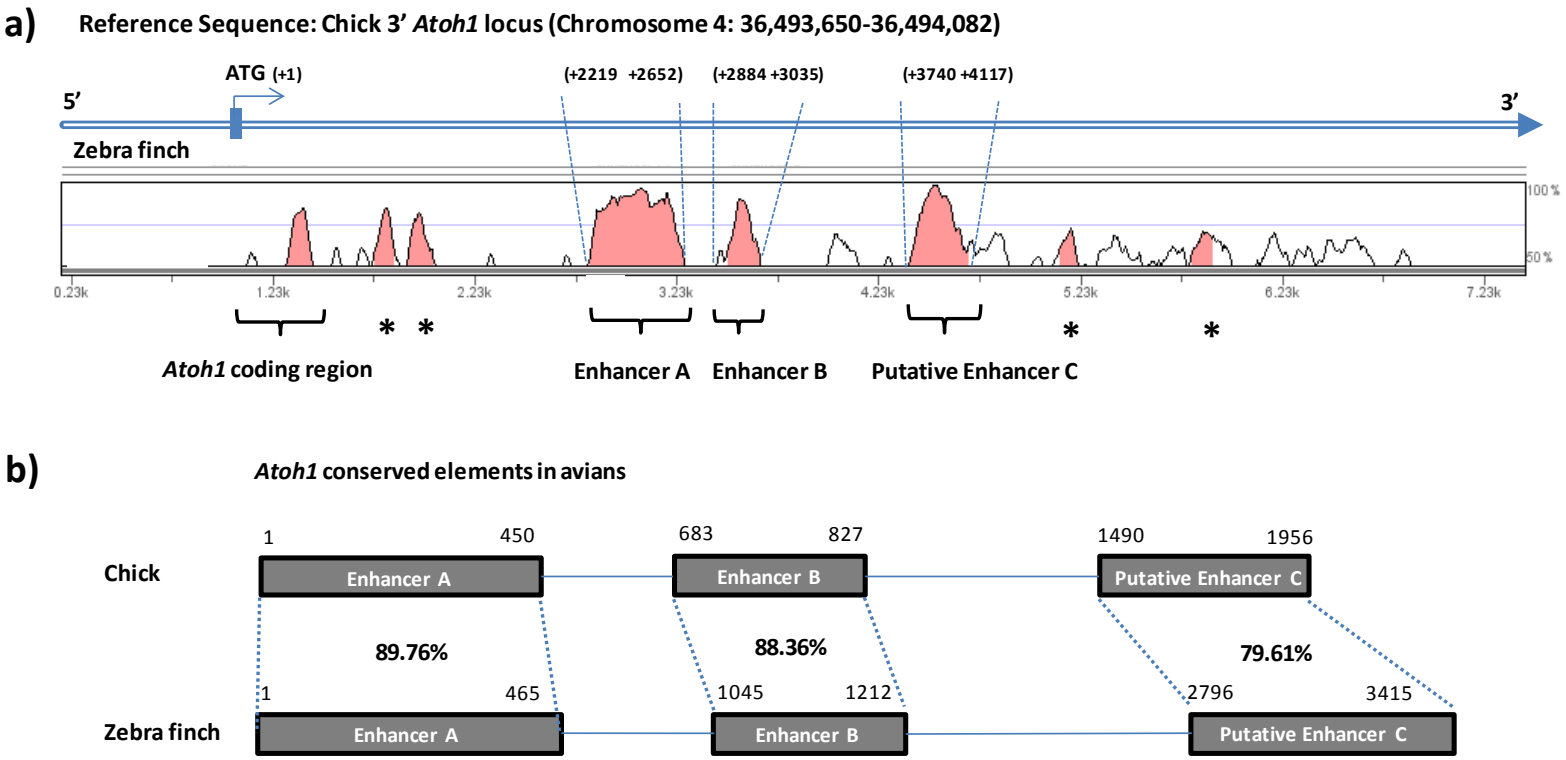

Figure 3.2. Alignment comparison between the chick and zebra finch *Atoh1* genome sequences. a) Sequence conservation analysis showing the degree of homology between chick and zebra finch *Atoh1* sequences. The schematic extracted from mVista (Mayor et al. 2000) shows conserved regions highlighted in pink, conservation level in the y axis (in percentages) and length of the conserved regions in the x axis (minimum length 100 bp). The chick *Atoh1* coding region (Chromosome 4: 36,493,650-36,494,082) shares some degree of homology with the zebra finch genome (*Atoh1* coding region in zebra finch is yet to be characterized). Two highly conserved regions shown correspond to the chick *Atoh1* enhancers A and B which were previously characterized by Ebert et al. 2003. An additional non-coding region with a high degree of homology between chick and zebra finch is shown annotated as putative enhancer C. Other non-coding regions with a lower degree of homology are marked with an asterisk. **b)** Schematic representation (not scaled) of the position of the *Atoh1* enhancers show the percentage homologies (using Clustal2.1 between chick and zebra finch). **c)** DNA sequences of the chick *Atoh1* evolutionary conserved elements (*Atoh1* AB enhancers and putative enhancer C).

c)

```
    5′
1   CTTTCTTTCTTTCTTTCTTTCTTTTTCTTTTCTTTTCTTTTCTTTTCTTTTCTTTTTTTTTTTCCCTAACACATCTCTGAAAGAGATGCGC
92  AGCGCATTTCCATGTTGAGGTTCAGCCCCGGAGTTTGCATAACAACCGCTTGGCAGCCCCCTCTCCCTCCCCCCGTTAACAAGCTGGAACG
183 TAGAGCTGCAGGTTGCTCTAATCTCATTAATATTTTGGAAAGTTGAATATTGAGCGTTTCGGAGCGCTCATTCCCCATATGCCGGGCCGCT
274 CCCGCTATGCTGGCTGCTTCCTTTCTCTCCATTATTAGCAATTAGCTCCTACCTTCCAAAGTGGGATCCAAGTATCCAAGATACTAGCAAA
365 GGCATCAACTCTGCGGTGCAAGCTAAGCACGCTCCCAAACAAACAAAGAGACAACATTTCTTTAAGTAATGAAGATGGATAAATCGCTTTA
456 TTGAGCTCGCGACAGTGTTTGTTTTGCACGGACGAGCGCAAAGTTTGCAAAGCGGAGAGCGCGCACTTCGCGGCTGCTTTGCTTTGTGCCA
547 TTTTTTATCGCTTTTTGAGGCATTTCTTTAAAGCGGGTCCGCTCGGTTTCGGCCGTAATGCTCCGTTTTCTTCGGGGTGCGGTTCTCCGGC
638 TGCTGTTTGCCCAACATCTGGCCCCGGGGATAGAAGGAAGGAAGGAGGGGGGGGAGAAAGGGTTAACCCCGGAGCTTCTTAATTAGAGCGG
729 GGCGGACAATGCGGCGGGGCGGCCCGGGGGGGGCTGGCCGCGCTCCCGGCCGCGGTGCGCCGTGTCTGGAGTGGAGCACGCGCTGTCAGCT
820 GGTGAGCGCGGCGCGGCGGCCTTTCAGGCGGCGCCCCGGGGAGCTGCGGCCCGCGGGGAGCTCCGCCGTGCTCCCCCCCCTCCCCCTCCGC
911 CCCGGCAGCCCGCGCTCGGGTCTCCCCCCGGCCCCCTCCTCGCCTCGCCCGAGGAGCGACGGCCGTCGGAGTGGGATACAAAAGCAACGCC
1002 TGCTTGCGCGGGGGGGTCTCACGCGTGTGCGTGCTCCCATGGCTCCTCTCCCTTTAGCCTCTTGCACACGTGGGGAGCCGGCGGAGCTCTC
1093 CAGGGACGCGCGGCTCTCGCATCTGCTGCAAAGCTCTGCGATATCGCCGCCGCTCCCCTGCAGGAATGTCACCGGCGGGGCCGCGCGGAGC
1184 CCCAAGATCCCTCCTCGCCGAGGGCAACCCCCCGCTGACTCGACTCCGGGGAAGGCAGAGAGCCCCTTCCGAAGGGCTATCGGGTGGCAGA
1275 GGGACGCCTTTGGGAGCGCGGCCAGGACGTGTCAACACGTCGAAGCGTTTCCTCGCTGCCCCCGCTGCCTTTCTGCCGTGCGCTCCCTCCC
1366 TCCCGGCTCGGGACGGGAACACCGGAGCCCTTCGCACCGGGCTGCCGCCGCTCGGAGCCGTGCCCCCGTGCGCCGGGCAGGGAAACCGAGA
1457 CCTGGGTCTAGGAGAGCGACATTCGGGACTAGGAAAACGAGTTTTGGGGCTGGCGGAGCAAATCGCACCCACTTACAACGACCTAATTTCT
1548 CATTCATCCAAACTTCCTTCTTTATCGTTTATTGTATTTGTGTTTAATCGCTGTAATCCCCGTGTCCTCTCGCCCGCCCTGGTGCGCGCTC
1639 CCGCGCCCAACGCGGGACAGCGACGCGCACCCGAGCGGTGCTGCCGCGCTTTATGGAGCGGTTAATCAACTGCGCATCAGCGAGACAGCGC
1730 ATCAGCCCATCTGCTTGATATATATTCAGGAGGGCTCCAGCCCTTTTGAAGTCTAATTTCTTCCCCGGGAGAACGCGCCGGGTAATTTACC
1821 ATCATTTCATACGCATCGCGGCCACCGAGTTAACCCTTTCCCCAAGCGCTGCCCGCACGGGATTTTCCTCCCGAAAAACGCCGGGTGCAAC
1912 GCTACAAACTTGTCAAAGCGTCTTTCCGATGATGCTCCTTGAAATAAGAGATCGCAGCTCACCGACACTGTAACCCCTTGGATCTGTCGGG
2003 TTAGAAAGGAGGGGTTGTGAAAGATCTGCTTGGGATAAGCAAACGCTTAGAACCGCCCATGCCAACGCGCATCATTTCATCCCCAACCACC
2094 TACTGCT   3′
```

Enhancer A

Enhancer B

Putative Enhancer C

3.2.3 Multi-species alignment of the *Atoh1* genomic sequence

Comparative alignment of the *Atoh1* loci sequence in avian species resulted in the identification of an additional conserved region, putative enhancer C, a region with a similar degree of conservation as the functionally characterized *Atoh1* enhancers A and B. A multi-species alignment analysis across the mammalian and avian *Atoh1* sequences was conducted in order to compare the conserved regions across both groups.

As shown in Figure 3.3, the chick Atoh1 sequence was aligned to the human, mouse and zebra finch sequences. Two regions appeared to be highly conserved across all four species. These sequences corresponded to the previously characterized *Atoh1* enhancers A and B. It was notable to find that the enhancers have retained their sequence identity even in species that are evolutionary distinct like human and chick. Several smaller regions were also found with a high degree of homology corresponding to the *Atoh1* coding region, as might be expected. However, there were no additional conserved regions downstream of the *Atoh1* enhancer that matched both the mammalian and avian sequences. Therefore, the putative enhancer C appeared to be unique to the avian genome.

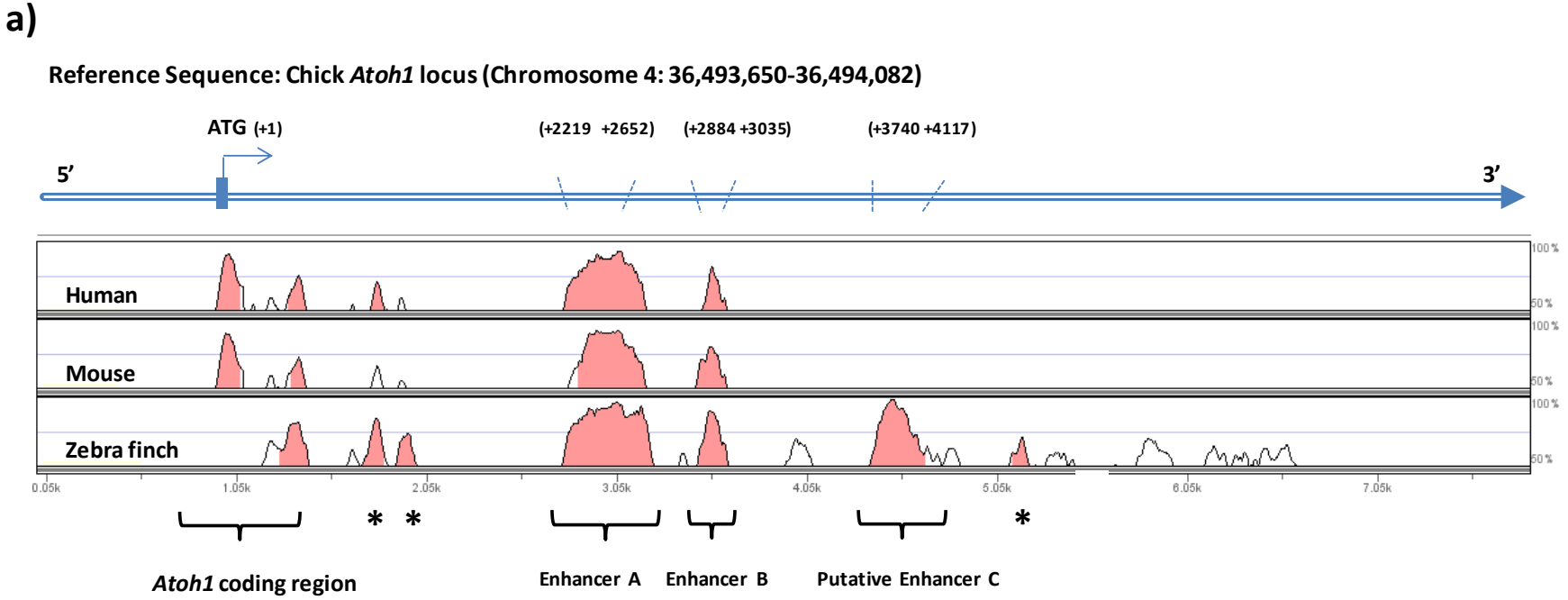

Figure 3.3. Alignment comparison between the chick, human, mouse and zebra finch *Atoh1* genome sequences. a) The chick *Atoh1* sequence was used as the basis for comparison and conserved regions are highlighted in pink. Conservation levels are represented in the y axis (in percentages) and the length of the conserved regions is presented in the x axis (minimum length 100 bp). The diagram extracted from mVista (Mayor et al. 2000) shows that some regions within the *Atoh1* coding sequence are highly conserved among chick, human, mouse and zebra finch (*Atoh1* coding sequences correspond to chromosome 6:64,729,125-64,731,245 in mouse, chromosome 4: 93,828,753-93,830,964 in human and chromosome 4: 36,493,650-36,494,082 in chick; forward strand). The two highly conserved regions previously characterized by Helms et al. 2000 and Ebert et al. 2003 and defined as the *Atoh1* enhancer A and B are also conserved among the four species including zebra finch. Two additional non-coding regions located ~500 bp downstream of the *Atoh1* coding region are conserved among chick, human, mouse and zebra finch (marked with an asterisk). The additional non-coding region (annotated as putative enhancer C; genomic location 4:36496979-36497355) with a high degree of homology between chick and zebra finch does not share homology with the 3' region of the mouse and human *Atoh1*. **b)** Schematic representation (not scaled) of the position *Atoh1* enhancers showing the percentages of homologies using Clustal2.1 between chick, human, mouse and zebra finch.

b)

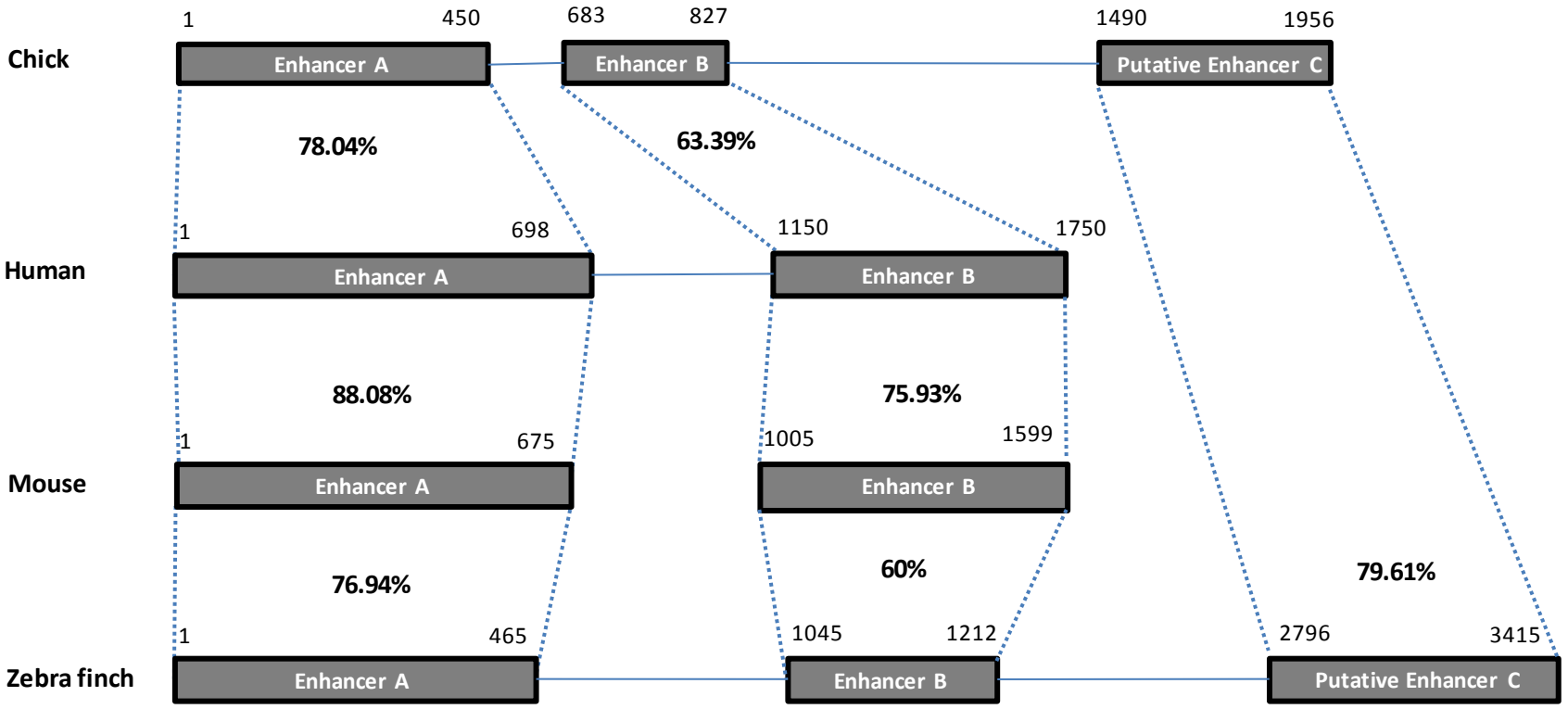
Atoh1 conserved elements – Multispecies alignment
Chick
1
450
683
827
1490
1956
Enhancer A
Enhancer B
Putative Enhancer C
78.04%
63.39%
Human
1
698
1150
1750
Enhancer A
Enhancer B
88.08%
75.93%
Mouse
1
675
1005
1599
Enhancer A
Enhancer B
76.94%
60%
79.61%
Zebra finch
1
465
1045
1212
2796
3415
Enhancer A
Enhancer B
Putative Enhancer C

3.3 Identification of putative transcription binding sites within ECRs

MatInspector from Genomatix is a bioinformatic software program that predicts transcription factor binding sites in DNA sequences (Cartharius et al. 2005). This software uses a matrix similarity approach in order to locate matches based on the nucleotide conservation of functionally proven binding sites (Quandt et al. 1995). This approach results in the construction of a library of transcription factor matrices based on experimental data from transcription factors binding sites that have previously been tested. At the time this investigation was conducted, the MatInspector library contained 1381 weight matrices classified in 411 families (version 9.0, August 2012) representing the largest database available to identify binding sites. In addition, unpublished experimental data conducted in our laboratory suggested that this software has a good accuracy in predicting transcription factor binding sites in comparison to other software packages. Therefore, the ECRs identified previously by mVista including enhancer A, B and putative enhancer C were analysed using MatInspector to identify transcription factor binding sites.

3.3.1 Predictions within *Atoh1* Enhancer A and Enhancer B

Using MatInspector, transcription factor binding sites common to both mammalian and avian species in enhancers A and B were predicted (Figure 3.4). The matches given by MatInspector were grouped into matrix families corresponding to functionally related transcription factor binding sites. A total number of 52 common matches were found in enhancer A and 62 transcription factor binding sites in enhancer B. Some of the transcription factors already shown to regulate *Atoh1* were predicted in this analysis. This includes ATOH1 binding sites necessary for autoregulating *Atoh1* expression (Helms et al. 2000). As shown in Figure 3.4c a V$NEUR matrix family match was predicted within mouse and human *Atoh1* enhancer B. This matrix family is categorized by MatInspector as a potential binding site for bHLH transcription factors. When checking the predicted binding site sequence for the V$NEUR site, it was found that it matched the E-box sequence where ATOH1 binds (Figure 3.4c). Other predictions in the *Atoh1* enhancers that matched functional transcription factors involved in the regulation of *Atoh1* were SOX2 (Family V$SORY in enhancer A), ZIC1 (Family

V$GLIF in enhancer B) (Figure 3.4). A number of additional conserved motifs consistent with the potential binding of POU3 and POU4 transcription factors (Family V$BRNF), BARHL1 (Family V$HOMF), GATA (Family V$GATA), LHXF (Family V$LHXF) and Id transcription factors (V$NEUR) were also predicted within enhancers A and B (highlighted by red boxes in Figure 3.4). These are transcription factors that are known to play roles during hair cell fate, differentiation and maturation of the sensory epithelium (see section 1.5.3). Hence, based on the analysis conducted by MatInspector, these transcription factor candidates could potentially bind to the *Atoh1* enhancers and are within sequences conserved across avian and mammalian species.

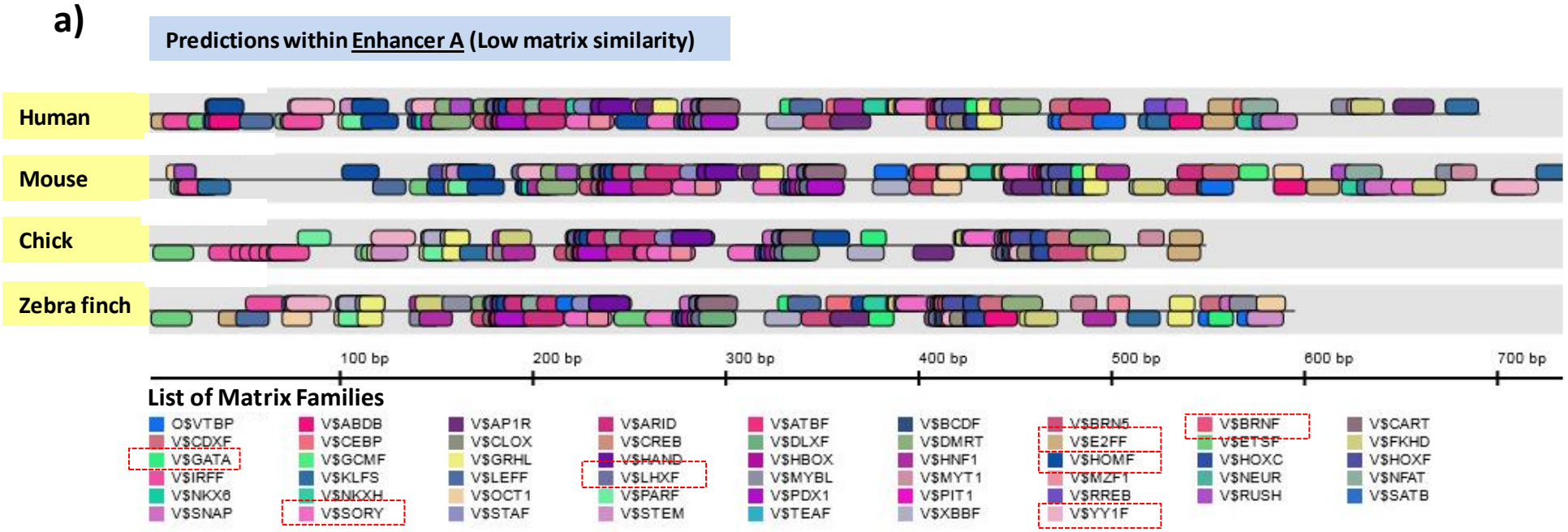

Figure 3.4. Common transcription factor binding sites predicted within *Atoh1* enhancer A and B. MatInspector predictions for common transcription factors in human, mouse, chick and zebra finch. The family names are given as a unique identifier for each match and displayed with a first letter corresponding to the section family they belong to (e.g. vertebrates (V$), other (O$). Each matrix match is represented by a coloured half round symbol with can be found in the positive or negative strand. Additionally, matrix family are presented in a list at the bottom of the figure. The matrix similarity is a parameter established by MatInspector showing how similar a prediction is in comparison to the consensus matrix **a)** Common transcription factor binding sites predicted within the *Atoh1* enhancer A in human, mouse, chick and zebra finch. A total number of 52 common transcription factor families matches were predicted on the enhancer A. **b)** Common transcription factor binding sites predicted within the *Atoh1* enhancer B in human, mouse, chick and zebra finch. A total number of 62 common transcription factor families matches were predicted on the enhancer B. **c)** A V$NEUR matrix family match was predicted for binding the mouse and human *Atoh1* enhancer B. The sequence of the predicted V$NEUR matrix family matched an E-box sequence which is the functional binding site for ATOH1. Other matrix families with roles in cell fate, differentiation and maturation are predicted for binding the *Atoh1* enhancers. These include the POU3 and POU4 transcription factors (Family V$BRNF), BARHL1 (Family V$HOMF), GATA (Family V$GATA), LHXF (Family V$LHXF), the Id transcription factors (Family V$NEUR), YY1 (Family V$YY1) and E2F (Family V$E2FF) (marked in red boxes in the list of matrix families).

b)

Predictions within Enhancer B (Low matrix similarity)

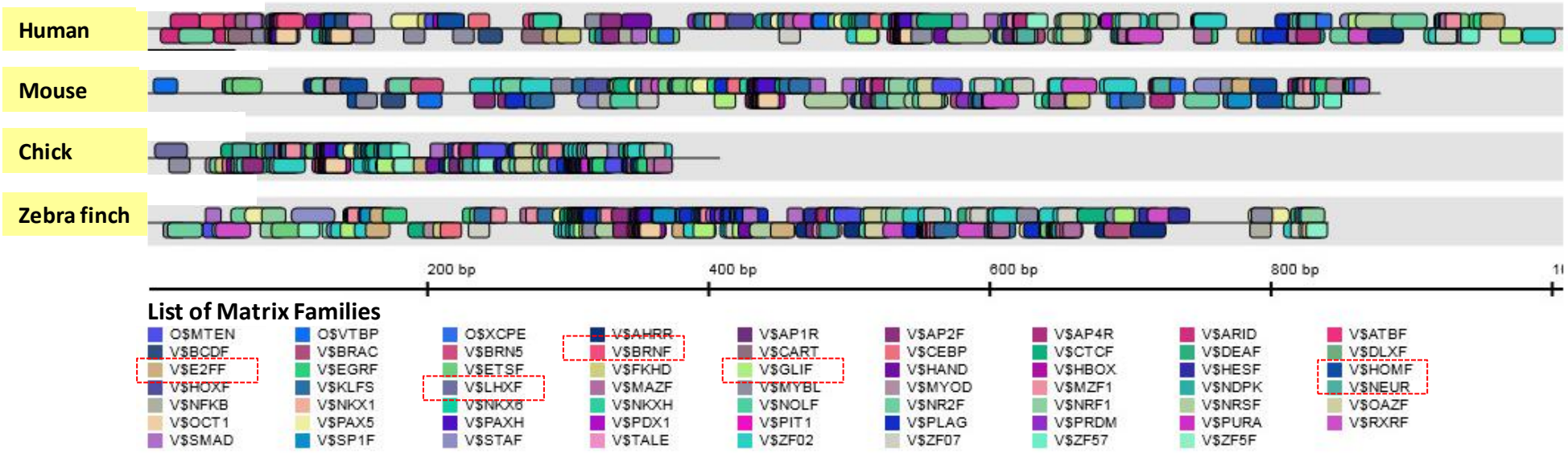

c)

tcccCAGCTGcgc

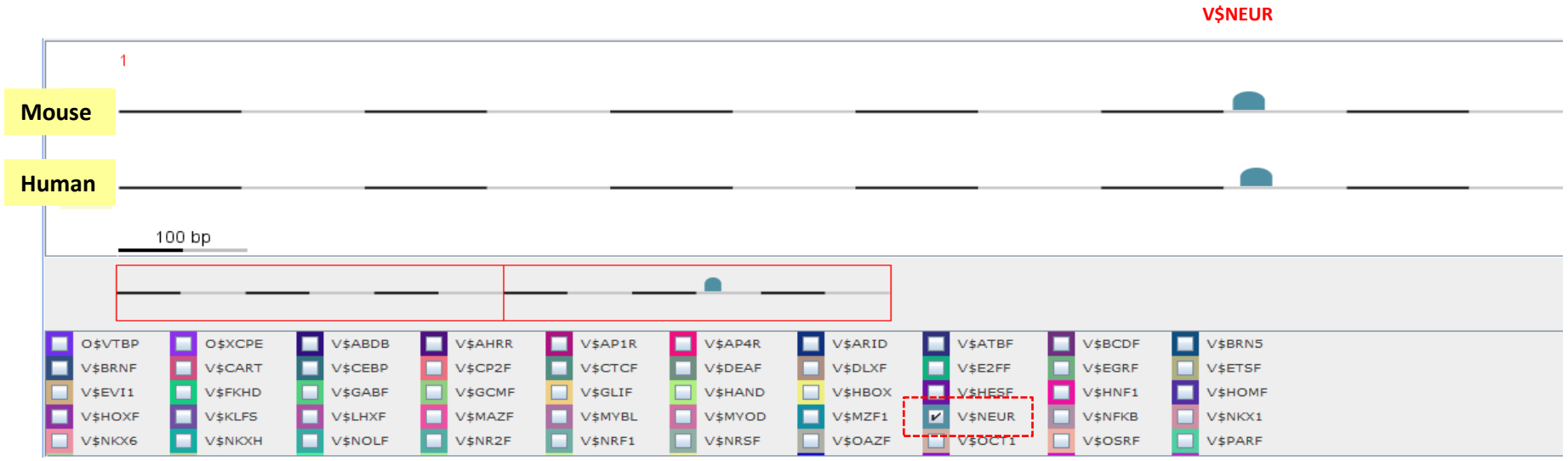

E-box

```
Human          TGCGGAGCGT CTGGAGCGGA GCACGCGCTG TCAGCTGGTG AGCGCACtct
Mouse          TGCGGAGCGT CTGGAGCGGA GCACGCGCTG TCAGCTGGTG AGCGCACtcg
Chick          TGCGCCGTGT CTGGAGTGGA GCACGCGCTG TCAGCTGGTG AGCGCggcgc
Zebra finch    TGCGCCGTGT CTGGAGCGGA GCACGCGTTG TCAGCTGGTG AGCGCA----
```

3.3.2 Predictions within putative Enhancer C

The additional conserved region found in the *Atoh1* sequence of chick and zebra finch, the putative enhancer C, was also examined by MatInspector. As in the previous analysis with the *Atoh1* enhancers, the putative enhancer C sequence from chick and zebra finch was retrieved from mVista and exported in FASTA format into MatInspector.

A total number of 53 transcription factor matrix families were identified by MatInspector within putative enhancer C in both chick and zebra finch. It was interesting to find that some of the predictions found in the *Atoh1* enhancer A and B were also found within putative enhancer C. This includes V$NEUR, V$E2F and V$NFKB matrix families (marked in Figure 3.5).

3.3.3 Predictions within other evolutionary conserved regions

In addition to the *Atoh1* enhancers and putative enhancer C, other evolutionary conserved regions were also found in the multi-species alignment of the *Atoh1* locus (Figure 3.3). Two regions (named ECR1 and ECR2 in Figure 3.6) were found at +1153 and +1246 downstream of the start codon of the chick *Atoh1* coding sequence. ECR1 and ECR2 were analysed for transcription factor binding sites with MatInspector to find 8 and 9 matches respectively. Some of the predictions identified correspond to binding sites for the POU transcription factor family (Family V$BRNF), BARHL1 (Family V$HOMF), GATA (Family V$GATA) and SOX transcription factor family (Family V$SORY) all known to be involved in controlling inner ear gene expression.

MatInspector analysis was also extended to another region of 83 bp (named ECR3 in Figure 3.6). The ECR3 is located 500 bp downstream of the putative enhancer C in chick and zebra finch and a low similarity was found against the mouse or human *Atoh1* locus using the set threshold given by mVista (50% similarity threshold). Only 2 putative binding sites were predicted in the ECR3 corresponding to the matrix family V$NACA (Nascent polypeptide associated complex and coactivator alpha) and V$NFAT (Nuclear factor of activated T-cells) (Figure 3.6).

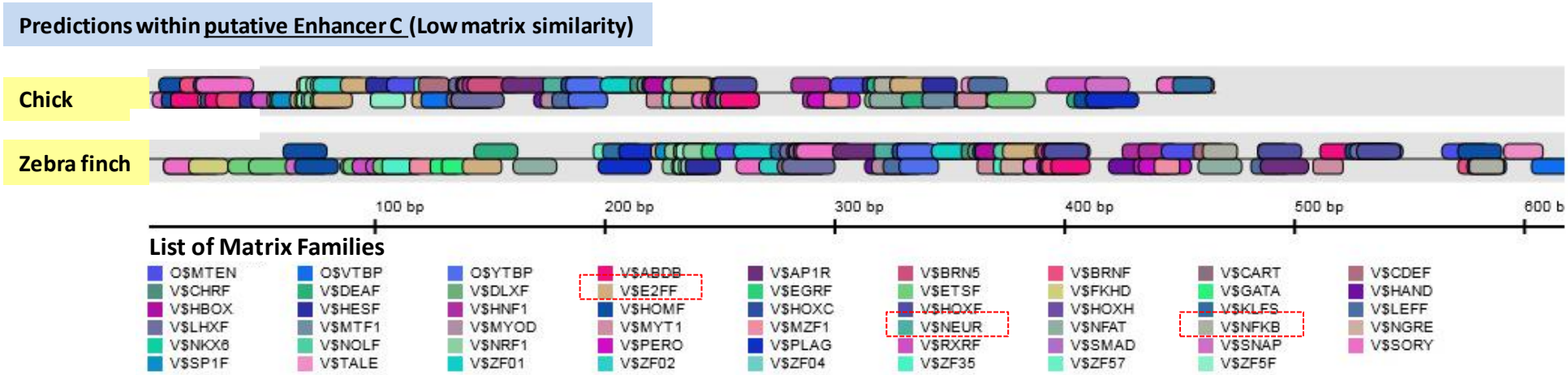

Figure 3.5. Common transcription factor binding sites predicted within *Atoh1* putative enhancer C in chick and zebra finch. MatInspector matches were grouped into matrix families. The family names were given as a unique identifier for the family and displayed with a first letter corresponding to the section family they belong to (e.g. vertebrates (V$), other (O$). As in the previous analysis, each matrix match was represented by a coloured half round symbol with can be found in the positive or negative strand. Additionally matrix families were presented in a list at the bottom of the figure. The matrix similarity is a parameter established by MatInspector showing how similar a prediction is in comparison to the consensus matrix. A total number of 53 common transcription factor families matches were predicted on putative enhancer C in chick and zebra finch. Some of the family matrices found in the putative enhancer C were also predicted for binding the *Atoh1* enhancer A and enhancer B. Some examples were marked in red squares such as the V$NEUR, V$E2F and V$NFKB matrix families.

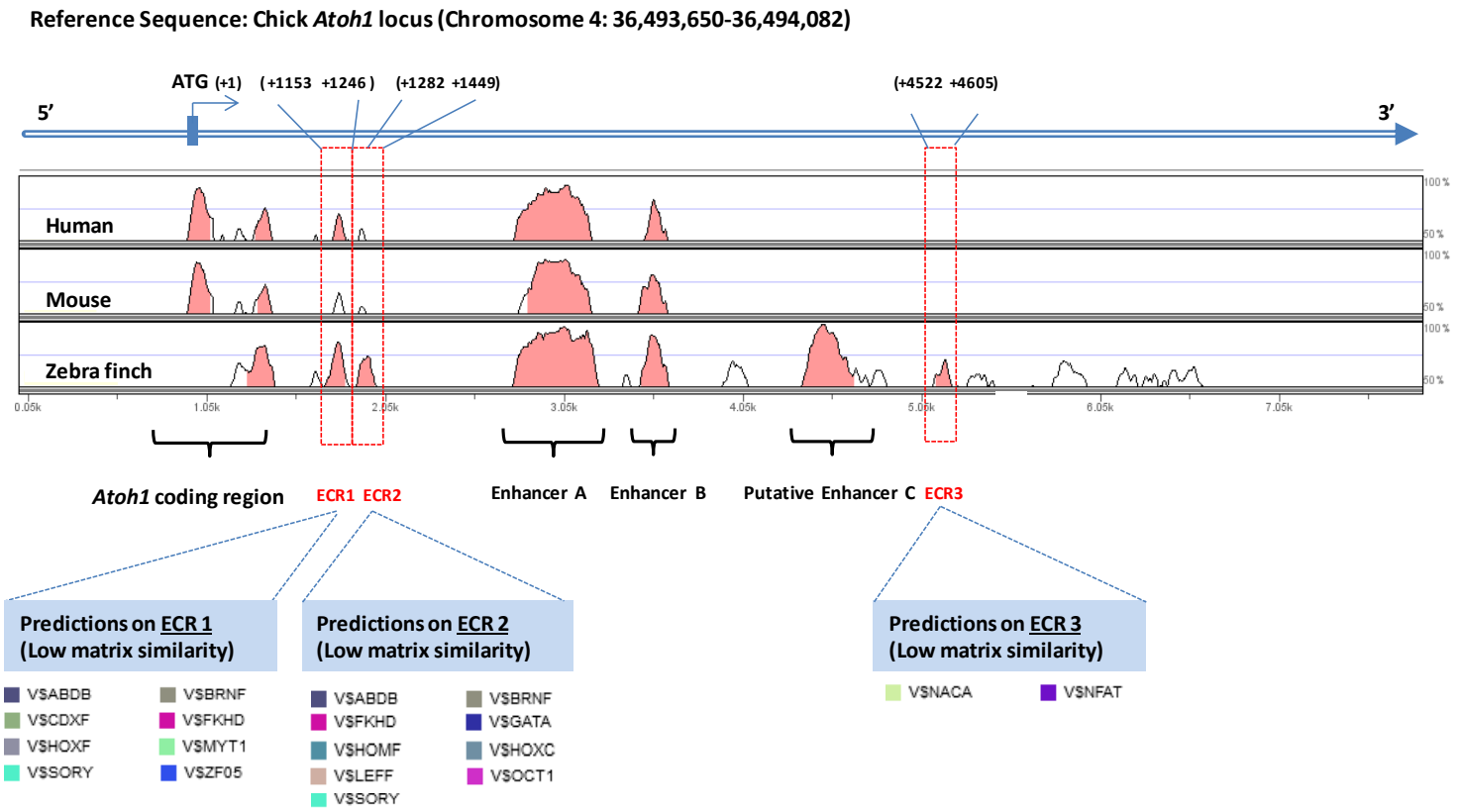

Figure 3.6. Common transcription factor binding sites within other evolutionary conserved regions at the *Atoh1* locus. Based on an *Atoh1* multi-species alignment, two small evolutionary conserved regions are found upstream of the *Atoh1* enhancers (ECR 1 and ECR2) which are present in chick, human, mouse and zebra finch. An additional conserved region among chick and zebra finch is also found downstream of the putative enhancer C (ECR3). The relative position of these regions is represented in the chick *Atoh1* sequence which is used as the basis for comparison. The transcription factor binding sites predicted for each region are listed using a low matrix similarity threshold. Some of the predictions identified in these regions include the POU3 and POU4 transcription factors (Family V$BRNF), BARHL1 (Family V$HOMF), GATA (Family V$GATA) and SOX transcription factor binding sites (Family V$SORY).

3.4 Refinement of predictions

Prioritization of novel candidates involved in the regulation of genes has always been a crucial as well as a difficult step for researchers. The complexity of regulatory gene networks makes the choice of potential candidates a very challenging and time consuming task. However, at different stages of any research project, scientists have to decide which genes will be experimentally tested and which ones will be left out because of limited resources. As many candidates were predicted in the bioinformatic analysis, it was necessary to simplify my investigation and prioritize some of the putative candidates for further experiments.

The first selection criteria was on the basis of the matrix similarity threshold. The matrix similarity score given by MatInspector shows how similar a prediction is in comparison to the consensus matrix. The highest matrix similarity score given by MatInspector is 1 and therefore is defined as the "perfect match" since all the base pairs in the binding site are identical to a functional consensus binding site. On the contrary, a low matrix similarity predicts more matches the predicted binding sites allow a lower percentage match to the consensus matrix which results in false positives as well as functional binding sites. As shown in Figure 3.7, the number of transcription factor families predicted within enhancer A of mouse and human was reduced from 73 to 28 when the matrix similarity was increased. Only the candidates with a predicted binding site close to the consensus matrix were retained, for example, transcription factor YY1 (marked with a red box in Figure 3.7). The position of this predicted binding site is also conserved across these two species.

As shown in the schematic diagram of Figure 3.8, the number of predicted candidates binding sites in both chick and zebra finch putative enhancer C was reduced from 53 to 13 when the matrix similarity was increased from low to high. Notable remaining predictions include multiple binding sites for the E2F and NF-κB transcription factors (marked with a red box in Figure 3.8).

Having completed a comparative alignment to identify highly conserved regions in the *Atoh1* locus followed by a MatInspector analysis to predict potential candidates binding to these regions, my investigation continued to select candidate transcription factors to investigate further based on the known biological functions in which they are involved.

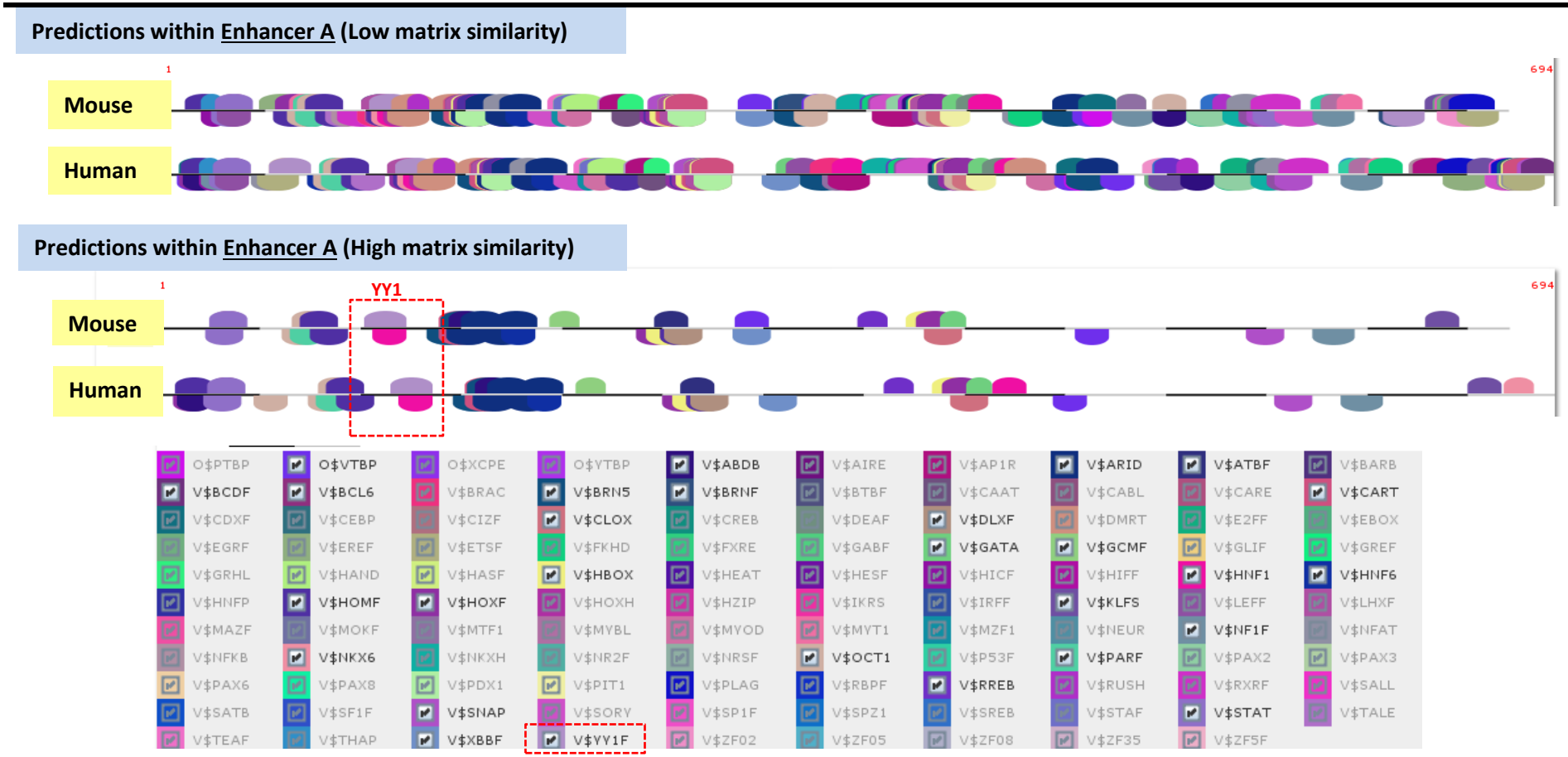

Figure 3.7. Common transcription factor binding sites predicted within *Atoh1* enhancer A of mouse and human. A total of 73 common matches were predicted in the *Atoh1* enhancer A with the lowest matrix similarity represented by a coloured half round symbol. When the matrix similarity was increased, the number of predictions was decreased to 28 since only the matches that were closer to the consensus matrix were displayed. Each matrix family is presented in the list at the bottom of the figure and the matches with a high matrix similarity are displayed in bold. As an example, the YY1 transcription factor (marked with a red box) was predicted as a strong candidate binding to the *Atoh1* enhancer A.

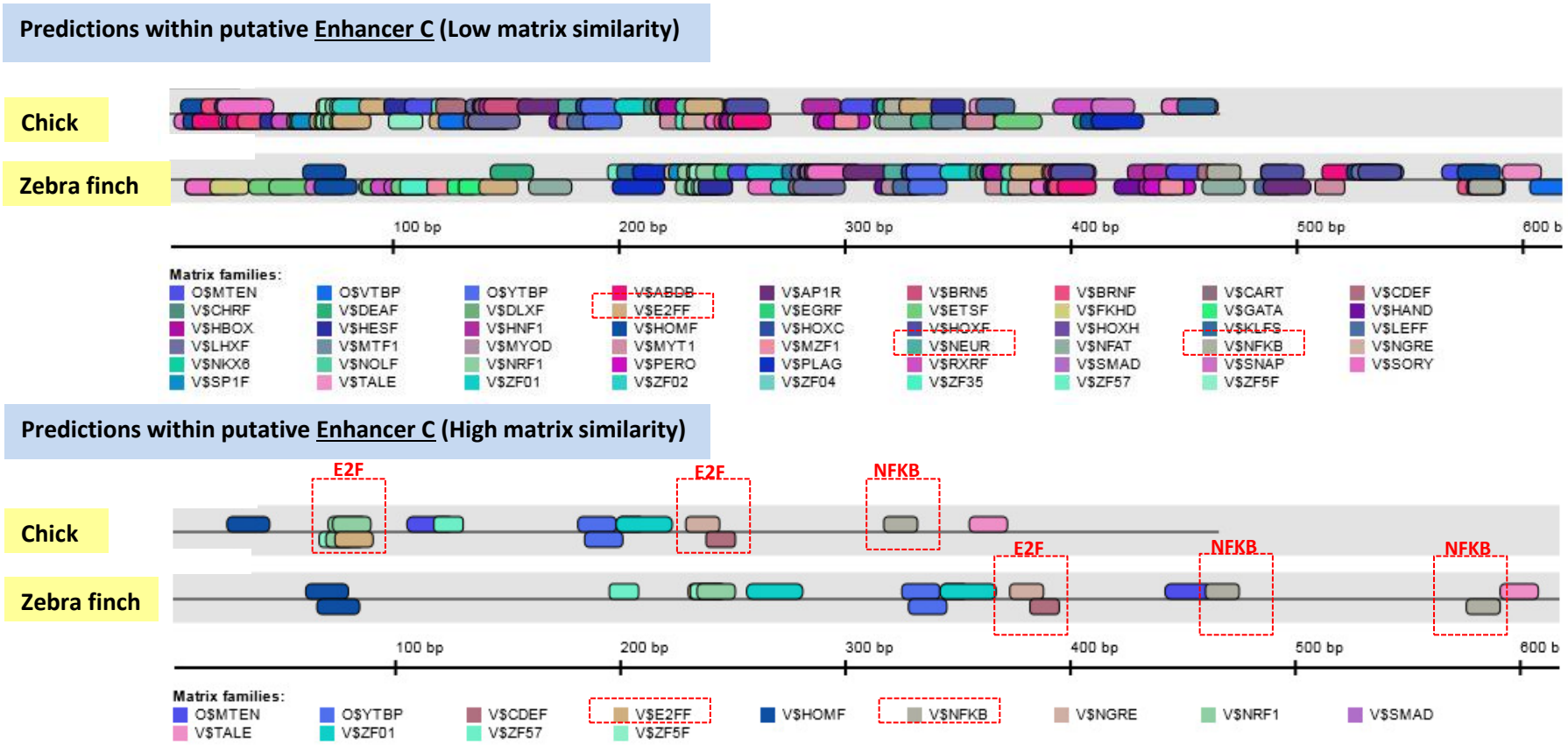

Figure 3.8. Common transcription factor binding sites predicted within putative enhancer C of chick and zebra finch. A total of 53 common matches were predicted for binding putative enhancer C with the lowest matrix similarity. Each coloured half round symbol corresponds to a predicted matrix family represented in the list. When the matrix similarity was increased to the highest parameter given by MatInspector, the number of predictions was decreased to 13 since only the matches that were closer to the consensus matrix were displayed. Multiple binding sites were predicted for the E2F and NFKB transcription factors (marked with a red box) which were predicted as strong candidates binding putative enhancer C.

3.5 Prioritization of YY1, NFKB, E2F and ATOH1

Following the bioinformatics predictions, four transcription factor candidates were prioritized based on their expression profiles and functions during hair cell development and survival. For the prioritization process, gene expression profiles were checked for most of the predicted transcription factors candidates that showed a high stringency in the bioinformatic analysis. Different gene expression databases were used for this purpose. For mammalian gene expression, the Allen Brain Atlas (www.brain-map.org) was used. The interactive Atlas viewer application provides a rapid method to assess gene expression based on annotated RNA sequencing and exon microarray techniques combined with high-resolution *in situ* hybridization image data from developing and adult human brain and brain section from 8-week old C57Bl/6J male mice. Gene expression profiles were also checked using GEISHA (Gallus Expression *In Situ* Hybridization Analysis: http://geisha.arizona.edu/geisha) and echick atlas (http://www.echickatlas.org/ecap/home.html) in order to obtain gene expression profiles from avian databases. Having checked gene expression from different mammalian and avian databases, transcription factor candidates whose expression was shown in the brain or inner ear were prioritized for follow-up. However, the possibility that expression data may not be available for all the candidates was taken into account. Hence, experimental and functional data from previous publications were also assessed in order to select potential regulators of *Atoh1*. The final prioritization criteria, was the selection of candidate genes involved in developmental pathways and biological processes that could be relevant to the inner ear.

Based on these criteria, four candidates were selected: YY1, NF-κB, E2F and ATOH1. The various reasons for their individual selection are described below.

3.5.1 YY1

The first selected candidate was YY1 (Ying Yang-1). YY1 is a zinc finger transcription factor that has the capacity to act as an activator or repressor of the transcription of its target genes (Shi et al. 1991). At the time my investigation started, expression of YY1 in the mouse and chick cochlea had been described (Street et al. 2011). In this study, immunohistochemistry data showed that YY1 is expressed in hair cells as well as in the spiral ganglion of mice aged 2 months. In chick, YY1 was also detected in different

tissues including brain and the basilar papilla (Street et al. 2011). Previous studies in *Xenopus* also observed YY1 protein in the neural tube at embryonic stages (Kwon and Chung 2003). YY1 has also been shown to be a transcriptional repressor of the MYO7A promoter. A single nucleotide polymorphism (SNP) was found at the position -4128 in the MYO7A promoter allele which is linked to severe hearing loss. The study conducted by Street et al., suggested that the SNP in the MYO7A promoter controls differential binding and regulation by the YY1 transcription factor. To confirm this, EMSA and reporter gene assays were carried out to demonstrate that the direct binding of YY1 to the -4128 SNP produces the transcriptional repression of the MYO7A expression in comparison to the wild-type allele. As hair cells are sensitive to the level of MYO7A expression, the reduction of MYO7A resulted in a hearing loss phenotype. Since YY1 seems to be involved in the transcriptional response of MYO7A, it may also be involved in the regulation other genes in the auditory system. As described in section 3.4, a YY1 binding site was identified with the highest matrix similarity in the mammalian *Atoh1* enhancer A (Figure 3.7). Therefore, based on the study by Street et al., the YY1 expression pattern in the auditory system in mouse and chick and the predictions from bioinformatic analysis, YY1 was selected for further experimentation and as putative candidate regulating *Atoh1*.

3.5.2 NF-κB

NF-κB (NF-kappa-B) is a well characterised transcription factor which has been described as a key regulator of genes involved in many biological processes including immunity and inflammation, cell survival, apoptosis, differentiation and development (Karin and Lin 2002; Gilmore 2006). In the inner ear NF-κB has been shown to be required for the survival of immature hair cells (Nagy et al. 2005). Expression studies conducted by Nagy et al. 2005 detected mRNA in the organ of Corti of p5 rats and protein expression by immunohistochemistry for some of the subunits that form NF-κB. Therefore, specific antibodies are commercially available for NF-κB as well as expression constructs from collaborators. Availability of reagents for further investigation was a secondary consideration taken into account in the selection of candidates. In addition, NF-κB binding sites were predicted with a high stringency within putative enhancer C (Figure 3.8). Therefore, based on the predictions given by the bioinformatic analysis combined with the biological roles of NF-κB and the

existence of reagents for functional studies, NF-κB was selected for further investigations in the transcriptional regulation of *Atoh1*.

3.5.3 E2F

The E2F transcription factor family was also predicted by the bioinformatics analysis to bind the mouse and chick *Atoh1* enhancer A and B (Figure 3.4) as well as the chick *Atoh1* putative enhancer C (Figure 3.8). E2F and its partner protein, the Retinoblastoma (Rb) play a critical role in the control of the cell cycle, cell proliferation and apoptosis (Bandara and La Thangue 1991; Chellappan et al. 1991; Kaelin Jr et al. 1991). Analysis of conditional knockout mice for a genetic deletion of Rb has demonstrated that their post-mitotic hair cells can re-enter the cell cycle and consequently proliferate for a longer period (Sage et al. 2006). The partnership role of E2F/Rb controlling developmental and proliferative processes has also been well established in other tissues. In addition, E2F1 expression has been described in the stria vascularis and spiral ganglion in mouse suggesting that E2F could have a significant role in the auditory organ (Raimundo et al. 2012). Therefore, the E2F family was selected for further investigation. Results from E2F experiments are presented in Chapter 5.

3.5.4 ATOH1

Finally, the ATOH1 transcription factor was also selected for further investigation. The interaction between ATOH1 and an E-box site located in the *Atoh1* enhancer B has been previously described as an autoregulatory feed-back system to control ATOH1 expression (Helms et al. 2000). The bioinformatic analysis performed here detected the presence of bHLH binding sites in the mouse and chick *Atoh1* enhancers (the V$NEUR matrix) which verified the efficiency of this approach to predict functional binding sites. Since the interaction between ATOH1 and its enhancer has already been proven (Jarman et al. 1993; Akazawa et al. 1995; Helms et al. 2000) but its response has not been quantified in an auditory cell line, the response of the *Atoh1* enhancers upon overexpression of ATOH1 was investigated in UB/OC2 cells. In addition, a bHLH binding site was also predicted in the chick *Atoh1* putative enhancer C (Figure 3.5, V$NEUR matrix). Previous studies conducted by Helm et al., suggested the possibility of additional autoregulatory elements in the *Atoh1* sequence beyond the *Atoh1*

enhancers. Therefore, this possibility was investigated by quantifying the response of the chick putative enhancer C, upon overexpression of ATOH1.

3.6 Binding profiles for YY1, NF-κB and ATOH1 transcription factors

The genomic location and the conservation profiles of the binding sites for YY1, NF-κB and ATOH1 were examined in more detail. This information was required for further experimentation especially for the design of EMSA probes or the mutagenesis of their binding site for reporter gene assays. Based on the data collected from the MatInspector analysis, the location of the predicted binding sites for YY1, NF-κB and ATOH1 was annotated (Figure 3.9). The degree of homology of the predicted binding sites across mammalian and avian species was also assessed by the use of DiAlign, one of the features included in the Genomatix software package. The YY1 binding site shows a high degree of homology in mammalian and avian species. The NF-κB and ATOH1 binding sites predicted in the putative enhancer C, were also almost identical in chick and zebra finch (Figure 3.9). In addition and in support of matrix predictions, Table 3.1 shows the binding sites for these transcription factor candidates. The matrix and core similarity scores are also shown which are between 0.8 and 1 respectively.

Figure 3.9. Location of the YY1, NF-κB and ATOH1 predicted binding sites within the *Atoh1* conserved regions. Summary of the genomic location of the binding sites predicted by MatInspector. A YY1 binding site was predicted within the *Atoh1* enhancer A whereas an ATOH1 and a NF-κB were predicted within putative enhancer C. The degree of homology across the mammalian and avian species is shown. The predicted YY1 binding site is highly conserved in mouse and human *Atoh1* enhancer A whereas the ATOH1 and NF-κB binding sites were highly conserved in chick and zebra finch *Atoh1* putative enhancer C.

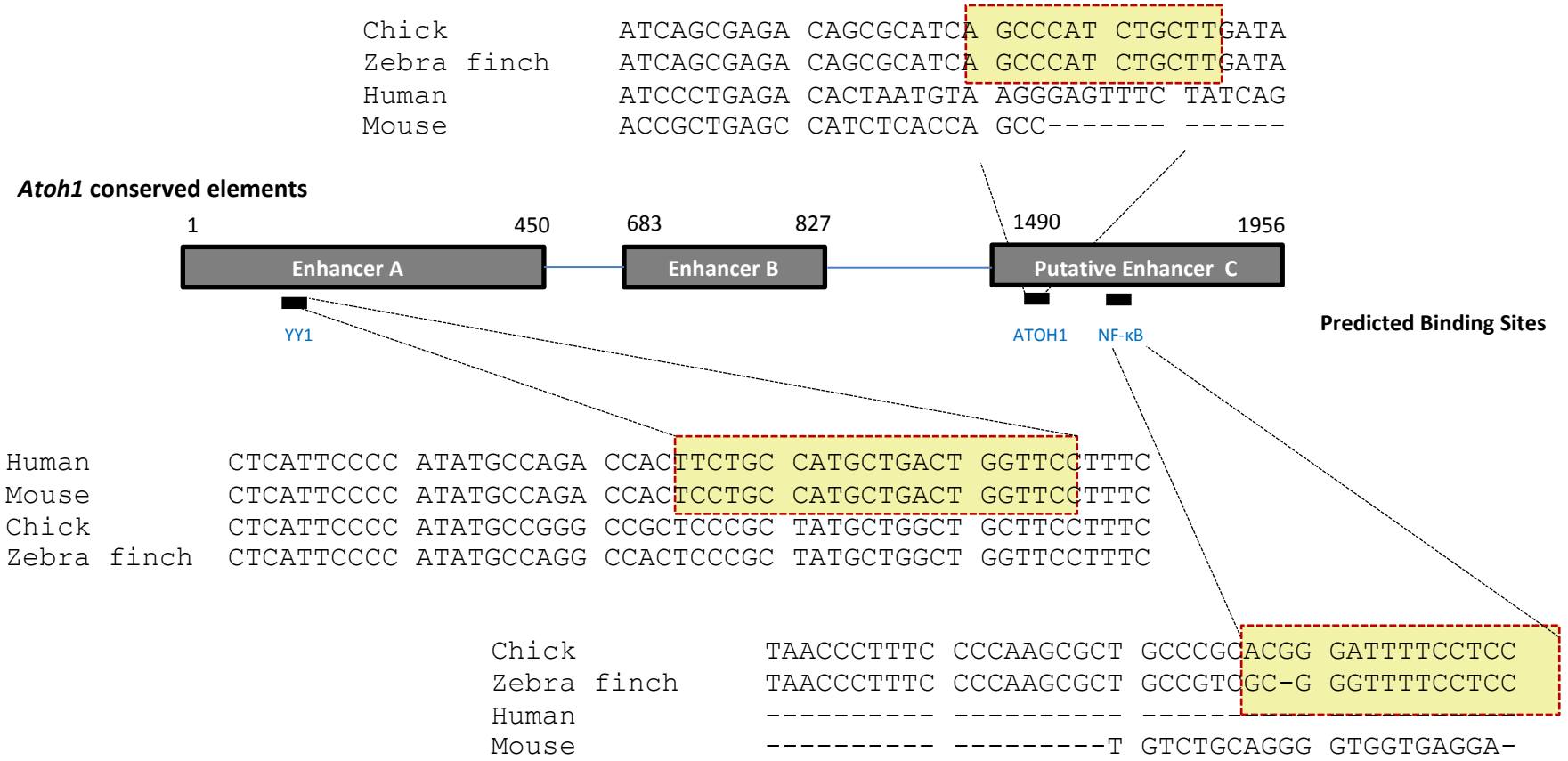

Table 3.1. MatInspector analysis of candidate genes. Conservation profiles of the binding sites for the different transcription factor candidates against a consensus binding site are represented by the Matrix and Core Similarity scores (> 0.8). The core base pairs of the predicted binding sites are represented in capital letters. Start and end positions represent the location of the binding sites relative to start of the enhancer A.

Candidate gene	Family/Matrix	Stringency level	Predicted expression	Start position	End position	DNA Strand	Matrix similarity	Core similarity	Predicted binding site
YY1	V$YY1F/V$YY1.01	0.05	Ubiquitous	179	200	+	0.853	1	tcctgCCATgctgactggttc
NF-κB	V$NFKB/ V$NFKAPPAB65.01	0.05	Blood cells, bone marrow cell, immuno system	1792	1902	+	0.982	1	acgggattTTCCtcc
ATOH1	V$NEUR	0	Brain, central neural system	1589	1606	+	0.985	1	agcccatCTGCtt

3.7 Binding profiles for the E2F transcription factor family

Nine putative E2F binding sites were identified by MatInspector at the chick and three at the mouse *Atoh1* gene locus (Figure 3.10). Based on the potential role that the E2F family could have in the regulation of *Atoh1*, these predictions were examined in greater detail.

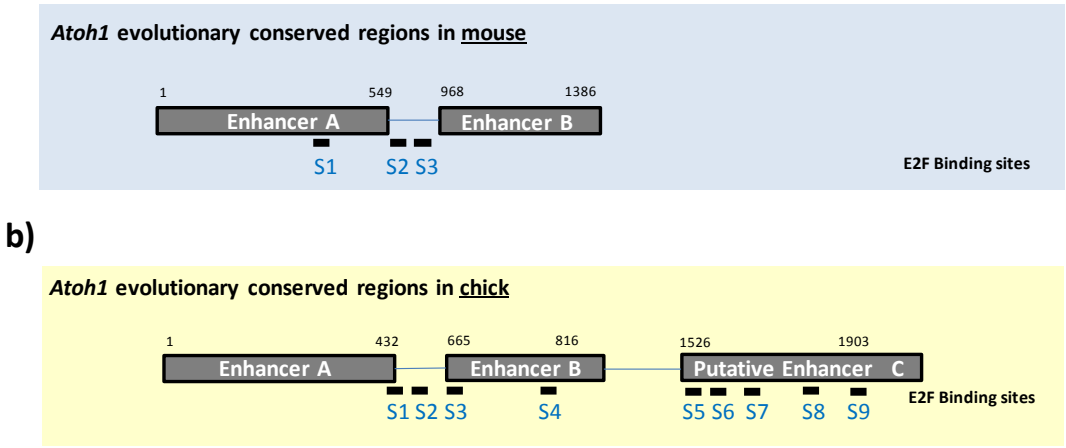

Figure 3.10. Predicted E2F binding sites in the mouse and chick *Atoh1* conserved regions. Summary of the E2F binding sites predicted by MatInspector. **a)** Three E2F binding sites were predicted in the mouse *Atoh1* conserved regions, one located within mouse *Atoh1* enhancer A and two located in the sequence between enhancer A and B. **b)** In the chick, nine E2F binding sites were predicted. One within chick *Atoh1* enhancer A, one in the sequence between enhancer A and B, two within chick enhancer B and five within putative enhancer C.

The genomic location of the predicted binding sites is summarized in Figure 3.10. In chick, four potential E2F binding sites were predicted within the chick *Atoh1* enhancer AB (sites 1-4 in Table 3.2) and five binding sites were predicted within the chick putative enhancer C (sites 5-9 in Table 3.3). In some cases, two or more overlapping E2F binding sites were predicted in the same genomic region and therefore were grouped as a single site (e.g. site 2 and 5 predicted in the chick *Atoh1*; Table 3.2 and Table 3.3). Almost all the predicted matches for E2F have a matrix similarity score higher than 0.8 which classify them as a good match. A few E2F binding sites within putative enhancer C score lower than 0.8 (Table 3.3). However, since the value is close to the 0.8 threshold and in some cases two or more binding

sites overlapped at the same DNA site, they were included as a potential E2F match (sites 5, 6, 8 and 9 in putative enhancer C). The core similarity scores described by MatInspector are also annotated in Table 3.2 and Table 3.3. As with the matrix similarity, the score for the core similarity is measured from 0 to 1 and in most cases were above or close to 0.8 for the E2F binding site predictions in the chick sequence.

A similar strategy was also conducted with the putative E2F binding sites predicted at the mouse *Atoh1* locus. Table 3.4 shows the three E2F binding sites that were predicted at the mouse *Atoh1* locus and their relative positions within the mouse *Atoh1* enhancer A and B region. The binding sites predicted in mouse were compared against those predicted in the chick *Atoh1* locus however no sequence homology between the chick and mouse E2F binding sites was found.

Table 3.2. Predicted E2F binding sites within chick *Atoh1* enhancer region. Summary of the MatInspector analysis with the location of the different E2F sites that were predicted in the positive and/or negative strand of chick *Atoh1* enhancer sequence. Conservation profiles of the different predictions against a consensus E2F site are represented by the matrix and core similarity. The matrix scores for all the E2F sites are > 0.8 and the core similarity is 1 which defines these predictions as good matches. The core of the binding site is presented in capital letters and the names given for each E2F binding site is represented from S1 to S4 based on the relative position within the chick *Atoh1* locus.

Family/Matrix	Predicted expression	Start position	End position	DNA Strand	Matrix similarity	Core similarity	Predicted binding site	Given name
V$E2FF/E2F2.01 V$E2FF/E2F3.01	ubiquitous	420	437	+ and -	0.934-0.944	1	ggagaGCGCgcacttcg	Site 1 (S1)
V$E2FF/E2F.02 V$E2FF/E2F1_DP2.01 V$E2FF/E2F4_DP2.01	ubiquitous	457	474	-	0.8	1	aaaaAGCGaTAAAaaat	Site 2 (S2)
V$E2FF/E2F2.01 V$E2FF/E2F3.01	ubiquitous	688	705	-	0.8	1	acacgGCGCaccgcggc	Site 3 (S3)
V$E2FF/E2F3.02	ubiquitous	756	773	+	0.8	1	aggcgGCGCcccgggga	Site 4 (S4)

Table 3.3. Predicted E2F binding sites within chick *Atoh1* putative enhancer C. MatInspector also predicted E2F binding sites in the chick putative enhancer C which were grouped in five sites (S5-S9). Matrix and core similarity scores were close or higher than 0.8 and therefore were considered as a potential match. The core of the binding site is presented in capital letters and the different E2F sites that were predicted in the positive and/or negative strand of chick putative enhancer C sequence.

Family/Matrix	Predicted expression	Start position	End position	DNA Strand	Matrix similarity	Core similarity	Predicted binding site	Given name
V$E2FF/E2F1_DP2.01 V$E2FF/E2F2.01 V$E2FF/E2F3.01	ubiquitous	1526	1553	+ and -	0.78-1	0.77-1	cctCGCGCGtggtcCCGCCcgctctcc	Site 5 (S5)
V$E2FF/E2F.03 V$E2FF/E2F1_DP2.01 V$E2FF/E2F2.01 V$E2FF/E2F3.01 V$E2FF/E2F4_DP2.01	ubiquitous	1543	1580	+ and -	0.79-1	0.79-1	tgcgcgctcccGCGCccaaCGCGGgacagcgacgcgc	Site 6 (S6)
V$E2FF/E2F2.01	ubiquitous	1589	1606	-	0.8	1	ataaaGCGCggcagcac	Site 7 (S7)
V$E2FF/E2F.01	ubiquitous	1702	1719	+	0.75	0.75	cttccccggGAGAacgc	Site 8 (S8)
V$E2FF/E2F.01	ubiquitous	1797	1814	+	0.78	1	tttcctcccGAAAaacg	Site 9 (S9)

Table 3.4. Predicted E2F binding sites within mouse *Atoh1* enhancer region. Summary of the MatInspector analysis of the different E2F sites predicted in the sequence region of the mouse *Atoh1* enhancers. Conservation profiles of the different predictions against a consensus E2F site are represented by the matrix and core similarity. The matrix scores for all the E2F sites is > 0.8 and the core similarity is close to 0.8 or above which define these predictions as good matches. The core of the binding site is presented in capital letters and the names given for each E2F binding site is represented from S1 to S4 based on the relative position within the mouse *Atoh1* locus.

Matrix	Detailed Matrix information	Tissue	Start position	End position	DNA Strand	Core similarity	Matrix similarity	Predicted binding site	Given name
V$E2F.02	E2F-myc activator/cell cycle regulator E2F, involved in cell cycle regulation, interacts with Rb p107 protein	ubiquitous	499	516	-	1	0.849	gtggtgagcCAAAaccc	Site 1 (S1)
V$E2F.02	E2F-myc activator/cell cycle regulator E2F, involved in cell cycle regulation, interacts with Rb p107 protein	ubiquitous	712	729	+	1	0.849	actgagcccCAAAgttg	Site 2 (S2)
V$E2F1_DP2.01	E2F-myc activator/cell cycle regulator E2F-1/DP-2 heterodimeric complex	ubiquitous	844	861	+	0.795	0.831	agatCGCGggcaaagac	Site 3 (S3)

3.8 Discussion

In this chapter a comparative analysis of the sequences at the *Atoh1* locus was conducted across mammalian and avian species. The 3' region downstream of the *Atoh1* coding sequence contains two evolutionary conserved elements, enhancer A and enhancer B, which have previously been described to be sufficient to drive *Atoh1* expression (Helms et al. 2000). By contrast, the same study showed that the 5' region, upstream of the *Atoh1* coding sequence, was not required for *Atoh1* expression (Helms et al. 2000). Based on this work using reporter constructs in transgenic mice, Helms et al. hypothesized the existence of other regulatory elements that participate in the regulation of *Atoh1*, in addition to the *Atoh1* A and B enhancers (see section 1.7.2). Therefore a comparative analysis was conducted to identify evolutionary conserved regions in mammalian and avian species. The results of this analysis supported the previous work (Helms et al. 2000; Ebert et al. 2003). Hence, in mammals the sequences within the *Atoh1* enhancer A and B share a high degree of conservation between mouse and human (90.73% for enhancer A and 88.79% for enhancer B) (Figure 3.1). Similarly, the comparison of the *Atoh1* enhancers in avian species showed that the homology of these enhancers was 89.76% and 88.36% respectively for enhancer A and B between chick and zebra finch suggesting that these also exist in avians (Figure 3.2). Interestingly, an additional highly conserved region was identified in chick and zebra finch. This region, termed putative enhancer C, is located about 700 bp downstream of enhancer B and shares 79.61% homology between chick and zebra finch (Figure 3.2). This putative enhancer C is a unique region to avian species and was not found in any of the mammalian species analysed in this study (Figure 3.3). Based on the degree of conservation of the putative enhancer C in avians, my investigation presented in subsequent chapters focused on determining whether putative enhancer C is involved in the regulation of *Atoh1* in chick (described in chapters 5 and 6).

Following the comparative alignment, a bioinformatic analysis was conducted using MatInspector from Genomatix (version 9.0) to identify putative transcription factors binding to the mammalian and avian *Atoh1* evolutionary conserved regions. In the inner ear, very little is known about which transcription factors contribute to the regulation of *Atoh1* expression (Ahmed et al. 2012; Neves et al. 2012). Having predicted over 200 putative candidates that potentially could bind to the *Atoh1* enhancer AB or putative

enhancer C, four candidates were selected for further functional analysis based on the conservation profiles of their predicted binding sites and their potential roles in auditory hair cell maintenance and survival.

The ability of these candidates to regulate *Atoh1* expression was subsequently tested in reporter gene assays and EMSA experiments (Chapter 4). In addition, expression data are also presented for one of these transcription factor candidates, providing strong evidence that this candidate could be involved on the regulation of *Atoh1* (Chapter 5).

Chapter 4

4 Investigation of putative candidates regulating *Atoh1*

Having identified the presence and location of YY1, NF-κB and ATOH1 binding site predictions within the *Atoh1* locus and based on the expression profiles and functions of the selected transcription factor candidates, I investigate whether YY1, NF-κB and ATOH1 do bind and regulate the *Atoh1* expression using electrophoresis mobility shift assays (EMSAs) and reporter gene assays.

4.1 EMSA analysis of candidate binding sites

To assess the ability of YY1 and NF-κB to bind the *Atoh1* conserved regions, EMSAs were conducted. This technique is used to detect interactions between protein complexes and nucleic acids based on the observation that the electrophoretic mobility of a protein-DNA complex is less than that of the free nucleic acid (Hellman and Fried 2007). In addition, sequence specificity of a given transcription factor binding site can be investigated in competition assays with known or consensus binding sites.

To perform these experiments, double stranded oligonucleotides were designed against the predicted binding site sequences for YY1 and NF-κB (Table 4.1). Oligonucleotides were radiolabelled as described in section 2.2.8.5 and incubated with nuclear extracts from UB/OC2 cells, either alone or in a competition assay with an excess of an unlabelled competitor.

The ability of YY1 to bind the *Atoh1* enhancer A was assessed using EMSA analysis shown in Figure 4.1. Several DNA-protein complexes (referred to as bandshifts) were observed when the radiolabelled oligonucleotide containing the predicted YY1 binding site was incubated with UB/OC2 cell nuclear protein extracts (Figure 4.1 bandshifts A_1, B_1, C_1). The banding pattern showed two slow-migration DNA-protein complexes (Figure 4.1 A_1 bandshifts) and two protein-DNA complexes with a faster migration (Figure 4.1 B_1 and C_1). On competition with an unlabelled YY1 consensus binding site, the A_1 and B_1 complexes were slightly attenuated by an excess of unlabelled YY1

consensus (lanes 3-6) whereas the C_1 protein-DNA complex was completely attenuated by x500 excess of unlabelled YY1 (lane 6). Competition with 500-fold of unlabelled non-specific competitor, had no effect on the A_1, B_1 and C_1 bandshifts (lane 7). This pattern suggests that the protein-DNA complex C_1 contains the YY1 transcription factor bound in a sequence dependent manner. The A_1 and B_1 protein-DNA complexes are less likely to be produced by YY1 since the level of competition by an excess of a YY1 consensus probe was much lower.

Table 4.1. Oligonucleotides for YY1 and NF-κB EMSA analysis. EMSA oligonucleotides containing the predicted binding sites given by MatInspector. Oligonucleotides for the consensus binding sites for YY1 and NF-κB were also designed and synthesised for EMSA competition assays. The sequences of the binding sites for the transcription factor candidates are presented and the core of the binding site is underlined.

Oligo name	Probe Sequence (5' to 3')	Length (bp)	Prediction
YY1_Sense	ACCACTCCTGCCATGCTGACTGGTTCCTTTC	31	Enhancer A
YY1_Antisense	GAAAGGAACCAGTCAGCATGGCAGGAGTGGT	31	Enhancer A
YY1_Con_Sense	CGCTCCCCGGCCATCTTGGCGGCTGGT	27	Consensus
YY1_Con_Antisense	ACCAGCCGCCAAGATGGCCGGGGAGCG	27	Consensus
NF-κB _Sense	CCCGCACGGGATTTTCCTCCCGAAA	25	Putative enhancer C
NF-κB _Antisense	TTTCGGGAGGAAAATCCCGTGCGGG	25	Putative enhancer C
NF-κB _Con_Sense	AGTTGAGGGGACTTTCCCAGGC	22	Consensus
NF-κB _Con_Antisense	GCCTGGGAAAGTCCCCTCAACT	22	Consensus

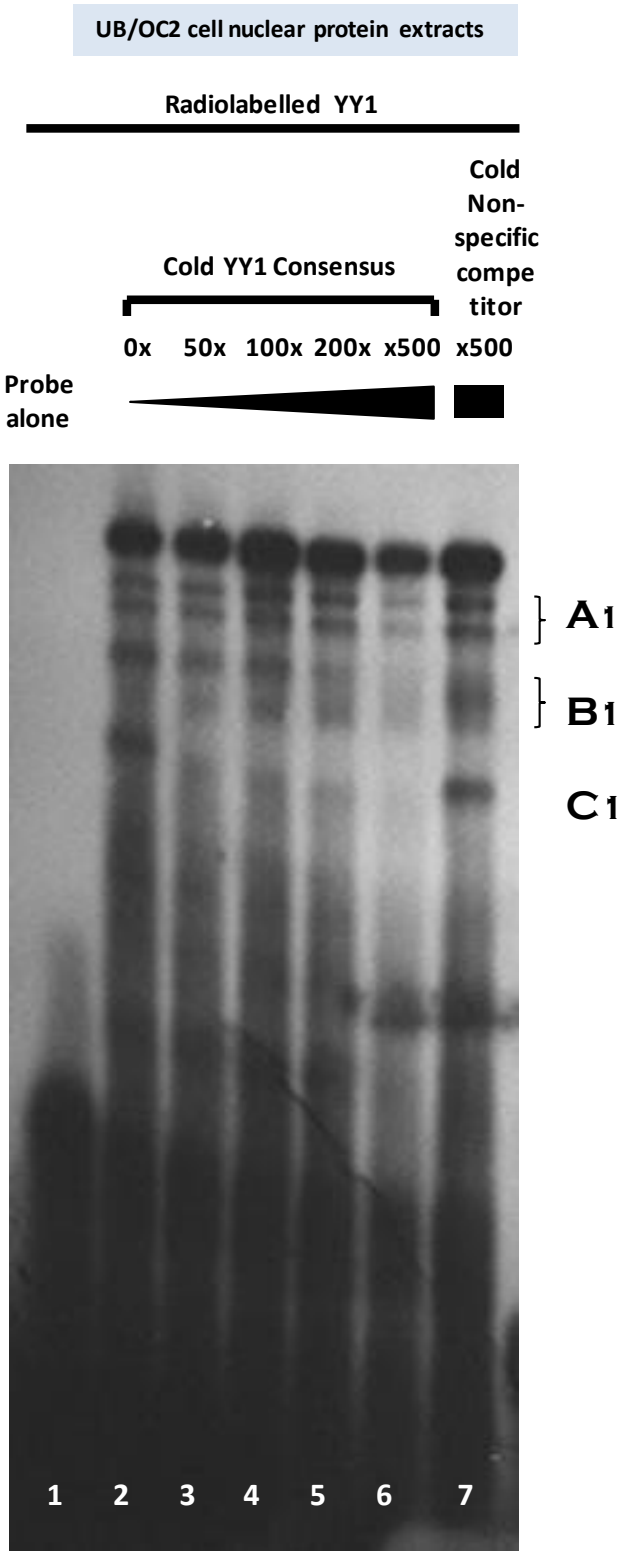

Figure 4.1. Binding of YY1 to *Atoh1* enhancer A binding site. A radiolabelled probe containing the predicted YY1 binding site sequence was incubated in the absence of nuclear extracts (lane 1) or with 10µg of UB/OC2 cell nuclear extracts (lanes 2-7) either in the absence of competitor (lane 2) or in a competition with an excess of unlabelled consensus YY1 (lanes 3-6) or with an unlabelled non-specific competitor (lane 7). The different shifted DNA-protein complexes were named as A_1, B_1 and C_1 and labelled on the right of the figure.

As with YY1, the ability of NF-κB to bind to the *Atoh1* putative enhancer C was also tested on EMSA assays. In EMSA analysis shown in Figure 4.2, the predicted NF-κB binding site sequence produced several distinct protein-DNA complexes when incubated with UB/OC2 cell nuclear extracts (Figure 4.2, lane 2 bandshifts A_2-D_2). On competition with unlabelled consensus NF-κB oligonucleotide, the A_2 and C_2 protein-DNA complexes were attenuated even at 50 fold competition (Figure 4.2, lanes 3-6) whereas bandshift D_2 was only significantly attenuated by 200 fold excess competition (Figure 4.2, lane 6). By contrast, competition was not seen in the complex that generated the bandshift B_2 suggesting that B_2 is not NF-κB sequence specific (Figure 4.2, lanes 3-6). Competition with 500-fold unlabelled non-specific competitor showed that both A_2 and C_2 bandshifts were not attenuated suggesting that the protein-DNA complexes A_2 and C_2 are NF-κB sequence specific (Figure 4.2, lane 7). In contrast, the D_2 bandshift was competed in a similar manner by both a consensus NF-κB (Figure 4.2, lane 6) and non-specific competitor (Figure 4.2, lane 7) suggesting that the protein-DNA complex D_2 is not NF-κB sequence dependent.

In summary, EMSA experiments suggested that YY1 and NF-κB have the capacity to bind to the putative binding sites identified by MatInspector in the *Atoh1* conserved elements. Given the evidence of an interaction between both YY1 and NF-κB with *Atoh1*, this regulation was investigated in reporter gene assays.

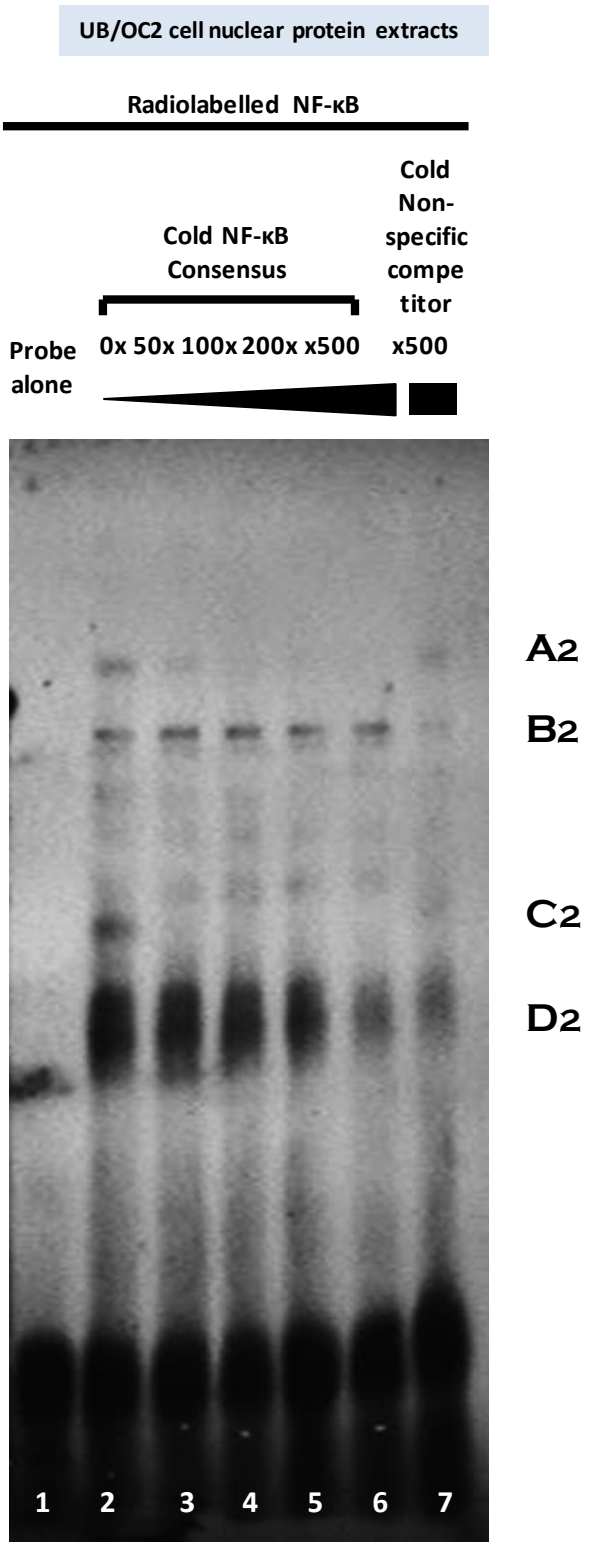

Figure 4.2. Binding of NF-κB to putative enhancer C. A radiolabelled probe containing the predicted NF-κB binding site sequence was incubated in the absence of nuclear extracts (lane 1) or with 10µg of UB/OC2 cell nuclear extracts (lanes 2-7) either in the absence of competitor (lane 2) or in a competition with an excess of unlabelled consensus NF-κB (lanes 3-6) or with an unlabelled non-specific competitor (lane 7). The different shifted DNA-protein complexes were named as A_2, B_2, C_2 and D_2 and labelled on the right of the figure.

4.2 Transcriptional activation of *Atoh1* conserved regions by candidate regulators

EMSA analysis showed evidence of specific binding of two of the transcription factor candidates to the *Atoh1* conserved regulatory elements. To further investigate the functional properties of the candidate genes in the regulation of *Atoh1*, reporter gene assays were conducted. The ability of the potential candidate regulators (NF-κB, YY1 and ATOH1) to control *Atoh1* was therefore tested in luciferase assays. Expression constructs for all the transcription factors, were obtained from different laboratories and used in co-transfections with the *Atoh1* luciferase reporters that had been constructed (see section 2.2.9.3 and section below). The UB/OC2 cell line derived from auditory epithelia pre-cursors was used for this functional analysis (kindly provided by Professor Matthew Holley, University of Sheffield). UB/OC2 cells represent a valuable resource for the study of gene regulation since they express several hair cell markers such as POU4F3, α9AChR, Myosin7a and Myosin6 (Rivolta and Holley 2002). In addition, *Atoh1* mRNA production was also detected in our laboratory by q-PCR in UB/OC2 cells (data not shown) which confirms that all the physiological machinery necessary to transcribe *Atoh1* is present in this cell line.

4.2.1 Cloning of the mouse and chick *Atoh1* conserved elements

To investigate the regulation of the mouse and chick *Atoh1* conserved regions by the selected transcription factor candidates, luciferase constructs containing the chick and mouse *Atoh1* conserved regions were produced. At the time my investigation started, a few publications reported studies with the mouse *Atoh1* enhancer A and B cloned into the pGL3 luciferase constructs (Shi et al. 2010; Terrinoni et al. 2013). However, luciferase constructs containing the chick *Atoh1* enhancer A and B and the novel putative enhancer C did not exist. Hence, the pGL4 luciferase constructs (Promega®) were chosen for the cloning of the *Atoh1* conserved regions. This generation of reporter vector has advantages in comparison to the pGL3 luciferase constructs. These include engineered the removal of many consensus transcription factor binding sites in the vector backbone reducing the risk of artefactual regulation of the base vector. Therefore the mouse and chick *Atoh1* enhancers and the chick putative enhancer C were cloned into the pGL4.23 luciferase construct. The pGL4.23 vector contains a minimal promoter 32 bp upstream of the transcription start site to drive basal expression of the *luc2*

reporter gene and facilitates the analysis of enhancer sequences cloned into the vector. The cloning strategy that was followed to generate all these constructs was described in detail in methods section 2.2.9.3. All *Atoh1* conserved regulatory elements were positioned either upstream or downstream of the minimal promoter sequence in the pGL4.23 luciferase construct. The position of the *Atoh1* conserved regulatory elements is shown for each reporter assay since it varies for each experiment. The dual luciferase assay system was used for these experiments because it allows sequential measurement of two independent luciferase reporters within a single sample. Hence, the activity of the Firefly luciferase *(Photinus pyralis)* from the experimental reporter is determined relative to the activity of the Renilla luciferase (*Renilla reniformis*) which is used as an internal control to adjust for differences in transfection rate and cell number.

4.2.2 Effect of YY1 on the *Atoh1* conserved non-coding elements

The ability of YY1 to regulate the mouse and chick *Atoh1* conserved regions was tested in luciferase assays. To conduct these experiments an expression construct containing the open reading frame of the human YY1 was obtained from Dr Yang Shi, Boston Children's Hospital, US (Shi et al. 1991). The response of the different *Atoh1* luciferase constructs (shown in Figure 4.3a) to YY1 expression was investigated. A modest upregulation of 1.3 and 1.2-fold activation was detected on co-transfections of the YY1 expression vector via the mouse and chick *Atoh1* AB enhancers respectively (Figure 4.3b). A similar 1.3-fold activation was also observed via the chick putative enhancer C. However, when a construct containing the chick *Atoh1* enhancer AB together with the putative enhancer C (construct referred to as chickABC in Figure 4.3a), the activation previously observed through the chick *Atoh1* enhancer AB was reduced and instead a 20% downregulation was obtained after co-transfecting YY1. The base pGL4.23 luciferase vector did not show a response when co-transfected with YY1. Therefore, the responses observed in the *Atoh1* luciferase constructs were due to the presence of *Atoh1* conserved regions and not due to an artefactual response of the backbone of the pGL4.23 construct.

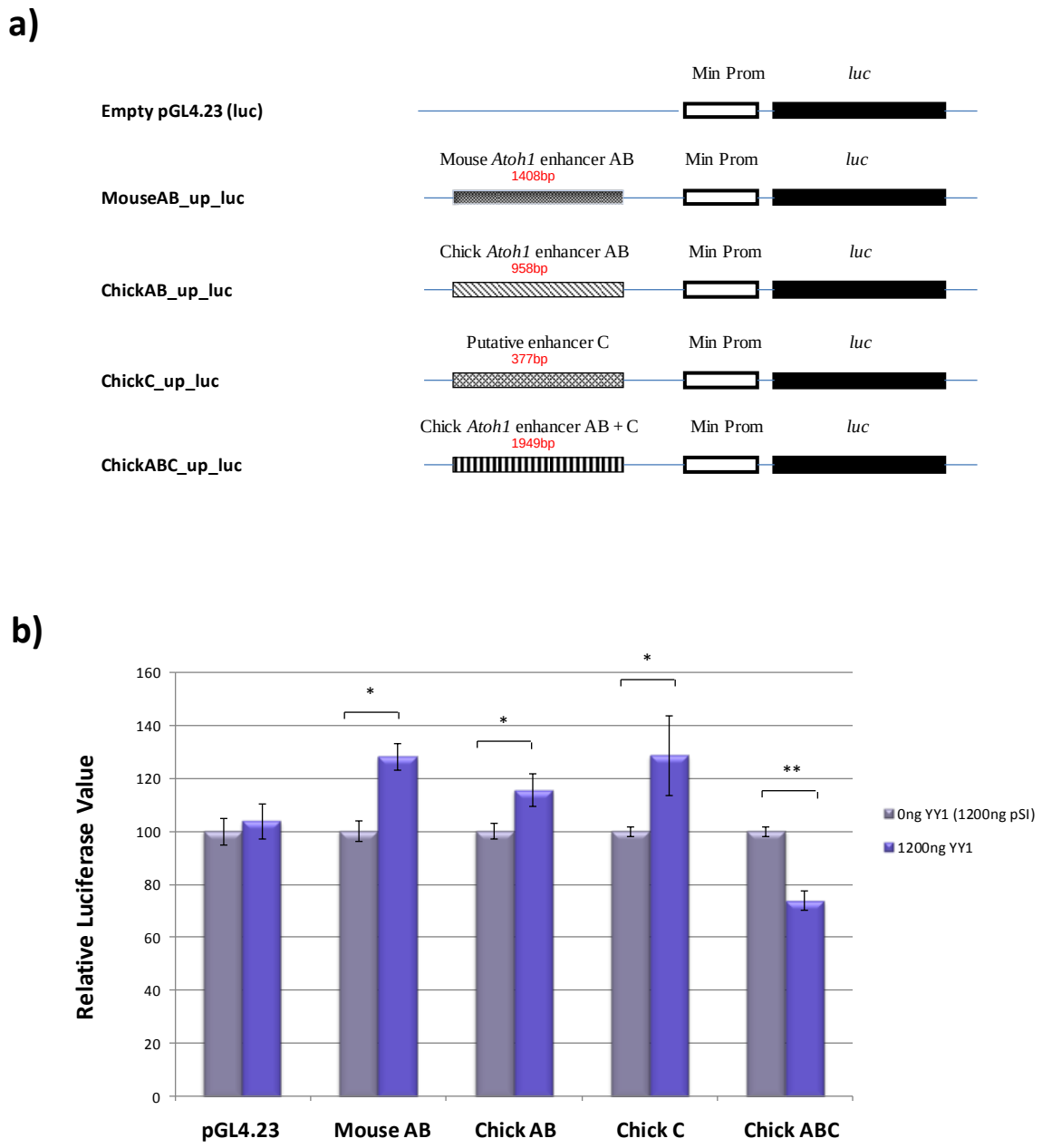

Figure 4.3. Effect of the YY1 transcription factor on the activity of the mouse and chick *Atoh1* enhancers and putative enhancer C. a) Schematic representation of the luciferase constructs containing the mouse or chick *Atoh1* conserved regions cloned into the luciferase vector pGL4.23 (referred as empty pGL4.23 luc). Both mouse and chick *Atoh1* conserved regions were located upstream of the luciferase gene for this reporter gene assay (constructs are referred as "up_luc"). **b)** UB/OC2 cells were co-transfected with 200ng of empty pGL4.23 and the different *Atoh1* luciferase constructs, 10ng of pRL-null and 1200ng of the expression constructs (pSI or YY1). The luciferase activity of each reporter is normalized to its response in the absent of stimulation (set at 100). Error bars on charts represent the standard error of the mean. Statistical significance was assessed using a paired Student t-test (**p< 0.01 or *p<0.05). Experiments were conducted in triplicate in two separate assays with different DNA preparations for each construct (n=6).

4.2.3 Effect of NF-κB on the *Atoh1* conserved non-coding elements

The ability of NF-κB to regulate the mammalian and avian *Atoh1* conserved regions was also tested in luciferase assays. An expression vector containing the human NF-κB p65 cDNA sequence was obtained from University of Michigan Medical Center, US (Schmid et al. 1991) and co-transfected with the *Atoh1* luciferase constructs (Figure 4.4a). The results from this experiment showed no significant response of mouse and chick *Atoh1* AB enhancers to NF-κB (Figure 4.4b). A similar response was obtained for the construct containing the chick putative enhancer C. However, the construct containing the chick *Atoh1* enhancer AB and putative enhancer C (referred to as chick ABC) showed a modest 25% downregulation when it was co-transfected with NF-κB.

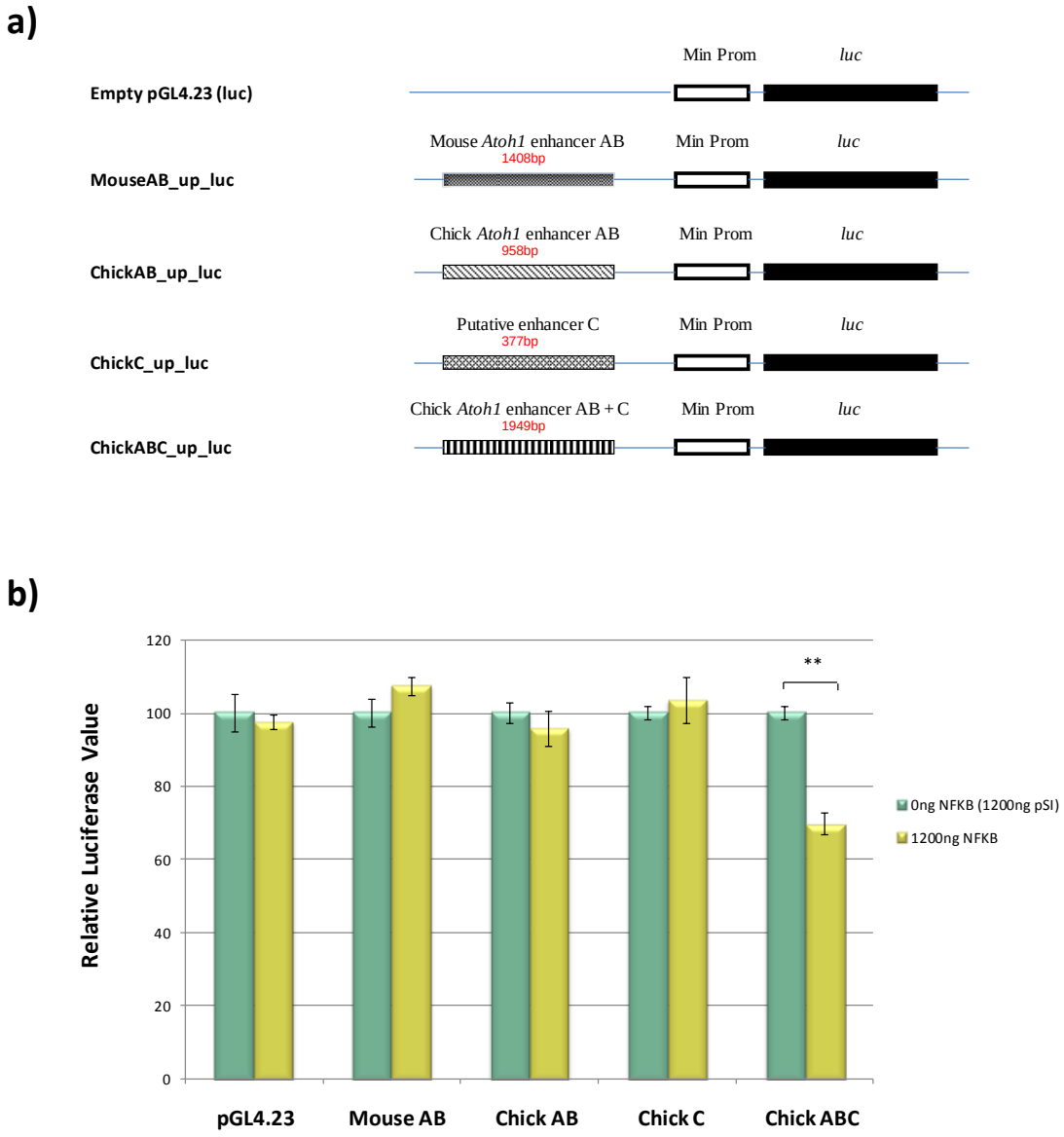

Figure 4.4. Effect of the NF-κB transcription factor on the mouse and chick *Atoh1* enhancers and putative enhancer C. a) Schematic representation of the luciferase constructs containing the mouse or chick *Atoh1* conserved regions cloned into the luciferase vector pGL4.23 (referred as empty pGL4.23 luc). Both mouse and chick *Atoh1* conserved regions were located upstream of the luciferase gene for this reporter gene assay (constructs are referred as "up_luc"). **b)** UB/OC2 cells were co-transfected with 200ng of the empty pGL4.23 and the different *Atoh1* luciferase constructs, 10ng of pRL-null and 1200ng of the expression constructs (pSI or NF-κB). The luciferase activity of each reporter is normalized to its response in the absent of stimulation (set at 100). Results showed a 1.3-fold downregulation when the Chick ABC construct is co-transfected with NF-κB (**p< 0.01). Error bars on charts represent the standard error of the mean. Statistical significance was assessed using a paired Student t-test. Experiments were conducted in triplicate in two separate assays with different DNA preparations for each construct (n=6).

4.2.4 Effect of ATOH1 on the *Atoh1* conserved non-coding elements

The interaction between ATOH1 itself and the *Atoh1* A and B mouse enhancers has been shown (Helms et al. 2000). ATOH1 has the ability to bind to E-box consensus sites (Jarman et al. 1993) (Akazawa et al. 1995). Interactions between ATOH1 and E-box sites within mouse *Atoh1* enhancer B, are essential for ATOH1 expression in the neural tube at E10.5 (Helms et al. 2000). ATOH1 is also required for the correct regulation of the *Atoh1* enhancers in the neural tube according to transgene studies in mice conducted at E10.5 (Helms et al. 2000). Expression of an *Atoh1*/*lacZ* reporter transgene in the neural tube is absent in an *Atoh1* knockout mouse model suggesting an autoregulatory feedback loop requiring ATOH1.

However, how the *Atoh1* A and B mouse enhancers and other regulatory elements respond in other tissues/cells expressing ATOH1 and at other stages during development still remains unexplored. Therefore the effect of ATOH1 on the *Atoh1* conserved regions was investigated under *in vitro* conditions by the use of reporter gene assays in UB/OC2 cells. It is important to consider that an approach based on *in vitro* techniques possess some limitations (discussed further in 4.3). However it can provide a useful insight into the molecular mechanism of *Atoh1* gene regulation in a cell line were ATOH1 is expressed.

Hence, to assess whether ATOH1 is able to activate the *Atoh1* A and B enhancers under *in vitro* conditions, luciferase assays were conducted. In addition, the effect of ATOH1 on the putative enhancer C was also investigated since a bHLH binding site (a putative ATOH1 binding site) was predicted in the putative enhancer C.

4.2.4.1 Investigating the autoregulation of ATOH1 via the *Atoh1* conserved elements

An initial investigation was carried out to quantify the response of the various mouse and chick *Atoh1* evolutionary conserved elements with increasing amounts of transfected ATOH1 in order to identify whether this response is dose-dependent. A dose response effect is a characteristic mechanism of direct binding between transcription factors and regulatory regions. Since previous evidence suggested the binding of ATOH1 to the E-box site in the *Atoh1* enhancer B (Helms et al. 2000), a gradient effect on the response of *Atoh1* enhancer AB was expected when the amount of ATOH1 was

increased. However, as shown in Figure 4.6, the expected activation of the mouse and chick *Atoh1* enhancer AB constructs was not observed. The experiments showed no significant effect on the response of the mouse *Atoh1* enhancer AB and the chick *Atoh1* enhancer AB constructs. Only a modest downregulation was observed when the highest amount of ATOH1 was co-transfected (1200ng of ATOH1 in Figure 4.6b). Similar results were obtained with the chick putative enhancer C construct giving a 10% downregulation when 800ng or 1200ng of ATOH1 were co-transfected. Only the construct containing both the chick enhancer AB and putative enhancer C (construct referred as chick ABC), showed a small upregulation of 1.2-fold when 400ng of ATOH1 were co-transfected. This effect was not observed when the amount of ATOH1 was increased to 800ng whereas a 30% downregulation was seen when 1200ng of ATOH1 were co-transfected. It is notable that a modest downregulation was obtained for all the *Atoh1* regulatory elements constructs when the highest amount of ATOH1 was used (1200ng). In addition, this small downregulation is only statistical significant in the chick *Atoh1* constructs but not in the mouse (Figure 4.5b).

In summary, these results were unable to demonstrate the predicted upregulation of ATOH1 on the various *Atoh1* regulatory elements and the observations vary between mouse and chick although none are dose dependent. One possible explanation for these results could be the relative position of the *Atoh1* conserved regions in the different luciferase constructs that were generated. For example, the mouse and chick *Atoh1* enhancer are cloned upstream of the minimal promoter whereas the putative enhancer C and the construct containing enhancers AB and putative C altogether were inserted downstream of the minimal promoter (Figure 4.5a). Therefore, the possibility of obtaining different results based on the relative position of the inserted regions in the luciferase constructs was considered. Hence, to minimize this possibility, the putative enhancer C and region ABC upstream of the minimal promoter were relocated and a new set of luciferase constructs was constructed (see section 2.2.9.3). Further experiments from this point on were conducted with the luciferase constructs containing all the *Atoh1* conserved elements upstream of the minimal promoter (constructs were referred with theirs corresponding name and as “up-luc” to indicate the position of the regulatory region).

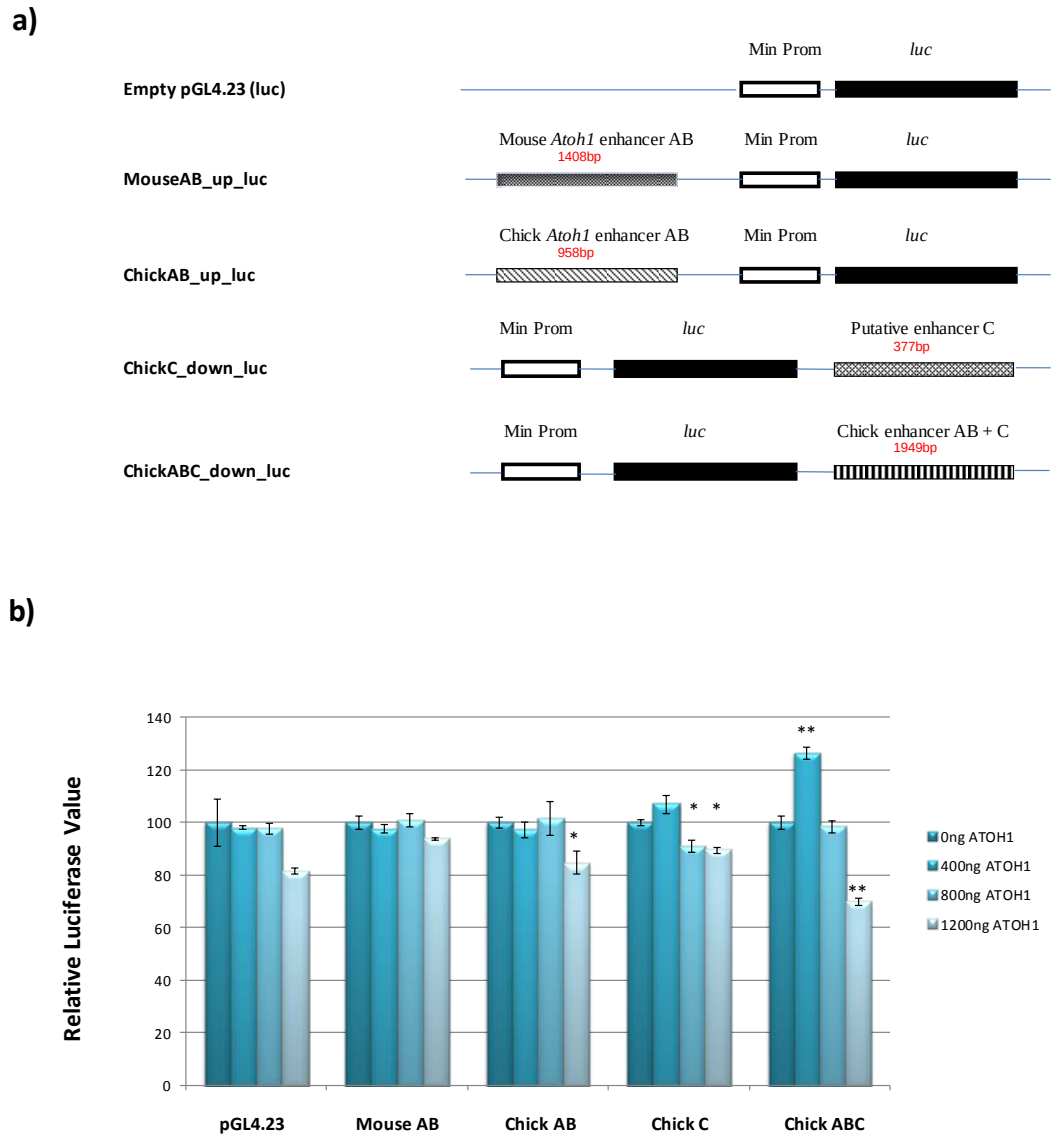

Figure 4.5. Dose-response effect of *ATOH1* on the *Atoh1* conserved elements. Initial investigation was conducted to assess response of the mouse and chick *Atoh1* enhancers and the putative enhancer C. **a)** Relative position of the *Atoh1* conserved elements in the luciferase constructs. The mouse and chick *Atoh1* enhancer were positioned upstream of the minimal promoter whereas the chick putative enhancer C and chick enhancer plus putative enhancer C were located downstream of the minimal promoter. **b**) Dose-responses of the different luciferase constructs when co-transfected with increasing amounts of ATOH1. The luciferase activity of each reporter is normalized to its response in the absent of stimulation (set at 100). Error bars on charts represent the standard error of the mean. Experiments were conducted in triplicate (n=3).

4.2.4.2 Effect of ATOH1 on the mouse and chick *Atoh1* enhancers AB and chick putative enhancer C

Having relocated the chick putative enhancer C and chick *Atoh1* enhancers plus putative C region upstream of the minimal promoter, all the *Atoh1* conserved elements were positioned in a similar relative location within the luciferase construct (Figure 4.6a). In order to assess the effect of ATOH1 on these new reporters, an additional set of luciferase experiments was conducted. Only the highest amount of ATOH1 was used in these experiments (1200ng) and the response of the *Atoh1* conserved elements was compared against the response with the same amount of the pSI construct (in the absence of exogenous ATOH1). In this experiment, no significant effect was observed on the mouse and chick *Atoh1* conserved elements when co-transfected with ATOH1 (Figure 4.6b). In addition, the relocation of the putative enhancer C and the putative enhancer C containing the ABC fragment did not give any significant differences in comparison to what it was observed before in previous experiments (Figure 4.5). These results suggest that ATOH1 on its own was not able to cause an upregulation on the *Atoh1* conserved elements in UB/OC2 cells. Consequently, I investigated whether ATOH1 needs the co-operation of other DNA binding proteins to produce the up-regulatory effect suggested in the literature (Akazawa et al. 1995) (Helms et al. 2000).

a)

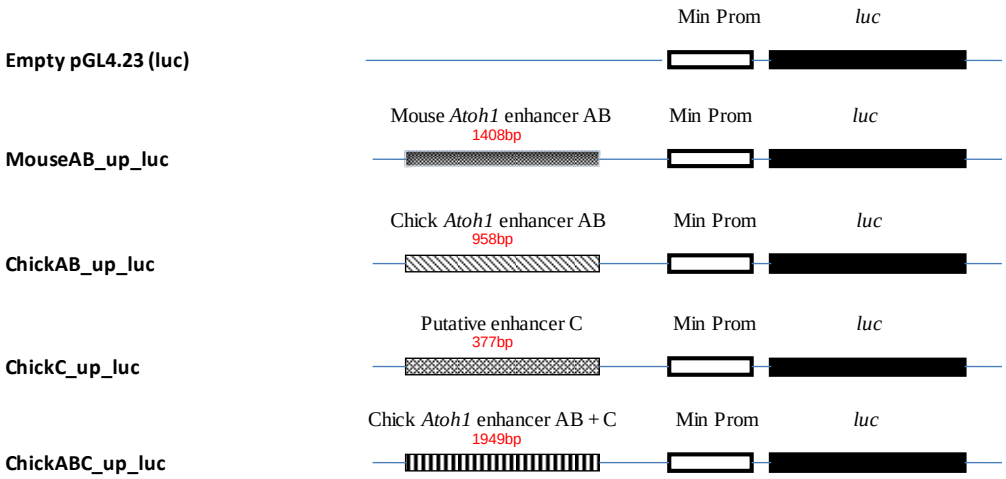

b)

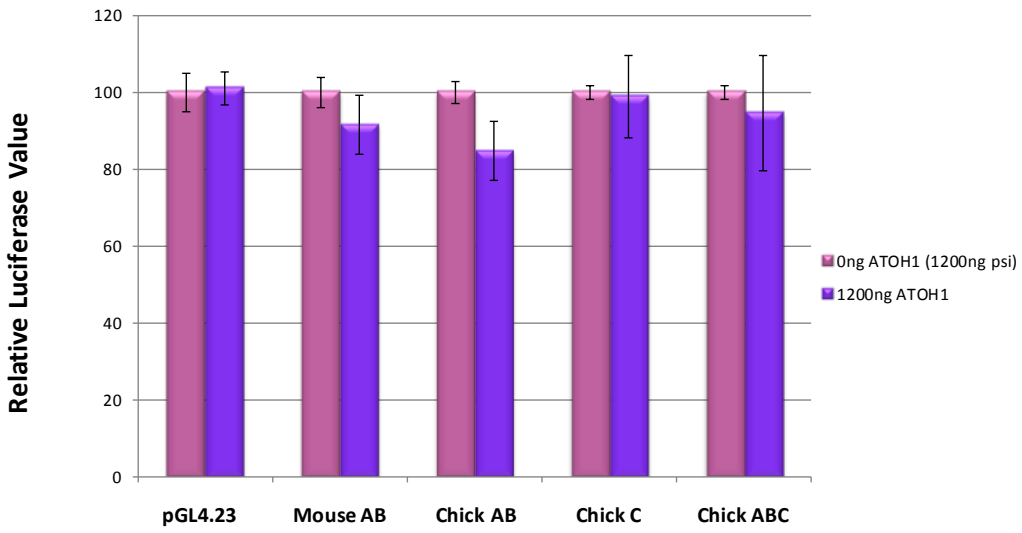

Figure 4.6. Effect of ATOH1 on the *Atoh1* non-coding conserved elements. a) Schematic representation of the *Atoh1* luciferase constructs. The putative enhancer C and the chick *Atoh1* plus putative enhancer C were repositioned upstream of the minimal promoter in comparison to previous experiment. **b)** UB/OC2 cells were co-transfected with the different *Atoh1* luciferase constructs (200ng) with and without ATOH1 (1200ng of ATOH1 or 1200ng of pSI). Luciferase activities are represented in comparison to the response without ATOH1 (set at 100) but transfecting the empty mammalian expression vector pSI to maintain the same amount of transfected DNA. Renilla expression vector phRL-null (10ng) was used as an internal control to correct differences in transfection efficiencies across experiments. Error bars on charts represent the standard error of the mean. The experiment was performed in triplicate and repeated twice with two different preparations of DNA (n=6).

4.2.5 Investigation of the effect of E47, the ATOH1 co-factor

In the previous section, it was observed that ATOH1 was not able to up-regulate the mouse or chick *Atoh1* enhancers. Previous transcriptional experiments using a mouse embryonic mesenchymal cell line, C3H10T1/2, have observed that interactions between ATOH1 and E-box sites are only possible when ATOH1 forms an heterodimer with the ubiquitous protein E47/E12 (Akazawa et al. 1995). In this study an upregulation of a construct containing seven sequential E-box sites was shown under the control of the β-actin promoter when ATOH1 was co-transfected with E47. In addition, EMSA experiments conducted by the same group and subsequent studies conducted by Helms et al., 2000, suggested that ATOH1 on its own cannot physically bind to E-box sites and that the binding is only possible when the ATOH1/E47 complex is formed. One explanation for the lack of activation of the *Atoh1* constructs therefore may have been the absence of E47. Based on these studies, I aimed to investigate whether the heterodimer formed by ATOH1 and E47 can activate consensus E-box sites and the *Atoh1* conserved regions in an auditory cell line (UB/OC2 cells).

4.2.5.1 Response of 3x *Atoh1* binding sites and mutant 3x *Atoh1* binding sites with and without E47

To investigate whether the heterodimer formed by ATOH1/E47 can activate consensus E-box sites in UB/OC2 cells, a luciferase construct was generated by cloning three sequential E-box sites downstream of a minimal promoter (described in section 2.2.9.3) and compared to a construct in which point mutations in the E-box sites had been introduced (Figure 4.7a). These two constructs were co-transfected with ATOH1 alone, E47 alone or ATOH1 and E47 together and compared against co-transfections without ATOH1 (transfected with the empty pSI expression vector). As observed in Figure 4.7b, transfection of ATOH1 alone did not show a significant effect on the response of the luciferase construct containing three E-box sites. However, co-transfections of E47 alone caused an upregulation of about 8-fold difference ($p<0.01$). By contrast, when both ATOH1 and E47 were co-transfected only a 4-fold upregulation was observed ($p<0.01$). For the construct containing the mutated E-box sites, none of the transfected expression constructs produced an effect. Since co-transfection of E47 activated the minimal promoter construct via E-box sites, I further investigated whether a similar response may be produced on the different *Atoh1* enhancers constructs as a consequence of the presence of E-box sites in these regions.

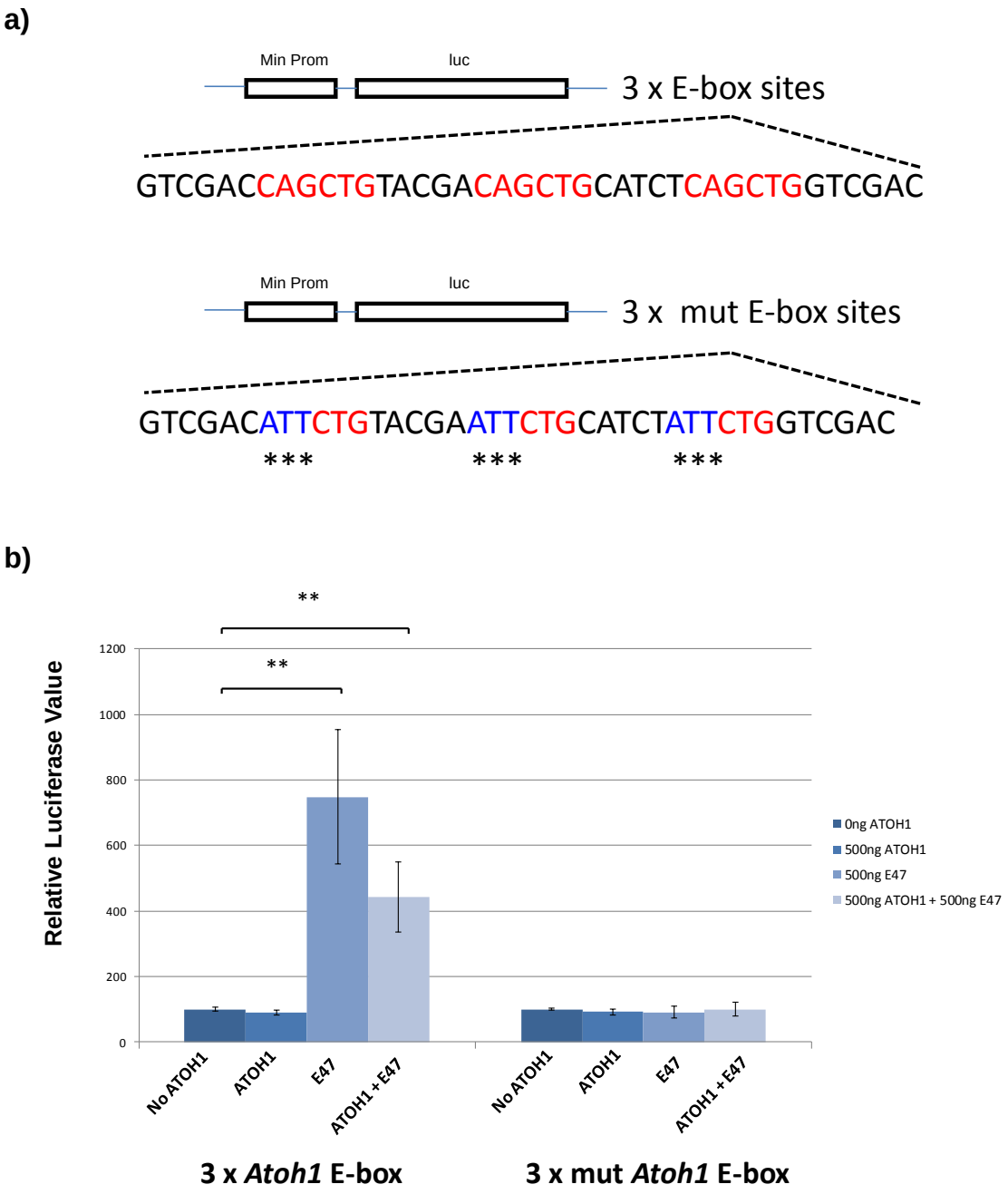

Figure 4.7. Effect of ATOH1 and E47 on the regulation of E-box sites. a) Schematic representation of the luciferase construct containing 3x E-box sites (represented in red) and the mutant version which carries 3xmutant E-box sites (in blue and marked by asterisks). Both luciferase constructs are driven by a minimal promoter sequence. **b)** UB/OC2 cells were co-transfected with either the 3x E-box sites or the 3x mut E-box sites luciferase construct with no ATOH1, ATOH1 alone, E47 alone or ATOH1 and E47 together. Luciferase responses are represented in comparison to the response given in the absence of stimulation with the empy pSIexpression vector (0ng of ATOH1). The empty pSI expression vector was also used to standarize concentrations of DNA across the different experiments. The renilla expression vector (phRL-null) was used as an internal control to normalize differences in transfection efficiencies. Error bars on charts represent the standard error of the mean. Statistical significance was assessed using a paired Student t-test (**p<0.01). The experiment was performed in triplicate and repeated twice with different preparations of DNA.

4.2.5.2 Effect of ATOH1 and E47 on the *Atoh1* enhancer and putative Enhancer C

Having observed an activation of the E-box sites by the E47, a further investigation was conducted to test whether similar results can be obtained on the mouse and chick *Atoh1* enhancer AB. Although, this approach would not verify the effectiveness of the E-box site in enhancer B, it would demonstrate the effect of E47 and the E47/ATOH1 complex on the entire enhancer sequence in an inner ear derived cell line. As shown in Figure 4.8, a 1.16-fold upregulation of the mouse *Atoh1* enhancer AB was observed when E47 was co-transfected, in comparison to the response observed in the absence of exogenous ATOH1. A greater effect on the mouse *Atoh1* enhancer AB was shown when ATOH1 and E47 were co-transfected together however, this response was small and not statistically significant (1.36-fold difference in Figure 4.8). The effect of ATOH1 and E47 on the chick *Atoh1* enhancer AB, chick putative enhancer C or on the chick *Atoh1* enhancer and putative enhancer C was also minimal and not statistically significant (chick AB, chick C and chick ABC constructs respectively in Figure 4.8).

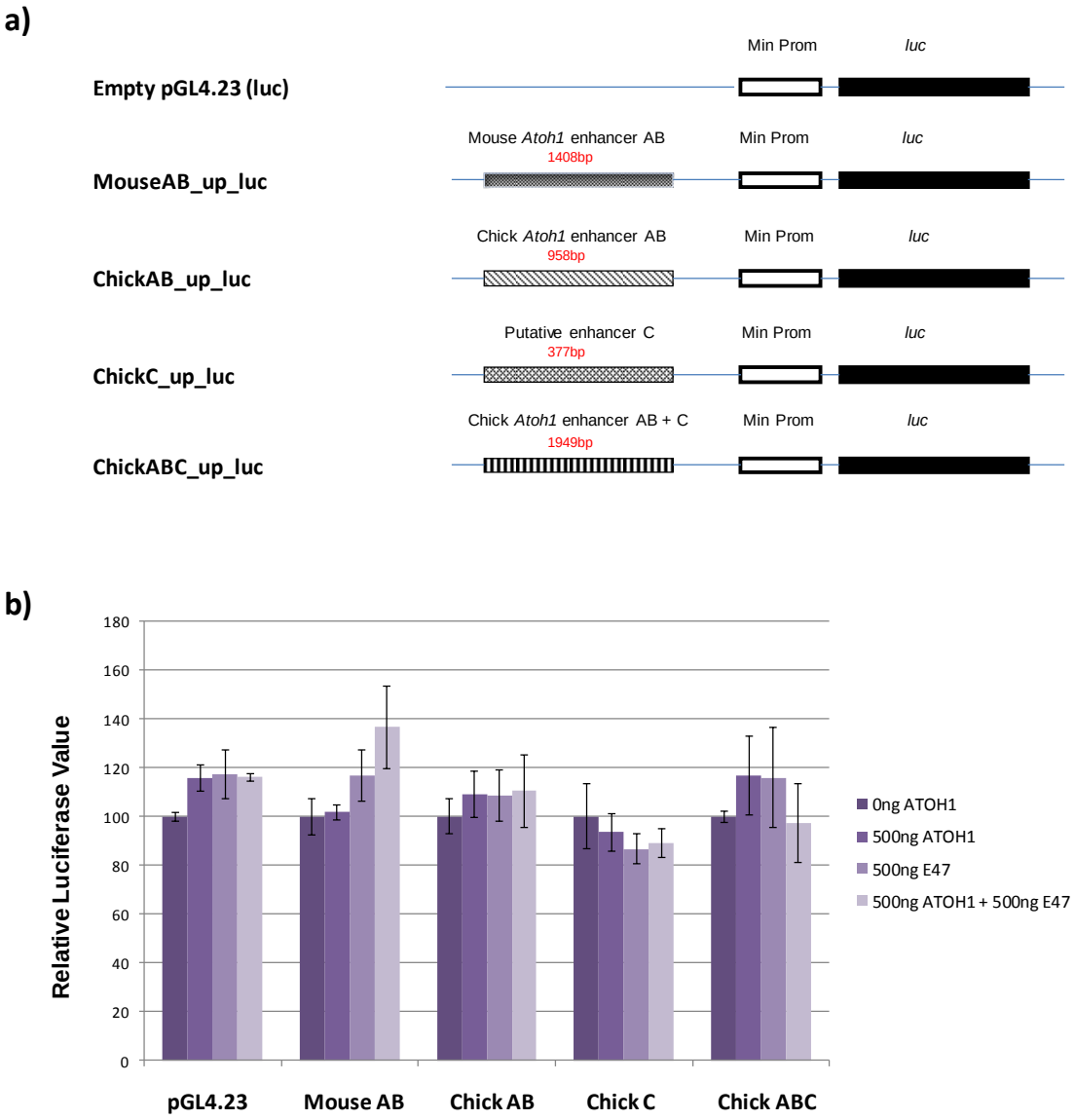

Figure 4.8. Effect of ATOH1 and E47 on the *Atoh1* evolutionary conserved regions. a) Schematic representation of the luciferase construct containing the *Atoh1* conserved regions upstream of the minimal promoter sequence. **b)** UB/OC2 cells were co-transfected with the luciferase construct containing the *Atoh1* conserved regions with the following expression constructs: ATOH1 alone, E47 alone or ATOH1 and E47 together. Luciferase responses are represented in comparison to the response given in the absence of exogenous ATOH1 (set at 100). The empty pSI expression vector was used to standardize concentrations of DNA across the different experiments. The Renilla expression vector (phRL-null) was used as an internal control to normalize differences in transfection efficiencies. Error bars on charts represent the standard error of the mean. Statistical significance was assessed using a paired Student t-test. No statistical differences were found in any of the constructs for all the treatments tested. The experiment was performed in triplicate and repeated twice with different preparations of DNA.

4.3 Discussion

Previous *in-vivo* studies have demonstrated that the *Atoh1* enhancers AB are sufficient to drive mouse ATOH1 expression (Helms et al. 2000). However, very little is known about how the interaction of different transcription factors may affect the regulation of the enhancers and consequently how this could influence the expression of ATOH1. Among others, YY1, NF-κB, and ATOH1 are transcription factors that were prioritized as putative candidates to bind to the *Atoh1* conserved elements based on the bioinformatic analysis conducted in this project. To define the strategy of the investigation, these candidates were prioritized for further investigation on the basis of their potential roles in hair cell development, maintenance and survival.

Ying Yang-1 (YY1), a zinc finger transcription factor was selected as a putative candidate to regulate *Atoh1* expression. It was predicted to bind the mammalian *Atoh1* enhancer A with the highest stringency given by MatInspector and therefore prioritized for being a strong putative candidate. Results from competition EMSA experiments demonstrated that some protein-DNA complexes (visualized on the gel as bandshifts) were YY1 sequence specific (Figure 4.1). However, further experiments with a YY1 antibody will be required in order to confirm whether the binding between YY1 and the *Atoh1* enhancer A is protein specific to confirm the presence of YY1 protein in the shift. In reporter gene assays, a 1.3 and 1.2-fold upregulation of the mouse and chick *Atoh1* enhancer AB constructs was observed in response to exogenous YY1 respectively (Figure 4.3). Although this modest upregulation was statistical significant when compared to the activation seen in the absence of exogenous YY1, it may not be physiologically relevant and may be within experimental error. In other studies, YY1 has been shown to stimulate promoters and regulatory regions with a stronger effect to that with the *Atoh1* reporter constructs. For instance, overexpression of YY1 upregulates via a 5-fold increase the response of the human liver DnaJ-like protein promoter (HLJI) in human lung cancer cells (Wang et al. 2005) and with a 25-fold increase the response of the ganglioside-induced differentiation associated protein 1 promoter (GDAP1) in HEK293 cells (Ratajewski and Pulaski 2009). Moreover, if a small effect is seen in *in vitro* experiments with other expression of proteins, the physiological response *in vivo* could be even lower. A binding site *in vitro* might not be accessible in an *in vivo* environment by the presence of histones and other chromatin modifiers. In addition, reporter gene assays, for example, were performed by cloning a

DNA fragment which was isolated from its endogenous form. The interaction with other regulatory regions could influence the cloned fragment might affect the observed response. Also the use of artificial promoters such as the minimal promoter used in the luciferase reporters may also influence the transcriptional response of genes to an altered signal that could be different to the response obtained by an endogenous promoter.

Nevertheless, the small activation of the mouse and chick *Atoh1* enhancer AB confirmed that the approach choosing the high stringency of the predicted binding site (Table 3.1) and the high grade of conservation of the binding site across mammalian and avian species (Figure 3.9) were appropriate to prioritize YY1 as a candidate to regulate *Atoh1*. However, the small upregulation seen in the putative enhancer C did not correlate with the MatInspector analysis since YY1 was not predicted to bind in this region. As with all other bioinformatics approach, MatInspector has limitations and it is possible that in this case the generation of matrices to detect a potential YY1 match were not accurate in predicting a binding site in the putative enhancer C. Another observation from the luciferase assays was the downregulation obtained when the three chick *Atoh1* conserved elements were co-transfected with YY1 (Figure 4.3). This downregulation was also observed when co-transfections were conducted with other candidates like NF-κB or ATOH1 (Figure 4.4 and Figure 4.5). It is possible that other transcription factors bound at the *Atoh1* conserved regions and promoter intervened in the formation of DNA loops and caused a differential transcriptional response in the construct containing the three chick *Atoh1* conserved regions (the Chick ABC luciferase construct) in comparison to the construct with the putative enhancer C alone. Also, I cannot eliminate the possibility that YY1 could associate with other proteins to change its activity and consequently upregulate or downregulate the *Atoh1* conserved elements. For instance, YY1 associates with the transcription factor SP1 to form a protein-protein complex to initiate the basal level of the transcription process (Lee et al. 1993) (Seto et al. 1993). There is also evidence of a physical interaction between YY1 and the basal transcription factor TFIIB which is involved in the formation of the RNA polymerase II complex (Usheva and Shenk 1994). Hence, since YY1 can work in co-operation with other proteins, it could also be possible that its activity can be modulated when binding to other partner proteins.

NF-κB, a member of the Rel/NF-κB family, is another transcription factor that was prioritized as a putative candidate to regulate *Atoh1* expression. NF-κB is considered as the central mediator of the human immune response since it is involved in the response of diverse effects including cell inflammation, proliferation and apoptotic processes (Karin and Lin 2002) (Gilmore 2006). If cell damage is produced, the different subunits that form NF-κB, which are inactive in the cytoplasm are translocated into the nucleus to activate a downstream cascade of target genes in an attempt to block cell death (Pahl 1999). As part of this protective role, the NF-κB pathway was seen to protect cochlear cells after aminoglycoside-induced ototoxicity (Jiang et al. 2005). This was concluded by the detection of NF-κB in hair cells and supporting cells after kanamycin-induced damage in comparison to controls where the nuclear translocation of the NF-κB subunits was not seen. In addition, the selective inhibition of NF-κB *in vitro* caused the degeneration of hair cells in P5 rats. Therefore, it is possible that NF-κB is also required for the survival of immature hair cells in an *in vitro* environment (Nagy et al. 2005). However, the role of NF-κB in the inner ear is still poorly understood.

A high stringency NF-κB binding site was predicted in the putative enhancer C, the additional evolutionary conserved element downstream the *Atoh1* enhancers found in avians. Since evidence was found in the literature of the role of NF-κB in the survival of hair cells, the potential of NF-κB to bind and regulate *Atoh1* expression was investigated. EMSA experiments suggested that NF-κB could have the potential to bind to the predicted site in the putative enhancer C. However, supershifts experiments with an antibody specific for NF-κB will be required in order to confirm the presence of NF-κB in the observed UB/OC2 protein shifts.

Co-transfections experiments were unable to demonstrate a significant activation of the mouse and chick *Atoh1* enhancers or the chick putative enhancer C in the presence of exogenous NF-κB (Figure 4.4). The chick ABC luciferase construct did show a repressive response (Figure 4.4) but this was not observed when the putative enhancer C was tested independently from the *Atoh1* AB enhancers. The selective effect of NF-κB on the putative enhancer C when it is on its own or along with the *Atoh1* enhancers could be tested by mutating the predicted NF-κB binding site on the putative enhancer C. This would verify whether the downregulation observed in the luciferase construct containing the *Atoh1* enhancer and putative enhancer C is due to the NF-κB binding site predicted in the putative enhancer C.

The ATOH1 transcription factor has been characterized by previous publications for autoregulating *Atoh1* expression in the neural tube (Helms et al. 2000). However, little evidence exists as to whether this is also true in other tissues such as the inner ear. Therefore, the ability of ATOH1 to activate the *Atoh1* regulatory elements was assessed in an *in vitro* inner ear cell line environment. The use of cell lines as a method to quantify the response of regulatory elements is frequently applied in molecular biology and it is a relatively fast procedure to explore the effect of a candidate gene. Initial experiments showed ATOH1 on its own had no effect on all the constructs tested including one containing consensus E-box binding sites. This suggests that the UB/OC-2 cell line did not contain the correct regulatory environment in which to investigate ATOH1's mechanism of action although further studies are necessary to confirm this. When ATOH1 co-factor E47 was used in co-transfection experiments a significant ~7 fold activation via consensus *Atoh1* E-box sites was observed (Figure 4.7). However, this activation was repressed when ATOH1 was co-transfected with E47. Whether E47 activation of E-box sites in UB/OC-2 requires endogenous ATOH1 or is independent of ATOH1 is unclear. It is possible that ATOH1 prevents E47 binding to repress its effect on the E-box sites. Subsequent transfections to test the effect on the mouse and chick *Atoh1* enhancers constructs showed only small and none are significant changes (Figure 4.8).

The results obtained in the *in vitro* experiments have some correlations with studies conducted by other authors in an *in vivo* system. Masuda et al., 2012 demonstrated in electroporations in mouse cochlear explants that ATOH1 or E47 have the capacity to induce Pou4f3/GFP expression in the greater epithelia ridge, a non-sensory region of the cochlea. Interestingly, E47 by itself also induced Pou4f3/GFP expression. In addition, electroporation with both ATOH1 and E47 induced more Pou4f3/GFP positive cells in the greater epithelia ridge than ATOH1 alone. It is possible therefore that the combination of ATOH1/E47 is necessary for the activation of *Atoh1* target genes like Pou4f3 (Masuda et al. 2012) or *Atoh1* itself. The expression and function of E47, one of the protein products of the gene TCF3 (also known as E2A) (Massari and Murre 2000; Sun and Baltimore 1991) has not been well studied in the cochlea. However, E47 could interact with other bHLH transcription factors including ATOH1. Dimerization between bHLH proteins is a common mechanism that is mediated through the HLH domains (Massari and Murre 2000). To further investigate the effect of E47 on the *Atoh1* enhancers, a dose effect of E47 and ATOH1 could be investigated since only single

doses (500ng) were tested in this study (Figure 4.8). In addition, a number of factors may have impacted on the results obtained in reporter gene assays. For example, proliferating UB/OC2 cells endogenously express ATOH1 which may have been sufficiently expressed to mask the variation induced by the co-transfected ATOH1 expression construct. Furthermore, the potential squelching effect of ATOH1 could be tested in order to demonstrate that high levels of ATOH1 may prevent the expected upregulatory effect on the mouse and chick *Atoh1* enhancer constructs and prevent the upregulatory effect of E47. Given these possibilities, the effect of ATOH1 on the *Atoh1* enhancers could be tested in other cell lines that do not endogenously express ATOH1.

Overall, the results presented in this chapter demonstrate that experimental validation of the binding sites predicted and prioritised in the bioinformatic analysis was not fully achieved. Although some evidence was obtained for interactions between the transcription factors and the predicted binding sites in EMSA analysis this was limited and not substantiated in reporter gene assays. The lack of a strong effect of the candidates tested so far suggests that a true physiological response may not be probable but it may also be the case that the cell line used does not provide an appropriate environment to explore ATOH1 gene regulation. My results so far confirm the need for experimental validation before predicted binding sites can be assessed as functionally important.

Chapter 5

5 Investigation of the E2F transcription factor family as a putative candidate regulator of *Atoh1*

Having identified several predicted putative E2F binding sites within the evolutionary conserved elements of mammalian and avian *Atoh1*, the E2F family was selected for further investigation. The prioritization of the E2F family as a candidate for follow-up was on the basis of its potential relevance to the inner ear and the high stringency of some of its predicted binding sites extracted from the bioinformatic analysis. The expression pattern of E2F in the inner ear has been poorly investigated previously with only one publication reporting E2F1 expression in the stria vascularis and spiral ganglion of adult mouse (Raimundo et al. 2012). However, the E2F binding partner Rb is known to control hair cell proliferation and cell cycle exit during development (Sage et al. 2006). Investigating the potential roles of E2F and the Rb/E2F pathway during the development, maturation or regeneration of hair cells could have a profound impact on the understanding of the process of normal cell growth and cell fate determination in the inner ear epithelium.

5.1 Introduction to the E2F family

5.1.1 Initial studies

The E2Fs are described as a family of transcription factors that are critical for the control and progression of the cell cycle. Originally known as the E2 promoter binding factor, E2F1 (the primary member of the E2F family) was first discovered as a cellular factor binding to the adenovirus E2 promoter (Kovesdi et al. 1986; Kovesdi et al. 1987). Following studies in human adenovirus, E2F1 was investigated for being involved in the changes that occur during the cell cycle progression. Further characterization of the

function of E2F1 was conducted when E2F1 was described as one of the binding proteins of the Retinoblastoma tumour suppressor gene (Rb), one of the key factors regulating the cell cycle. E2F1 was found to form a complex with Rb during the G_1 stage in the cell cycle and this complex is disrupted upon the entry into the DNA synthesis phase (stage S) (Chellappan et al. 1991; Bagchi et al. 1991).

5.1.2 E2F family members

The E2F family has been described in different organisms including mammals with a conserved protein structure. In mammals, the E2F family is composed of eight members (E2F1-E2F8) represented in Figure 5.1.

The E2F family is divided in to two subclasses based on their sequence homology and transcriptional functions. E2F1-E2F3a are known as transcriptional activators since they participate in the activation of the expression of their target genes (Attwooll et al. 2004; Ivey-Hoyle et al. 1993; Lees, 1993). By contrast, E2F4-E2F6, the other subclass of the E2F family, were identified as repressors. They were originally identified for binding Rb and the other structural related pocket proteins, such as p107 and p130 (Beijersbergen et al. 1994; Hijmans et al. 1995; Trimarchi et al. 1998). E2F4 and E2F5 were mainly detected in quiescent (G_0) cells in contrast to E2F1-3 that are mainly restricted to dividing cells (Ikeda, 1996; Moberg et al. 1996). In addition, E2F4 and E2F5 lack the capacity to drive cells into the cell cycle (Müller et al. 1997). Among their functions, the cellular localization of the activating and repressing E2F members is also another representative characteristic of the two subclasses. In the molecular structure of E2F1-3, a canonical basic nuclear localization signal is found (NLS in Figure 5.1) that confers the nuclear localization of this subgroup (Müller et al. 1997; Verona et al. 1997; Magae, 1996). By contrast, the molecular structures of E2F4 and E2F5 contain a leucine/isoleucine-rich hydrophobic nuclear exporting signal (NES in Figure 5.1) which promotes the cytoplasmic localization of these E2F members (Gaubatz et al. 2001). Recently two more members of the E2F family have been identified, E2F7 and E2F8, which hold a separate conserved structure in comparison to the rest of the group. They contain two distinct DNA binding domains (DBD1 in Figure 5.1) and lack the dimerization and transactivation domains. Therefore they bind to their targets without forming a complex with the DP co-factors. The different molecular structures of E2F7 and E2F8 suggest that they probably have unique roles in

comparison to the other members, as transcriptional repressors of cellular proliferation (de Bruin et al. 2003; Di Stefano et al. 2003; Logan et al. 2004; Logan et al. 2005).

Picture removed for copyright purposes

Figure 5.1. The E2F family. Representation of the E2F family members and their molecular structure as reviewed in Chen, 2009. The molecular structure of the E2F family is characterized by the presence of winged-helix DNA binding domain (DBD), a DP binding domain consisting in a leucine zipper (LZ) and a marked box motif (MB). These sequences are required for the dimerization of the E2F-DP complex. The E2F1-6 members are also characterized by the presence of a transactivation domain located in the C-terminal region which mediates the interaction with the Retinoblastoma tumour suppressor (RB). Figure reproduced from Chen et al. 2009.

5.1.3 E2F co-factors: The DP family

The majority of the members of the E2F family enhance their functionality when they bind to their partners, the DP family (DP1, DP2 and DP4). DP1, the primary member of the family, was originally discovered as DRTF-polypeptide-1, a partner for E2F1 (Girling et al. 1993). It was observed that DP1 shared the same binding domains as the E2Fs and it was able to recognize the same binding sites in the DNA.

Following the discovery of DP1, it was demonstrated that E2F1 was able to form a complex with the co-factor DP1, improving the binding capabilities of E2F1 (Helin et al. 1993; Girling et al. 1993). The human DP2 was characterized as the second member of the DP family (Ormondroyd E 1995; Zhang Y 1995). Unlike DP1, this new member produces different transcripts (called α β γ) and their cellular localization varies depending on the tissue or cell line. However, like the previous member, DP2 also plays important roles in enhancing the binding affinities of E2F members during the regulation of the cell cycle. On the contrary, DP4 has been described for reducing DNA binding properties of E2F. It was also suggested that DP4 delays cell cycle progression when binding to E2F1 (Milton et al. 2006).

5.1.4 E2F functions

The E2F family is characterized for being involved in different regulatory and cellular events. However, the role and functions of E2Fs are complex and in some cases not well understood. Therefore, a summary of the more relevant aspects of the E2F family are described in the following sections.

5.1.4.1 E2F as controllers of the cell cycle

The role of E2Fs in the control of the cell cycle is in part linked to Rb, a protein that belongs to a family known as the "pocket" proteins. The Rb-E2F complex is one of the main components responsible for the progression of the cell cycle. The cell cycle is divided into four different stages (Sherr and Roberts 1999): G_1 is the growth phase, S phase corresponds to the stage at which DNA replication occurs, followed by G_2 which precedes to the M (mitosis) phase during which cell division occurs. During the G_1 phase, positive and negative growth factors are produced in order to undergo DNA replication or to maintain the cell in a latent stage. During the G_0/early G_1 phase of the cell cycle, the unphosphorylated Rb binds to E2F1-3 to form the Rb-E2F complex (Bagchi et al. 1991; Bandara and La Thangue 1991; Chellappan et al. 1991). The formation of the Rb-E2F complex inhibits the activation of the genes required for the S-phase and therefore the progression of the cell cycle is blocked. Growth-inhibitory signals, including the transforming growth factor (TBF-β) and the p53/p21 pathway block the phosphorylation of the Rb protein (DeGregori et al. 1995; Schwarz et al. 1995; Mann and Jones 1996).

Picture removed for copyright purposes

Figure 5.2. Schematic representation of the role of the E2F/Rb complex in the control of the cell cycle. Cell cycle progression and therefore the entry into S-phase is dependent on the phosphorylation of Rb by cyclin D1–cyclin-dependent kinase (CDK)-4, cyclin D1–CDK6 and cyclin E–CDK2 complexes. This causes the release of the free E2F1-3 and consequently the activation of downstream target genes required for the progression of the cell cycle. Image adapted from Coller, 2007.

By the late G_1 phase, the sequential activation of the cyclin-dependent kinases (CdKs) Cdk4/Cdk6-cyclin D (Ewen et al. 1993; Jun-ya Kato 1993) and Cdk2-cyclin E (Akiyama et al. 1992; Hinds et al. 1992) produces the phosphorylation of Rb. The centrosome duplication in mammalian somatic cells requires the phosphorylation of Rb and the activity of E2F and Cdk2 (Meraldi et al. 1999). The phosphorylated Rb releases the E2F transcription factors which results in the activation of genes required for the entry into S-phase including genes coding for enzymes needed for the synthesis of dNTPs and DNA such as thymidylate synthase, ribonucleotide reductase 2 and DNA polymerase α (Dimova and Dyson 2005). It is also known that in quiescent (G_0) cells, E2F4 and E2F5 associate with Rb to maintain the repression of S-phase genes as well as the activation of genes required for the exit out of the cell cycle and cell differentiation (Mann and Jones 1996; Gaubatz et al. 2001; Wu et al. 2001).

All these events, including the phosphorylation of Rb and consequent release of the E2F transcription factors are essential steps for the progression of the cell cycle.

5.1.4.2 E2F and cell proliferation

The role of the E2F family in cell proliferation has been described by different studies. Initial evidence was found by the identification of E2F binding sites in the promoters of genes directly linked to cell proliferation. Among others, this is the case of various gene promoters such as adenovirus E2 (Kovesdi et al. 1986), human Thyrimide kinase (Kim and Lee 1991), the dihydrofolate reductase gene (DHFR) (Blake and Azizkhan 1989) and DNA polymerase α (Pearson et al. 1991) whose promoter sequences were functionally validated in EMSA competition assays for having the ability to be bound by E2F and consequently activate the transcription of these genes.

E2F1 has also been described to activate cell proliferation upon ectopic overexpression in quiescent cells. The transfection of an E2F1 cDNA plasmid resulted in an increase of BrdU positive cells as a consequence of newly synthesized DNA in comparison to cells transfected with a mutant E2F1 protein (Johnson et al. 1993). Moreover, studies in serum-starved cells co-transfected with an E2F1 expression construct along with other constructs containing promoters that are known for containing E2F binding sites, resulted in the up-regulation of those promoters. Hence, it was concluded that E2F1 has the potential to stimulate transcription and therefore proliferation of genes without the action of normal growth stimulation signals. In addition to the previous studies it was also demonstrated that the combined loss of E2F1, E2F2 and E2F3 is sufficient to abolish cell proliferation in mouse embryonic fibroblasts (Wu et al. 2001).
More recent studies also associated E2F1 in proliferative activities during the melanoma and metastasis progression. It was observed that when endogenous E2F1 is knocked down via E2F1 small hairpin RNA (shRNA), metastatic cells reduced their invasive potential and melanoma progression was decreased (Alla et al. 2010).

5.1.4.3 E2F and apoptosis

The relationship between E2F1 and apoptosis has been defined by at least three different mechanisms. Firstly, E2F1 can inhibit survival signals from the death receptor pathway. It is unclear whether E2F1 directly induces the degradation of these signals or whether E2F1 actives the expression of downstream genes to produce these events (Phillips et al. 1999). Secondly, ectopic or endogenous E2F1 can induce the

transcriptional activation of tumour suppressor proteins such as p53 and p73 and consequently programme cell death (Stiewe and Putzer 2000). Thirdly, and in addition to the previous one, E2F1 can also induce the p53 tumour suppressor protein by an indirect mechanism. In normal cells, the level of p53 protein is low and is controlled by a feed-back loop mechanism. However, under stress conditions, p53 is unable to auto-regulate correctly and eventually is degraded (Ashcroft et al. 2000). E2F1 has been linked with promoting the stabilization of p53 under stress conditions and therefore may extend the apoptotic function of the p53 protein. This mechanism was shown to occur via the $p14^{ARF}$ protein which is a downstream target of E2F1 (Bates et al. 1998).
In summary, it is unclear whether the contrasting proliferative and apoptotic roles of E2F1 are due to the loss of potential activators or due to the up-regulation of negative factors of the cell cycle.

5.1.5 E2F and the inner ear

Most of the studies focused on the control of the cell cycle in the inner ear have been linked to the Rb protein and its function during early development and maturation of hair cells. Whether the E2Fs are also involved in these processes remains unexplored. However, based on the partnership that E2F and Rb share (see section 5.1.4) it seems logical to think that their functions in the inner ear are somehow connected.

Studies with Rb homozygous mutant mice ($Rb^{-/-}$) revealed that these mice die at embryonic stages and show multiple defects including in brain and nervous system (Classon and Harlow 2002). A more recent study carried out by Sage et al. with a conditional Rb knockout where the Rb was deleted in the inner ear, showed that in embryonic stages, hair cells appear normal but continue to divide for a longer period. At early post-natal stages, conditional Rb knockout mice, showed an increased number of IHC and OHC in the organ of Corti but in a disorganized distribution in comparison with normal cochleae (Sage et al. 2006). Vestibular and cochlear hair cells were still proliferating at post-natal stages as detected by a proliferating cell nuclear antibody (anti-PCNA) in comparison to controls where PCNA was not detected in neither hair cells nor supporting cells. Multiple rows of HCs and SCs were also observed in the Rb conditional knockout cochlear explants at P4. Whether the increase in the number of hair cells is due to the effect of "free" E2F inducing cell proliferation is unknown. In the vestibular system, anti-PCNA was shown only in hair cells but not in supporting cells,

suggesting that in the absence of Rb in the inner ear, there are different mechanisms controlling the proliferation of vestibular hair cells and supporting cells.
At late post-embryonic stages it was shown that Rb is required for the maturation and survival of both cochlear and vestibular hair cells. The lack of prestin expression, a protein essential in auditory processing, in Rb conditional knockout mice confirmed the requirement of Rb to form a functional inner ear.
In summary the work conducted by Sage et al. showed that post-natal vestibular hair cells undergo cell division up to 6 weeks and survived for 6 months in the absence of Rb. However whether E2F is involved in the maintenance of hair cells within the cell cycle due to the lack of Rb was not studied.

In mouse, hair cells stop dividing between embryonic day 13 (E13) and E14. It has been shown that the expression of $p27^{kip1}$, a cyclin-dependent kinase inhibitor, is upregulated in the organ of Corti between E13-14 which correlates with the cell cycle withdrawal (Chen and Segil 1999). As mentioned in section 1.5.1, this was demonstrated by immunohistochemistry of an anti- $p27^{kip1}$ antibody showing an up-regulation of this inhibitor protein between E12 and E14. In differentiated hair cells, $p27^{kip1}$ is downregulated however its expression remains in mature supporting cells suggesting that $p27^{kip1}$ is perhaps involved in maintaining supporting cells in a quiescent state (Chen and Segil 1999). The loss of $p27^{kip1}$ was also examined in mutant mice. In these animals, cells in the developing epithelium continue dividing for a longer period in comparison to controls and an increase in the number of hair cells and supporting cells was observed. However, $p27^{kip1}$ mutants also showed a severe hearing impairment, revealing the importance of $p27^{kip1}$ in the control of exit from the cell cycle.
In addition to Chen et al. studies, another group showed that the loss of $p27^{kip1}$ reduces Cdk4/6-cyclin D complexes (Cerqueira et al. 2014). Cdk4/6-cyclin D complexes are up-stream regulators of Rb and responsible for causing its phosphorylation and consequently the release of E2F from the Rb-E2F complex. If Rb is not phosphorylated appropriately because of the absence of $p27^{kip1}$, it is possible that the control of the exit from cell cycle is disrupted and cells continue proliferating.

A recent study conducted by Raimundo et al. showed that E2F1 could be linked to a mechanism of maternally inherited deafness. In this investigation it was found that a

mutation in human mitochondrial DNA leads to a dysfunction of the mitochondrial ribosome which results in the activation of AMP kinases and E2F1 (Raimundo et al. 2012). The mechanism involved in this process has been linked to the hypermethylation of rRNA which triggers a form of mitochondrial stress signalling. This upregulates E2F1 transcriptional activity which results in the apoptosis of cells involved in hearing such as the stria vascularis cells and spiral ganglion neurons. A microarray was also conducted and showed an enrichment of E2F1 target genes after the hypermethylation of the rRNA. On the other hand the hypermethylation of rRNA leads to an increase of phosphorylated Rb. In addition when the hypermethylation of rRNA was suppressed via knock down in mice, the upregulation of E2F1 is no longer seen and apoptosis measured by the Caspase 3/7 activity is reduced. Altogether results from Raimundo's group concluded that cell-type-specific mitochondrial stress produced by the hypermethylation of rRNA induces the Rb-E2F apoptotic pathway. This process leads therefore to an inner ear pathology affecting some cells involved in hearing and as a result causes deafness.

To summarise the role of E2F in the inner ear, different studies have investigated the function of Rb in various tissues and organisms however very little is known about the function of E2F itself. Both E2F and Rb proteins appear to be involved at multiple levels of the complex regulatory pathway controlling the cell cycle. Therefore, the investigation of E2F and Rb and the interaction with other upstream and downstream proteins could bring new insights in the study of hair cell formation, maintenance and proliferation.

5.1.6 The E2F family and the study of *Atoh1* regulation

One of the key questions that remains poorly understood in hair cell development and maintenance is the identification of genes that regulate the permanent exit of the cell cycle and genes that maintain the quiescent post-mitotic state of hair cells and supporting cells. Investigating whether the E2F family is responsible for the re-entry into the cell cycle of quiescent post-mitotic supporting cells to reactivate ATOH1 expression could provide insights to understand the regeneration process of the inner ear sensory epithelium.

Target genes of the E2F family were identified in a microarray experiment for changing expression when E2F1, E2F2 or E2F3 were overexpressed (Muller et al. 2001).

However, up to date, it is unknown whether ATOH1 is one of the downstream targets of the E2F family. Since Rb, the partner protein of E2F1-3, plays important roles in the cell cycle as well as in differentiation and survival in the inner ear, it would be important to investigate whether the E2F family is also involved in these processes. Hence, in order to elucidate the role of the E2F family in the inner ear, E2F was prioritized as a putative regulator of *Atoh1* transcription. If the re-activation of ATOH1 expression due to E2F1-3 could be demonstrated, then the manipulation of the Rb/E2F pathway could be a potential strategy to regenerate hair cells in the mature inner ear.

5.2 Regulation of the mammalian and avian *Atoh1* conserved regions by E2F1

The ability of E2F1 to regulate the mouse and chick *Atoh1* enhancers and putative enhancer C was investigated to verify the predictions extracted from the bioinformatic analysis. To test this, luciferase plasmids containing the mouse and chick *Atoh1* enhancers and putative enhancer C were generated (cloned upstream of the minimal promoter; see section 2.2.9.3) and co-transfected with increasing amounts of a human E2F1 expression construct cloned in pcDNA3 (kindly obtained from Professor Kristian Helin, University of Copenhagen, Denmark) (Helin et al. 1992).

Figure 5.3 (in blue) shows the responses of the different luciferase constructs containing specified mouse or chick *Atoh1* conserved regions when transfected with increasing amounts of the E2F1 expression construct (from 0 to 1200ng of E2F1). The mouse *Atoh1* AB enhancer construct showed 2, 2.4 and 3.1-fold activation when co-transfected with increasing amounts of E2F1. In the same luciferase assay, the response of the chick *Atoh1* conserved regions was also assessed. The chick *Atoh1* AB enhancer construct showed 8, 17 and 23-fold activation when co-transfected with increasing amounts of E2F1. In a similar way, the chick *Atoh1* putative enhancer C construct showed a 10, 18 and 34-fold activation with increasing amount of E2F1. The highest response was obtained with the construct containing all three chick *Atoh1* conserved elements, construct ABC, which gave a response of 27, 61 and 145-fold activation when the amount of E2F1 was increased from 400 to 1200ng. The response observed for all *Atoh1* luciferase constructs, both mouse and chick, correlates with a dose-dependent activation. However, the response obtained by the chick *Atoh1* AB enhancer, chick

Atoh1 putative enhancer C and chick *Atoh1* ABC constructs is much larger than the response obtained by the mouse *Atoh1* AB enhancer construct (145 fold compared to 3.1 fold). Moreover, the empty luciferase vector (pGL4.23) showed an increase of 2, 2.47 and 2.44-fold activation when co-transfected with increasing amount of E2F1 similar to the one observed in the mouse *Atoh1* AB construct suggesting that the activation in the mouse *Atoh1* AB could be due to effects on the base vector.

The results so far suggest that E2F1 is a powerful activator of the chick *Atoh1* conserved elements potentially by binding to one or more of the E2F binding sites predicted by the bioinformatic analysis. To further investigate whether the activation of the mouse and chick *Atoh1* conserved regions is dependent on a functionally active E2F1, another series of luciferase assays were performed but with a mutant E2F1 expression construct (Yu et al. 2011). This mutant E2F1 contains a change in the DNA binding domain located in exon 3 of the E2F1 gene which results in the substitution of an arginine into a histidine residue in the E2F1 protein. This amino acid site is highly conserved across different species, including mouse and chick and is essential for the binding of E2F1 to its targets genes (Yu et al. 2011). When the mutant E2F1 construct was co-transfected, the large up-regulation that was previously observed in the chick *Atoh1* constructs was no longer seen, confirming that the activation is dependent on a functional E2F1 (Figure 5.3 in red). In contrast, for the mouse *Atoh1* AB enhancer a similar response was observed when co-transfected with the wild type E2F1 or the mutant E2F1 expression construct (in Figure 5.3 comparing mouse AB response with wild type E2F1-in blue and mutant E2F1-in red). Therefore, the small upregulation seen in the mouse *Atoh1* AB enhancer when co-transfecting the wild type E2F1 is still observed when the mutant E2F1 is used.

In summary, although the mouse *Atoh1* AB enhancer construct demonstrated a small upregulation when E2F1 was co-transfected, a similar response was observed when using the mutant E2F1. This activation is statistically significant but might not reflect a physiological response since similar response was observed with the empty luciferase construct (pGL4.23 in Figure 5.3) suggesting that this response may be artefactual.
In chick, since an up-regulation was observed with the chick *Atoh1* AB construct and also with the construct containing the chick *Atoh1* putative enhancer C, at least two independent E2F binding sites may be functional in the chick *Atoh1* sequence.

Moreover, since the response is much larger in the chick ABC construct, the effect of E2F1 is greater when both, the chick *Atoh1* AB enhancer and putative enhancer C are present sustaining the hypothesis of multiple and independent E2F binding sites. In addition, the response observed with the chick *Atoh1* conserved regions is much larger and beyond any artefactual response produced by the luciferase backbone. Therefore, since the response in chick is large and dependent on active E2F1, further investigation was conducted to examine which of the predicted binding sites in the chick *Atoh1* mediates this E2F regulation.

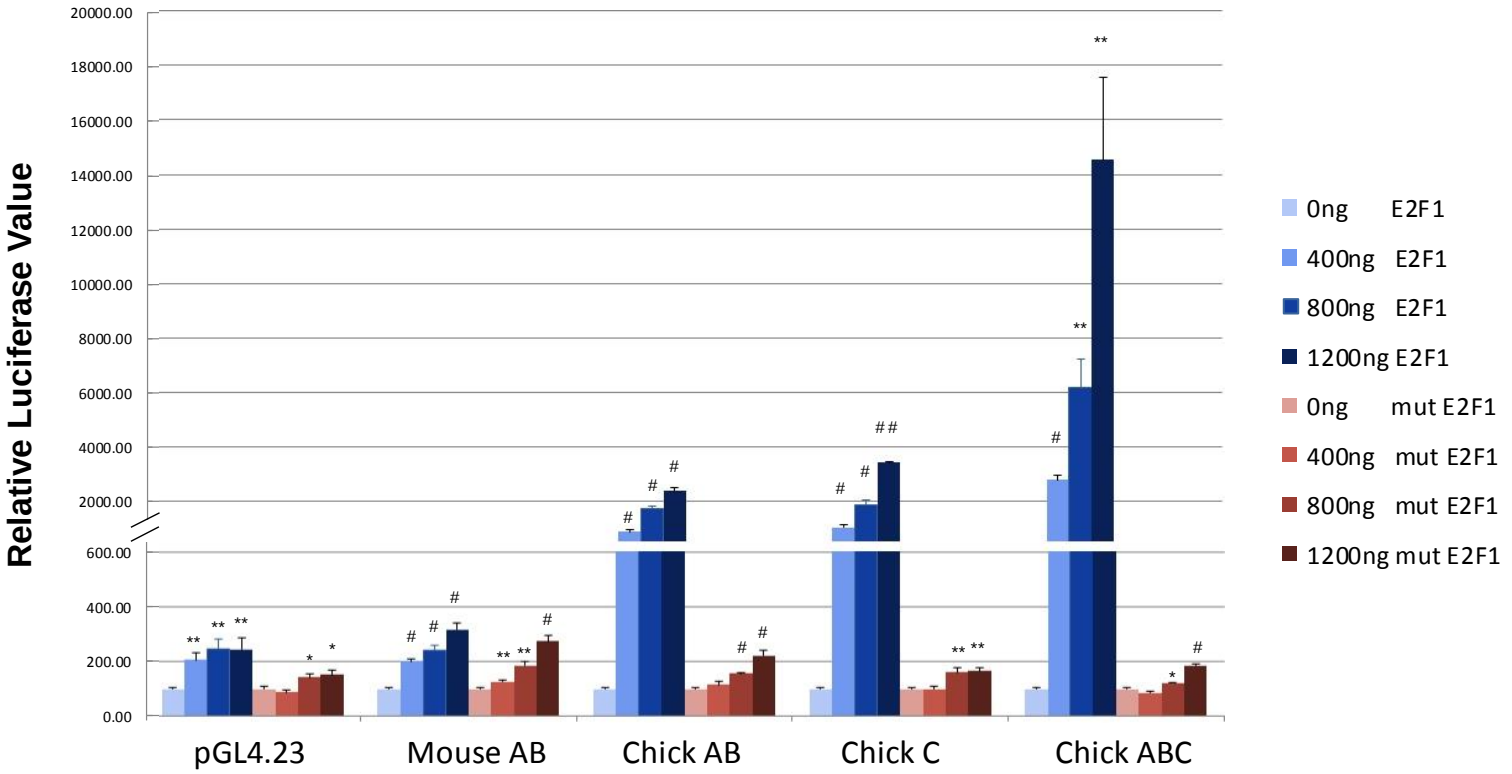

Figure 5.3. Dose-response effect of the E2F1 transcription factor on the *Atoh1* conserved regions. UB/OC2 cells were transfected with increasing amounts of an E2F1 expression construct (in blue) or a mutant E2F1 (in red). 10ng of the pRL-null luciferase construct (Promega) were co-transfected for all conditions and the pcDNA3 expression construct was also used to maintain the same amount of DNA across experiments. Each dose of E2F1 was normalized against the luciferase activity obtained when E2F1 was absent (0ng of E2F1 and therefore 1200ng of pcDNA3). Experiments were conducted in triplicate in two separate assays with different DNA preparations for each plasmid in each assay (n=6). Student t-test was conducted. (*$p< 0.05$; **$p < 0.01$; #$p<10^{-5}$; ## $p< 10^{-10}$). The mean value and standard error of the mean from 6 experiments are presented.

5.3 EMSA analysis of the predicted E2F binding sites in the chick *Atoh1* conserved regions.

In total nine E2F binding sites were predicted by the Genomatix MatInspector analysis in the chick *Atoh1* enhancers A and B and putative enhancer C (Figure 3.10, Table 3.2 and Table 3.3). Having shown an activation of the chick *Atoh1* enhancer AB and chick putative enhancer C by E2F1, the investigation was focused on characterizing which of the nine predicted binding sites can be bound by the E2F transcription factors. Interactions between DNA-protein are typically a sign of regulatory mechanisms and therefore can result in a functional response such as the regulation of the transcriptional process to activate or repress the expression of a gene. Identifying whether the E2F family can bind to the chick *Atoh1* regulatory regions to activate transcription and where exactly this interaction takes place, will provide additional evidence of a direct interaction of E2F1 with *Atoh1* to regulate ATOH1 gene expression.

To test this interaction, EMSA experiments were conducted using UB/OC2 nuclear protein extracts. As previously mentioned, different hair cell markers are expressed in these cells (Rivolta et al. 1998) in addition to *Atoh1* which was detected by q-PCR in our laboratory (data not shown). This suggests that the transcriptional background for *Atoh1* transcription is present in UB/OC2 cells. However, expression of E2F1 has never been tested in UB/OC2 cells and therefore before proceeding with the EMSA experiments E2F1 expression was examined in this cell line.

5.3.1 Analysis of E2F1 expression in UB/OC2 cells

The expression of the best characterized member of the E2F family, E2F1, was tested in proliferating UB/OC2 cells by immunohistochemistry and E2F1 mRNA production was assessed by RT-PCR.

Figure 5.4 shows endogenous expression of E2F1 protein in UB/OC2 cells. Immunolabeling is predominantly nuclear or perinuclear in proliferating UB/OC2 cells cultured at 33^{o}C as would be expected for E2F1.

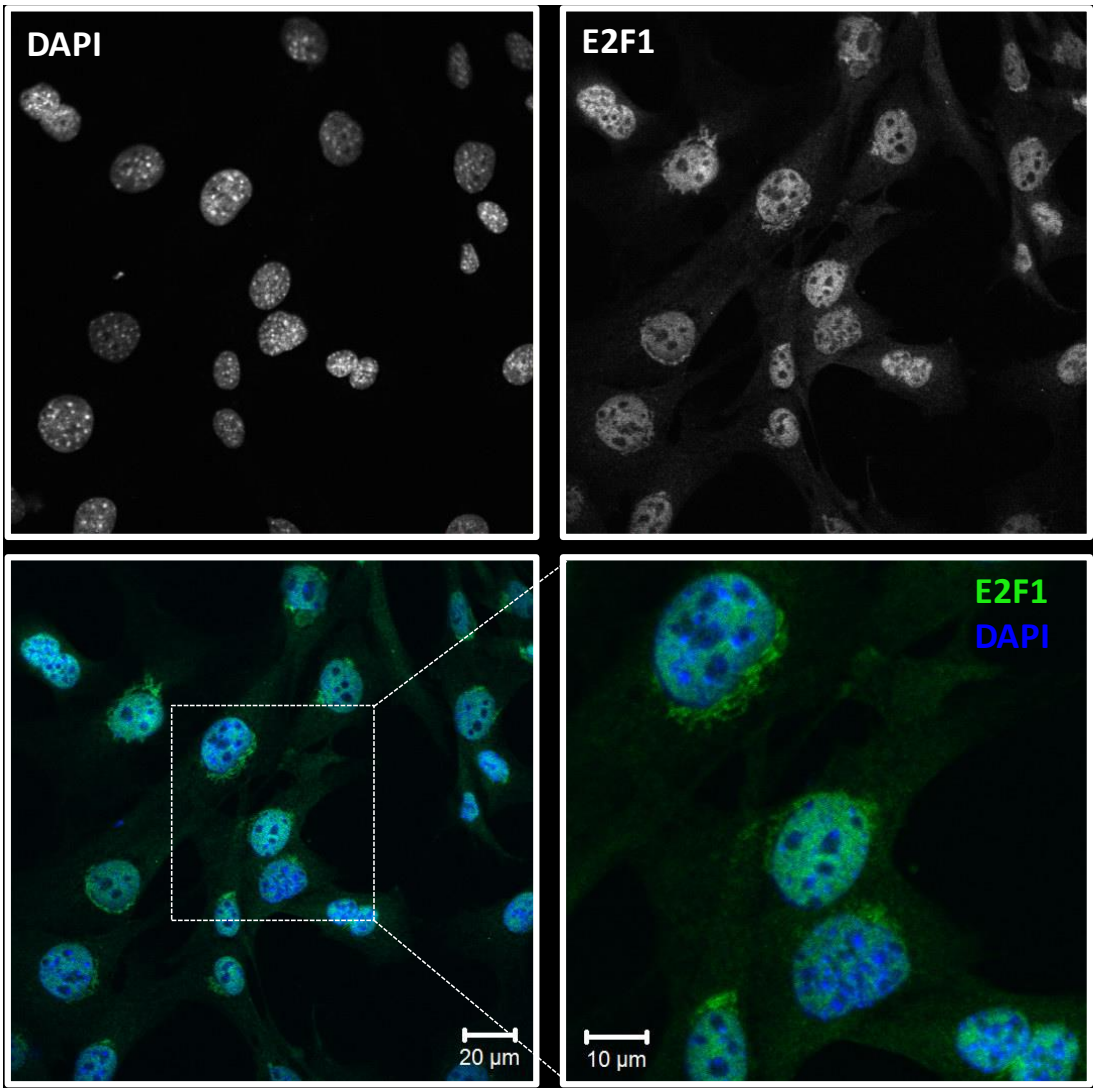

Figure 5.4. Endogenous expression of E2F1 in UB/OC2 cells. Confocal images of proliferating UB/OC2 cells immunostained with E2F1 (in green) and DAPI (in blue). Immunostaining was conducted with a rabbit polyclonal anti-E2F1 antibody. Alexa Fluor 488® provided the fluorescent labelling of the E2F1 antibody (in green) and 4′,6-diamidino-2-phenylindole (DAPI- in blue), was used to label nuclear DNA. Immunohistochemistry results show endogenous expression of E2F1 in proliferating UB/OC2 cells cultured at 33°C.

Figure 5.5 shows the results of the RT-PCR to detect E2F1 and GAPDH expression (using primer 25-28; Table 2.1 in material and methods). When cDNA from untransfected UB/OC2 cells was used for the PCR reaction, a very faint band of 341 bp can be visualized on the agarose gel corresponding to the expected size based on the E2F1 transcript amplification. When cDNA from UB/OC2 cells transfected with E2F1 was used, a stronger band of the same size was produced confirming that the signal of

the band correlates to the correct E2F1 transcript in transfected and untransfected UB/OC2 cells but suggesting it may be lowly expressed in UB/OC2 cells under normal conditions (Figure 5.5). E2F1 protein expression was also analysed and compared in untransfected UB/OC2 cells and cells transfected with an E2F1 expression vector. As shown in Figure 5.6, E2F1 immunolabeling in transfected UB/OC2 cells was stronger in some cells after transfection of the E2F1 expression plasmid since a higher amount of E2F1 protein was detected by the E2F1 antibody. In summary, the presence of E2F1 mRNA and E2F1 protein was confirmed in UB/OC2 cells. Therefore, nuclear extracts from UB/OC2 are suitable to conduct EMSA experiments as they contain E2F1 and the regulatory machinery that is required for its activity and production. The comparison between non-transfected and E2F1 transfected cells demonstrates the successful exogenous expression of E2F1 in UB/OC2.

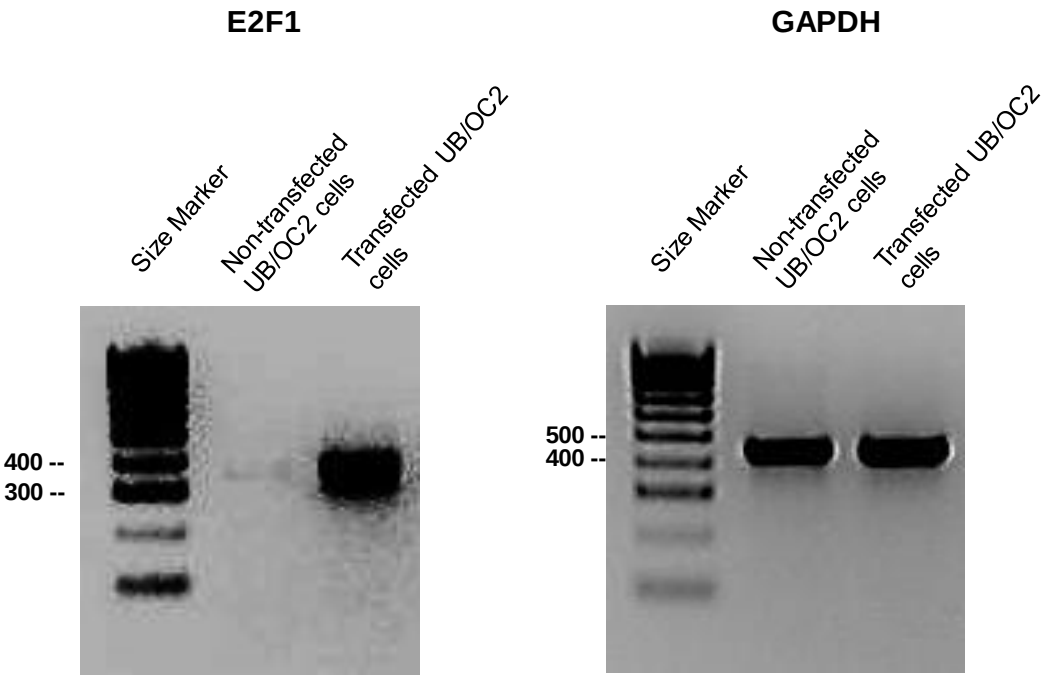

Figure 5.5. RT-PCR for E2F1. RT-PCR of non-transfected UB/OC2 cells and cells transfected with the E2F1 expression construct generate a band of the same size (341 bp). A faint band is observed in the non-transfected cells indicating that the presence of endogenous E2F1 is low. However, the band is much stronger when using cDNA from cells transfected with E2F1. Expression levels of GAPDH were used as a reference to verify that mRNA content did not vary under the different experimental conditions (in non-transfected and transfected cells).

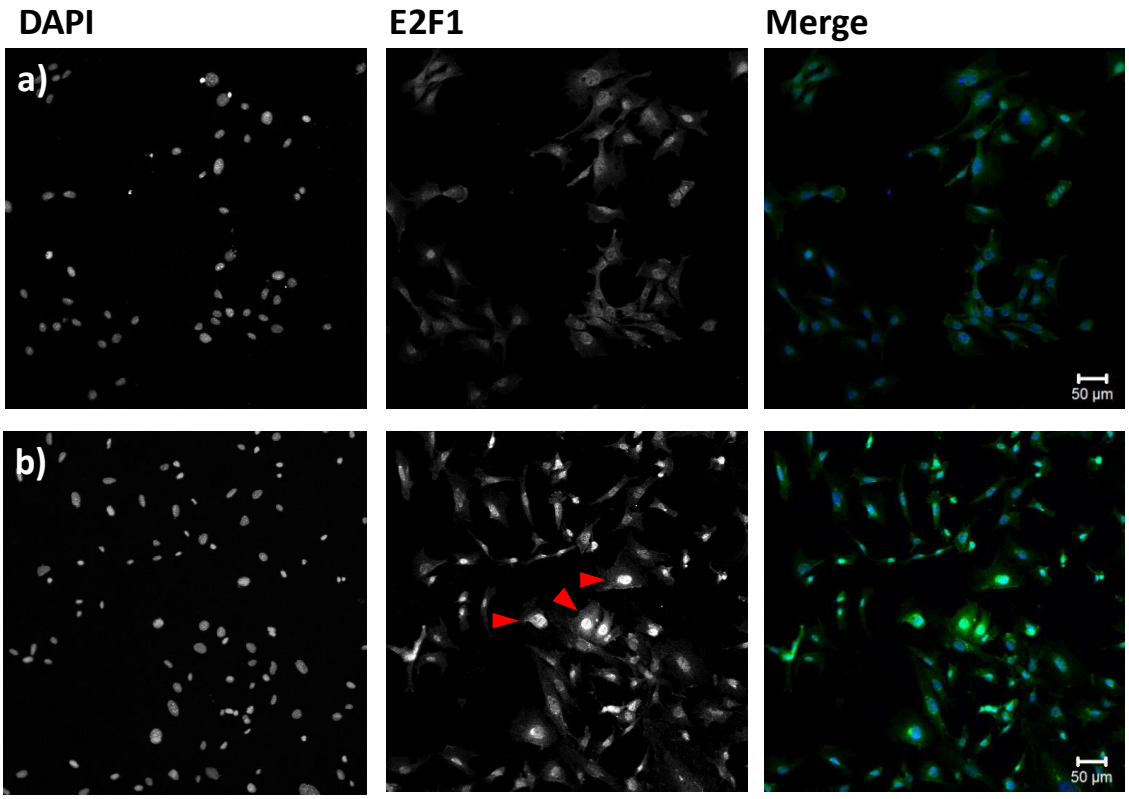

Figure 5.6. Comparison between E2F1 transfected and non-transfected UB/OC2 cells. Confocal images of UB/OC2 cells immunostained with E2F1 (in green) and DAPI (in blue). **a)** Untransfected UB/OC2 cells and **b)** transfected cells with an E2F1 expression construct. Immunostaining was conducted with a rabbit polyclonal E2F-1 antibody incubated overnight in a 1:400 dilution. Alexa Fluor 488® provided the fluorescent labelling for the E2F1 antibody (in green) and 4′,6-diamidino-2-phenylindole (DAPI- in blue), used to label nuclear DNA, were incubated in a 1:1000 dilution for 2h at room temperature. E2F1 protein expression was stronger in cells transfected with E2F1 and the nuclei of some cells are notably stronger possibly due to greater transfection efficiencies (red arrowheads). Images in **a)** and **b)** were taken using identical confocal microscopy settings.

5.3.2 Binding of E2F in EMSA experiments

After confirming expression of E2F1 in UB/OC2 cells, EMSA experiments were conducted to investigate interactions between E2F and the chick *Atoh1* enhancers and the putative enhancer C.

Initial results of EMSA experiments to assess E2F binding were problematic and required a great degree of optimization. These included changes in the incubation temperature, nuclear extract protein concentration, optimization of salts in buffer solutions and EMSAs with E2F1 and DP1 *in vitro* using translated proteins (see appendix section for these experiments). For the optimization procedure and further EMSA experiments, double stranded oligonucleotides were designed. Table 5.1 shows the oligonucleotide sequences corresponding to E2F1 consensus and mutant sequences (Lees et al. 1993) as well as the "A2 probe", an experimentally verified site located in the imprinted tumor suppressor gene promoter which has been shown to be bound by E2F1 (Lu et al. 2006). These oligonucleotides were used in competition EMSA assays.

Table 5.1: Consensus oligonucleotides for EMSA experiments. E2F binding sites are underlined.

Oligo name	Primer Sequence (5' to 3')	Predicted Binding site
E2F1_Cons_Sense	ATTTAAGTTTCGCGCCCTTTCTCAA	Consensus E2F
E2F1_Cons_Antisense	TTGAGAAAGGGCGCGAAACTTAAAT	Consensus E2F
E2F1_MutCons_Sense	ATTTAAGTTTATATCCCTTTCTCAA	Mutant E2F
E2F1_MutCons_Antisense	TTGAGAAAGGGATATAAACTTAAAT	Mutant E2F
A2_Sense	TTATTTTTGGCGGGGGGGAATCTATAG	E2F1 (Z Lu et at)
A2_Antisense	CTATAGATTCCCCCCCGCCAAAAATAA	E2F1 (Z Lu et at)

The first aim in the EMSA analysis was to demonstrate that known E2F binding sites and consensus probes were able to be bound by E2F in the assay conditions. Preliminary tests with DP1 (the co-factor for E2F) and E2F1 *in vitro* translated proteins incubated into the same binding reaction showed a small improvement in the E2F-DP1 complex interacting with a consensus E2F binding site (see appendix section). Therefore, an EMSA experiment was conducted comparing nuclear extracts from non-transfected UB/OC2 cells and nuclear extracts from UB/OC2 cells transfected with

E2F1 and DP1 when incubated with a radiolabelled E2F probe (the A2-E2F1) alone or in competition with non-radiolabelled probes.

In Figure 5.7, an EMSA assay is presented showing the comparison of the different protein-DNA complexes (referred to as bandshifts) produced by both non-transfected and transfected UB/OC2 nuclear extracts when incubated with a radiolabelled probe known for being bound by E2F (the A2-E2F1 probe). When incubating the A2-E2F1 probe with non-transfected nuclear extracts, several different protein-DNA complexes were generated (bandshifts A, B, C and D in lane 2). In order to demonstrate which, if any, of these bandshifts corresponds to the E2F complex, a competition assay was performed where the nuclear extracts were incubated with a non-radiolabelled A2-E2F1 probe for 1-2h before adding the radiolabelled A2-E2F1 probe. Since the extracts were incubated first with the cold probe, less E2F protein would be available to bind to the radiolabelled probe. This resulted in competition between both probes for E2F binding and consequently the disappearance of one the bandshifts (Figure 5.7 bandshift B, lane 3). To confirm that the competed bandshift B is E2F-sequence dependent, rather than due to competition for a non-specific protein, a probe containing a mutated E2F1 consensus probe was incubated with nuclear extracts before adding the radiolabelled A2-E2F1 probe. The mutated E2F1 consensus probe did not compete for the binding suggesting that bandshift B is sequence specific (Figure 5.7 bandshift B, lane 4). To further analyse the specificity of the E2F complex, a similar experiment was performed using a non-specific probe instead of the mutated E2F1 probe. This non-specific probe was designed using a distal sequence relative to the E2F binding site sequence. As expected, the non-specific probe caused the same effect as the mutated E2F1 consensus probe verifying that both probes do not compete for bandshift B (Figure 5.7 bandshift B, lane 5). A supershift was also performed to further confirm the presence of E2F protein in complex B. 1µg of E2F1 antibody was incubated for 1h before adding the radiolabelled probe. This resulted in an attenuation of the complex B suggesting that the addition of the antibody interfered with the binding between E2F protein and the radiolabelled probe (Figure 5.7, bandshift B, lane 6). Further supershift assays will be described in subsequent sections.

Competition and supershift assays were also performed using nuclear extracts from UB/OC2 cells transfected with E2F1 and DP1 expression constructs (Figure 5.7 lanes 7-12). Similar results were observed to the non-transfected extracts. The bandshift B

generated by the protein-DNA complex was competed when using the consensus A2-E2F1 probe as a competitor (lane 9). As it was previously observed, the radiolabelled probe incubated with nuclear extracts cells transfected with E2F1 and DP1 did not compete for binding when incubated with the mutated E2F1 consensus probe (lane 10) or a non-specific probe (lane 11). Furthermore, bandshift B was more intense when using nuclear extracts from UB/OC2 cells transfected with E2F1 and DP1 in comparison to the bandshift B generated using non-transfected nuclear extracts. Conversely, the rest of the bandshifts (A, C and D) remained with the same intensity when using transfected and non-transfected nuclear extracts suggesting that these are not E2F dependent.

In summary when taken together the competition assays with a known E2F probe (the A2-E2F1 probe), the supershift with the E2F1 antibody and the increased binding of the same shift when using transfected nuclear extracts, were consistent with bandshift B corresponding to E2F.

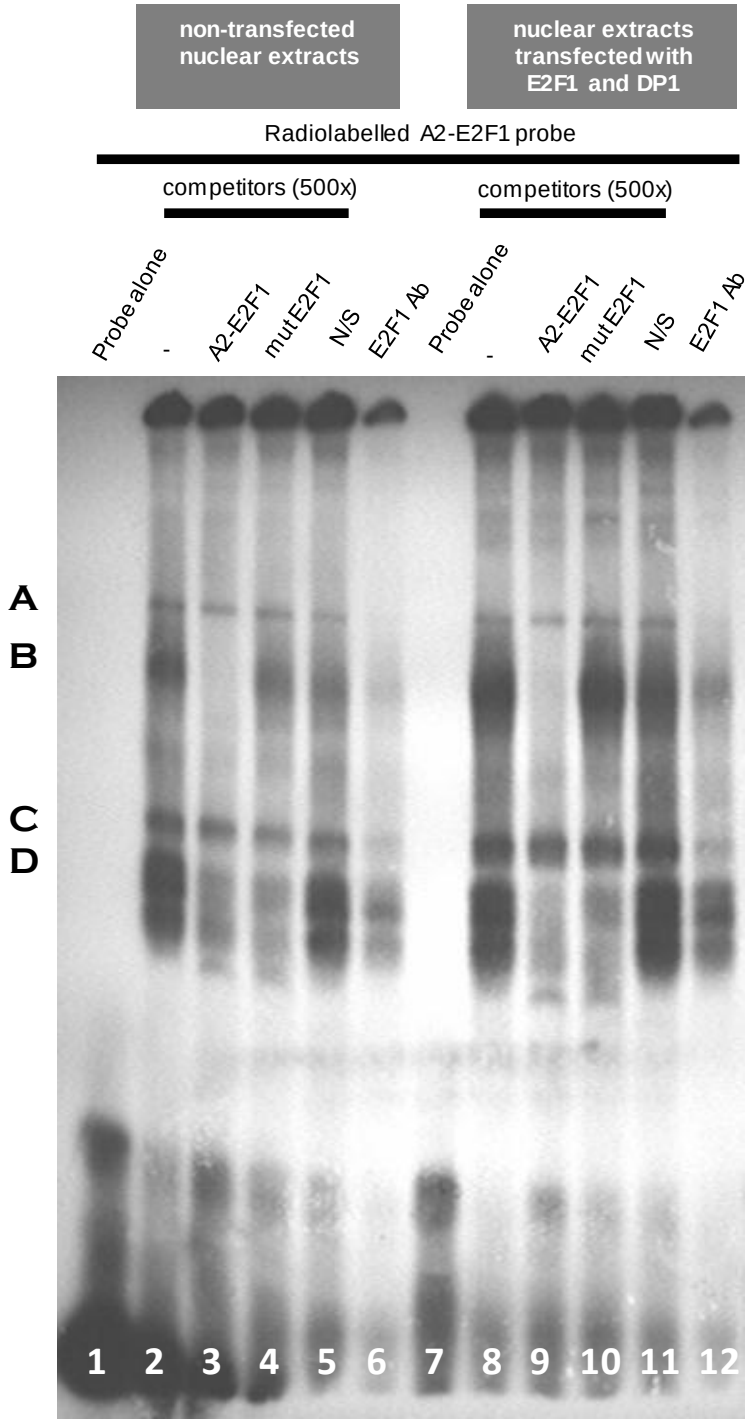

Figure 5.7. Comparison of the binding of a known E2F1 binding site incubated with nuclear protein extracts from non-transfected UB/OC2 cells or nuclear protein extracts from UB/OC2 cells transfected with E2F1 and DP1. EMSA was performed using the A2 probe (referred to as A2-E2F1), known for containing a functional E2F1 binding site, labelled with [γ-32P] ATP. The labelled A2-E2F1 probe was incubated with nuclear protein extracts from non-transfected UB/OC2 cells or nuclear protein extracts from UB/OC2 cells transfected with E2F1 and DP1, in the absence of competition (lanes 2 and 8) or in competition with an excess of 500ng of non-radiolabelled competitors (A2-E2F1 in lanes 3 and 9; mutant E2F1-lanes 4 and 10; non-specific probe (N/S)-lanes 5 and 11). For supershift assays (lanes 6 and 12), 1µl of rabbit polyclonal anti-E2F1 (C-20) sc-193X (Santa Cruz Biotechnology, Inc) was added to the binding reaction 1h before the labelled A2-E2F1 probe was added.

5.3.3 Characterization of binding affinities of the predicted E2F sites in the *Atoh1* regulatory elements

Having confirmed that a known E2F probe can be bound by the E2F protein in nuclear extracts from UB/OC2 cells, the investigation then focused on assessing which of the E2F binding sites predicted in the chick *Atoh1* enhancers and putative enhancer C can also be bound by E2F. In order to test whether there is such interaction between E2F and the chick *Atoh1* regulatory elements, oligonucleotides were designed containing the E2F binding sites located in the chick *Atoh1* conserved regions predicted by bioinformatics analysis. These probes are represented in Table 5.2, referred to as probe 1 to probe 9 based on the relative position within the chick *Atoh1* enhancers and the putative enhancer C shown in Figure 5.8.

Table 5.2. EMSA oligonucleotides containing the putative E2F sites in the *Atoh1* regulatory regions. Each probe contains an E2F binding site predicted by the Genomatix analysis. The predicted E2F binding sites are underlined in each probe. Probes were referred to as probe 1-9 corresponding to the nine E2F sites predicted in the chick *Atoh1* regulatory elements.

Oligo name	Primer Sequence (5' to 3')	Predicted Binding site
Probe 1_Sense	AGCCGCGAAGTGCGCGCTCTCCGCTTTGC	E2F2 and E2F3
Probe 1_Antisense	GCAAAGCGGAGAGCGCGCACTTCGCGGCT	E2F2 and E2F3
Probe 2_Sense	GCCTCAAAAAGCGATAAAAAATGGCACA	E2F1&E2F4
Probe 2_Antisense	TGTGCCATTTTTTATCGCTTTTTGAGGC	E2F1&E2F4
Probe 3_Sense	TCCCGGCCGCGGTGCGCCGTGTCTGGA	E2F2 and E2F3
Probe 3_Antisense	TCCAGACACGGCGCACCGCGGCCGGGA	E2F2 and E2F3
Probe 4_Sense	CTTTCAGGCGGCGCCCCGGGGAGCTGC	E2F3
Probe 4_Antisense	GCAGCTCCCCGGGGCGCCGCCTGAAAG	E2F3
Probe 5_Sense	TGTCCTCTCGCCCGCCCTGGTGCGCGCTCCCGC	E2F1, E2F2 and E2F3
Probe 5_Antisense	GGAGCGCGCACCAGGGCGGGCGAGAGGACA	E2F1, E2F2 and E2F3
Probe 6_Sense	TGCGCGCTCCCGCGCCCAACGCGGGACAGCGACGCGC	E2F1 and E2F4
Probe 6_Antsense	GCGCGTCGCTGTCCCGCGTTGGGCGCGGGAGCGCGCA	E2F1 and E2F4
Probe 7_Sense	GAGCGGTGCTGCCGCGCTTTATGGAGC	E2F2
Probe 7_Antisense	GCTCCATAAAGCGCGGCAGCACCGCTC	E2F2
Probe 8_Sense	ATTTCTTCCCCGGGAGAACGCGCCGG	E2F1
Probe 8_Antisense	CCGGCGCGTTCTCCCGGGGAAGAAAT	E2F1
Probe 9_Sense	GATTTTCCTCCCGAAAAACGCCGGGT	E2F1
Probe 9_Antisense	ACCCGGCGTTTTTCGGGAGGAAAATC	E2F1

Figure 5.8. Location of the predicted E2F binding sites in the chick *Atoh1* enhancers and putative enhancer C. Summary of the relative position of the nine E2F binding sites predicted by MatInspector. When two predicted binding sites were close to each other, we defined them as a single site (e.g. site 5 and site 6). The core of the binding site is represented in red capital letters. Two or more overlapping binding sites were marked in green/red (e.g. site 2).

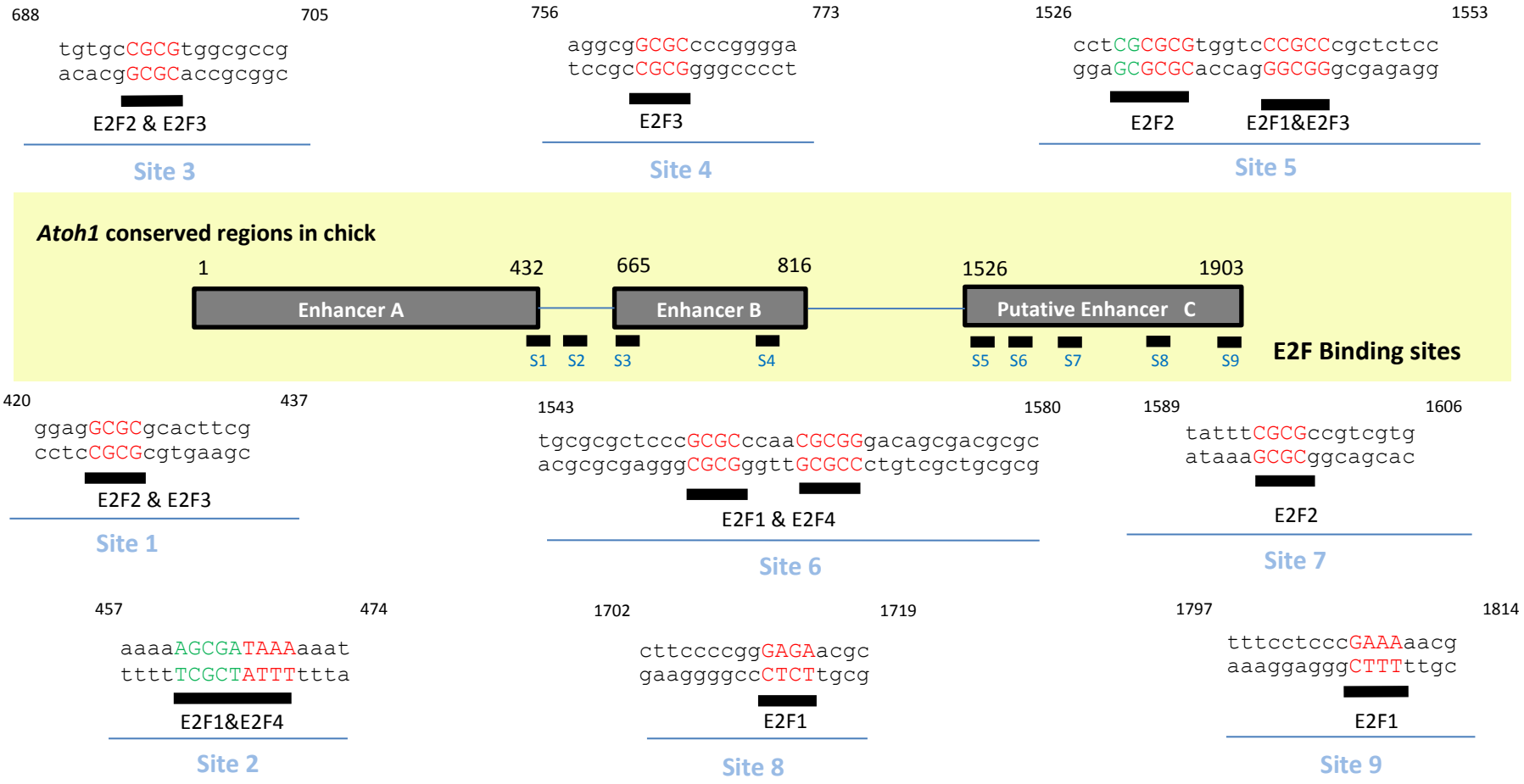

As in the previous EMSA experiment, a known E2F probe (the A2-E2F1 probe) was radiolabelled and incubated with nuclear extracts from UB/OC2 transfected with E2F1 and DP1 expression constructs. As shown in Figure 5.9, one protein-DNA complex (bandshift B in lane 3) was competed by the cold consensus E2F probe (the A2-E2F1 probe). This bandshift was not competed by the mutated E2F1 probe or the non-specific probe (Figure 5.9, bandshift B, lane 4-5).

To investigate whether the predicted E2F sites in the chick *Atoh1* regulatory regions can compete with the known E2F probe (the A2-E2F1 probe) for binding E2F, the oligonucleotides (probes) containing the putative E2F sites in the chick *Atoh1* were used in competition assays (probes 1-9 and lanes 7-15 from Figure 5.9). Competition was performed by adding an excess of x500 of the cold competitors to the nuclear extracts before the addition of the radiolabelled A2-E2F1 probe. As shown in Figure 5.9, two probes, probe 2 and especially probe 6, showed signs of competition for E2F binding in EMSA suggesting that these sites could be bound by E2F1 (Figure 5.9 bandshift B, comparing lane 3 with lanes 8 and 12).

In contrast to probes 2 and 6, the rest of the probes predicted to be bound by E2F did not show any competition when incubated with the A2-E2F1 probe and therefore were not further analysed. To further investigate the specificity of probes 2 and 6 and to confirm that E2F can bind to these sites in the *Atoh1* regulatory elements, additional competition assays and supershift assays were performed.

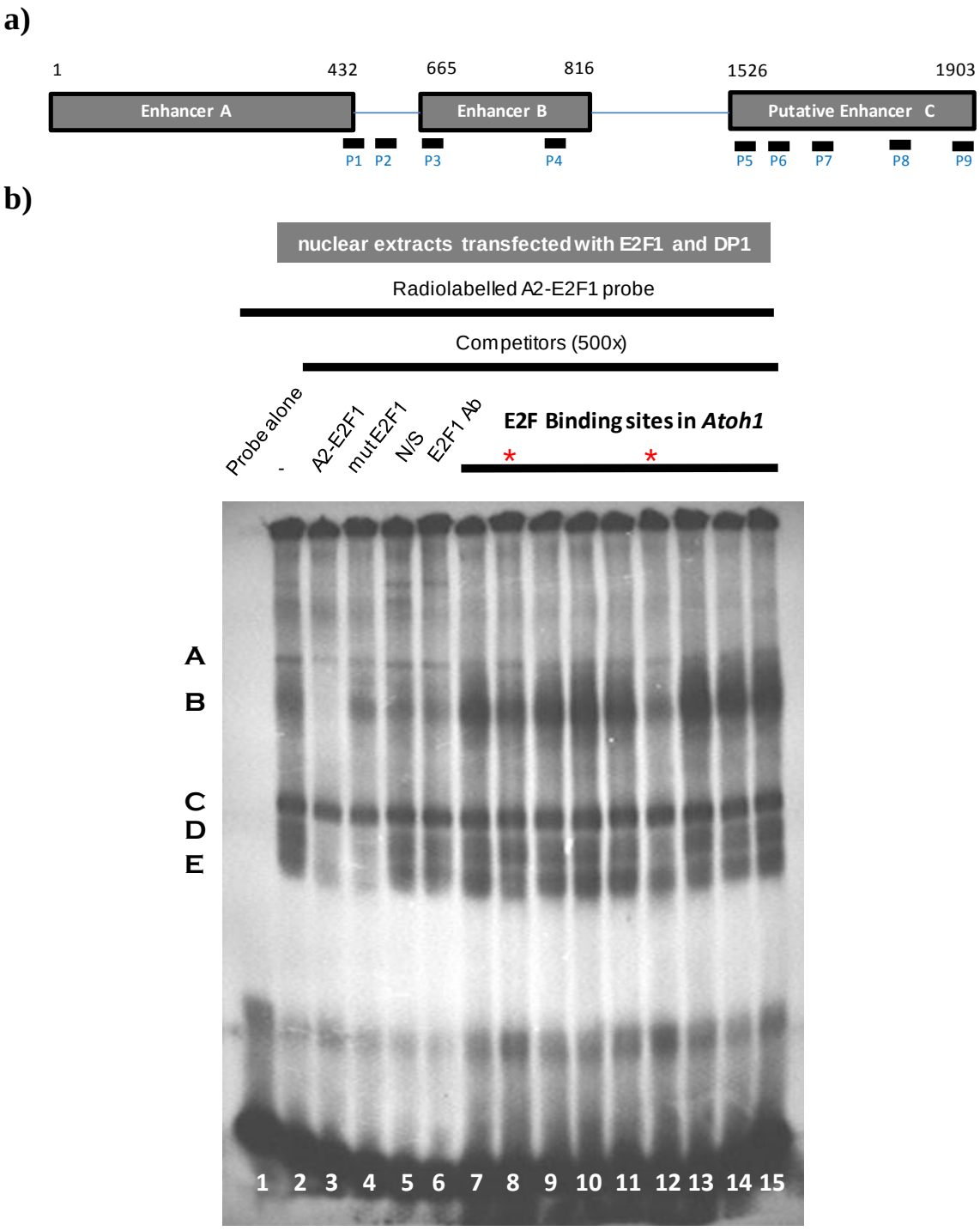

Figure 5.9. EMSA analysis of the predicted E2F sites in the chick *Atoh1* conserved regions. a) Nine probes were designed (P1-P9) corresponding to the E2F binding sites predicted in the chick *Atoh1* conserved regions. **b)** EMSA was performed using the A2-E2F1 probe, known for containing a functional E2F1 binding site, labelled with [γ-32P] ATP. The labelled A2-E2F1 probe was incubated alone (lane 1) or with nuclear extracts transfected with E2F1 and DP1 (lanes 2-15). Competition assays were performed with an excess of 500ng of non-radiolabelled competitors (A2-E2F1-lane 3), mutant E2F1 (lanes 4), non-specific (N/S) probe (lane 5). For supershift assays (lane 6), 1µl of rabbit polyclonal anti-E2F1 was added to the binding reaction 1h before the labelled A2-E2F1 probe was added. A competition assay was also performed using an excess of 500ng of non-radiolabelled E2F probes sequences predicted in the chick *Atoh1* conserved regions (lanes 7-15) corresponding to sites 1 to 9 as described in **a)**.

5.3.4 Further analysis of *Atoh1* probes 2 and 6 as putative E2F binding sites

The preliminary results presented so far show that two of the E2F binding sites predicted by Genomatix, probe 2 and 6, have some capacity to compete for E2F proteins when incubated with a probe containing a known E2F binding site. To further investigate the specificity of probe 2 and 6, a competition gradient experiment was conducted where the radiolabelled probe 2 and 6 were incubated with increasing amounts of cold competitors.

An EMSA assay with radiolabelled probe 2 and nuclear extracts from UB/OC2 cells transfected with E2F1 and DP1 is shown in Figure 5.10. Increasing amounts of cold probe 2 and cold A2-E2F1 were used as competitors for E2F protein. This resulted in faint attenuation of bandshift A when incubated with increasing amounts of cold probe 2 (Figure 5.10b lanes 2-4). However, no competition was observed when the radiolabelled probe 2 was incubated with the cold A2-E2F1 probe (Figure 5.10b, lanes 5-7). A mutated probe 2 (mut P2) was designed containing a mutation in the core sequence of the predicted E2F binding site of probe 2 (Table 5.3). The mutated P2 probe was used in order to test whether competition was dependent on presence of the E2F binding site. However, mutated P2 probe still competes with the labelled P2 for E2F protein suggesting is not specific to E2F.

The presence of E2F protein in the complex with probe 2 was also investigated in a supershift assay by the addition of an E2F1 antibody to the nuclear extracts before or after adding the labelled probe 2. As is shown in Figure 5.10c, lane 9, when the E2F1 antibody was incubated before adding the labelled probe 2, the formation of a heavier "supershifted" complex was observed in shift A. This larger DNA probe-protein-antibody complex was observed as a result of a slower migration on the gel after the addition of the E2F1 antibody to the DNA probe-protein complex. When using a non-specific antibody against E2F1, no supershift was formed (Figure 5.10c, lane 10). The supershift assay was also performed by adding the antibody after the radiolabelled probe 2. When the E2F1 antibody was added after the labelled probe 2, a supershift was also observed although fainter than when adding the antibody before the radiolabelled probe 2 (Figure 5.10c, lane 11). When adding a non-specific antibody after the radiolabelled probe 2, a supershift was not observed (Figure 5.10, lane 12).

The supershift results suggest that shift A includes an E2F transcription factor.

Table 5.3. Oligonucleotides used for EMSA experiments containing point mutations in Probe 2 and Probe 6. Mutations were introduced into the core of the predicted E2F binding sites. In site 6, two E2F binding sites were predicted therefore the binding sites were mutated alternatively (Probe6mut_a and Probe6mut_b). The core of the binding site is underlined and the mutations are in bold.

Oligo name	Primer Sequence (5' to 3')	Predicted Binding site
Probe 2mut_Sense	GCCTCAAAAA**TT**GATAAAAAATGGCACA	E2F1 and E2F4
Probe 2mut_Antisense	TGTGCCATTTTTTATC**AA**TTTTTGAGGC	E2F1 and E2F4
Probe 6mut_a_Sense	TGCGCGCTCCCG**TT**CCCAACGCGGGACAGCGACGCGC	E2F1 and E2F4
Probe 6mut_a_Antisense	GCGCGTCGCTGTCCCGCGTTGGG**AA**CGGGAGCGCGCA	E2F1 and E2F4
Probe 6mut_b_Sense	TGCGCGCTCCCGCGCCCAAC**TT**GGGACAGCGACGCGC	E2F1 and E2F4
Probe 6mut_b_Antisense	GCGCGTCGCTGTCC**AA**GTTGGGCGCGGGAGCGCGCA	E2F1 and E2F4

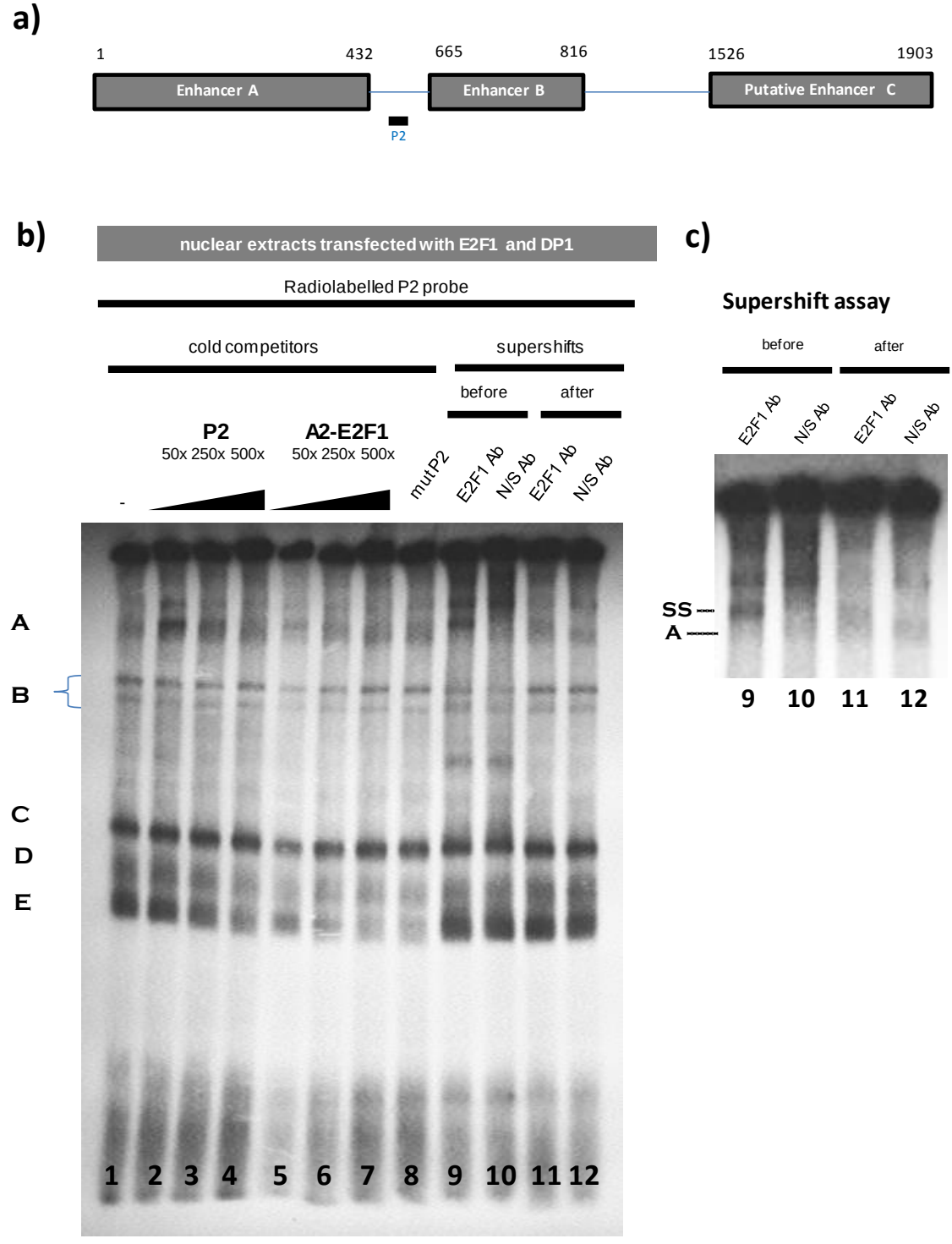

Figure 5.10. Competition assay to test specificity of Probe 2. a) Schematic representation of the location of the predicted E2F binding site, named site 2, in the chick *Atoh1* 3' sequence. Site 2 was predicted between the chick *Atoh1* enhancer A and B. An oligonucleotide probe (Probe 2) was designed containing the sequence of the predicted E2F binding site 2 for EMSA experiments. **b)** The radiolabelled Probe 2 was incubated with nuclear extracts from UB/OC2 transfected with E2F1 and DP1 in competition with cold P2 (lanes 2-4), cold known E2F1 (A2-E2F1 probe) (lanes5-7) or a cold mutant for Probe 2 (mut P2) (lane 8). **c)** Enlarged image of the supershift represented in **b)**. Supershift was conducted with a rabbit polyclonal anti-E2F1 (C-20) sc-193X (lanes 9 and 11) and rabbit polyclonal anti-SP1 antibody H-225X (lanes 10 and 12) used as a non-specific control added before or after the addition of the labelled Probe 2.

Probe 6 contains two putative E2F binding sites in the putative chick enhancer C located downstream of the *Atoh1* enhancers (see Figure 5.8) and was also analysed in EMSA experiments. A gradient competition assay was performed using increasing amounts of cold probe 6 and cold A2-E2F1 probe as competitors. Both probes competed for binding with the labelled P6 probe and caused a slight attenuation of bandshift B (Figure 5.11, lanes 2-7). To further investigate whether E2F binding is specific to the presence of the E2F site within probe 6, a mutated probe 6 was designed. Since probe 6 contains two putative E2F binding sites (Figure 5.8), two different mutated probes were designed containing independent mutations in the E2F binding sites located in probe 6 (referred to as mutant probe 6_a and mutant Probe 6_b in Table 5.3). These two mutated probes were used in the competition assay (lane 8 and 9 in Figure 5.11). As shown in Figure 5.11 lane 9, when the cold mutant corresponding to probe 6_mut_b was used as a competitor, the attenuated bandshift B was slightly restored suggesting that E2F binding is specific to site b in probe 6. In contrast, the probe containing a mutation in the first E2F site in probe 6 (probe6_mut_a) still competes with probe 6 for bandshift B suggesting that E2F binding is not specific to site a in probe 6.

In addition, a supershift was conducted in order to confirm the presence of E2F protein in the E2F-probe 6 binding complex (Figure 5.11). In the presence of an E2F1 antibody, added before or after the radiolabelled probe 6 (lane 10 and 12), a shifted complex was observed (SS on Figure 5.11) confirming that E2F is a component of the binding complex.

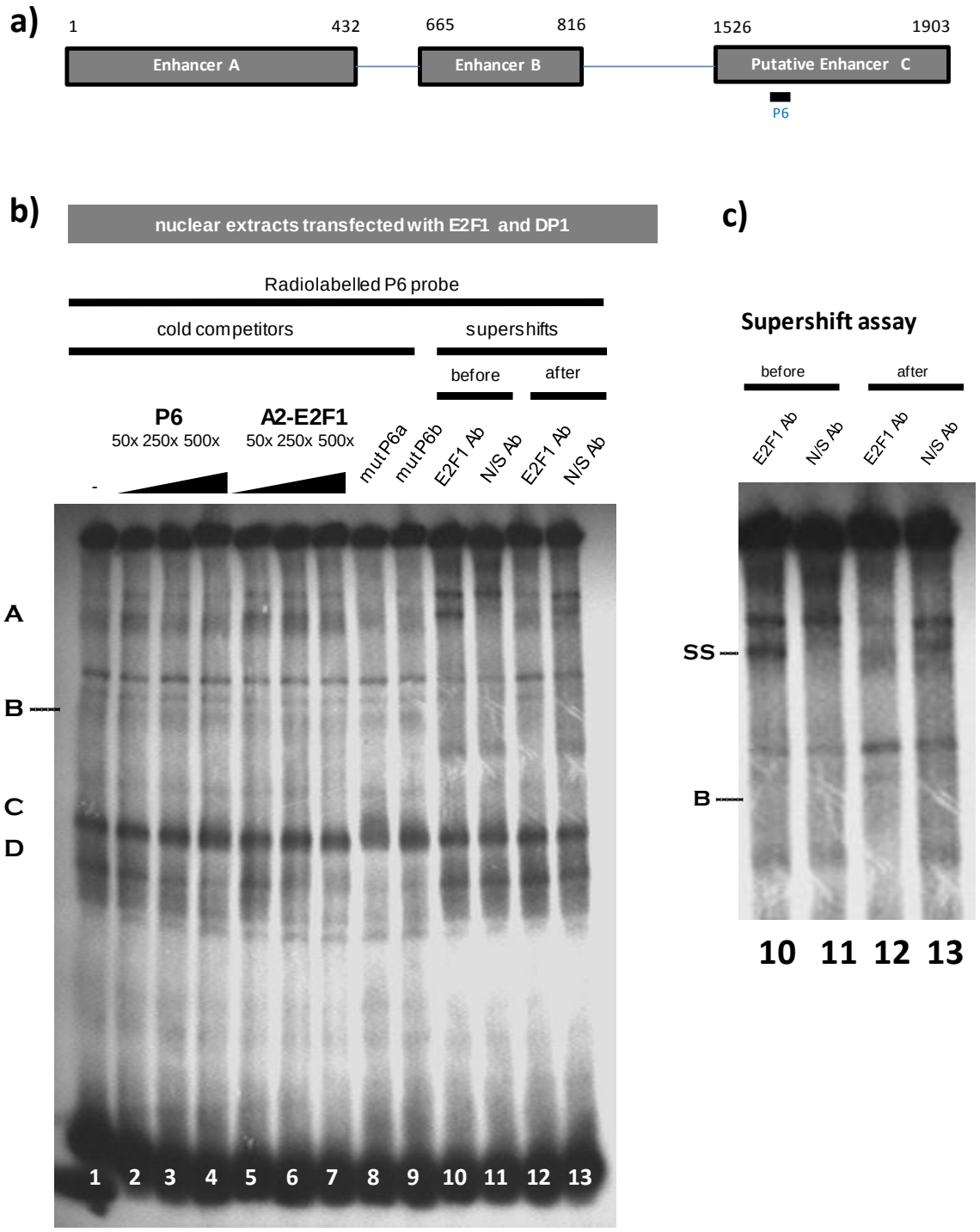

Figure 5.11. Competition assay to test specificity of Probe 6. a) Schematic representation of the location of the predicted E2F binding site (site 6) in the chick putative enhancer C. An oligonucleotide probe (probe 6) was designed containing the sequence of the predicted E2F binding site 6 for EMSA experiments. **b)** The radiolabelled probe 6 was incubated with nuclear extracts from UB/OC2 cells transfected with E2F1 and DP1 in competition with cold P6 (lanes 2-4), cold known E2F1 (A2-E2F1 probe) (lanes 5-7) or with a cold mutant for probe 6 (mutP6a or mutP6b) (lanes 8 and 9). **c)** Enlarged image of the supershift represented in **b)**. Supershift was conducted with a rabbit polyclonal anti-E2F1 (C-20) sc-193X (lanes 10 and 12) and rabbit polyclonal anti-SP1 antibody H-225X (lanes 11 and 13) used as a non-specific control added before or after the addition of the labelled probe 6.

The evidence provided by the EMSA experiments suggests that two of the nine E2F binding sites predicted by the Genomatix analysis have the capacity to be bound by E2F. Combining the results obtained so far, it can be hypothesized that these two binding sites may be responsible for the upregulation observed in the luciferase assays. It is notable that the location of these binding sites correlates with the responses obtained by the different chick *Atoh1* conserved regulatory regions when co-transfected with E2F1. For example, the chick *Atoh1* enhancer AB was upregulated when co-transfected with E2F1 and one of the specific binding sites defined by the EMSA experiments, site 2, is located between these two enhancers, a sequence that is present in the chick *Atoh1* enhancer AB luciferase construct. Similarly, a response was obtained with the putative enhancer C when co-transfected with E2F1 and site 6 located in this region, was found to be bound by E2F1 in EMSA experiments.

To finally confirm whether E2F upregulates the chick *Atoh1* enhancer AB and putative enhancer C via these two sites, point mutations were introduced into the two specific E2F binding sites in the luciferase constructs (site 2 and site 6 represented on Figure 5.8).

5.4 Site Directed Mutagenesis of sites 2 and 6 within the avian *Atoh1* conserved regions

EMSA experiments suggested that two of the putative E2F binding sites (site 2 and site 6) were the most likely sites to be bound by E2F. Having predicted and tested these two sites, the investigation was focused on verifying whether site 2 and site 6 were functional binding sites by creating point mutations in their sequences in the *Atoh1* luciferase constructs.

5.4.1 Design of mutagenesis sites

In order to identify which nucleotides need to be mutated, the sequence of site 2 and site 6 was compared against the consensus E2F1 binding site (Tao et al. 1997) (Figure 5.12a and b). In addition, a cross species alignment was performed to identify which nucleotides are evolutionary conserved in site 2 and site 6 and therefore more likely to be necessary for binding and regulation of E2F (Figure 5.12b).

A reduction of the E2F binding activity when some base pairs of the E2F binding site are mutated has already been demonstrated in previous studies (Lu et al. 2006). Based on this analysis, it was found that the GCGC sequence within the core of the E2F binding site is the most effective site in abolishing E2F binding in EMSA experiments. Moreover, the GCGC sequence is well conserved across different avian and mammalian species (Figure 5.12b) and it is contained within the consensus E2F1 (Figure 5.12a). Thus, two point mutations were incorporated in the GCGC sequence of site 2 and site 6 by site-directed mutagenesis (Figure 5.12c).

a)

Picture removed for copyright purposes

b)

Conservation profile of Site 2

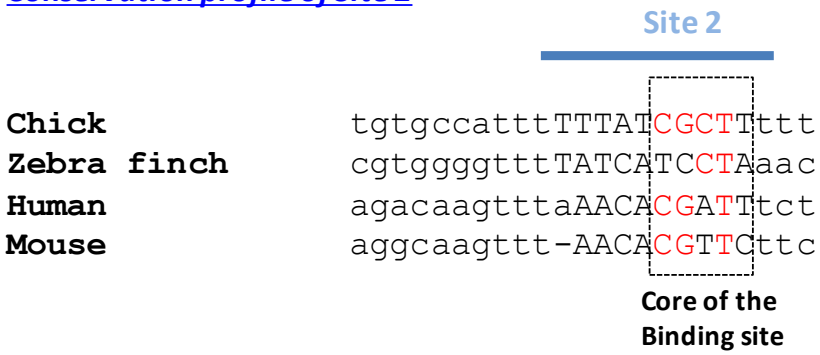

Conservation profile of Site 6

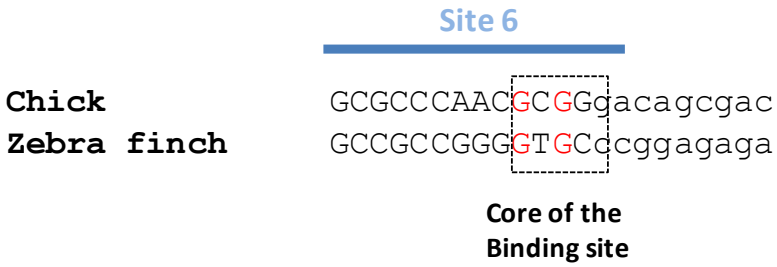

c)

Mut Site 2 tgtgccatttTTTATCTTTTttt

Mut Site 6 GCGCCCAACTTGGgacagcgac

Figure 5.12. Comparison between the consensus E2F1 binding site and the predicted site 2 and site 6. a) Consensus E2F1 binding site given by MatInspector, Genomatix. The core of the binding site is defined as the most critical part of the sequence for E2F binding. **b)** Cross species alignment of site 2 and site 6 in the *Atoh1* regulatory regions. Alignments were conducted against different avian and mammalian species in order to find out which nucleotides are more likely to be required for the binding of E2F. Conserved nucleotides within the core sequence of site 2 and site 6 were marked in red. **c)** Mutations (marked in blue and with asterisk) incorporated in the core of the predicted E2F binding site (core shown in red and blue) of site 2 and site 6.

5.4.2 Site-directed mutagenesis of sites 2 and 6

The *in vitro* site-directed mutagenesis kit from Stratagene (QuikChange II Site-Directed Mutagenesis) was used to introduce modifications into the *Atoh1* luciferase constructs containing the chick *Atoh1* conserved elements (see section 2.2.10). The technique requires the design of primers containing the desired mutation in the E2F binding sites in site 2 and site 6 (primers 16-19 in Table 2.1). Mutagenic primers were designed using Stratagene's web-based QuikChange® Primer Design Program available online at http://www.stratagene.com/qcprimerdesign.

The mutations in E2F predicted binding sites 2 and 6 were introduced in the GCGC region of the E2F binding site, as is the most likely region to abolish E2F binding based on previous experiments. Only two nucleotide changes were introduced in each site since the site-directed mutagenesis technique has some limitations and the success of the protocols is, in part, defined by the number of base pairs to be mutated (Novoradovsky et al. 2005). Mutations were introduced in the construct containing all three *Atoh1* conserved elements found in chick (construct referred to as Chick ABC containing the chick conserved regions upstream of the luciferase). This is because this construct contains both E2F site 2 and the E2F binding site corresponding to site 6 so the effect of mutating each of these could be assessed in the same construct. Following the manufacturer's protocol with the thermal conditions described in section 2.2.10, mutations were successfully integrated in both sites. The Chick ABC construct containing the mutations in the E2F binding sites in probe 2 and 6 was sequenced in order to verify that mutations were incorporated in the desired location. The primers used for the sequencing (primers 23 and 24 in Table 2.1) and chromatograms confirming the introduction of the point mutations are presented in Figure 5.13.

Figure 5.13. Verification of the nucleotide substitutions by Site-directed mutagenesis. Sequencing chromatograms showing that the two point mutations were successfully introduced in site 2 and site 6 (marked with an asterisk).

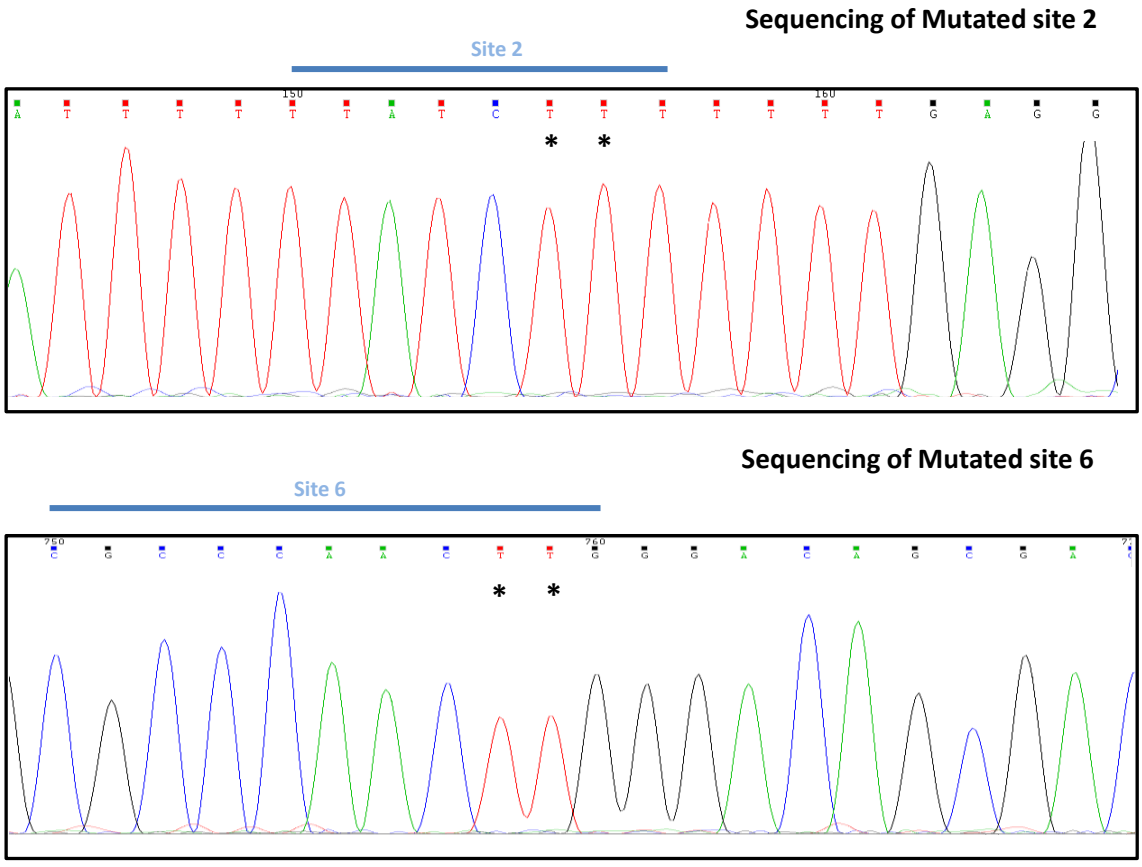

5.5 Response of the *Atoh1* conserved regions to E2F1 when putative E2F sites are mutated

As previously shown, the chick *Atoh1* enhancers and putative enhancer C were upregulated when co-transfected with E2F1 (Figure 5.3). Since mutations were successfully introduced in two putative E2F binding sites in the chick ABC luciferase construct, I aimed to assess whether these mutations were sufficient to reduce the upregulation observed in the wild type luciferase construct containing the chick *Atoh1* conserved regions by E2F1.

In section 5.2, a large upregulation of 27, 61 and 145-fold difference was observed when the luciferase construct containing the chick *Atoh1* conserved regions was co-transfected with increasing amounts of E2F1 (from 400ng to 1200ng respectively). To examine the effect of the mutations on each putative binding site, the mutated constructs, denoted Chick ABC_ p2mut and Chick ABC_p6mut, were co-transfected with increasing amounts of E2F1 in UB/OC2 cells. The ability of the mutated constructs to respond to E2F1 was quantified and compared against the response obtained with the wild type construct (denoted as Chick ABC_wt).

As shown in Figure 5.14, the wild type construct (Chick ABC_wt) generated a large response when co-transfected with E2F1 (Figure 5.14b). This response was similar to the one previously observed and described in section 5.2. However, the large response observed in the wild type luciferase construct was attenuated when using the constructs containing the E2F binding site mutations. The mutation of the putative E2F site 2 for instance, reduced the upregulatory effect of E2F1 by 37%. This reduction was observed only when 1200ng of E2F1 was transfected in comparison to the response given by the wild type construct ($p<0.05$ in Figure 5.14b). By contrast, the Chick ABC_p6mut showed a 77% decrease when 1200ng of E2F1 was co-transfected. The mutation in site 6 within the putative enhancer C also attenuated the effect by 40% and 68% downregulation when 400 and 800ng of E2F1 were co-transfected respectively (Figure 5.14b). This reduction in the response of the construct containing the mutation in site 6 (chick ABC_p6mut) was statistically significant in comparison to the response given by the wild type construct ($p<0.001$ in Figure 5.14b).

Based on these results, a direct interaction between the E2F1 transcription factor and site 2 and site 6 in the *Atoh1* regulatory regions can be suggested.

Figure 5.14. Response of the *Atoh1* regulatory regions to E2F1 when the putative E2F sites are mutated. a) Diagram representing two of the putative E2F sites: site 2 which contains two overlapped putative binding sites for E2F1 or/and E2F4 (in green and red respectively) and site 6 which also contains a putative binding site for E2F1 and/or E2F4 (in red). Point mutations were introduced in these sites (positions marked with asterisks). **b)** Luciferase assays show a reduced response of the Chick_ABCp2mut (*p<0.05) and the Chick_ABCp6mut (***p<0.001) when E2F1 is co-transfected in comparison with the wild type luciferase construct. The experiment was conducted in triplicate in two separate assays with different DNA preparations. Student t-test was conducted.

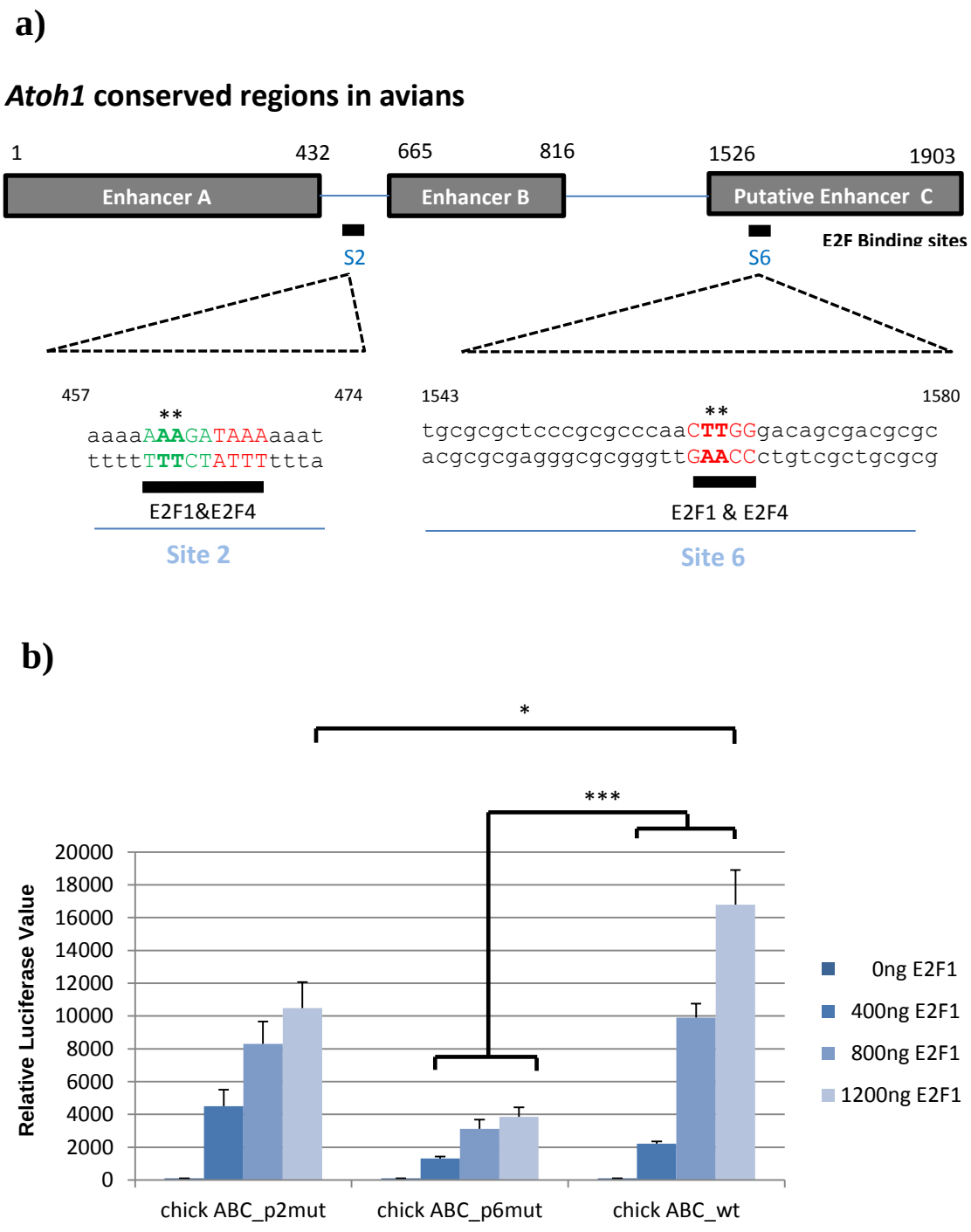

5.6 Transcriptional regulation of the *Atoh1* conserved regions by other E2F transcription factors

In addition to the study of E2F1, other members of the E2F family were also analysed in luciferase assays to assess their putative regulatory roles on the *Atoh1* conserved elements. Based on the similarity of the binding site sequence of the different E2F members and their similar functions (see section 5.1.2), it may be possible that they also play roles in the regulation of *Atoh1*.

To assess this possibility, luciferase plasmids containing the mouse and chick *Atoh1* regulatory elements cloned upstream of the firefly luciferase reporter gene (section 2.2.9.3) were co-transfected in UB/OC2 cells with 1200ng of E2F2, E2F3 and E2F4 expression constructs in separate assays. Expression constructs for E2F2, E2F3 and E2F4 have been previously described and therefore were obtained from other laboratories to perform these experiments. The E2F2 is a pCMV-Neo-Bam construct (Wu et al. 1995), the E2F3 is a pcDNA3 construct (Lui and Baron 2013) and the E2F4 is a pcDNA3 construct (Beijersbergen et al. 1994). The ability of the E2Fs to activate the *Atoh1* luciferase constructs was compared against the response with the empty pcDNA3 expression construct (Figure 2.5).

As shown in Figure 5.15a, E2F2 activated the mouse *Atoh1* AB enhancer 2-fold. The response obtained, was almost identical to the response obtained in the empty luciferase construct, suggesting that although the response was statistically significant, it could be artefactual and not due to the mouse *Atoh1* enhancer. However, E2F2 has the capacity to activate the chick *Atoh1* AB enhancer as well as the putative enhancer C with a 15.3-fold and 17.8-fold activation respectively. Moreover, the response given by the construct containing the three *Atoh1* conserved regions, the Chick ABC luciferase construct, showed a greater response, giving a 66.3-fold upregulation. The ability of E2F2 to activate the luciferase construct containing the mutation in the putative E2F site 6 was also tested. The mutant ChickABC_p6 (ChickABC_p6mut) showed a significant decrease in its response when co-transfected with E2F2 showing a 34.4-fold difference in comparison to the 66.3-fold upregulation shown in the wild type ChickABC construct (Figure 5.15a). These results support the hypothesis that the E2F binding site 6 located

in the putative enhancer C can also be directly be bound by E2F2 as these luciferase experiments demonstrate.

The response obtained when E2F3 was co-transfected with the *Atoh1* luciferase constructs was also tested (Figure 5.15b). The *E2f3* locus encodes two gene products, E2F3a and E2F3b, which are transcribed through two different promoters (Adams et al. 2000). Only the effect of the E2F3a product was tested. The effect of E2F3 on the mouse and chick *Atoh1* enhancers was very similar to the one obtained with E2F2. The mouse *Atoh1* enhancer showed a response of 3-fold difference in comparison to the response in the absence of exogenous E2F3. However, E2F3 had a higher capacity to activate the chick *Atoh1* enhancer AB and putative enhancer C showing a response of 14.2-fold and 22.3-fold difference in comparison with the response obtained with the basal empty pcDNA3. When the chick *Atoh1* AB enhancer and putative enhancer C were present in the same construct, the Chick ABC luciferase construct, the response observed when co-transfected with E2F3 was a 51.8-fold activation. The ability of E2F3 to activate the mutant ABC_p6 construct was also tested which showed a 30-fold activation. This response was close to reaching statistical significance ($p=0.098$) when compared to the response obtained by the wild type construct.

Finally, the response of the *Atoh1* luciferase constructs was also tested with E2F4 (Figure 5.15c). As described in section 5.1.2, E2F4 has been defined as a repressor (Ginsberg et al. 1994). E2F4 did not cause a statistically significant effect on the mouse and chick *Atoh1* enhancer AB (Figure 5.15c). However, a repressive effect was observed in the putative enhancer C by E2F4. This downregulation was also observed in the empty luciferase construct however, the level of repression was greater in the putative enhancer C by the effect of E2F4. The downregulation was not observed in the Chick ABC luciferase construct however, it is observed when site 6 located in the putative enhancer C is mutated.

Altogether, the luciferase results suggested that E2F2 and E2F3 have the potential to activate the chick *Atoh1* enhancers and chick putative enhancer C but not the mouse *Atoh1* enhancer. Although this activation is lower than the response observed by E2F1 (145-fold), it seems that based on the homology of the binding site sequence of these three E2F members and their activation functions, E2F1, E2F2 and E2F3 have the potential to upregulate *Atoh1* transcription in chick. Moreover, it was observed that the

transcriptional response is enhanced when the putative enhancer C is combined with the chick *Atoh1* AB enhancers. By contrast, E2F4 causes the downregulation of the putative enhancer C and this downregulation may be partially dependent on the E2F site 6.

Figure 5.15. Effect of E2F2, E2F3 and E2F4 on the *Atoh1* conserved regions. UB/OC2 cells were transfected with 1200ng of E2F2 **(a)**, E2F3a **(b)** and E2F4 **(c)** expression constructs. 10ng of the pRL-null luciferase construct (Promega) were co-transfected and 1200ng of the empty pcDNA3 expression construct was also used to compare with E2F. **a)** A significant response was observed when the Chick *Atoh1* luciferase constructs were co-transfected with E2F2 in comparison to the response obtained with the empty pcDNA3 construct. **b)** A significant response was also observed when the Chick *Atoh1* luciferase constructs were co-transfected with E2F3 in comparison to the response obtained with the empty pcDNA3 construct. **c)** No significant response was obtained with E2F4. Experiments were conducted in triplicate in two separate assays with different DNA preparations for each plasmid in each assay (n=6). The luciferase activity of each reporter is normalized to its response in the absent of stimulation (set at 100). Student t-test was conducted. The mean value and standard error of the mean from 6 experiments are presented **p < 0.01 or *p<0.05.

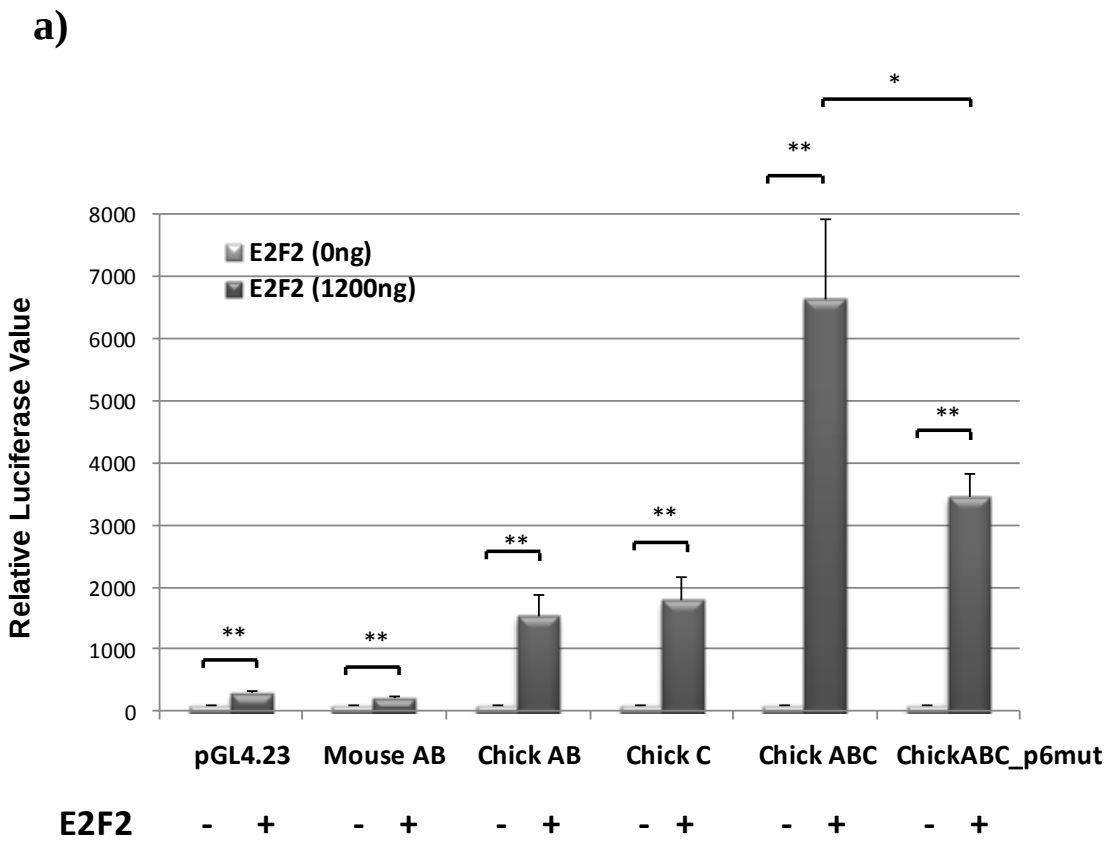

b)

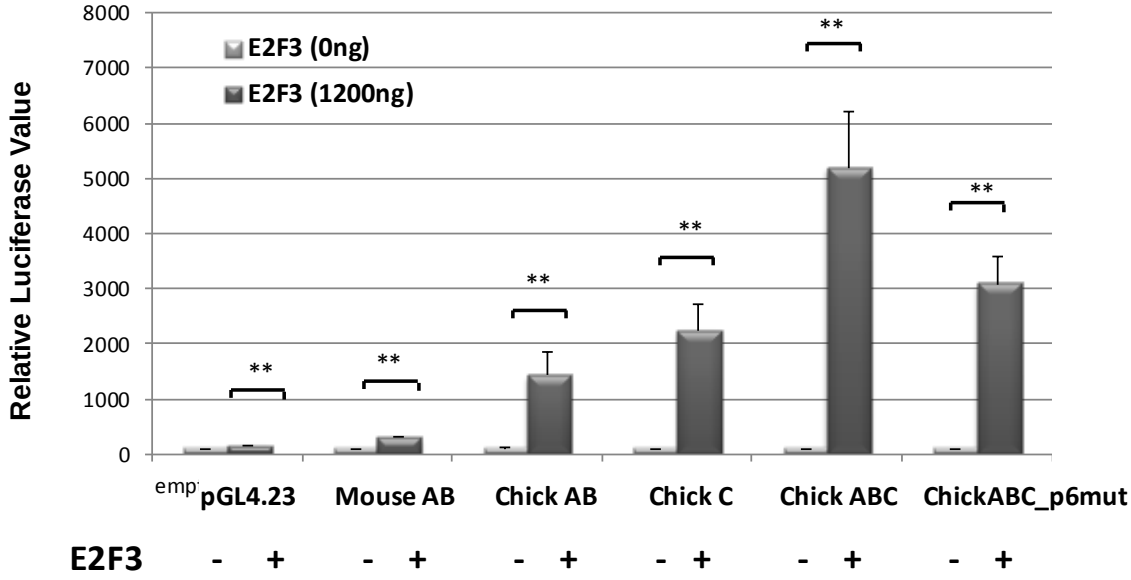
Relative Luciferase Value
8000
7000
6000
5000
4000
3000
2000
1000
0
E2F3 (0ng)
E2F3 (1200ng)
**
emp
pGL4.23
Mouse AB
Chick AB
Chick C
Chick ABC
ChickABC_p6mut
E2F3
- + - + - + - + - + - +

c)

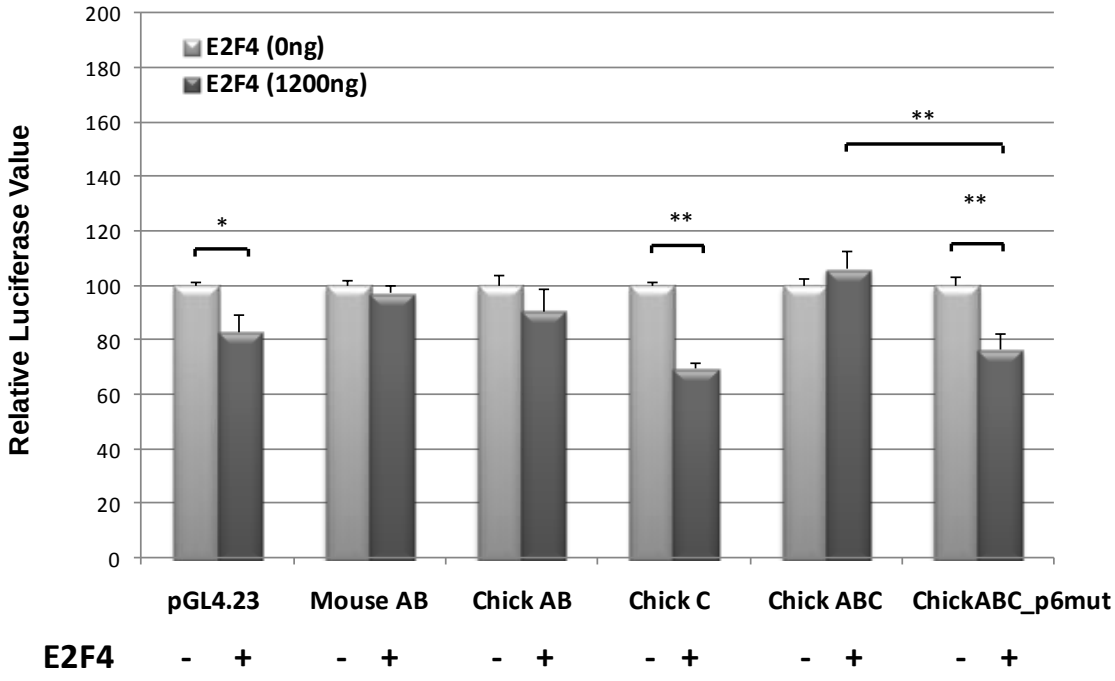
Relative Luciferase Value
200
180
160
140
120
100
80
60
40
20
0
E2F4 (0ng)
E2F4 (1200ng)
*
**
pGL4.23
Mouse AB
Chick AB
Chick C
Chick ABC
ChickABC_p6mut
E2F4
- + - + - + - + - + - +

5.7 Characterization of E2F1 expression in the mammalian and avian developing inner ear epithelium

The results presented so far, suggest that E2F1, as well as E2F2 and E2F3, are strong candidates for regulating *Atoh1* expression in the avian inner ear. Based on this hypothesis, the investigation focused on characterizing the expression of E2F1, the primary member of the E2F family, to assess potential correlations between E2F1 and ATOH1 expression.

All E2F transcription factors are expressed during embryonic development of the murine central nervous system (Dagnino et al. 1997; Kusek et al. 2001; Li et al. 2008). The expression of E2F1, E2F2 and E2F5, as assessed by *in situ* hybridization, is enriched in neural proliferating progenitors such as the neuroblastic layer of the retina, neuroepithelium and spinal cord (Dagnino et al. 1997). On the other hand, expression of E2F3 and E2F4 was found in proliferating as well as non-proliferating regions (Dagnino et al. 1997; Ruzhynsky et al. 2007).

The Єmage database (http://www.emouseatlas.org/emage) and the Allen Brain Atlas (http://www.brain-map.org) also provide evidence of E2F1 expression in embryonic and adult mouse tissues by *in situ* hybridization. These databases indicate that E2F1 mRNA is expressed in the hindbrain, spinal cord and in the developing limbs of mouse embryonic tissue whereas in the adult mouse, E2F1 was observed in different parts of the nervous system including the isocortex, hippocampus and cerebellum. In chick, the GEISHA database (Gallus Expression *In Situ* Hybridization Analysis (http://geisha.arizona.edu/geisha) and the echick atlas (http://www.echickatlas.org) provide some expression data for the E2F family. According to these databases, E2F1-8 mRNA is expressed in the hindbrain of embryonic chick stage 21, 24 and 27 (embryonic day 3.5, 4 and 5). In addition E2F1 mRNA appears to be expressed in the inner ear at E3.5 and E4.

Apart from the minimal data shown in the above websites, no reports in the inner ear describing expression of E2F1 in avian species and in mammals were found. E2F1 has been described only in adult mouse where it was suggested that it is expressed in the stria vascularis and spiral ganglion (Raimundo et al. 2012). Therefore, E2F1 expression was assessed in the mammalian and avian inner ear during development.

5.7.1 E2F1 expression in the developing chick inner ear epithelium

As described in section 5.3.1, E2F1 was found to be expressed in UB/OC2 cells, a conditional immortalized cell line derived from E13 primary cultures of the developing mouse organ of Corti. This expression was described using a rabbit polyclonal anti E2F1-1 (C-20) from Santa Cruz which was also used to assess E2F1 expression in chick and mouse inner ear tissue.

E2F1 expression was tested in the chick inner ear at E7 and E10. At E7, vestibular hair cells are already formed whereas cochlear hair cells in the basilar papilla are formed at around E10 (Goodyear and Richardson 1997). Therefore, cryosections were prepared from E7 and E10 chick specimens (see section 2.2.12) for immunofluorescence with the E2F1 antibody described above and anti-Myosin7a which was used as a hair cell marker. Figure 5.16a shows E2F1 expression in an E7 developing crista. The Myosin7a antibody strongly labelled the hair cells in the crista whereas E2F1 expression was relatively ubiquitous in the epithelium.

To test E2F1 expression in hair cells at a more advanced stage in development, expression of E2F1 was assessed at E10 (Figure 5.17a). At E10 vestibular hair cells in the crista labelled with E2F1 antibody showed that E2F1 expression still remains relatively weak and uniform throughout the developing crista epithelium. To test the specificity of the E2F1 antibody in chick tissues, controls were performed without the E2F1 antibody (primary antibody) and only with the Alexa Fluor® 488-conjugated anti-rabbit IgG (secondary antibody). The controls examined at embryonic day 7 and 10 (E7 and E10) showed a similar staining pattering in the crista as the samples labelled with the E2F1 antibody (Figure 5.16b and Figure 5.17b). Therefore, it is possible that the E2F1 antibody is not recognizing the chick E2F1 and the stain observed represents non-specific secondary antibody staining.

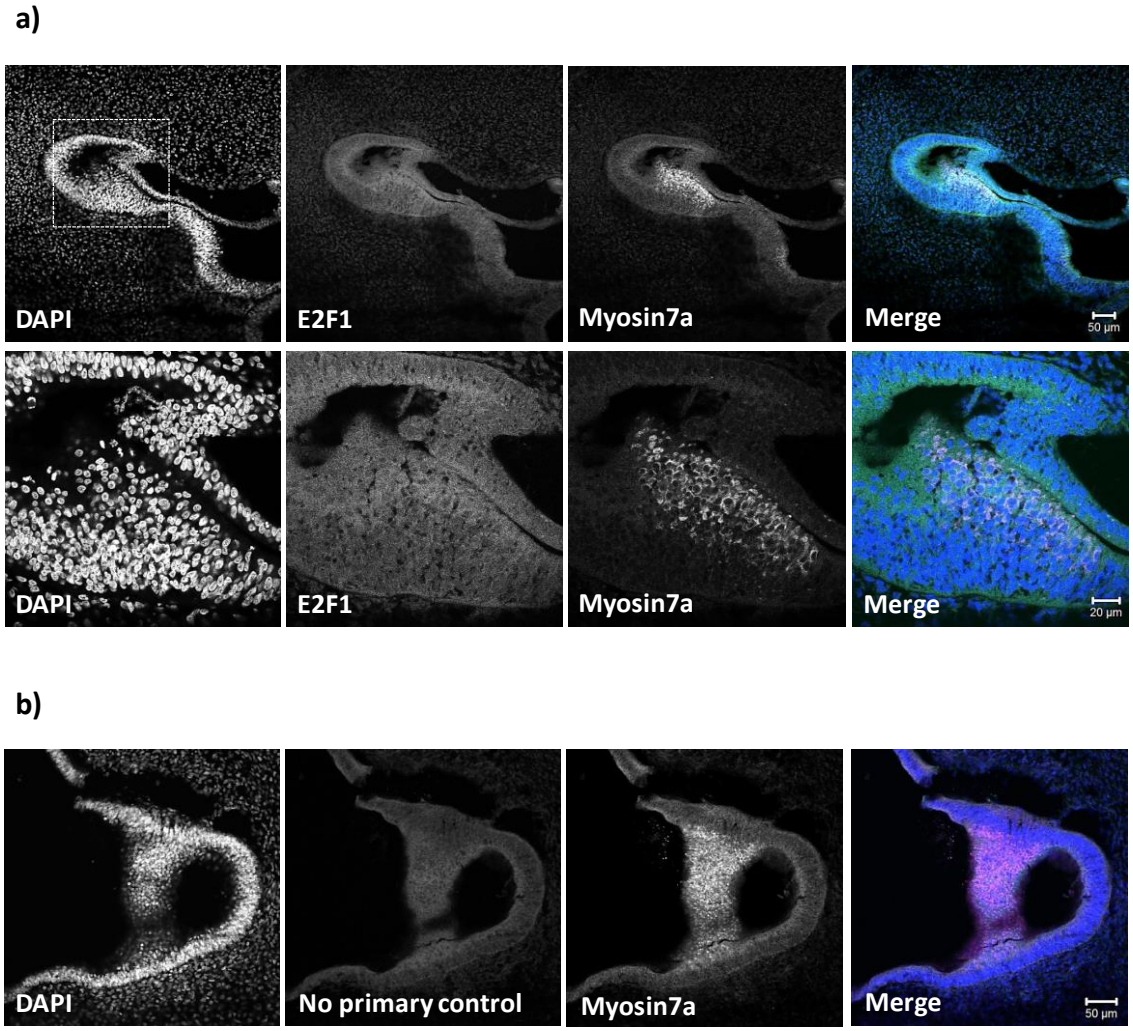

Figure 5.16. Immunolabeling of E2F1 in E7 chick crista. Transverse sections of chick embryonic tissue through the hindbrain and inner ear. **a)** E7 chick specimens were immunolabeled with a rabbit polyclonal anti E2F1-1 (1:400) and Myosin7a (1:250) which was used as a hair cell marker (in pink in the merged image). Alexa Fluor 488®-conjugated anti-rabbit IgG (secondary antibody) provided the fluorescent labelling for the E2F1 antibody (in green) and 4′,6-diamidino-2-phenylindole (DAPI- in blue), was used to label nuclear DNA (1:1000). The confocal images show an E7 crista (enlarged image is shown in the second row; magnification 63X) with vestibular hair cells labelled with Myosin7a. E2F1 labelling is weak and does not appear to be specific to hair cells (n= 4). **b)** Controls for the immunolabeling of E2F1. Confocal images of cross sections of E7 crista shows immunohistochemistry with DAPI (1:1000), Alexa 488 (1:1000) without E2F1 antibody and the hair cell marker Myosin7a (1:250). In the absence of E2F1 antibody (primary antibody), the Alexa Fluor 488®-conjugated anti-rabbit IgG (secondary antibody) provided a similar labelling as the experiment where the primary E2F1 antibody was used (n=3). Magnification 20X.

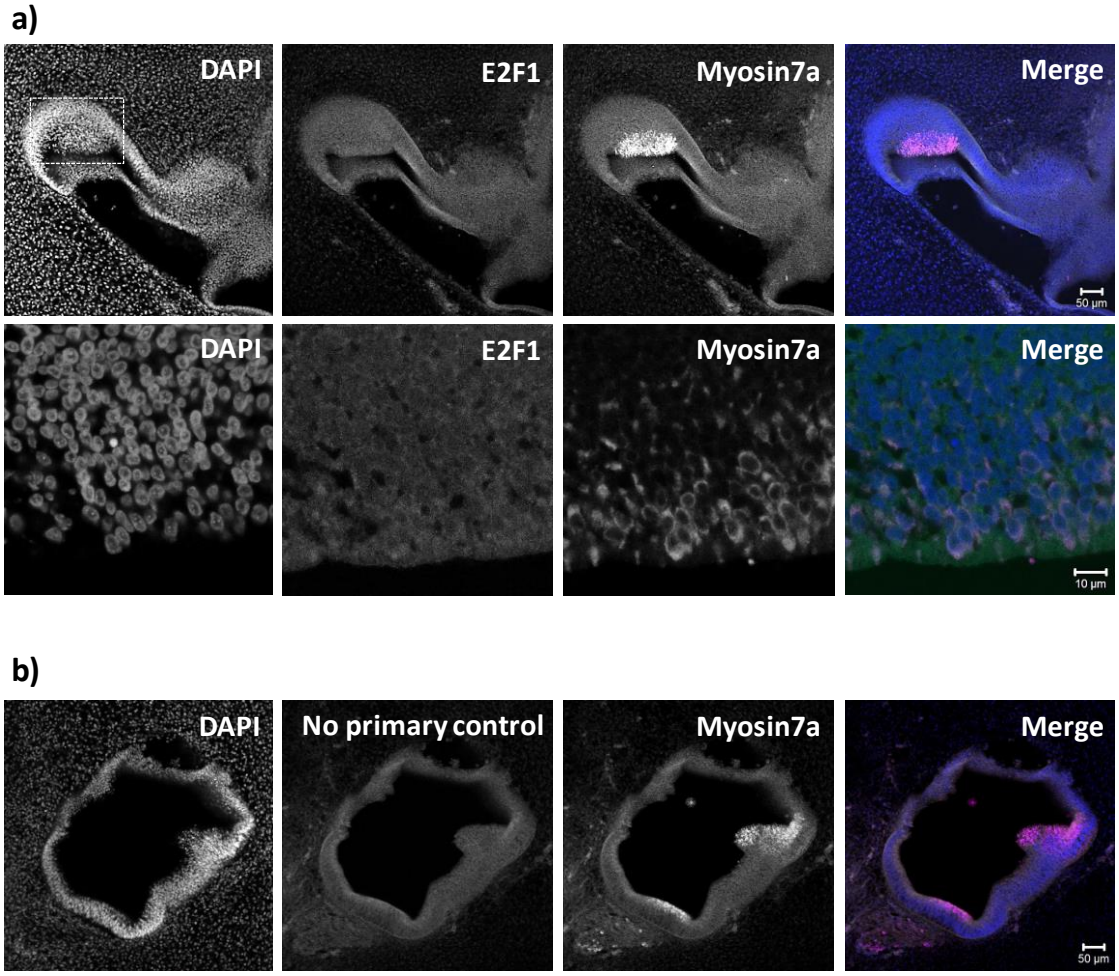

Figure 5.17. Immunolabeling of E2F1 in E10 chick crista. Cross sections of E10 immunolabeled with an anti E2F1-1 antibody (1:400) and Myosin7a (1:250) which was used as a hair cell marker (in pink in the merged image). Alexa Fluor 488®-conjugated anti-rabbit IgG provided the fluorescent labelling for the E2F1 antibody (in green) and 4′,6-diamidino-2-phenylindole (DAPI- in blue) was used to label nuclear DNA (1:1000). The confocal images show an E10 crista (enlarged image is shown in the second row; magnification 63X) with vestibular hair cells labelled with Myosin7a. At this stage (E10) the number of hair cells is higher in comparison to the previous stage (E7). However, E2F1 labelling remains weak and does not appear to be specific to hair cells (n=4). **b)** Control specimens at E10 in the absence of the anti E2F1 antibody (no primary control) show a similar labelling of the Alexa Fluor 488®-conjugated anti-rabbit IgG in comparison to the previous experiment at the same stage (n=3). Magnification 20X.

Based on the control data (no primary antibody for E2F1) and the homology between the human and chick c-terminus amino acid sequence recognized by the E2F1 antibody (64%), it is possible that the human E2F1 antibody does not recognize chick E2F1. Additional tests (n=30) in chick retina and inner ear and subsequent controls were conducted to test the species specificity of the E2F1 antibody in chick tissues. Retinal tissue was chosen as a good positive control tissue since E2F1 is strongly expressed up to E10 in chick, as previously confirmed by *in situ* hybridization (Pasteau et al. 1995). Different fixation methods (MetOH and 4% PFA) and fixation times (5, 15, 30min, 60min) were tested at different stages (E3, E5, E7, E10 and E16). However, no above background staining of E2F1 was observed in comparison with controls treated with Alexa Fluor® 488 secondary alone throughout the retinal development. Therefore, as an alternative method, E2F1 expression in chick was assessed by *in situ* hybridization (ISH). A chick E2F1 cDNA clone was obtained (Dr. Mathew Towers, University of Sheffield, UK) and used to generate an RNA probe labelled with digoxigenin (described in section 2.2.15.2). The same chick E2F1 cDNA clone has been successfully used to describe the expression of E2F1 during chick wing development (Towers et al. 2009) and therefore this procedure was used to examine E2F1 expression in the chick inner ear.

The chick E2F1 RNA probe was first tested in the retina which was used as a positive control for E2F1 expression and confirmed that the signal given by the RNA probe was greater than the one achieved by the E2F1 immunolabeling (Figure 5.18). It also showed that the E2F1 mRNA probe labelled specifically the inner nuclear layer of the retina in comparison to other layers such as the ganglion where E2F1 is not expressed. In addition, negative controls with the use of a sense E2F1 probe demonstrated that the expression pattern given by the antisense E2F1 probe is sequence specific (Figure 5.18). These results were similar to those of Pasteau et al. 1995 in chick retinal tissue with the use of a chick E2F1 mRNA probe. Therefore the E2F1 mRNA probe was chosen as a suitable approach to investigate E2F1 expression in chick tissues by ISH.

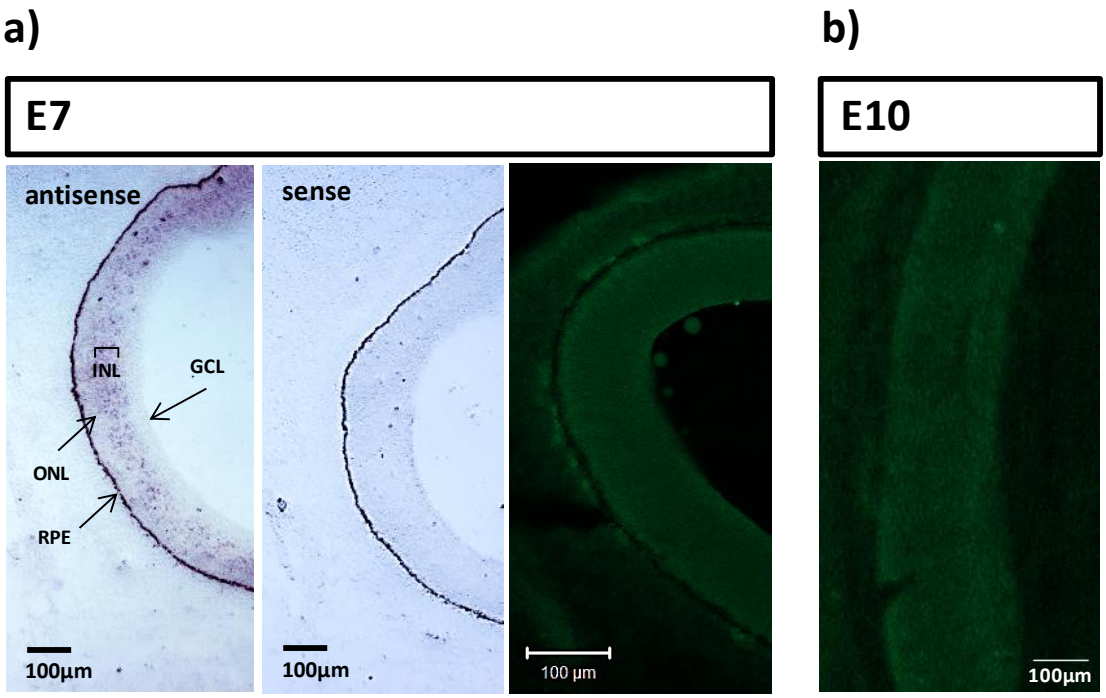

Figure 5.18. E2F1 expression in chick retina assessed by *in situ* hybridization and by immunolabeling. a) Comparison of E2F1 expression by ISH and immunolabeling in the E7 chick retina. The ISH technique showed a greater E2F1 signal in comparison to immunohistochemistry results. The antisense E2F1 mRNA probe labelled specifically at high levels the inner nuclear layer (INL) of the retina in comparison to other layers such as the ganglion cell layer (GCL) or the outer nuclear layer (ONL) where E2F1 is not expressed. The sense E2F1 probe did not show specific binding in any of these layers under the same experimental conditions. The lower thin layer corresponds to non-specific staining of the retinal pigmented epithelium (RPE) which was observed both with the sense or antisense probes. **b)** Example of E2F1 immunolabeling at E10 in the chick retina. Immunolabeling in retinal sections at different stages (E3, E5, E7, E10, E16) were tested giving similar expression results (data not shown). Different fixation methods (4% PFA or MetOH) and timings (15min, 30min, 60min) were also tested. Controls with no primary for E2F1 gave similar results to samples labelled with E2F1 antibody for all stages and fixation methods tested (n=2 for each stage and treatment).

E2F1 expression was investigated at different stages of chick inner ear development. At embryonic day (E) 3, E2F1 appears to be expressed in the otic vesicle (Figure 5.19 A and A'). At E7, hair cells have already emerged in the vestibular sensory patches and E2F1 transcripts were detected in the vestibular sensory system (Figure 5.19 B and B'). Moreover, the location of E2F1 transcripts was restricted to presumptive hair cells. Specimens were also analysed at E10. At this stage the sensory patches are well developed and contain a large number of more mature hair cells. At E10, E2F1 expression was observed in the sensory patches of the vestibular system and also in the basilar papilla (Figure 5.19 C). In addition, E2F1 transcripts appear to be restricted to the hair cell layer (Figure 5.19 C'; C''; C''', C'''). Although further tests are required

to assess whether E2F1 is restricted to hair cells and whether its expression is associated with proliferative regions in the developing epithelium, this is the first report of E2F1 expression in the avian inner ear.

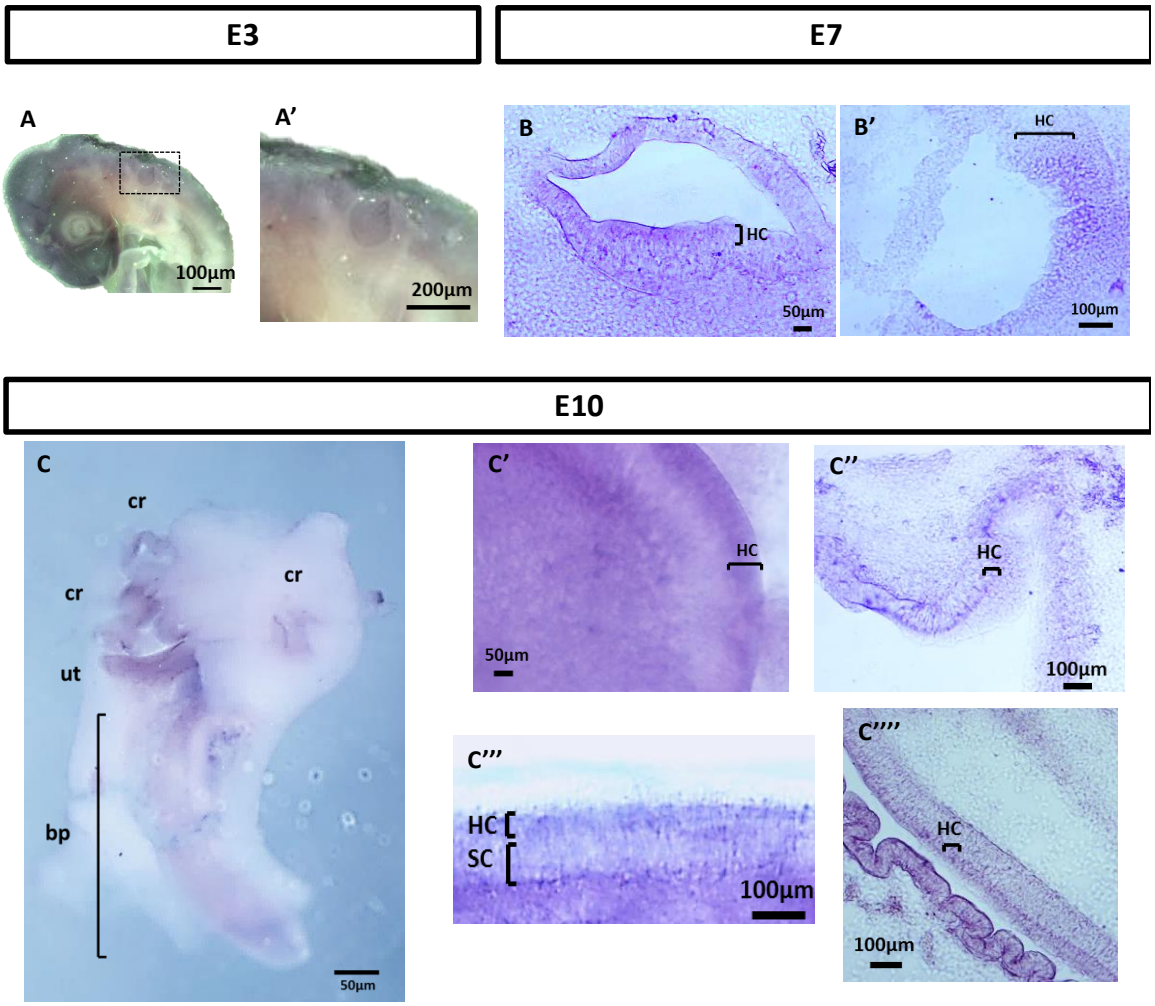

Figure 5.19. E2F1 expression in the chick inner ear by *in situ* hybridization (ISH). **A and A')** E2F1 mRNA showed faint levels of expression at E3 in the otic vesicle. **B and B')** Transverse cryosections through the E7 cristae reveals E2F1 transcripts in the hair cell layer. **C)** Whole mount of an E10 chick inner ear showed that E2F1 transcripts are still expressed in the vestibular system and in the basilar papilla. **C' and C'')** Whole mount and transverse cryosections through an E10 crista revealed E2F1 transcripts in the hair cell layer. **C''' and C'''')** Whole mount and transverse cryosections through the E10 basilar papilla showed E2F1 transcripts in the hair cell layer. Abbreviations: crista (cr); utricle (ut); basilar papilla (bp); hair cell layer (HC); supporting cell layer (SC).

5.7.2 E2F1 expression in the developing mouse inner ear epithelium

Based on the luciferase assay experiments presented in previous sections, E2F1 was not able to activate the mouse *Atoh1* enhancer construct. However, a recent publication showed that E2F1 is expressed in the stria vascularis and spiral ganglion of 1 year old mouse and its expression was suggested to be upregulated in response to mitochondrial malfunctions (Raimundo et al. 2012). Whether E2F1 is expressed in the organ of Corti remains unexplored. Since very few expression studies have been conducted in the inner ear, E2F1 expression was also tested in mouse at early post-embryonic stages, P0, P4 and P8, and expression was followed up to P21 in order to examine whether E2F1 expression changes as hair cells mature.

Ex-vivo cochlear explants of P0 mouse were prepared (see section 2.2.11.1) and immunofluorescence was carried out with the anti-E2F1 and Myosin7a antibodies. At early post-natal stages such as P0, ATOH1 expression is still present (Lanford et al. 2000; Matei et al. 2005; Scheffer et al. 2007) therefore it represents a good stage to investigate potential correlations between the expression of the E2F1 and ATOH1 transcription factors. Figure 5.20a presents P0 cochleae explants immunostained with E2F1 and Myosin7a. Strong E2F1 expression was found in the three rows of outer hair cells and also in the single row of inner hair cells labelled with the hair cell marker Myosin7a. These results could suggest that expression of both transcription factors, ATOH1 and E2F1, overlaps in the cochlear epithelium. Control explants were also tested in the absence of the anti-E2F1 antibody (primary antibody) maintaining the same microscopy settings (Figure 5.20b). These controls were labelled with Myosin7a and the Alexa Fluor® 488-conjugated anti-rabbit IgG alone (secondary antibody). As shown in Figure 5.20b, a faint background expression is present, visualized by the green-fluorescent from the Alexa Fluor® 488-conjugated anti-rabbit IgG (secondary antibody). However, the E2F1 expression observed in the presence of the primary antibody was above the background levels produced by the secondary antibody.

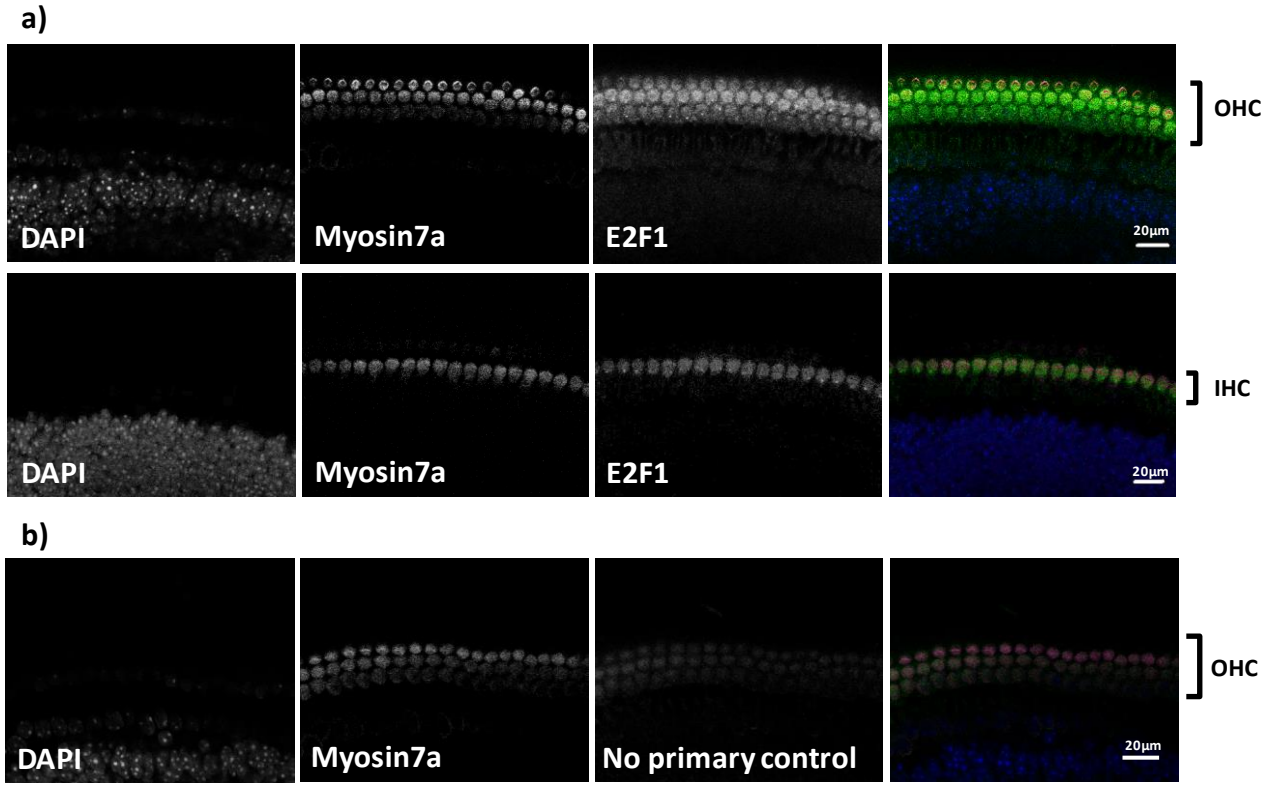

Figure 5.20. Expression of E2F1 in P0 cochlear explants. Cochleae were isolated from post-natal day 0 (P0) from C57BL/6 mice. Immunolabeling was performed with anti E2F1 (1:400) antibody and Myosin7a (1:250) which was used as a hair cell marker. The confocal pictures represent Z-stack images of **a)** E2F1 expression (in green) in outer hair cells (OHC) and inner hair cells (IHC) labelled with Myosin7a (in red) and DAPI (in blue) (n=3). **b)** Control experiments carried out in the absence of anti-E2F1 antibody (primary antibody) but keeping the same microscopy settings as in a). In these explants, Myosin7a was only used with the corresponding secondary antibodies: Alexa Fluor® 488, Alexa Fluor® 568 and DAPI 405. The confocal image shows that the Alexa Fluor® 488-conjugated anti-rabbit IgG alone (secondary antibody) gave some background labelling in outer hair cells (OHC) labelled with Myosin7a using the same confocal setting as with the E2F1 immunostaining (n=3).

In addition to the cochlear explants, cryosections of native tissue from P0, P4, P8 and P21 mice were also tested to further assess E2F1 expression in the organ of Corti epithelium (Figure 5.21). The antibody concentration for the anti E2F1 and Myosin7a labelling was the same as previously used with the cochlear explants. As with the cochlear explants, E2F1 expression was observed in the inner and outer hair cells in the organ of Corti of P0 mouse. Nuclear and cytoplasmic E2F1 expression was present in hair cells whereas the rest of the organ of Corti epithelium did not appear to be specifically labelled with E2F1. Controls with the Alexa Fluor® 488-conjugated anti-rabbit IgG alone (secondary antibody) suggested that weak background staining from the secondary antibody was present in hair cells in the mouse cochlea.

E2F1 expression was also assessed at later stages. At P4 and P8, E2F1 expression was still observed and its expression appeared to be maintained at later stages, with post-embryonic day 21 (P21) being the latest stage analysed in this study (Figure 5.22). At these stages, both nuclear and cytoplasmic E2F1 expression was observed. In the stria vascularis and spiral ganglion, E2F1 was also present (Figure 5.22) which correlates with previous findings of E2F1 expression in 1 year old mouse (Raimundo et al. 2012).

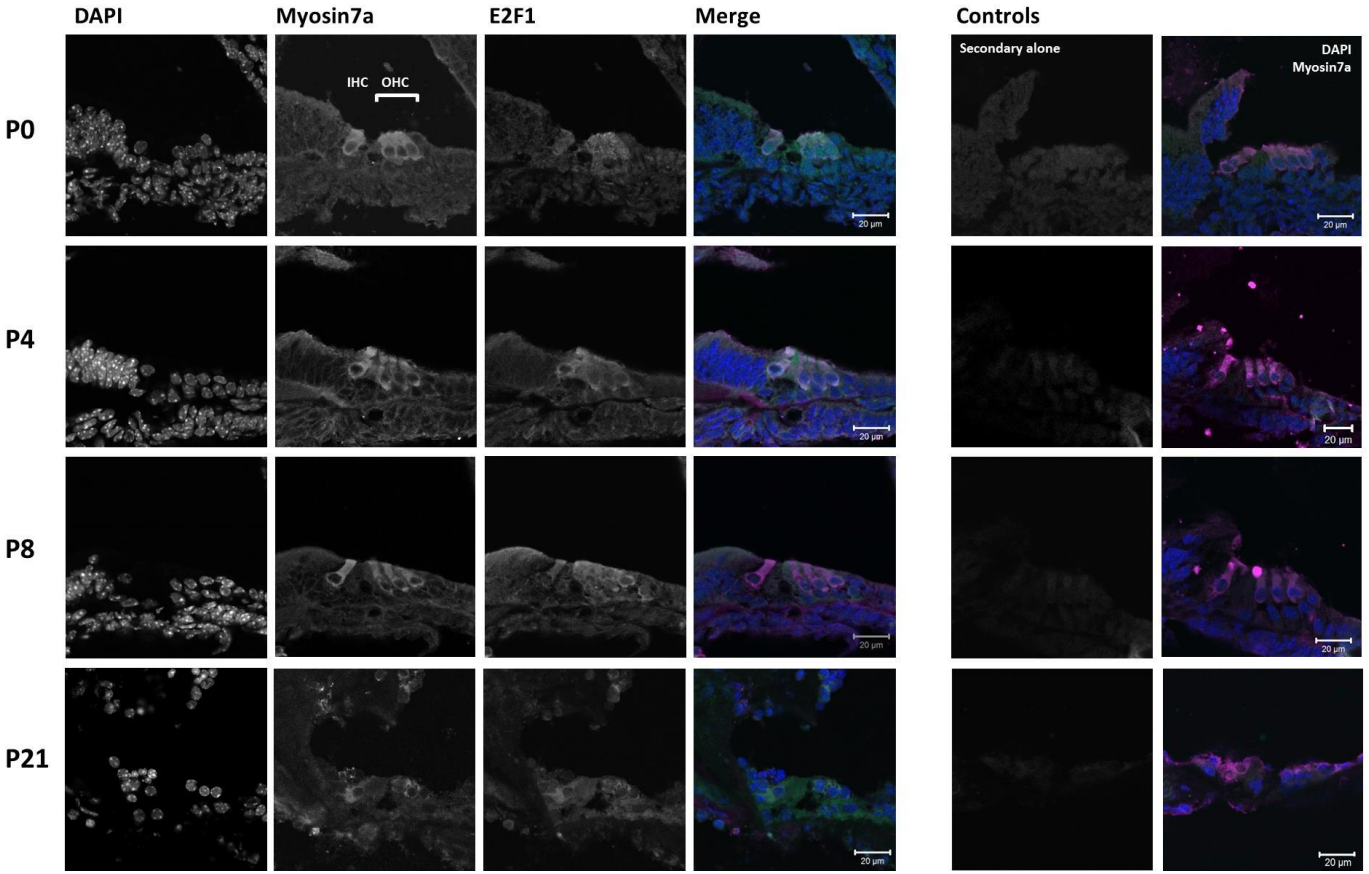

Figure 5.21. Expression of E2F1 in the mouse organ of Corti. Cryosections were immunolabeled with anti E2F1-1 (C-20) from Santa Cruz (1:400) and Myosin7a (138-1-c) from DSHB (1:250) used as a hair cell marker. E2F1 (green) was examined in post-embryonic stages at P0, P4, P8 and P21. In the organ of Corti, E2F1 was observed in the outer and inner hair cells labelled with Myosin7a (magenta) and DAPI (blue) (n=3 from different animals for each stage). Controls were performed in the absence of E2F1 antibody (primary antibody) using identical confocal microscopy settings (n=3 from different animals for each stage).

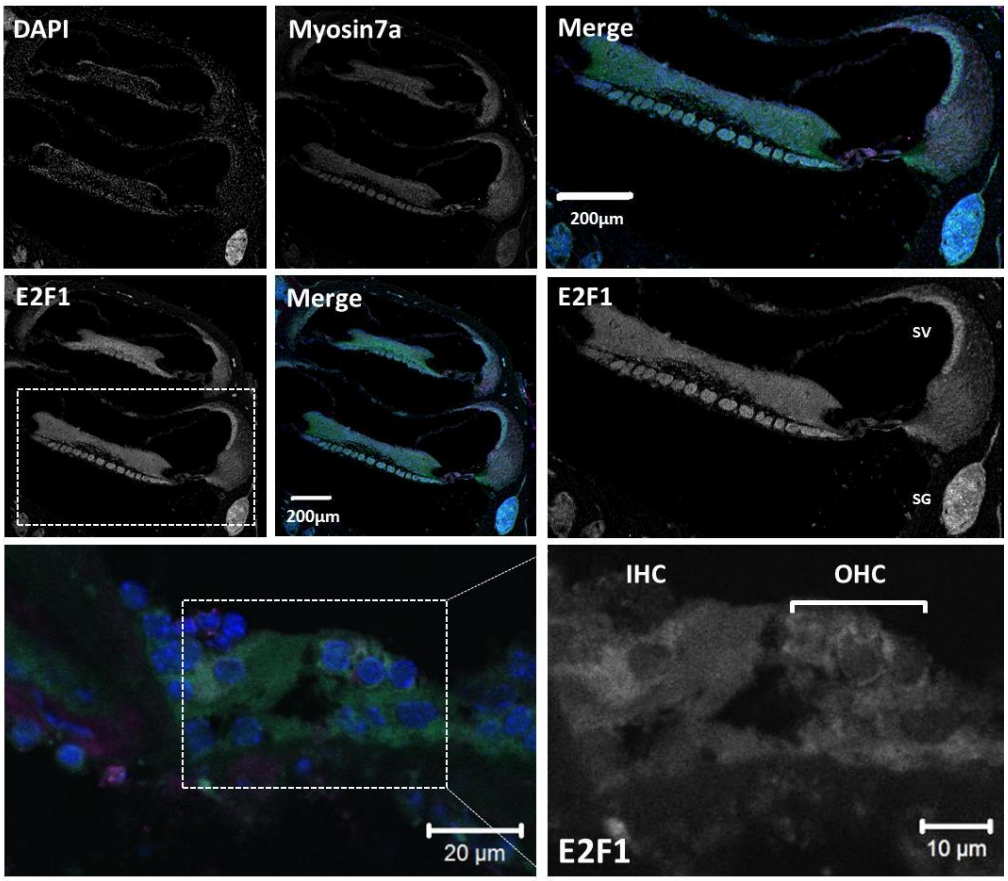

Figure 5.22. Cellular localization of E2F1 expression at P21. P21 cryosections immunolabeled with anti E2F1-1 (C-20) from Santa Cruz (1:400) and Myosin7a (138-1-c) from DSHB (1:250). E2F1 immunoreactivity (green) was strongly observed in the spiral ganglion (SG) and stria vascularis (SV). In the organ of Corti, E2F1 was observed in the outer hair cells (OHC) and inner hair cells (IHC) labelled with Myosin7a (magenta) and DAPI (blue). E2F1 appeared to be expressed in the nuclei and cytoplasm in tissue sections, with cytoplasmic localization stronger in the inner hair cells (n=3).

Altogether, these results describe E2F1 expression in the developing inner ear epithelium of chick and mouse for the very first time. In chick, E2F1 mRNA was detected at embryonic stages by *in situ* hybridization and in mouse, E2F1 protein was detected by immunohistochemistry. In chick, the embryonic expression of E2F1, combined with the known function of E2F1 as a controller of the cell cycle and the response caused in the chick *Atoh1* enhancer, could suggest a potential role for E2F1 to regulate the transcription of *Atoh1* during chick inner ear development. In mouse, E2F1 was detected in early post-natal post-mitotic hair cells (P0) and its expression continued as the hair cells matured. This is similar to the expression found in chick at embryonic stages and therefore could suggest the potential role of E2F1 as a key candidate involved in the development of the inner ear.

5.8 Summary and Discussion

The E2F family was identified as a putative candidate to regulate the transcription of *Atoh1*. Based on the known roles of the E2F family in the cell cycle and its partnership with the Retinoblastoma (Rb) protein, it was hypothesized that some members of the E2F family could participate in the *Atoh1*-driven mechanism that induces hair cells to either regenerate or transdifferentiate from supporting cells after inner ear injury in non-mammalian species. If this regulatory mechanism occurs via E2F1-3, I first hypothesize that E2F would bind to the chick *Atoh1* regulatory elements to activate its expression. Secondly, I would expect to observe E2F1 expression in the auditory system.

Taking a bioinformatics approach, the E2F family was predicted to bind the 3' *Atoh1* evolutionary conserved elements and it was further selected for its roles in the control of the cell cycle. The E2F transcription factor family is also involved in the Rb regulatory network which appears to be a critical pathway in the development and maintenance of hair cells and supporting cells in the inner ear (Sage et al. 2006). Based on these initial observations, the E2F family was investigated in functional *in vitro* experiments to further assess its role in the inner ear.

E2F1, the primary member of the E2F family, was found to upregulate the chick, but not the mouse, *Atoh1* regulatory elements according to *in vitro* luciferase reporter assays. Not only was it able to activate the chick regulatory *Atoh1* enhancers AB, but also a highly conserved region identified in avians and defined as putative enhancer C. This up-regulation was observed when constructs containing the *Atoh1* conserved regions were co-transfected with increasing amounts of E2F1 in UB/OC2 cells. Moreover this up-regulation was very large (145-fold) and dose dependent. A dose response effect is characteristic of a direct binding mechanism and therefore it suggests that E2F1 may directly interact with the chick *Atoh1* 3' conserved elements.

This interaction between E2F1 and the chick *Atoh1* 3' conserved elements was further examined in EMSA experiments. These results suggested that at least two E2F binding sites could be involved in the up-regulation of the chick *Atoh1*. One E2F binding site was identified between the chick *Atoh1* enhancer A and B (named site 2) and the other E2F binding site was located in the chick putative enhancer C (named site 6). To better characterize the effect of E2F on the chick *Atoh1*, independent point mutations were

introduced in these two E2F binding sites to determine their contribution to the regulation of *Atoh1*. A reduction in the activation of chick *Atoh1* by E2F1 was observed when each of these mutations was introduced independently. The largest reduction was observed when the E2F site located in the putative enhancer C, site 6, was mutated. Therefore, it is possible that this binding site is a required site for the up-regulation of chick *Atoh1*. In future work, the ability of E2F to bind to their specific sites in the chick *Atoh1* conserved elements could be further investigated by chromatin immunoprecipitation in UB/OC2 cells or in chick inner ear tissue. However, this technique may be restricted by the lack of specificity of the human anti-E2F1 antibody to recognize chick E2F1 protein.

In summary, luciferase and EMSA experiments confirmed that E2F1 has the capacity to directly bind and activate the chick *Atoh1* enhancers AB and the chick putative enhancer C but not the mouse *Atoh1* enhancers AB. Therefore, the response caused by E2F1 is specific to chick *Atoh1* and not to mouse.

In addition to the activation of the chick *Atoh1* conserved regions by E2F1, the ability of other members of the E2F family to regulate *Atoh1* transcription was also investigated (Figure 5.15). Similar responses were obtained when the *Atoh1* conserved regions were co-transfected with E2F2 and E2F3 confirming the activating roles of the E2F1-E2F3 sub-group (Figure 5.15a/b). Since E2F1-3 present a high grade of conservation in their DNA-binding domains for binding to the consensus motif (Helin et al. 1993), it was expected to find very similar binding capacities to the chick *Atoh1* conserved sequences and therefore similar responses. By contrast, E2F4 did not cause a statistically significant response in the mouse or chick *Atoh1* enhancers AB. However, downregulation was observed in the chick putative enhancer C when transfected with E2F4 (Figure 5.15c). This downregulation is no longer observed in the chick ABC luciferase construct but the downregulation reappears when the E2F site 6 located in the putative enhancer C is mutated. Therefore, there must be a mechanism that explains the differential effect caused by E2F4 in the putative enhancer C and chick ABC luciferase constructs. As previously demonstrated, E2F1 directly binds to chick *Atoh1* and this interaction is dependent on two E2F binding sites, site 2 in between the chick *Atoh1* enhancer AB and site 6 in the putative enhancer C. Therefore, it is possible that when overexpressing E2F4, a competition for binding to E2F sites takes place between endogenous E2F1 contained in UB/OC2 cells and exogenous E2F4. This would explain

the minimal response observed in the chick ABC luciferase construct since the effect of E2F4 could be masked by the upregulatory effect of endogenous E2F1 binding to E2F sites in the chick *Atoh1* enhancer AB (for example via site 2). When site 6, located in the putative enhancer C, is mutated in the chick ABC luciferase construct, the binding of endogenous E2F1 is reduced in that E2F site and the repressive effect of E2F4 is observed again (Figure 5.15c). In fact, previous publications based on ChIP-seq experiments found that E2F4 showed strong binding affinities at promoters regulated by E2F1-E2F3, estimating that about 70% of the E2F1 target genes overlapped with E2F4 targets (Lee et al. 2011). In future work, further experiments could be performed by co-transfecting E2F1 and E2F4 expression constructs in UB/OC2 cells and evaluating whether E2F4 has the ability to block the E2F1 response in the chick *Atoh1* enhancer AB and putative enhancer C luciferase constructs.

The classical model for E2F regulation during the cell cycle indicates that E2F4 forms complexes with other proteins such as p130 and histone deacetylase during the G_0/G_1 phase to repress E2F target genes and consequently to block cell cycle progression (Magnaghi et al. 1998; Brehm et al. 1998; Luo et al. 1998). Therefore, it is possible that E2F4 acts as a repressor of *Atoh1* to keep hair cells and supporting cells in a quiescent post-mitotic state. Whereas, if hair cell damage occurs, it is possible that other E2Fs such as E2F1-3 take the place of E2F4 and mediate the re-entry of quiescent hair cells and supporting cells into the cell cycle and co-ordinate that with the re-activation of ATOH1 expression to specify a hair cell fate. Studies using chromatin immunoprecipitation to asses promoter occupancy in living glioblastoma cells entering the cell cycle from quiescence suggested that E2F4 represses the transcription of different gene promoters during G_0 and early G_1 whereas E2F1, E2F2 and E2F3 bind to those promoters, coincident with the activation of these genes (Takahashi et al. 2000).

E2F1 expression was also investigated in this chapter, describing for the very first time expression of E2F1 in UB/OC2 cells and in the developing inner ear of chick and mouse. In proliferating UB/OC2 cells, the expression of E2F1 protein is localised in the nucleus. The canonical basic nuclear localization domain in the E2F1 molecular structure is a determinant nuclear targeting signal that could confer its nuclear localization (Marfori et al. 2011). However, E2F1 mRNA detected by RT-PCR was low in comparison to protein expression detected by immunohistochemistry. Poor correlations between the level of mRNA and the level of protein are often reported in

the literature (reviewed in Greenbaum et al. 2003). Post-translational mechanisms involved in turning mRNA into protein are not yet sufficiently understood to determine protein concentrations from mRNA. In addition, proteins may differ in their half-lives and stabilities in comparison to mRNAs. All these factors may explain the different E2F1 mRNA and protein levels found in UB/OC2 cells.

In chick, E2F1 mRNA was detected in the developing inner ear at E3, E7 and E10. (Figure 5.19). Based on the known roles of E2F1 in cell proliferation and since E2F1 was detected at stages where cell division is actively taking place, the potential role of E2F1 as a major component during ear development can be hypothesized.

In chick wing development for example, E2F1-3 mRNA is detected between E2.5-E4 in the posterior-distal region of the wing bud which is consistent with the active cell proliferation taking place in this zone (Towers et al. 2009). At later stages, by E6-E7, E2F1-3 expression is less visible in the interdigital mesenchyme in the handplates whereas some of the repressing E2F members (E2F4-7) become more detectable in comparison to early stages. This could suggest that the balance between the activating E2Fs (E2F1-3) and the repressing E2F members (E2F4-8) can promote the transition between the activation of proliferation and the exit of the cell cycle. Therefore, the observations of Towers et al. are consistent with the proliferative role of E2F1-3 during the early phases of development in chick whereas the repressing E2F members including E2F4, might be functional at later stages when differentiation occurs. Further expression data are needed in order to fully characterize E2F1 expression as well as the expression of other members of the E2F family throughout the chick inner ear development. However, the lack of an E2F1 antibody to detect chick E2F1 protein limited the experimental expression data in the chick inner ear detailed in this chapter. Therefore, ISH was chosen as experimental procedure to investigate E2F1 mRNA expression in the chick inner ear. The E2F1 mRNA probe used for these expression studies has previously been characterized and validated in the scientific literature (Towers et al. 2009). In addition, when the E2F1 cDNA used to generate the E2F1 probe is BLASTed against the chick genomic sequence, it was found to be, not only homologous, but 100% specific to E2F1. This was checked prior experimentation to confirm that the E2F1 mRNA probe is able to recognize specifically E2F1 and not other closely related mRNA sequences like for instance, other members of the E2F family. The expression of E2F1 in the chick retina was also shown with the use of a sense E2F1

probe as a negative control. The use of a sense probe, containing the same sequence as the target E2F1 mRNA provided information about non-specific probe binding to the tissue due to the chemical properties of the probe. Positive and negative controls are shown in retinal tissue where specific binding is observed in the inner nuclear layer of the retina with the use of the antisense E2F1 probe. This was not detected with the use of the sense E2F1 probe under the same experimental conditions which confirms that the expression pattern given by the antisense probe is not background signal (Figure 5.18). This correlates with the studies conducted by Pasteau et al. 1995 at higher magnification with histological preparations of the whole thickness of the retina with sense and antisense chick E2F1 mRNA probes.

Although further investigation is required, based on the initial data presented in this chapter and in addition to what has been found during chick development in other systems, it can be suggested that E2F1 is a putative transcription factor involved in the development of the chick inner ear.

In mouse, E2F1 protein was detected by immunolabeling at different post-natal stages. Although E2F1 has already been described in the stria vascularis and spiral ganglion in adult mice (Raimundo et al. 2012), E2F1 expression was detected for the very first time in the organ of Corti. At P0, E2F1 expression was assessed in cochlear explants (Figure 5.20) and in cochlear cryosections (Figure 5.21). At this stage, E2F1 was detectable in inner and outer hair cells and its expression overlaps with Myosin7a which was used as a hair cell marker. It is also clear that E2F1 is restricted to inner and outer hair cells in comparison with the signal observed in the rest of the inner ear epithelium and the controls in the absence of E2F1 antibody (Figure 5.21). Furthermore, cytoplasmic and nuclear E2F1 expression was detected at P4, P8 and P21 in mouse cochlear hair cells (Figure 5.21). Therefore, the expression pattern of E2F1 in hair cells supports the possibility of a potential regulatory relationship between *Atoh1* and E2F1. Although the luciferase data demonstrates that E2F1 does not regulate the mouse *Atoh1* enhancer and that specific activation was only found in chick, expression data for E2F1 in mouse can give insights into the expression of E2F1 in avians since a chick E2F1 antibody is not currently available. If E2F1 expression in chick overlaps with ATOH1, the potential role of E2F1 to control ATOH1 expression in avians can be sustained.

Having shown preliminary immunohistochemistry and ISH experiments which provided information about protein and mRNA localization of E2F1 expression within the inner ear, further experimentation should be focused on quantifying E2F1 expression by q-PCR. This will represent a more quantitative method to describe E2F1 mRNA expression. Furthermore, if E2F1 is expressed in the inner ear as our preliminary data suggest, additional experimentation could be also conducted to assess the expression of other member of the E2F family in the inner ear.

In summary, the data presented in this chapter provide strong evidence that support a role for E2F1 as a novel transcription factor involved in the regulation of *Atoh1*. This is particularly relevant in chick where a direct interaction was suggested between E2F1 and the *Atoh1* conserved regions, resulting in a large activation of *Atoh1* (145-fold activation). Although characterization of the E2F expression data requires further investigation, the initial expression data assessed in this chapter showed a good foundation for additional experimentation. A better characterization, for instance, of the precise time at which E2F1 is expressed will be required as well as the verification with a higher number of animal samples. It would also be interesting to investigate at which stage E2F1 begins to be expressed at embryonic stages and follow its expression throughout the inner ear development and so assess potential variations in comparison to post-natal and post-mitotic stages. Since expression of ATOH1 is downregulated as hair cells differentiate, the study of E2F1 expression will help us to reveal a more solid conclusion of the relationship between E2F1 and *Atoh1* during the process of hair cell fate. This assessment could verify the involvement of E2F1 as a potential activating factor of ATOH1 expression at embryonic stages and its potential downregulation once hair cells exit the cell cycle and differentiate.

Another interesting finding is the different effect that E2F causes in avian and mammalian *Atoh1*. Activation due to E2F1-3 is only seen in an avian *Atoh1* enhancer and not in a mammalian *Atoh1* enhancer. The differences obtained in the response of *Atoh1* in avians and mammals may represent real differences in the responsiveness of the *Atoh1* enhancers to E2F1. In addition, activation also occurs via a putative enhancer which is present in avians but absent in mammalian species. Therefore it is also possible that mammalian *Atoh1* does not respond to E2F1-3 because of the lack of the putative enhancer C region. If proliferation of supporting cells after hair cell damage in the chick is linked with re-activation of *Atoh1* via E2F factors binding to enhancer C, this could

lead to a hair cell fate explaining the different abilities of mammalian and avian species to regenerate hair cells via re-activation of *Atoh1* after hair cell damage.

Based on the activating roles of E2F1-3 and the repressive role of E2F4 observed in the luciferase experiments, it can be hypothesized that E2F4 is a component of the maintenance of the quiescent post-mitotic state of hair cells and supporting cells to repress ATOH1 expression whereas E2F1-3 could be responsible for the re-entry of supporting cells into the cell cycle to reactivate ATOH1 expression upon damage in avian species. Such investigations could identify a new *Atoh1* regulatory network linking proliferation and ATOH1 re-activation and prompt novel approaches to the design of hair cell regeneration therapies.

Chapter 6

6 *In vivo* investigation of the role of putative enhancer C and E2F1 on the regulation of chick *Atoh1*

In this chapter the activity of putative enhancer C found in avians but not mammals was investigated in hair cells. Having quantified the responses of the mouse and chick *Atoh1* conserved regions when co-transfected with different transcription factors in *in vitro* luciferase assays, the functional responses of the chick *Atoh1* conserved regions were characterized *in vivo*. The investigation focused on testing whether putative enhancer C is active during chick inner ear development and if so how its activity is comparable to that of the previously characterized chick enhancers A and B. Activity of putative enhancer C in the inner ear could suggest a role for this regulatory element in the re-activation of chick ATOH1 expression during formation or regeneration of hair cells. The *in vivo* characterization of the chick *Atoh1* conserved regions, including putative enhancer C, was assessed by transfecting reporter constructs containing these regions into the chick inner ear using the Tol2 transposon vectors. The Tol2 vector system has been established as an efficient method to stably introduce DNA transgenes in chick embryos by *in ovo* electroporation (Sato et al. 2007).

In addition, in this chapter the ability of E2F1 to activate *Atoh1 in vivo* in the chick inner ear was also investigated. Results presented in chapter 5 demonstrate that E2F1-3 have the capacity to strongly activate the chick *Atoh1* conserved regions *in vitro*, giving a response of 145-fold when E2F1 is co-transfected in UB/OC2 cells. Here, the effect of E2F1 on endogenous ATOH1 expression when transfected *in vivo* into the chick inner ear was investigated.

6.1 Introduction to the Tol2 system

The Tol2 system uses a transposon-mediated gene transfer technique in order to stably integrate an exogenous DNA sequence into nuclear DNA (Sato et al. 2007). Tol2 carries

in its sequence a transposon mobile element that is active only when transposase activity is present. Therefore, when the transposase encoding plasmid is co-electroporated with a Tol2 transposon reporter, the transgene carried by the Tol2 is excised from the reporter and subsequently integrated into the cell's genome (Sato et al. 2007). This allows the stable expression of any gene cassette cloned in a Tol2 transposon vector after electroporation.

The Tol2 system offers several advantages over the conventional use of DNA plasmids or viral vectors. Firstly, several Tol2 vectors can be electroporated into the same cell. Therefore, here a constitutively expressed marker for transfection was also used in addition to the Tol2-*Atoh1* enhancer constructs. The use of a Tol2-mEGFP vector was chosen, driving expression of a membrane localized GFP, as a marker to visualise the electroporated cells (generated in our laboratory by Dr Nicolas Daudet). Hence, Tol2-mEGFP was expressed in the cellular membrane of the electroporated cells and its expression was maintained throughout inner ear development after electroporation (see Figure 6.1a).

Secondly, the Tol2 vectors can accommodate larger inserts than retroviral RCAS vectors (Kiernan AE 1997). For the Tol2-*Atoh1* reporters, for example, a fragment corresponding to the chick AB enhancers plus putative enhancer C (~2 kb) was inserted in addition to the sequences corresponding to the minimal promoter and fluorescence proteins, giving a total length of 4.3 kb inserted between the 5' and 3' Tol2 ends. Previous studies have demonstrated that the Tol2 vectors can carry fragments longer than 11 kb without reducing transcriptional activity of the reporter and without causing any anomalies in its structure (Urasaki et al. 2006).

Finally, the transfection of the Tol2 is mosaic which allows gene expression and regulation at the single-cell level to be compared between transfected and non-transfected cells *in situ*.

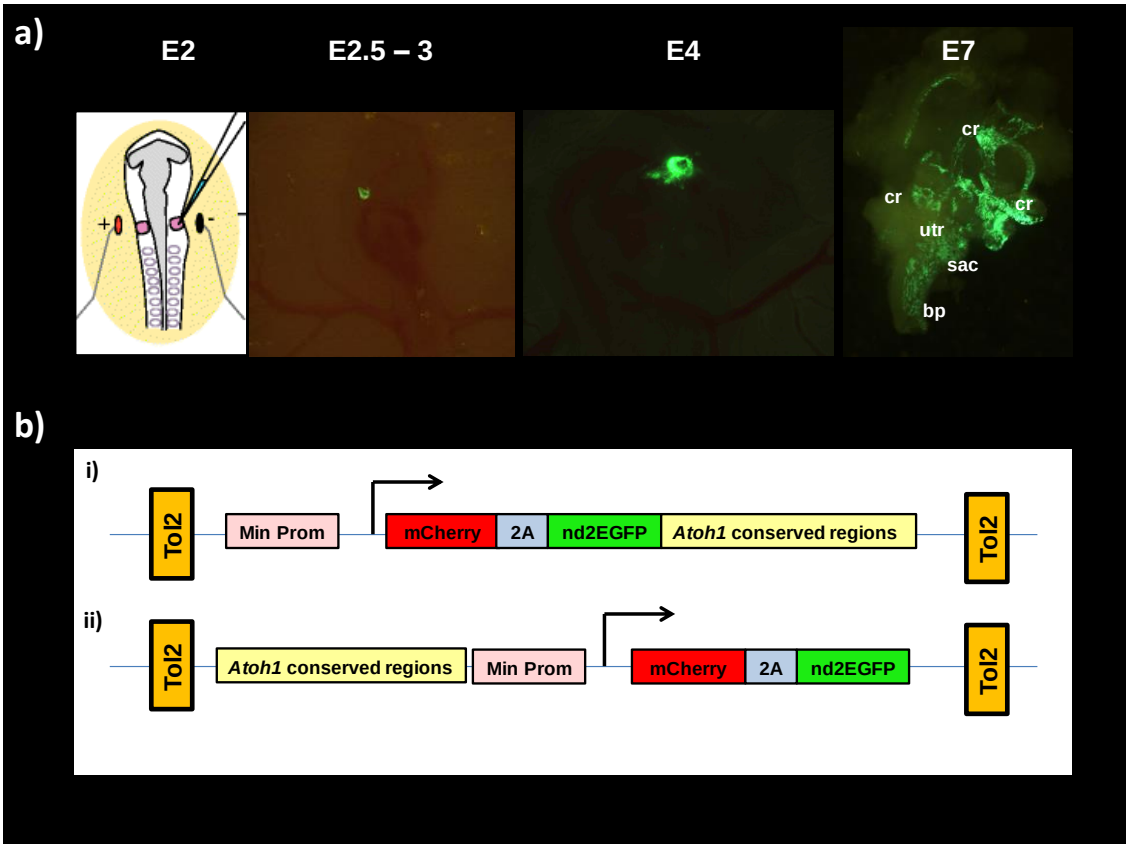

Figure 6.1. Constitutive expression of Tol2 reporters via *in ovo* electroporation. a) *In ovo* electroporations were conducted at embryonic day 2 (control) into the chick otic cup. Tol2-mEGFP was used as electroporation marker to label transfected cells. This is visible in the electroporated otic cups (in green). Reporter activity of the Tol2-mEGFP construct is constitutively maintained several days after transfection (see E2.5 to E4). At E7, the different structures of the dissected inner ear are visible by the expression of Tol2-mEGFP (see in green in E7 inner ear: basilar papilla-bp; crista-cr; utricle-ut; saccule-sac). **b)** Constructs generated for the constitutive expression of the *Atoh1* conserved regions. **i)** Initially three constructs were generated containing the *Atoh1* conserved regions (chick *Atoh1* enhancer AB, chick putative enhancer C and chick *Atoh1* ABC) downstream of the minimal promoter. **ii)** Two more constructs were also generated containing the chick putative enhancer C and chick *Atoh1* enhancer AB upstream of the minimal promoter.

6.2 *In vivo* characterization of the chick *Atoh1* conserved regions by the use of the Tol2 system.

To test the activity of the various chick *Atoh1* conserved regions in the inner ear *in vivo*, different Tol2 bi-colour fluorescent reporters driven by the *Atoh1* conserved regions were constructed (see Figure 6.1b and 2.2.14.3). The Tol2 bi-colour reporters contain

two fluorescent proteins with different half-lives, a destabilized enhanced green fluorescent protein (nd2EGFP; referred to as nEGFP) and a much more stable H2B-mCherry fusion protein (referred to as mCherry). nEGFP is localised to the nucleus and encodes for a protein in a destabilized form with a half-life of 2h (Li et al. 1998). The destabilization of the nEGFP protein is conferred by the addition of a PEST sequence which reduces the stabilization of the protein and increases its degradation rate. The other fluorescent protein, mCherry, is also localised to the nucleus but it is a stable protein with a longer half-life. These two fluorescent proteins are separated by a 2A self-cleaving sequence, a small viral polypeptide sequence which causes the self-cleavage of both proteins after translation resulting in the expression of both fluorescent proteins at the same ratio (Stewart et al. 2009).

This feature allows the dynamic temporal and spatial changes of *Atoh1* reporter activity to be studied with EGFP marking cells with recent activation of *Atoh1* reporters and mCherry marking cells with a previous history of *Atoh1* activation through inner ear development. The activity of the chick *Atoh1* conserved regions was therefore investigated by assessing the expression of the nEGFP and mCherry fluorescent proteins in electroporated chick inner ears. Initially, the *Atoh1* conserved elements were cloned downstream of the nEGFP and mCherry fluorescent proteins coding sequences (see section 2.2.14.3), this being the most straightforward cloning strategy. Transcriptional activity of the chick *Atoh1* regions and the fluorescent proteins coding, nEGFP and mCherry, was driven by a minimal promoter sequence (Figure 6.1b).

To test whether the various chick *Atoh1* conserved region constructs were functionally active during hair cell development, electroporation of the *Atoh1*-Tol2 constructs was conducted as described in section 2.2.14.4. Since hair cell formation in chick peaks at E9-E12 in the vestibular system (Goodyear et al. 1999) and between E5-E11 in the basilar papilla (Corwin 1989; Goodyear and Richardson 1997), *Atoh1* reporter activity was assessed between E7 and E9 in the sensory patches of the inner ear.
Experiments were conducted by co-electroporating two Tol2 reporters. (i) a Tol2-mEGPF vector, driving expression of a membrane localized GFP, used as a marker to visualise transfected cells and (ii) a second Tol2 reporter containing two other nuclear-localised fluorescent proteins (nEGFP and mCherry) driven by the *Atoh1* conserved

regions (initially cloned downstream of the minimal promoter). Myosin7a expression was used to mark hair cells in these experiments.

Results from experiments conducted with the Tol2 reporter containing the chick *Atoh1* enhancer AB (designated as *Atoh1*-ChickAB-down::nEGFP-mCherry) showed that in all the samples where mEGFP expression was detected, mCherry fluorescence was visible in some differentiated hair cells indicating that the *Atoh1*-ChickAB-down::nEGFP-mCherry had been active (Figure 6.2). Similar results were obtained for both E9 basilar papilla and crista. However, nuclear localised EGFP was not observed at E7 or E9 suggesting that AB reporter activity was historic rather than current or recent.

Activity of the conserved putative enhancer C was also analysed at E7 and E9 after the electroporation of the *Atoh1*-ChickC-down::nEGFP-mCherry. In these experiments, cells positive for mEGFP were found in the crista, saccule/utricle and basilar papilla indicating successful transfection (Figure 6.3 and Figure 6.4). However, as shown in Figure 6.3, neither mCherry or nuclear EGFP were found in any of the transfected patches at E7 suggesting this construct was not active. Specimens were also examined at E9 and transfected hair cells marked with mEGFP were detected in the basilar papilla and crista. Once again, activity from the *Atoh1* putative enhancer C was not detected since expression of the fluorescent proteins was not found (Figure 6.4).

In order to test whether putative enhancer C has any influence on the activity of the *Atoh1* enhancers AB, a construct containing the chick enhancer AB together with putative enhancer C was electroporated. Reporter activity of the *Atoh1*-ChickABC-down::nEGFP-mCherry construct was observed in sensory patches indicated by the expression of mCherry, but as with the AB enhancer alone, nuclear EGFP was not detected suggesting the activity was not current or recent (Figure 6.5).

The activity of the enhancerless version of the Tol2 construct, pT2K-MinProm-bicolor vector, was tested between E7 and E9 after electroporation. No activity was detected in any of the samples that were successfully electroporated (marked by mEGFP expression, Figure 6.6). This confirmed the absence of background activity from the Tol2 reporters and that the activity detected in Figure 6.2-Figure 6.5 is due to the presence of the conserved enhancer elements.

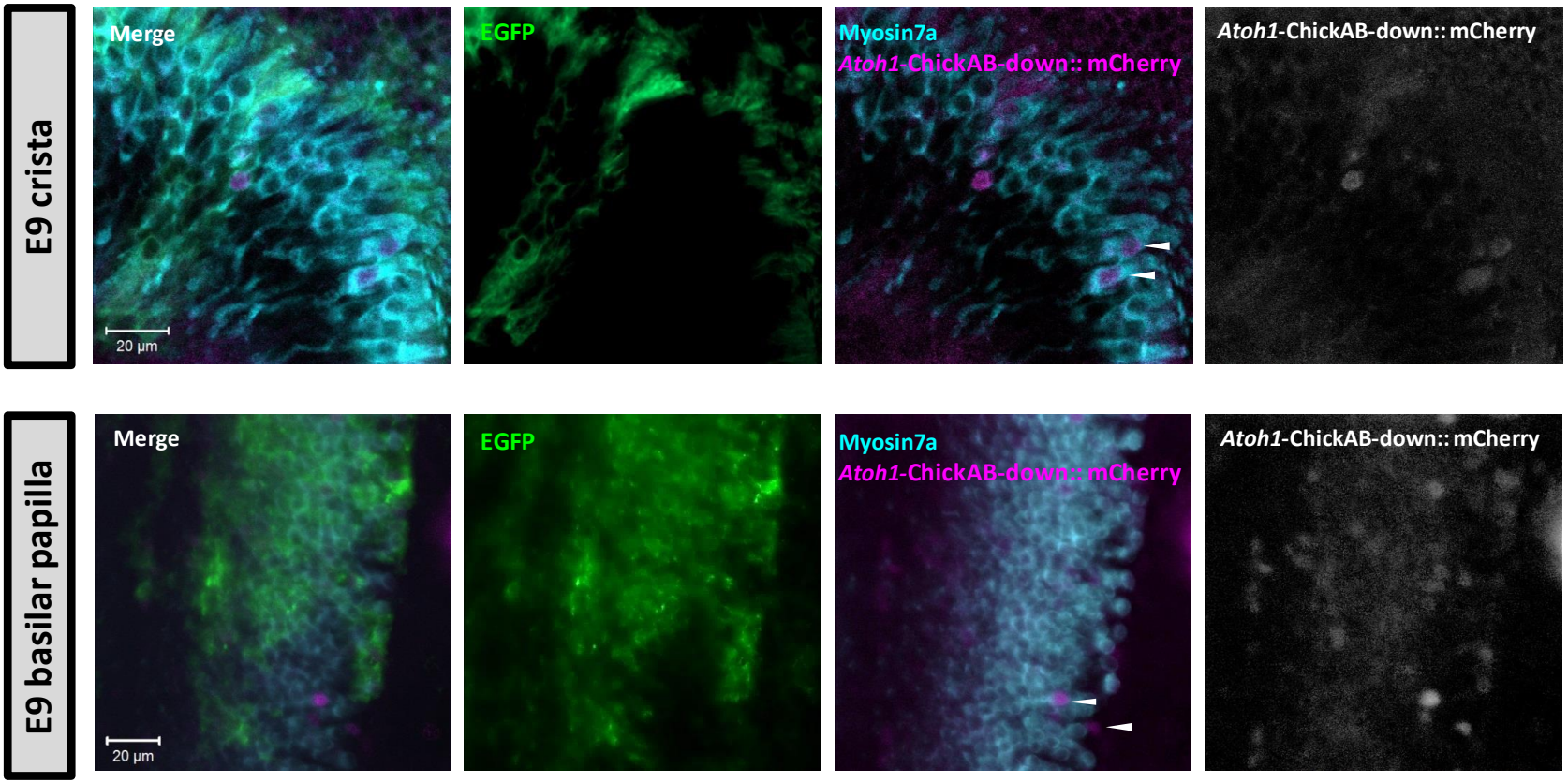

Figure 6.2. Activity of the *Atoh1*-ChickAB-down::nEGFP-mCherry. Confocal images of E9 crista and basilar papilla electroporated with the Tol2-mEGFP and the *Atoh1*-ChickAB::nEGFP-mCherry. The Tol2-mEGFP reporter was used to mark the electroporated tissue (in green). In both, crista and basilar papilla, mEGFP (in green) was detected in tissue containing hair cells immunostained with Myosin7a (in blue). Activity of the chick *Atoh1* enhancer AB reporter is observed in some transfected hair cells (arrowheads) by the expression of mCherry (in magenta). However, nuclear EGFP (nEGFP) was not observed suggesting no recent *Atoh1* enhancer AB reporter activity. The levels of *Atoh1*-ChickAB::mCherry fluorescence varied greatly among the tissue. The images are representative of at least 7 well transfected sensory patches (marked by the mEGFP) from different animals.

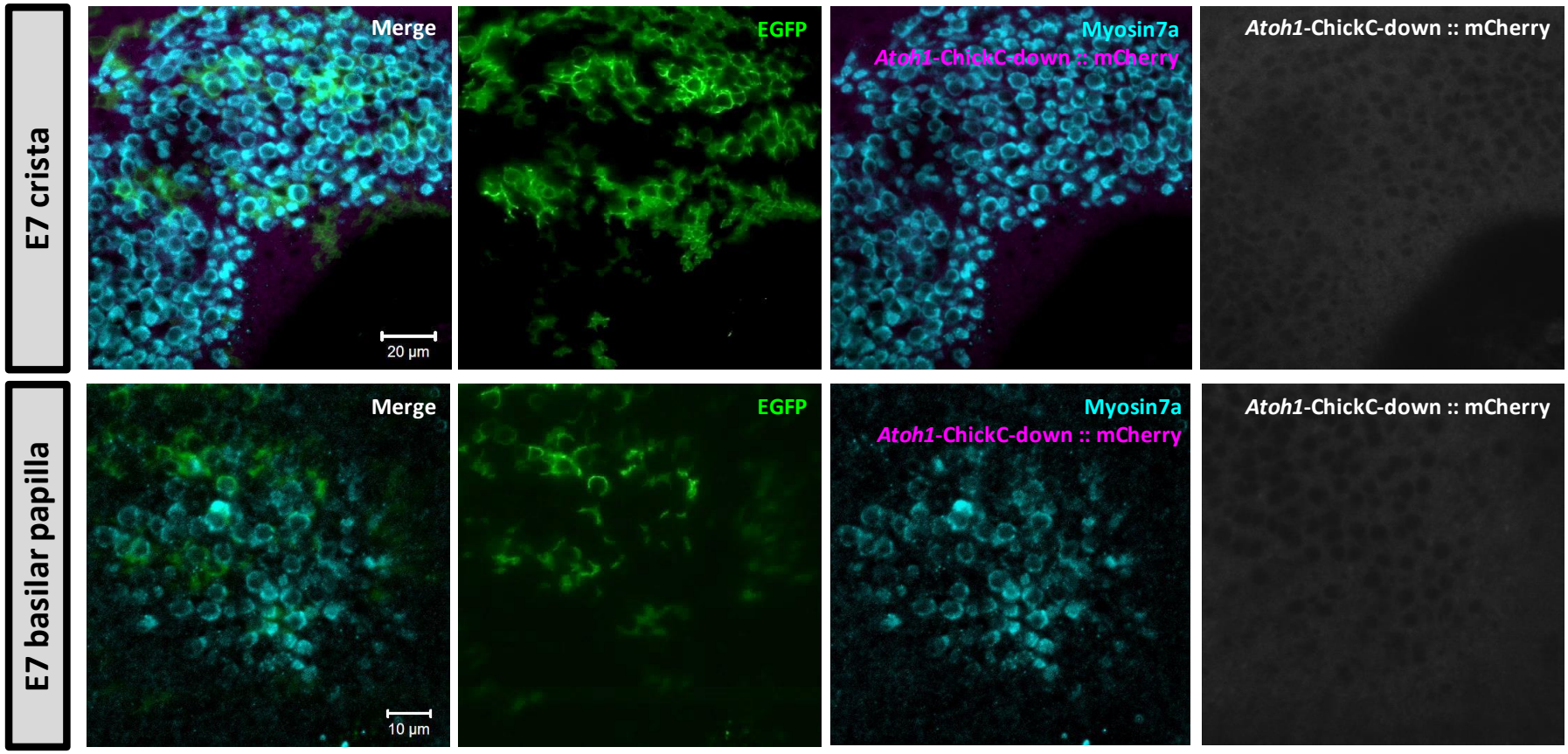

Figure 6.3. Activity of the *Atoh1*-ChickC-down::nEGFP-mCherry at E7. Confocal images of E7 crista and basilar papilla electroporated with the chick *Atoh1* putative enhancer C and mEGFP Tol2 reporters. Multiple areas in the crista and basilar papilla were well transfected since mEGFP activity (in green) was expressed in different parts of the sensory patches containing hair cells immunostained with Myosin7a (in blue). In tissue that was mEGFP positive, no reporter activity from the chick *Atoh1*-ChickC::nEGFP-mCherry was observed in any of the sensory patches that were analysed. Data are representative from sensory patches of 4 different animals.

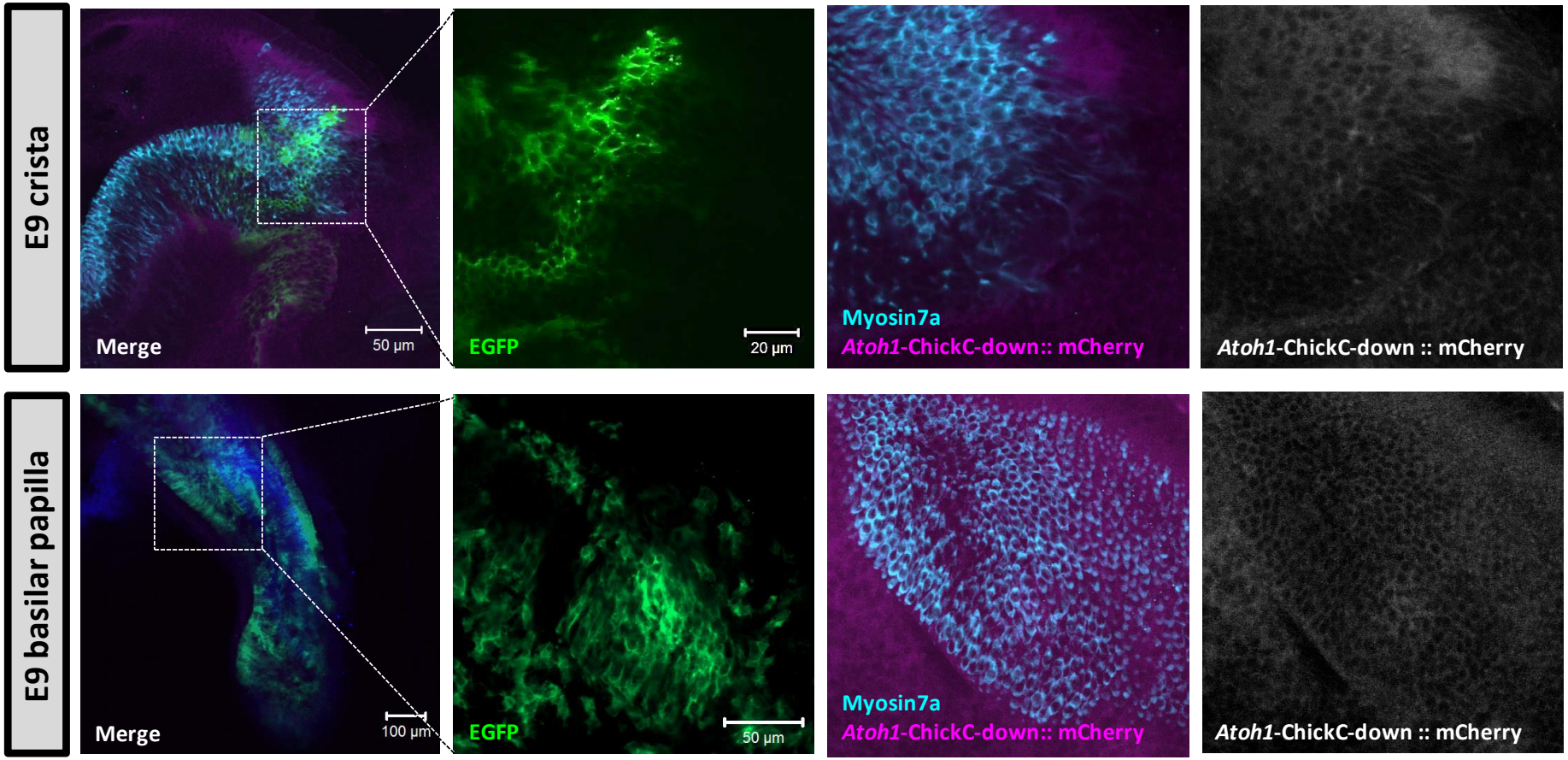

Figure 6.4. Activity of the *Atoh1*-ChickC-down::nEGFP-mCherry at E9. Confocal images of E9 crista and basilar papilla electroporated with the chick *Atoh1* putative enhancer C and mEGFP Tol2 reporters. Vestibular and cochlear hair cells (in blue) immunostained with Myosin7a (1:250) were detected in this sensory patches. Multiple areas in the tissue were successfully transfected since the mEGFP Tol2 activity was observed in several parts of the sensory patches. Reporter activity from the chick *Atoh1*-ChickC::nEGFP-mCherry was also not observed at later stages in development (E9). Images are representative of at least 8 successfully electroporated animals.

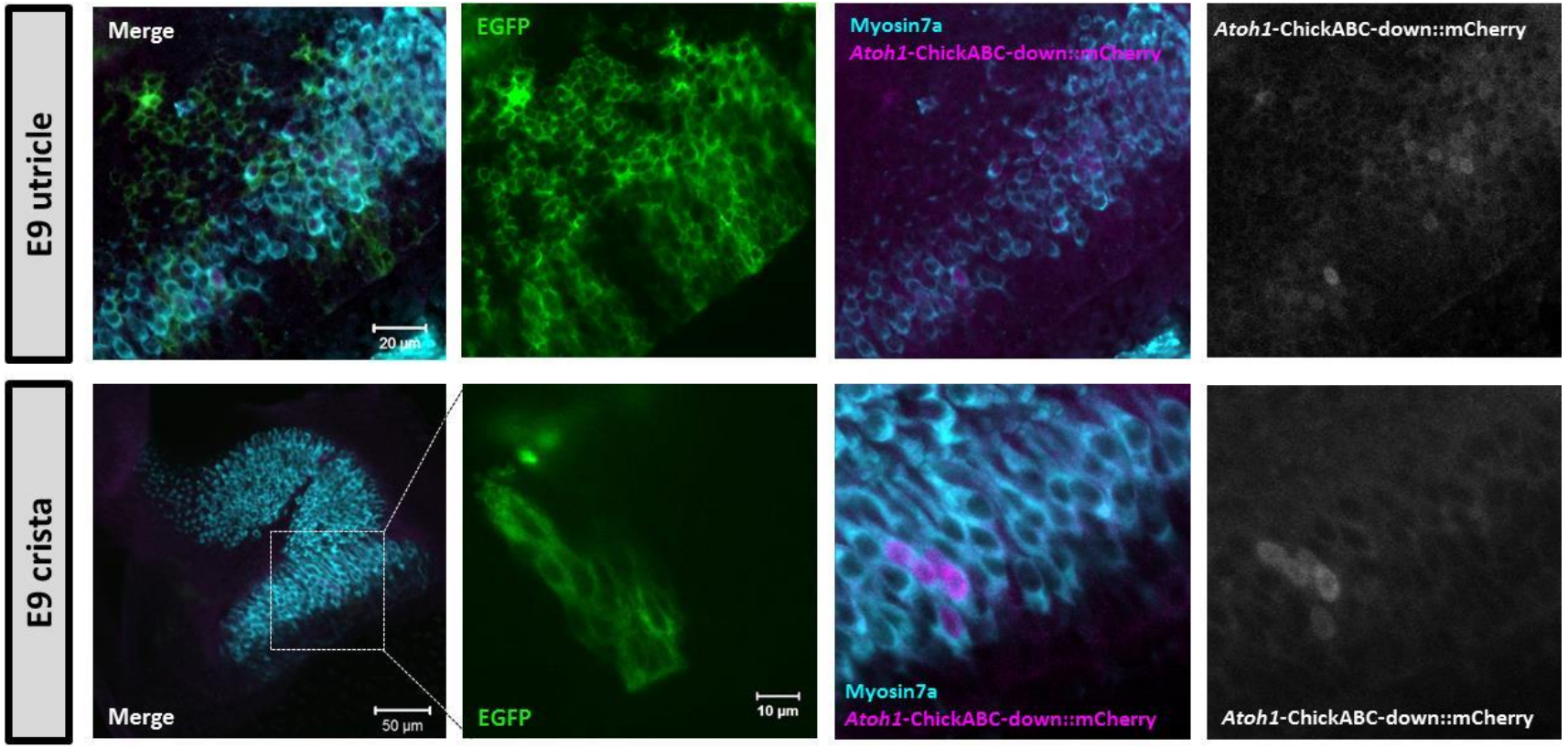

Figure 6.5. Activity of the chick *Atoh1*-ChickABC-down::nEGFP-mCherry at E9. Embryonic otic cups of a two days old chick were electroporated with the construct containing the chick *Atoh1* enhancers and putative enhancer C, the chick *Atoh1*-ChickABC::nEGFP-mCherry reporter, and the mEGFP construct. Samples were examined at E9 by confocal microscopy. Multiple areas in the tissue were successfully transfected since the mEGFP Tol2 activity was observed in different parts of the sensory patches. At this stage (E9) sensory patches contain hair cells marked by the Myosin7a antibody (1:250). Reporter activity of the chick *Atoh1*-ChickABC::nEGFP-mCherry reporter was still observed in hair cells labelled with Myosin7a in the sensory patches (n=8) indicated by the expression of mCherry (in magenta)**.** Nuclear EGFP (nEGFP) from the *Atoh1*-ChickABC::nEGFP-mCherry reporter was not observed.

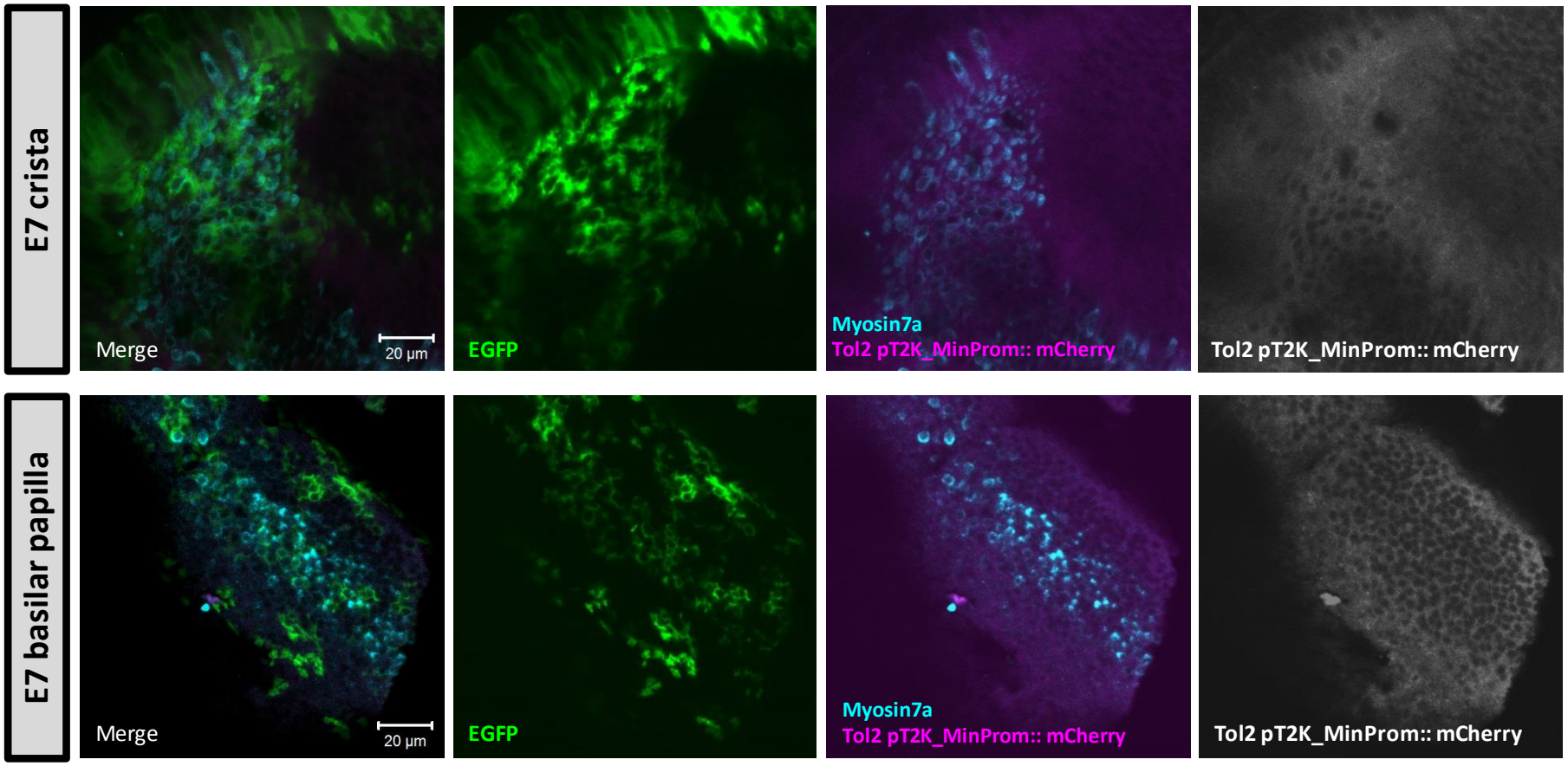

Figure 6.6. Activity of the base Tol2 vector at E7. The enhancerless Tol2 pT2K_MinProm::nEGFP-mCherry and the mEGFP construct were electroporated in the chick inner ear. Reporter activity was examined at E7 by confocal microscopy. Tissue that was successfully transfected produced mEGFP expression in different parts of the sensory patches. Tol2 pT2K_MinProm::nEGFP-mCherry activity was not found in any of the samples analysed (n=5 at E7 and n=5 at E9). Images are representative of the samples that were examined in the vestibular and cochlear system. Hair cells were immunostained with a Myosin7a antibody (1:250).

6.2.1 Effect of the relative position of the *Atoh1* conserved regions on the Tol2 reporter activity

Electroporation of the various Tol2-*Atoh1* reporters demonstrated that chick *Atoh1* enhancer AB was active in the hair cells (Figure 6.2). However, activity was not observed with the reporter containing the putative enhancer C alone (Figure 6.3 and Figure 6.4). In these reporter constructs, the *Atoh1* regulatory regions were located 2 kb downstream of the minimal promoter (Figure 6.1b). In principle, the relative position and orientation of the enhancers is irrelevant since enhancers have the capacity to work either upstream or downstream to the gene they regulate. However, a recent study suggested that in some cases, enhancers can be sensitive to the position and orientation within a reporter construct (Hozumi et al. 2013).

To test this possibility, the chick *Atoh1* enhancer AB and chick putative enhancer C were relocated upstream of the transcription start site (upstream of the minimal promoter). As described in section 2.2.14.3, both inserts were cloned in the same insertion site in the Tol2 pT2K-MinProm-bicolor vector.

When electroporations were conducted with the chick *Atoh1* enhancer AB located upstream of the transcription start site (construct referred to as *Atoh1*-ChickAB-up::nEGFP-mCherry), mCherry fluorescence was detected in the sensory patches at E7 (Figure 6.7). The mCherry positive cells co-localized with transfected regions marked by the Tol2-mEGFP. When compared with the previous results in Figure 6.2, these experiments show that *Atoh1* enhancer AB activity in hair cells is independent of the relative position of the enhancer. The activity of the nEGFP fluorescent protein was also investigated 24h after electroporation at E7. As previously observed, nEGFP activity from the *Atoh1*-ChickAB-up::nEGFP-mCherry was not observed in any of the electroporated samples at E7 indicating that the activity is not current.

The reporter containing putative enhancer C upstream of the transcription start site, was also tested in electroporations (construct referred to as *Atoh1*-ChickC-up::nEGFP-mCherry). However, as in the previous experiment, no reporter activity was observed from the *Atoh1*-ChickC-up::nEGFP-mCherry reporter containing the putative enhancer C upstream of the minimal promoter and fluorescent proteins. Successfully transfected areas were analysed as shown by the expression of the

mEGFP (Figure 6.8) which contained hair cells as shown by the Myosin7a immunostaining. However, no activity of the putative enhancer C reporter was detected in the sensory patches in spite of being relocated upstream of the minimal promoter.

Taken together, these results showed that the position of the different *Atoh1* conserved regions relative to the minimal promoter did not affect the reporter activity since similar results were obtained when the *Atoh1* conserved regions were positioned either upstream or downstream of the reporter cassette.

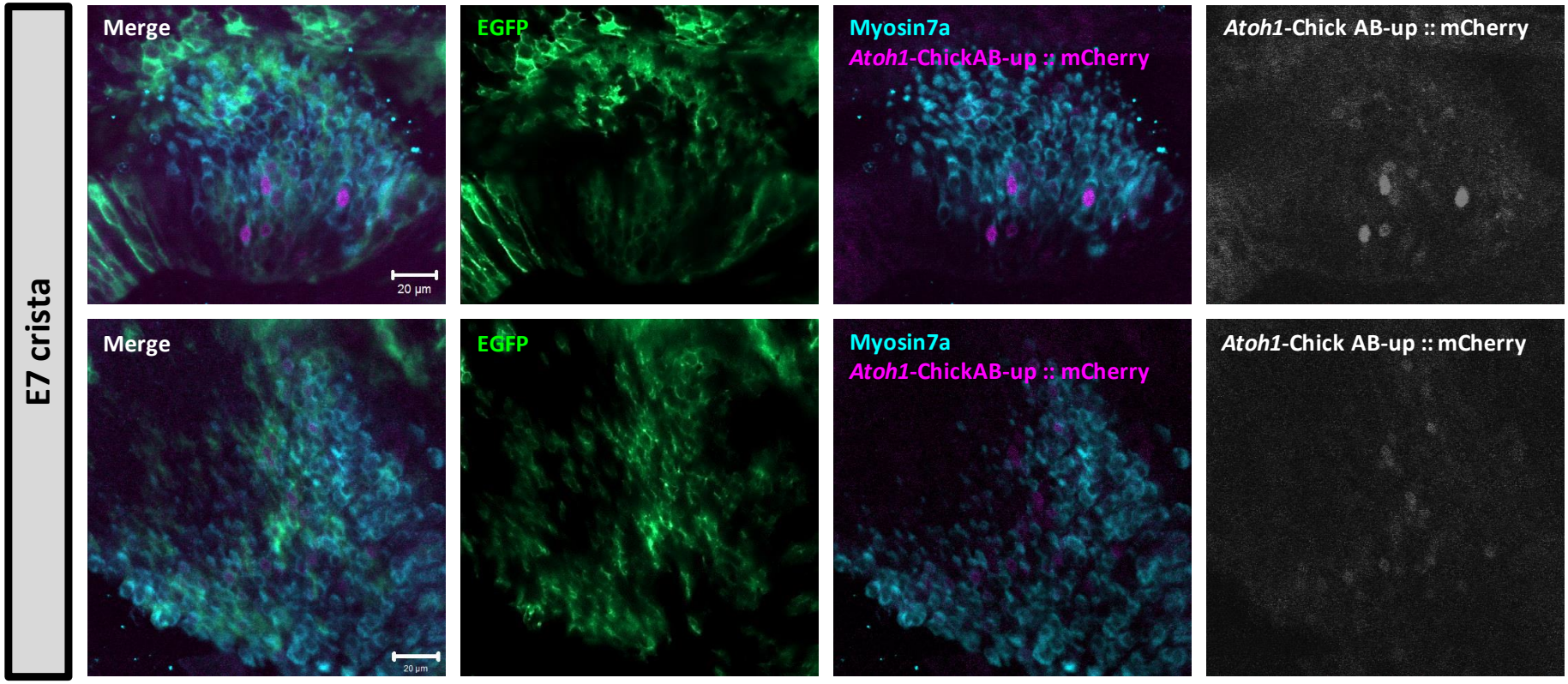

Figure 6.7. Activity of the *Atoh1*-ChickAB-up::nEGFP-mCherry at E7. As in previous experiments, embryonic otic cups of a two days old chick were electroporated with the construct containing the chick *Atoh1* enhancers AB located upstream of the minimal promoter (referred to as *Atoh1*-ChickAB-up::nEGFP-mCherry) and the Tol2 mEGFP construct. In this construct the *Atoh1* enhancer AB was relocated in a closer position to the minimal promoter. Samples were examined at E7 by confocal microscopy. Multiple areas in the tissue were successfully transfected since the Tol2 mEGFP activity was observed in different parts of the sensory patches. At this stage (E7) sensory patches contain hair cells marked with the Myosin7a antibody (1:250) by immunohistochemistry. Reporter activity of the chick *Atoh1*-ChickAB-up::nEGFP-mCherry reporter was observed in hair cells labelled with Myosin7a in the cristae, observed by the expression of mCherry (in magenta). The nuclear EGFP (nEGFP) from the *Atoh1*-ChickAB-up::nEGFP-mCherry reporter was not observed. Images are representative of 4 different samples (n=4).

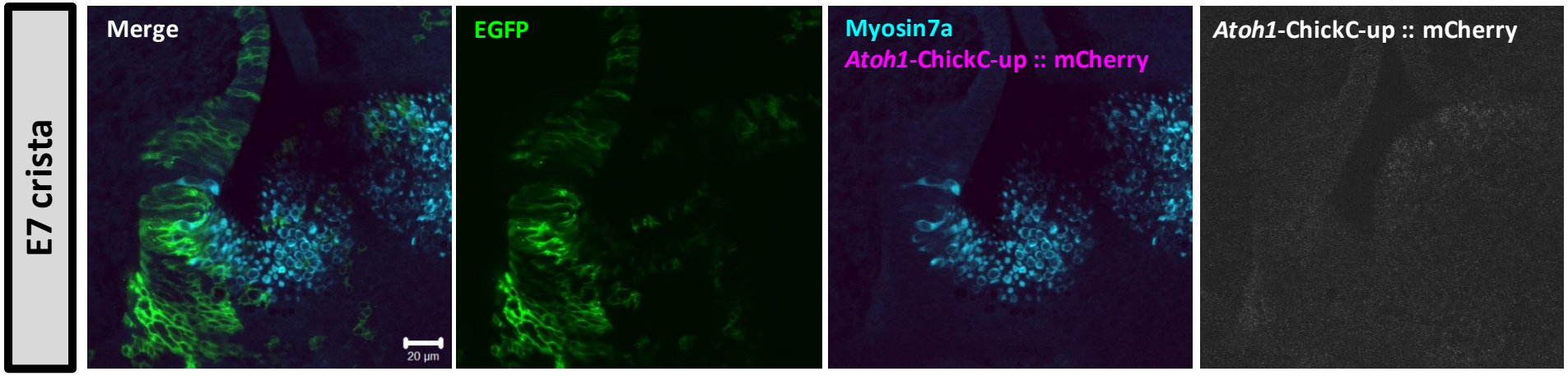

Figure 6.8. Activity of the *Atoh1*-ChickC-up::nEGFP-mCherry at E7. Embryonic otic cups of two days old chick (control) were electroporated with the construct containing the putative enhancer C upstream of the minimal promoter (referred to as *Atoh1*-ChickC-up::nEGFP-mCherry). The Tol2 mEGFP construct (in green) was also electroporated to mark the tissue that was well transfected. Samples were examined at E7 by confocal microscopy. Different areas in the tissue (in this case a crista) were well transfected since the Tol2 mEGFP activity was observed in different parts of the sensory patches. Hair cells (in blue) within sensory patches were labelled with the hair cell marker Myosin7a (1:250) by immunohistochemistry. Reporter activity of the chick *Atoh1*-ChickC-up::nEGFP-mCherry reporter was not observed in hair cells labelled with Myosin7a. The nuclear EGFP (nEGFP) from the *Atoh1*-ChickC-up::nEGFP-mCherry reporter was not observed. Images are representative from at least 13 examined sensory patches from different animals at E7.

6.3 *In vivo* effect of E2F1 in the chick inner ear at early stages

In chapter 5, a transcriptional activation of the chick *Atoh1* luciferase constructs containing the *Atoh1* conserved regions, including the chick *Atoh1* enhancers was observed when E2F1 is co-transfected in UB/OC2 cells. Furthermore, EMSA and site-directed mutagenesis results suggested that this occurs via a direct interaction between E2F1 and its binding sites in the *Atoh1* conserved regions. To assess whether E2F1 is able to activate ATOH1 expression *in vivo*, exogenous expression of E2F1 was performed in E2 chick inner ear using *in ovo* electroporation of the E2F1-pcDNA3 expression construct (see section 2.2.14.4). After electroporation of the E2F1 construct in the inner ear, *Atoh1* expression was investigated by immunohistochemistry at E4.

E2F1-pcDNA3 was co-electroporated with i) a Tol2 construct driving constitutive expression of a membrane EGFP fusion protein (generated in our laboratory by Dr Nicolas Daudet) to visualize the cells that were successfully electroporated and ii) a

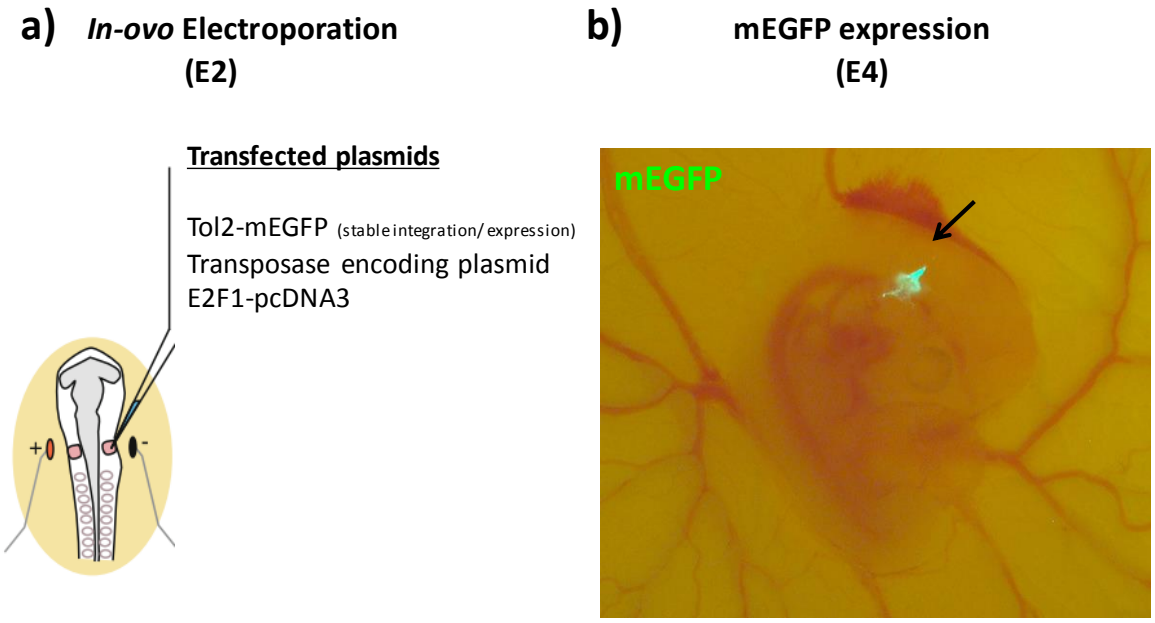

Figure 6.9. Gene transfer by *in ovo* electroporation. a) In-ovo electroporations were conducted in two days old chick embryos (schematic) in order to transfect: the Tol2-mEGFP reporter, used to mark the electroporated tissue, a transposase encoding plasmid used for the stable integration of the Tol2 reporter and an E2F1-pcDNA3 expression construct. **b)** After electroporation, at E4, expression of the Tol2-mEGFP is visualized in the otic cup (arrow) confirming that the transfection was successful. Only samples positive for mEGFP were examined in further experiments to assess *Atoh1* expression.

transposase-encoding plasmid used for the stable integration of the Tol2-mEGFP (Sato et al. 2007).

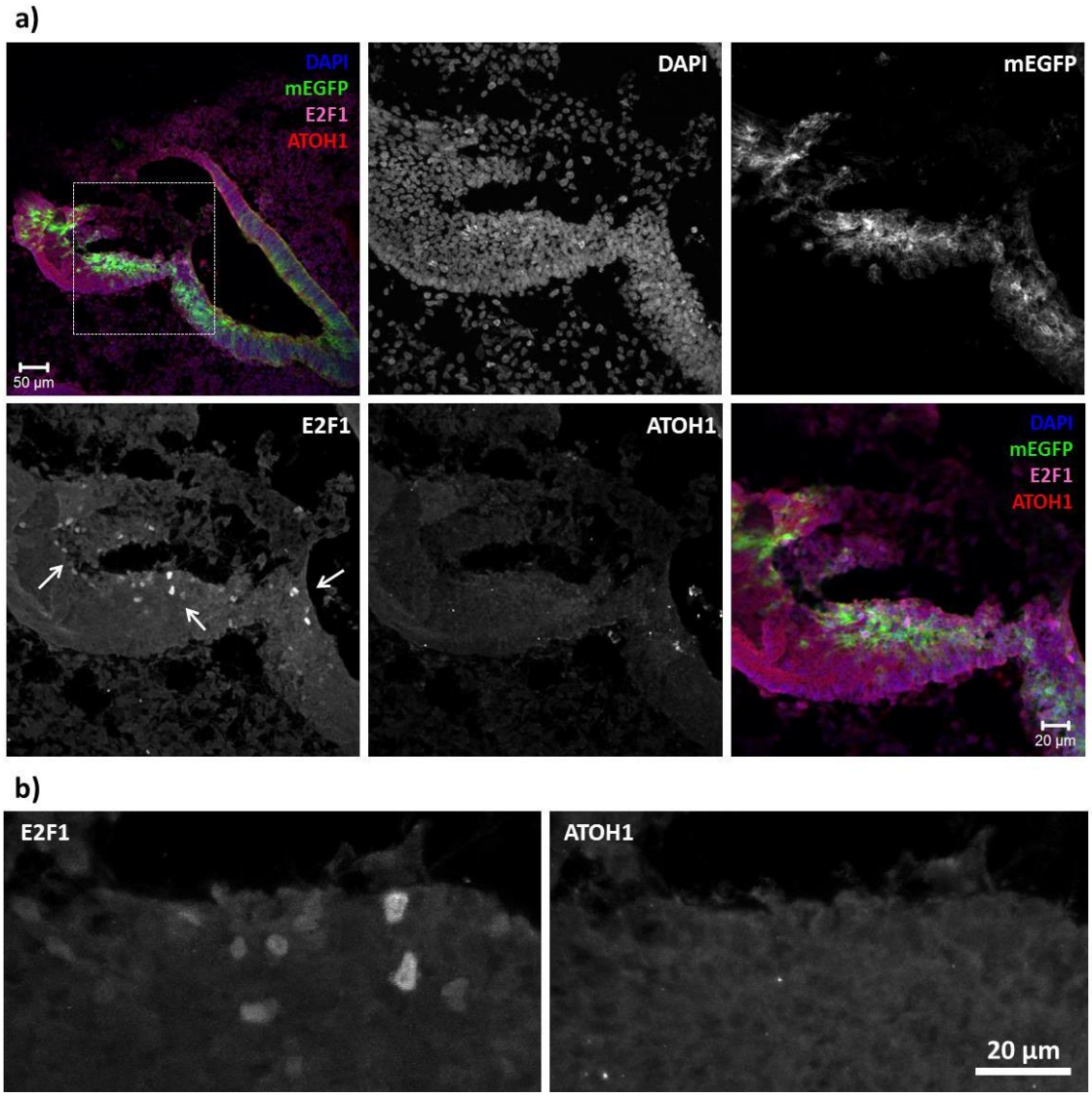

Figure 6.10. E4 chick otocyst electroporated with E2F1. a) Confocal microscopy images of cryo-sections from an E4 chick inner ear. mEGFP (in green) marks cells that were successfully electroporated. E2F1 positive cells expressing the transfected human E2F1 were observed in the electroporated regions (in purple in the merged image or marked with an arrow in the black and white image). However, ATOH1 expression was not found in any of the cryo-sections from an entire inner ear processed for immunostaining (some red background staining is visible in the merged image). **b)** Enlarged confocal images showing cells overexpressing the exogenous E2F1. In these cells, ATOH1 expression was not detected. No other hair cell marker was used therefore it is not clear whether E2F1 expressing cells are hair cells or any other inner ear cell type. The images are representative of 3 electroporated samples (n=3) containing E2F1 expressing cells. The entire inner ear was cryo-sectioned and immunostaining was performed in all the sections (~60 sections of 15µm were obtained from a single E4 ear).

A summary of the plasmids used and an example of an electroporated E4 otic cup is represented in Figure 6.9. Following electroporation of the otic cup, embryos were incubated until E4, a stage at which the non-constitutive E2F1 construct was still present in the transfected cells. Previous studies have shown that the onset of ATOH1 expression in chick occurs at E4 (Pujades et al. 2006; Stone et al. 2003). Therefore, E4 represents a good stage to investigate the effect of exogenous E2F1 on ATOH1 activation.

At E4, embryos were sacrificed, fixed and processed for cryosectioning as described in section 2.2.13.2. Sections were then immunostained with a human E2F1 antibody and with a chicken anti-peptide generated against the mouse ATOH1 (Driver et al. 2013). As shown in Figure 6.10, an electroporated E4 otocyst showed expression of mEGFP in the cells that were electroporated. Moreover, in these regions, some cells exhibited strong E2F1 immunostaining, indicating that these cells had been transfected with the E2F1 pcDNA3 plasmid. It is clear that the E2F1 positive cells are those that were expressing the exogenous human E2F1 produced by the E2F1 pcDNA3 plasmid since the human E2F1 antibody does not recognize the chick E2F1 protein (see chapter 5). However, after examining the tissue expressing exogenous E2F1, upregulation of ATOH1 expression was not observed in the transfected regions. In fact, ATOH1 expression was not found in any of the samples processed for ATOH1 immunostaining. To ensure that our assay was able to detect ATOH1, the hindbrain was analysed as a positive control for ATOH1 expression. As shown in Figure 6.11, ATOH1 expression was detected in the anterior part of the chick hindbrain which suggests that the fixation method and the ATOH1 antibody were appropriate to detect ATOH1 protein. However, ATOH1 expression was not detected in the E4 otic cup, perhaps due to the relative immaturity of hair cells at this stage.

In summary the results presented here do not show that E2F1 has the capacity to upregulate ATOH1 expression *in vivo*. However, it remains possible that E2F1 contributes to the regulation of ATOH1 after its initial onset of expression in committed hair cells. Therefore, performing similar experiments with E2F1 at later stages once ATOH1 expression is already present in the sensory patches could help to resolve this issue. However, my experiments were limited to the use of a non-stable E2F1-pcDNA3 expression construct which is diluted in the inner ear epithelium as the cells divide.

Hence, the generation of new Tol2 constructs is required in order to induce E2F1 expression at later stages, when ATOH1 expression is already present in the sensory patches, such as E5-6. This would provide a better insight into the function of E2F1 in the control of ATOH1 expression *in vivo*.

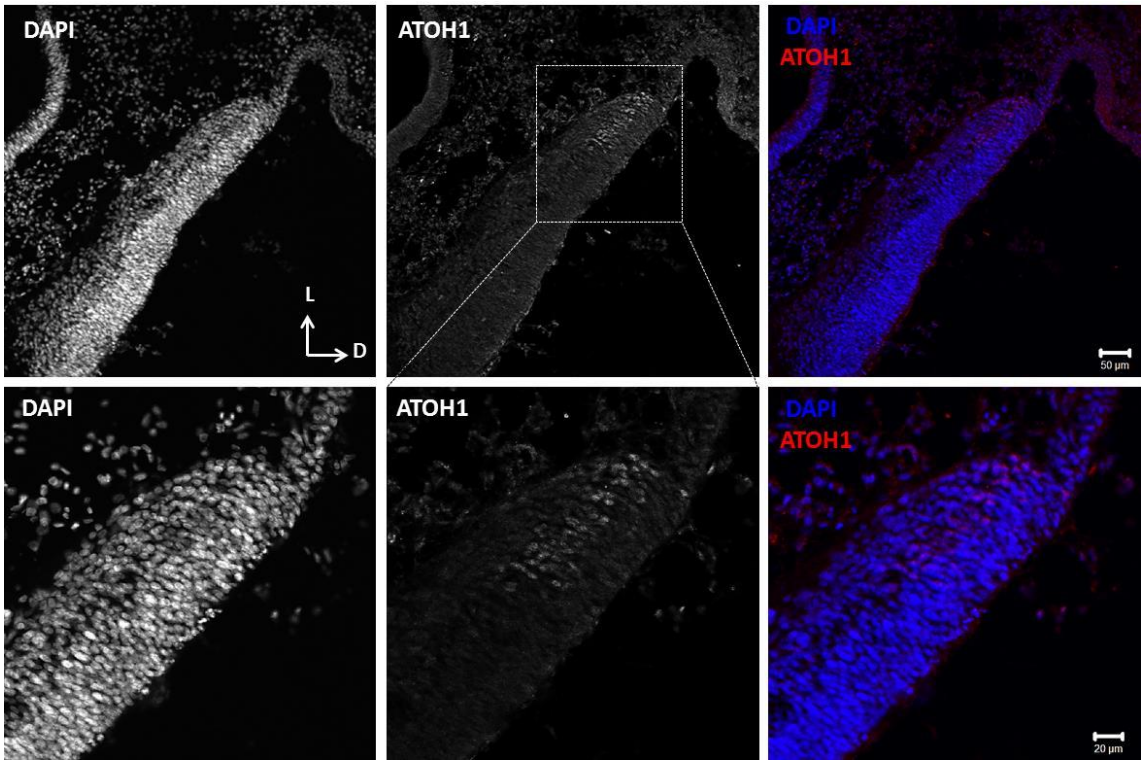

Figure 6.11: ATOH1 expression in the E4 chick hindbrain. Confocal microscopy images of cryosections from an E4 chick hindbrain stained with an ATOH1 antibody. A short fixation time was used as described in Driver et al., 2013. As expected, endogenous ATOH1 expression was detected in the anterior part of the chick hindbrain (n=3) demonstrating that effectiveness of the staining protocol. DAPI stain marks the nucleus of the cells.

6.4 Summary and Discussion

Based on the results obtained in previous chapters with the *Atoh1* luciferase assays, the activities of the chick *Atoh1* AB enhancers and putative enhancer C were investigated in the chick inner ear *in vivo*. The most common system to induce long term transgene expression in avian cells previously has involved the use of retrovirus. However, these systems present some limitations in terms of the size of the transgene to be transfected and they also have additional difficulties in ensuring long term expression. Hence, here the Tol2 transposon system was used. This system has proven to be an efficient method to induce transgene expression in different species including avians. Initially, three Tol2 constructs were generated, one containing the chick *Atoh1* AB enhancer region, one with the conserved putative enhancer C and another containing the chick AB enhancer and putative enhancer C altogether. The *Atoh1* regions in these constructs were positioned downstream of the minimal promoter and with a spacing of 2 kb between promoter-enhancer.

The results obtained for these constructs confirmed that the chick *Atoh1* enhancers AB were functionally active during hair cell development. Initial studies conducted by Helms et al., 2000 defined the *Atoh1* enhancers AB as being sufficient to recapitulate ATOH1 expression in most of *Atoh1* expressing tissues. Later studies conducted by Ebert et al., 2003 described the activity of the mouse and chick *Atoh1* AB enhancers in the neural tube in E10.5 chick embryos. Other studies have tested the functionality of the mouse *Atoh1* enhancers AB in the inner ear (Chen et al. 2002; Freeman and Daudet 2012; Neves et al. 2012; Driver et al. 2013).

In my studies, the response of the Tol2 *Atoh1*-ChickAB-down::nEGFP-nEGFP-mCherry reporter confirmed the importance of the chick *Atoh1* enhancers AB in hair cells. Therefore, since the mammalian and avian *Atoh1* AB enhancers have activity in hair cells, the phylogenetic conservation of the *Atoh1* AB enhancers goes beyond the neural tube and also applies to the inner ear.

However, in the results obtained with the various *Atoh1* Tol2 reporters generated here the accumulation and stability of the fluorescence proteins was not as high as expected. Other Tol2 reporters generated in our laboratory with a Tomato fluorescent protein driven by the mouse *Atoh1* AB enhancer generated a greater response in the embryonic hair cells (Freeman and Daudet 2012). It is therefore possible that the accumulation and stability of the nEGFP and mCherry fluorescent protein used in my *Atoh1* Tol2

reporters were not as great as the Tomato protein. This was especially notable for the signal given by the nEGFP which I was not able to detect in any of the electroporated samples. If real, this result suggests that the *Atoh1* reporter activity was not current or recent at any of the time points tested. This would be surprising based on the results of others described above and it may instead suggest that this nEGFP protein is not an efficient reporter for detecting activity in this system.

The studies conducted by Helms et al., 2000 also suggested the possibility of additional regions outside the enhancers that could be important for the regulation of the expression of *Atoh1* (Helms et al. 2000). Therefore, I aimed to investigate whether the conserved region found in avians, the putative enhancer C, could be an additional region involved in the regulation of *Atoh1* in avians. The fact that it is a well conserved region across different avian species could suggest that it has potential roles in gene regulation. Therefore, in order to assess the activity of putative enhancer C *in vivo*, the Tol2 system was used to address this question. *In ovo* electroporations with the Tol2 *Atoh1*-ChickC-down::nEGFP-mCherry construct were conducted. However, the putative enhancer C was unable to induce reporter activity in hair cells (Figure 6.3 and Figure 6.4). On the other hand, the presence of putative enhancer C did not prevent reporter activity from the *Atoh1* enhancer AB. This was demonstrated by the electroporations conducted with the Tol2 *Atoh1*-ChickABC-down::nEGFP-mCherry reporter which still demonstrated functional activity in the hair cells even when putative enhancer C was present (Figure 6.5).

The relative position of the *Atoh1* conserved regions in the Tol2 reporters was also investigated in this chapter. In the experiments mentioned previously, the *Atoh1* conserved regions in the Tol2 reporters were located downstream of the minimal promoter. Since the putative enhancer C downstream of the minimal promoter did not appear to drive reporter activity, I tested whether the relative position of putative enhancer C within the reporter could be responsible for the negative results. In fact, previous studies demonstrated the importance of enhancer-promoter communication (Palstra and Grosveld 2012). It appears that in some cases the spacing between promoter and enhancer is critical for the binding of transcription factors and therefore for the activity of the enhancer (Giese et al. 1995; Passamaneck et al. 2009). To test this possibility, the putative enhancer C was relocated upstream of the minimal promoter.

When the construct containing the *Atoh1* enhancers AB close to the promoter was electroporated, reporter activity was still present in hair cells (construct referred to as *Atoh1*-ChickAB-up::nEGFP-mCherry) (Figure 6.7). However, the construct containing putative enhancer C in a closer position to the promoter (*Atoh1*-ChickC-up::nEGFP-mCherry) did not report any activity when electroporated in the inner ear suggesting that the relocation of putative enhancer C did not have any effect on its response (Figure 6.8). Altogether, these results do not mean that the putative enhancer C is not involved in *Atoh1* regulation in chick, they show that it is not sufficient in itself to induce hair cell expression at the time points that were investigated.

Based on the large activation of the *Atoh1* putative enhancer C by E2F1 in the *in vitro* experiments in chapter 5, the activation of *Atoh1* by E2F1 was also tested in *in vivo* experiments. However, evidence of the activation of endogenous ATOH1 expression was not found when E2F1 was electroporated in the chick inner ear (Figure 6.10). Some technical limitations could explain the negative results obtained in my experiments. One of the limitations was the use of a non-stable plasmid, the E2F1-pcDNA3 expression construct. This construct does not confer long-term expression since the plasmid does not integrate into the chromosomes and therefore is diluted in the inner ear epithelium as the cells divide. Even though the electroporation was successful as shown by the use of the electroporation marker, Tol2-mEGP, only a few of these cells exhibited increased E2F1 expression (Figure 6.10). It is possible that the amount of E2F1 present was not sufficient to activate endogenous ATOH1 expression. At early stages of development, the inner ear undergoes a very active process of cell division and therefore the amount of exogenous E2F1 within the cells may not be sufficient to produce the activation of ATOH1 expression (Figure 6.10). The use of a Tol2-E2F1 transposon vector as described by Sato et al. 2007, would have been a more appropriate reporter for these experiments in order to maintain E2F1 expression for a longer period of time. Due to time limitations, I was unable to generate a Tol2-E2F1 transposon vector in order to stably induce E2F1 in the chick inner ear and so maintain its expression at later stages.

A further limitation on these experiments was the stage at which ATOH1 expression was examined. Previous authors showed expression of *Atoh1* mRNA as early as E4 in the chick otic cup (Pujades et al. 2006) and demonstrated very low levels of ATOH1 protein by the use of a rabbit anti-MATH1 antibody at the same stage (Stone et al. 2003). Therefore, the level of ATOH1 protein present at E4 in the inner ear may be very

low. Confirming this, ATOH1 protein was not detected in non-electroporated ears with the use of the mouse ATOH1 antibody. In contrast, ATOH1 was detected by immunohistochemistry at E4 in the chick hindbrain however, expression reminded low at this stage confirming the ability to detect ATOH1 (Figure 6.11). Ideally, I would have liked to investigate the effects of E2F1 on ATOH1 expression in the mature avian epithelium after damage. However, such experiments were not possible because of the lack of a long term E2F1 expressing vector and the difficulties involved in post-natal experiments in the inner ear.

There may be other explanations for the lack of an effect of E2F1 on ATOH1 in these experiments. During development, epigenetic modifications such as changes in chromatin structure, histone modifications and DNA methylation are mechanisms that participate on the control of gene expression (Arney and Fisher, 2004). During inner ear development, epigenetic changes are thought to allow/disable ATOH1 expression at different developmental stages as has recently been suggested by Stojanova et al. 2015. Such developmental dependent changes could prevent the ability of transcription factors, such as E2F1, to access their binding site in the *Atoh1* sequence blocking its regulation at the stage tested in my experiments.

In summary, the results obtained here show *in vivo* activity of the chick *Atoh1* conserved regions in hair cells in the developing chick inner ear. The investigations focused on the study of the putative enhancer C as a potential avian-specific regulatory region controlling ATOH1 expression. Although these experiments failed to detect enhancer C activity *in vivo*, the possibility that E2F1, may bind and upregulate this region under other circumstances cannot be excluded. For example, the putative enhancer C may be active only after hair cell damage in the mature epithelium and so contribute to the re-activation of ATOH1 expression. Further work would be needed to investigate whether the putative enhancer C is active during this process.

Chapter 7

7 General discussion

Transcription factors can regulate the expression of multiple genes to determine a specific cell fate or to organise a cell's response to some stimulus. One of the approaches that has been suggested to artificially induce the regeneration of hair cells in mammals to restore hearing is the introduction of transcriptional regulators of *Atoh1* to re-active its expression in differentiated hair cells or supporting cells (Ahmed et al., 2012). To this end, the work presented in this thesis aimed to identify novel transcription factors involved in the regulation of *Atoh1* expression. In particular, this work focused on identifying distinct *Atoh1* regulatory mechanisms in avian and mammals that might be responsible for the ability of avian species to re-activate ATOH1 expression and regenerate hair cells after damage.

These results suggest there may be different conserved elements in the mammalian and avian *Atoh1* regulatory elements which might be critical for the understanding of the regenerative capabilities of hair cells. It is known that the pro-hair cell gene *Atoh1*, is required for the formation of hair cells (Bermingham et al. 1999), however it is unclear whether there are variations in its transcriptional activity due to species-specific properties of its regulatory elements. Therefore, the differences between mouse and chick in the regulation of *Atoh1* were explored to compare the function of evolutionary conserved regulatory sequences. The outcome of this investigation can be separated in three main findings, however the data suggest that they are all related to each other.

First, the investigation focused on a comparative analysis of the *Atoh1* 3' sequence to identify non-coding conserved regions across divergent species. A highly conserved region was identified in different avian species as part of this comparative analysis. Since this region, named putative enhancer C, was found in avians but not in mammals, the putative enhancer C was further investigated to assess whether its sequence could be responsible for a differential regulation of *Atoh1* across species. However, the putative enhancer C was not sufficient on its own to drive expression of a reporter construct in

the developing chick inner ear during *in vivo* experiments. It remains to be investigated whether putative enhancer C plays a role in *Atoh1* activation after hair cell damage in avian species, a possibility that would be very valuable to investigate. Subsequent to my original analysis, when the comparative analysis was extended to other avian species such as turkey and duck, only recently available in the ensembl database (Ensembl release 83 - December 2015), the putative enhancer C was also found to be present in turkey and with less homology in duck (Figure 7.1).

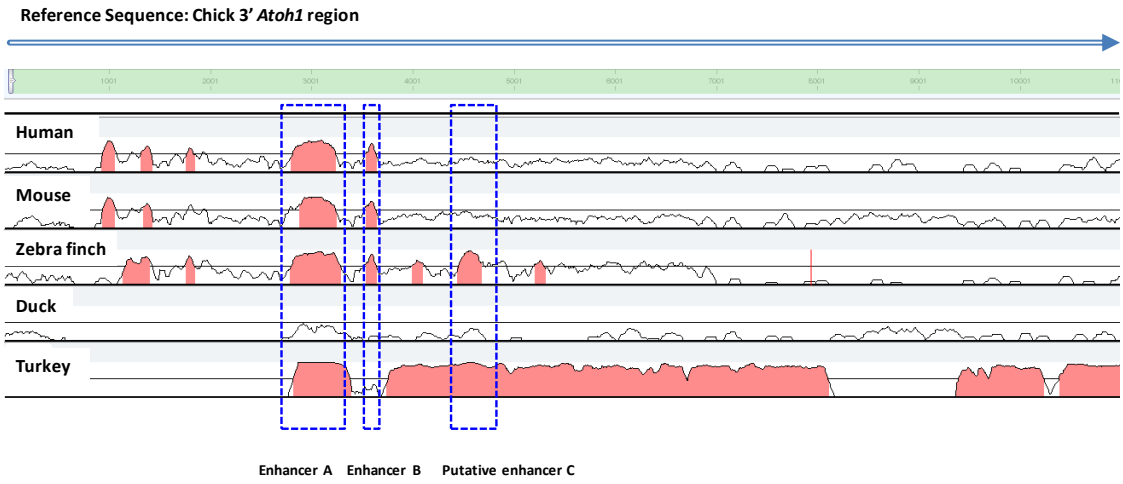

Figure 7.1. Updated comparative analysis of the *Atoh1* 3' sequence in mammalian and avian species. The comparative alignment described in Chapter 3 (Figure 3.3) was extended to further avian species whose sequences were recently released in the ensembl database (Ensembl release 83 - December 2015). As shown, the putative enhancer C is a conserved region also present in duck and turkey. The diagram was extracted from mVista following the same procedure as described in Chapter 3.

It is also possible that the putative enhancer C, although not sufficient on its own for driving *Atoh1* expression at the stage of development tested, requires the presence of a group of transcription factors in order to activate *Atoh1* which may not be present at this stage of development. A similar mechanism has recently been hypothesized in the work conducted by Ahmed and collaborators. In this work it was suggested that the cooperative interaction between the transcription factors SOX2, SIX1 and EYA1 at the *Atoh1* AB enhancers mediates a specific conformation of the enhancers DNA to activate the transcriptional machinery and consequently induce hair cell fate in the cochlea (Ahmed et al. 2012).

Therefore, the second part of my results focused on identifying putative transcription factor binding sites in the various *Atoh1* conserved regions. Vertebrate development is controlled by cis-regulatory elements which usually contain a large number of transcription factor binding sites to collectively create a regulatory network of developmental genes. Over 150 transcription factor candidates were predicted for potentially binding the *Atoh1* conserved regions. Due to the time taken to follow up each of these candidates, four were prioritized: NFKB, YY1, ATOH1 and E2F. The method for which the four putative candidates were selected for investigation can be seen as a somewhat subjective approach. Inevitably, their selection was reliant on prior knowledge of the role of the transcription factors candidates in the inner ear. From the selected candidates predicted by the bioinformatics analysis, only one was found to be a true upregulator of *Atoh1* in reporter gene assays and associated experiments.

The third set of data presented in this thesis is based on the investigation of the E2F family as novel and putative candidates regulating *Atoh1*. As previously discussed, the E2F family and the product of the retinoblastoma tumour suppressor gene (Rb) are considered the major regulators of the cell cycle machinery (Dyson 1998; Nevins 1998). Based on the important roles on the control of cell cycle combined with the lack of studies in the inner ear, the E2F family was selected for investigation.

There is solid evidence for a regulatory relationship between the E2F family and chick *Atoh1* based on the results described in this thesis. First, a strong and significant upregulation was found in the chick *Atoh1* enhancers when the E2F activating members E2F1-3 were co-transfected in proliferating UB/OC2 cells. This activation was not observed with the mouse *Atoh1* enhancer sequences. Secondly, the level of activation by E2F1-3 was at its strongest via chick putative enhancer C, either on its own or when combined with the chick *Atoh1* enhancers A and B and was highly attenuated when the E2F site in putative enhancer C was mutagenized. These data link the chick putative enhancer C as an *Atoh1* regulatory region and the E2F family as a novel transcription factor controlling chick *Atoh1* transcription via the same enhancer. Activation of the chick *Atoh1* conserved regions was shown to occur at two identified binding sites tested by EMSA experiments and site-directed mutagenesis. These two E2F binding sites, previously predicted by a bioinformatics approach, are located between the enhancer A and B and also in the putative enhancer C. It would be interesting to investigate whether a similar response is obtained for the *Atoh1* enhancers and putative enhancer C upon the

overexpression of E2F1-3 in cell lines derived from other tissues expressing ATOH1 to assess whether it is cell-specific. The use of cell lines that express ATOH1, such as H1770 (derived from lung carcinoma), LS 174T (derived from colorectal adenocarcinoma) and SNU-16 (derived from gastric carcinoma) could provide a potential strategy to conduct further experimentation to test the effect of E2F1-3 on *Atoh1* in other tissues (data extracted from https://genevisible.com/cell-lines/HS/Gene%20Symbol/ATOH1).

Although the evidence of the ability of E2F to bind to the chick *Atoh1* conserved elements through reporter gene assays, EMSAs and mutagenesis presented is strong it could be tested in a more physiological environment with the use of *in vivo* analysis. Chromatin immunoprecipitation would be the most suitable approach. Identification of novel E2F-regulated regions in DNA has been previously assayed using this technique (Weinmann et al. 2001). One major advantage of utilizing the chromatin immunoprecipitation approach is the selection of sites bound by the endogenous transcription factor of interest, eliminating the problem of indirect effects. Therefore, this method could be used to verify the *in vivo* binding of E2F to site 2 and site 6 in the *Atoh1* sequence. However, the limited amount of tissue, particularly cell specific tissue which can be obtained from the avian and mammalian inner ear for such experiments is extremely limiting and insufficient for chromatin immunoprecipitation. It is possible to perform these experiments using material from a cell line instead, such as UB/OC-2 cells but since this regulatory relationship is thought to be avian species and no such inner ear cell lines exist then it is difficult to envisage how they could be performed successfully given these limitations.

Another possible approach to confirm the relationship between E2F and *Atoh1* in the inner ear would be the use of E2F knockout mice. Knockout mice have been generated for almost all E2F members (Cooper-Kuhn et al. 2002; Tsai et al. 1998; Wang et al. 2007; McClellan et al. 2007; Ziebold et al. 2001; Chong et al. 2009; Lindeman et al. 1998). The study of E2F mutant mice suggested unique and tissue-specific roles for each E2F member during mouse development. For instance, E2F1 mutants have a decreased number of stem cell progenitors in the brain and in the proliferative zones of the hippocampus (Cooper-Kuhn et al. 2002). These results suggested the involvement of E2F1 in controlling proliferation and neural cell number in the brain. However, some

E2F members have some redundant roles. In the absence of E2F1, there seems to exist a compensatory effect of E2F3 which results in the normal development of some tissues (Cloud et al. 2002).

In spite of multiple studies with E2F mutant mice, the phenotype in the inner ear has not been examined in knockout animals (phenotypes in E2F mutants are summarized in Rocha-Sanchez et al. 2007). This is an area that should be explored. Only a few studies with Rb mutants examined the phenotype in the inner ear (Clarke et al. 1992; Sage 2000; Mantela et al. 2005; Sage et al. 2006). One of the common features shared in these studies with Rb mutants is the abnormal proliferation of vestibular and cochlear hair cells. Whether this is caused by the effect of free E2Fs to stimulate the cell cycle in the absence of Rb is unknown.

In addition, studies with Rb and $p27^{kip1}$ mutant mice suggested that cochlear and vestibular hair cells as well as sensory cell progenitors in the developing inner ear epithelium continue dividing for a longer period (Chen and Segil 1999; Sage et al. 2006). Again, it can be speculated that since both Rb and $p27^{kip1}$ are proteins involved in the control of the cell cycle, it is possible that the deregulation of these proteins has an effect on other partner proteins including the E2Fs.

One possibility that can be raised based on the well-known E2F family's role in proliferation is whether the E2Fs are involved in the spontaneous regeneration of hair cells observed in lower vertebrates after damage. In the avian inner ear, the mechanisms controlling the maintenance of post-mitotic quiescent state of hair cells and supporting cells and the regulators of the cell cycle are not well characterized. Therefore, it would be very valuable to characterize the regulatory molecules involved in the re-entry of the cell cycle upon regeneration. The data presented here provide evidence of a link between E2F transcription factors and its potential role in the control of re-entry into the cell cycle to re-activate *Atoh1* in the chick. Although the role of any such relationship in regeneration of hair cells after damage is speculative, it is one is worthy of more investigation.

Based on the data extracted from the literature and the results of this thesis, the following hypothesis can be raised.

Figure 7.2. Hypothesis of the role of the E2F1-4 on the control of *Atoh1*expression. E2F1-3 could potentially be involved in the re-entry of post-mitotic supporting cells into the cell cycle (from G_0 phase to G_1 phase). The mitotic activity of the E2F1-3 may re-activate the chick *Atoh1* enhancer and the putative enhancer C and consequently link re-entry if the cell cycle and the re-activation of ATOH1 expression. This regulatory network could be responsible for the spontaneous hair cell regeneration in avian species. In contrast, mouse *Atoh1* enhancers are not responsive to E2F1-3 and consequently cell cycle re-entry is not linked to *Atoh1* activation and hair cell fate. The repressive effect of E2F4 could potentially be involved in maintaining hair cells and supporting cells in a quiescent state (G_0 phase) once they have committed to their specific cell fates.

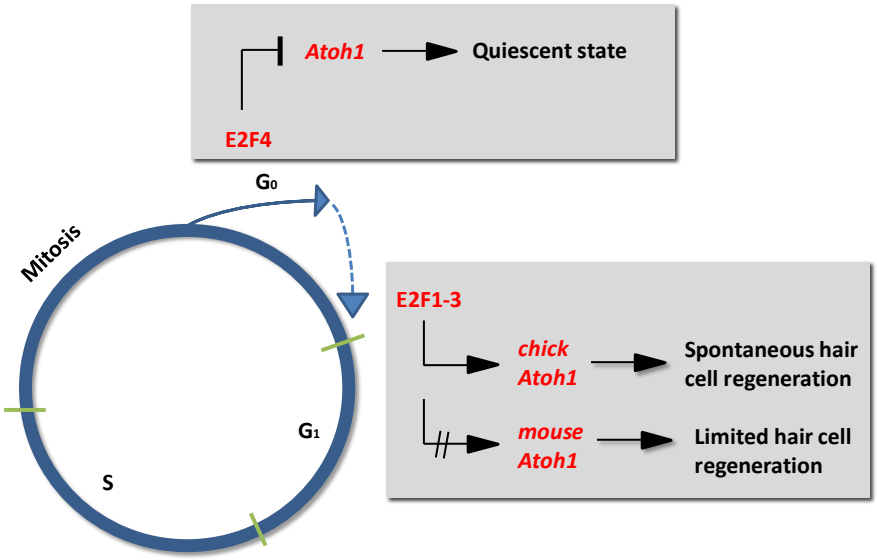

Hypothesis:

E2F1-3 may be involved in the re-entry of post-mitotic quiescent supporting cells into the cell cycle to reactivate ATOH1 expression upon damage in avian species via interaction with putative enhancer C. In contrast, E2F4, the repressive form of the E2F family could be involved in maintaining hair cells and supporting cells in a quiescent fate while repressing ATOH1 expression (Figure 7.2).

To confirm this hypothesis additional experiments are necessary in order to demonstrate that endogenous ATOH1 expression is re-activated by the effect of the E2F1-3 transcription factors. Based on the known functions of the E2F family as regulators of the cell cycle, it would be interesting to assess the role of E2F before and after hair cell damage in avians. Since one of the regenerative mechanisms after hair cell damage is conducted by mitosis of the remaining supporting cells to form new hair cells and

supporting cells, it would relevant to investigate whether the activating E2Fs (E2F1-3) are upregulated during this process in supporting cells. If this is the case, the likelihood of E2F1-3 driving supporting cells to re-enter into the cell cycle linked with a re-activation of ATOH1 expression can be enhanced.

One method that could be used to examine changes in endogenous ATOH1 mRNA levels is q-PCR. However, if using a mammalian cell line like for instance the UB/OC2 cells used in this study, a major limitation is the potential low response expected in the endogenous mammalian ATOH1. Based on the luciferase data presented in this thesis, the mouse *Atoh1* enhancer does not respond to the effect of E2F1 or E2F4. Therefore, minimal expression changes are expected in the mammalian endogenous ATOH1 expression upon the overexpression of E2F1 if using UB/OC2 cells. To overcome this limitation, a suitable method of investigating the potential changes of the expression of ATOH1, E2F1 and E2F4 could be the use of q-PCR in differentiated chick inner ear tissue and compare this with regenerated chick inner ear epithelium after damage. This approach could be assessed after aminoglycoside treatment (to cause hair cell death) in mature chick basilar papilla explants leading to supporting cell proliferation and subsequent hair cell regeneration. Changes in E2F1, E2F4 and ATOH1 expression levels could then be assessed during this process by q-PCR.

A recent study has demonstrated changes in some members of the E2F family during the process of hair cell regeneration in chick tissues. The RNAseq analysis revealed that almost 500 putative genes specific to hair cells are involved in the process of hair cell regeneration in chick (Ku et al. 2014). In addition, the analysis identified over 200 transcription factors which are differentially expressed during the time course of hair cell regeneration. The data from this RNAseq analysis revealed that E2F1, E2F7 and E2F8 are significantly upregulated in chick utricle and cochlea just prior to re-activation of ATOH1 after hair cell damage induced by streptomycin (personal communication with Professor Michael Lovett and Mark Warchol) (Figure 7.3).

In addition, a previous microarray study also demonstrated that E2F1 is significantly enriched in post-hatched chick basilar papilla cultures treated with forskolin in order to identify genes that are upregulated during the regeneration of the chick inner ear (Frucht et al. 2010). These findings support the hypothesis of the involvement of the E2F family during the process of hair cell regeneration in avians after post-natal hair cell damage.

Picture removed for copyright purposes

Figure 7.3. Changes in ATOH1, E2F1, E2F7 and E2F8 during hair cell regeneration. The x-axis indicates individual time points. The y-axis shows the fold change of streptomycin-treated versus control samples on a log2 scale. Expression profiles of ATOH1, E2F1, E2F7 and E2F8 at 24h intervals (1 in graph) across the 168h time course (8 in the graph) in the utricle **a)** and in the cochlea **b)**. In both utricle and cochlea, E2F1 expression is upregulated before the upregulation of ATOH1 in streptomycin-treated samples. Data kindly provided by Professor Michael Lovett and Mark Warchol.

If E2F1-3 are proven to be necessary for the re-activation of ATOH1 expression in chick tissues, then it would be necessary to investigate potential therapies to regenerate post-mitotic mammalian/human hair cells. Since evidence suggests that the mammalian *Atoh1* enhancer is unable to respond to E2F1-3 as it lacks the putative enhancer C, it would be interesting to assess the effect of modifications at the mammalian *Atoh1* locus, for instance, using CRISPR technology. The introduction of changes in genomic sequences into living cells has become a powerful tool to investigate different genetic diseases (review in Sander and Joung 2014). All these recent advances based on genome and epigenome editing could have an important role toward therapeutic applications to re-activate ATOH1 expression and therefore a potential avenue to reverse hearing loss in humans.

In conclusion, this thesis has provided valuable information about transcription factor candidates regulating *Atoh1*. The work emphasizes the potential role that a novel chick regulatory region (the putative enhancer C) and novel transcription factor candidates (the E2F family) could have on the study of the *Atoh1* regulatory network. The complexity of *Atoh1* regulation is high and investigations in chick and mammalian inner

ear are far from straightforward. So the challenge of regenerating human hearing cells to restore human hearing is still likely to be some distance away. Nevertheless, ATOH1 remains the strongest candidate for such an approach and revealing the distinct regulatory mechanism of ATOH1 re-activation in avians is one method which should be pursued.

Chapter 8

8 Conclusions

The work performed during the course of this thesis contributes to the understanding of the regulation of ATOH1 expression in different species. The investigations undertaken within this PhD produced three major conclusions:

A comparative analysis of the mammalian and avian *Atoh1* locus identified evolutionary conserved regions that are both common to, and distinct to, mammalian and avian species. In particular, a region was identified that was conserved within avian species but not in mammals, designated as putative enhancer C. This was subjected to further investigation and evidence suggests that this region is involved in the regulation of chick ATOH1 expression.

Bioinformatic analysis identified several putative transcription factor binding sites within the mammalian and avian *Atoh1* conserved regions. Some of these transcription factor candidates were selected for further investigation. Amongst all the candidates tested experimentally, evidence suggests that only the E2F1-3 transcription factors are regulators of chick *Atoh1* but not mouse *Atoh1* expression.

Activation of chick *Atoh1* by E2F1-3 is conducted primarily via a binding site in putative enhancer C suggesting a link between the avian-specific enhancer C and capacity to induce *Atoh1* activation in avians but not in mammals.

A plausible hypothesis can be built about the role of the E2F family and putative avian enhancer C in the regulation of *Atoh1* and hair cell regeneration based on these results. The presence of E2F regulatory elements within avian-specific enhancer C links hair cell cycle re-entry with re-activation of ATOH1 in avians but not mammals. This ATOH1 re-activation could confer a hair cell fate upon the newly produced cells in avians whereas this relationship is absent in mammalian species so that new hair cells are not produced. This hypothesis needs further investigation in order establish whether the E2F family are involved in the mechanism that drives supporting cells in avians to

re-activate ATOH1 expression after hair cell damage. If confirmed, this may in time lead to the exploration of novel therapeutic approaches to regenerate post-mitotic human hair cells that could benefit those affected by hearing loss.

Appendix

Optimization of the binding of E2F in EMSA experiments

On EMSA analysis in Appendix Figure 1, all bandshifts produced by the interactions between nuclear extracts proteins incubated with a radiolabelled E2F consensus probe failed to be competed by a known E2F1 probe as a competitor (the A2 probe). This was performed by testing different salt concentrations in the Parker Buffer solution as well as different concentration of nuclear extracts and different temperatures for the binding reaction (data not shown). However, in spite of all our efforts, no competition was shown between the consensus E2F and nuclear extracts from UB/OC2 cells. Nevertheless, Parker B^o 2 (see material and methods in section 2.2.8.2) gave stronger bands which could suggest that the addition of $MgCl_2$ improved protein-DNA binding affinities. Therefore, Parker B^o 2 was used for all the EMSA experiments.

Since, no competition was observed with nuclear protein extracts from UB/OC2 cells, the ability of E2F to bind a consensus E2F site was tested by in vitro translated protein.

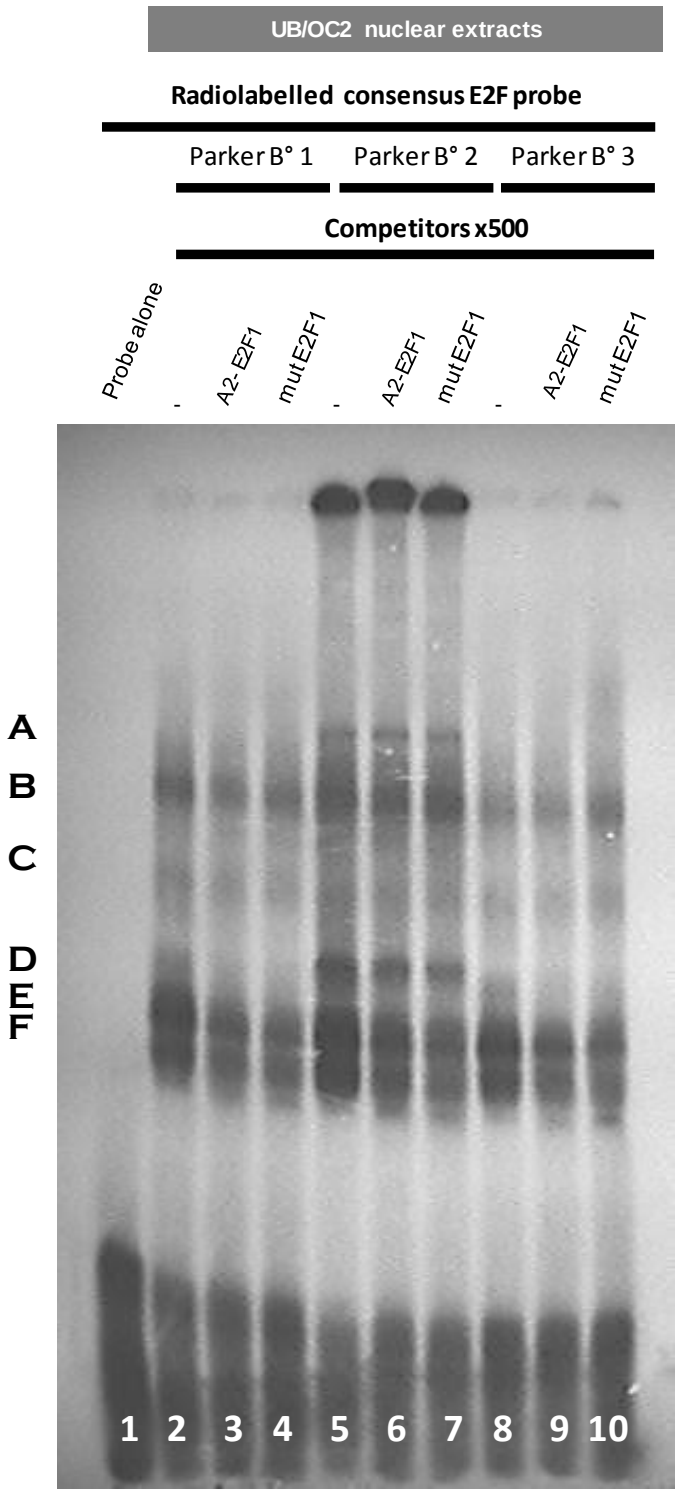

Appendix Figure 1: Attempt to show binding of UB/OC2 cell nuclear protein extract to a consensus E2F binding site. EMSA experiments were performed using a consensus E2F1probe labelled with [γ-32P]. Different Parker buffers were used to optimize the binding with different salt concentrations (Parker B^o1 was as described in section 2.2.8.2, Parker B^o2 was the same as B^o1 but with an addition of 4mmM $MgCl_2$ and Parker B^o3 was same as B^o1 but with the addition of 100mM of NaCl). Competition assay with the known E2F1 competitor (A2-E2F1 probe) failed to compete for any of the bandshifts (A-F) with all the Parker B^o tested. However Parker B^o 2 gave stronger bands suggesting that the addition of $MgCl_2$ improved protein-DNA binding affinities.

In vitro translation of E2F1 protein and its co-factor DP1

Since the tests described in the previous section failed to demonstrate the ability of E2F to bind a consensus E2F probe, I tested whether *in vitro* translated E2F protein was capable to show binding capacities.

E2F1 *in vitro* translated protein was made as described in section 2.2.7. as well as *in vitro* translated luciferase protein provided in the TNT® Transcription/Translation System which was used as control to discriminate between any protein from the rabbit reticulocyte lysate system which might bind to the radiolabelled probe in EMSA experiments. The T7 TNT® Transcription/Translation System was the chosen kit since the E2F1 expression construct is driven by the T7 promoter in the E2F1_pcDNA3 construct. Therefore, this system will produce a transcript due to T7-driven transcription and subsequent translation to generate *in vitro* translated E2F1.

The radiolabelled E2F consensus probe (Table 5.1) was incubated alone, with *in vitro* translated E2F1 protein or with *in vitro* translated luciferase protein and electrophoresed on a 4% polyacrylamide gel at room temperature for 2h. In Appendix Figure 2 a) represents the bandshifts (labelled A_1, B_1 and C_1) generated by *in vitro* translated E2F1 and *in vitro* translated luciferase. As it is shown in the figure, the bandshifts generated by both *in vitro* proteins were almost identical suggesting that all bandshifts in this experiment were possibly produced by proteins contained in the transcription/translation rabbit reticulocyte lysate system machinery (compare lane 2 and 3) binding to the radiolabelled consensus E2F probe.

Following this experiment and since neither E2F1 from UB/OC cells nuclear extract nor E2F1 *in vitro* translated protein were capable of binding to a consensus E2F site, I further investigated whether DP1, the co-factor for E2F, is necessary for E2F binding.

The DP proteins have been shown to form complexes with some members of the E2F family to activate transcription of genes containing E2F binding sites. Furthermore, the formation of E2F-DP complex enhances binding affinities and promote stable interactions to E2F sites in the DNA in comparison with the affinities of E2F alone (Helin et al. 1993). Since the presence of DP1 could be necessary to observe a specific binding between E2F and the predicted binding sites in the *Atoh1* conserved regions, I

performed an EMSA experiment where E2F1 and DP1 *in vitro* translated proteins were incubated together.

A human DP1 expression construct was obtained containing the human DP1 cDNA (accession number: L23959) cloned in a pCMV-Neo-Bam1 (a gift from Dr Tony Kouzarides, The Gurdon Institute, University of Cambridge, UK). The cDNA of the human DP1 was subcloned into the pcDNA3 expression construct (see section 2.2.7.1) to be able to produce *in vitro* translated DP1 using the T7 TNT® Transcription/Translation System.

Having successfully cloned the DP1 in pcDNA3, *in vitro* translated DP1 protein was used in EMSA experiments to test whether the E2F-DP complex improves the E2F binding capacity. DP1 and E2F1 *in vitro* translated proteins were incubated together for 1h at room temperature in order for them to form the E2F-DP1 complex before adding the radiolabelled consensus E2F probe. As with the previous experiment, the luciferase *in vitro* translated protein was used as a negative control.

The incubation of *in vitro* E2F with the DP1 co-factor resulted in the observation of a stronger bandshift in comparison with the bandshifts produced when *in vitro* translated E2F1 was incubated alone. In addition, an extra bandshift was generated when the *in vitro* E2F1 with the DP1 co-factor were incubated together in comparison to the bandshifts generated by the *in vitro* translated luciferase (bandshift B_2, compare lane 2 and lane 3 in Appendix Figure 2 b). Although this bandshift was weak, it was a small sign of improvement suggesting that the presence of DP1 enhanced the binding capacity of the E2F to the DNA. Based on these observations, EMSA experiments presented in chapter 5 were performed with UB/OC2 cells transfected with E2F1 and DP1.

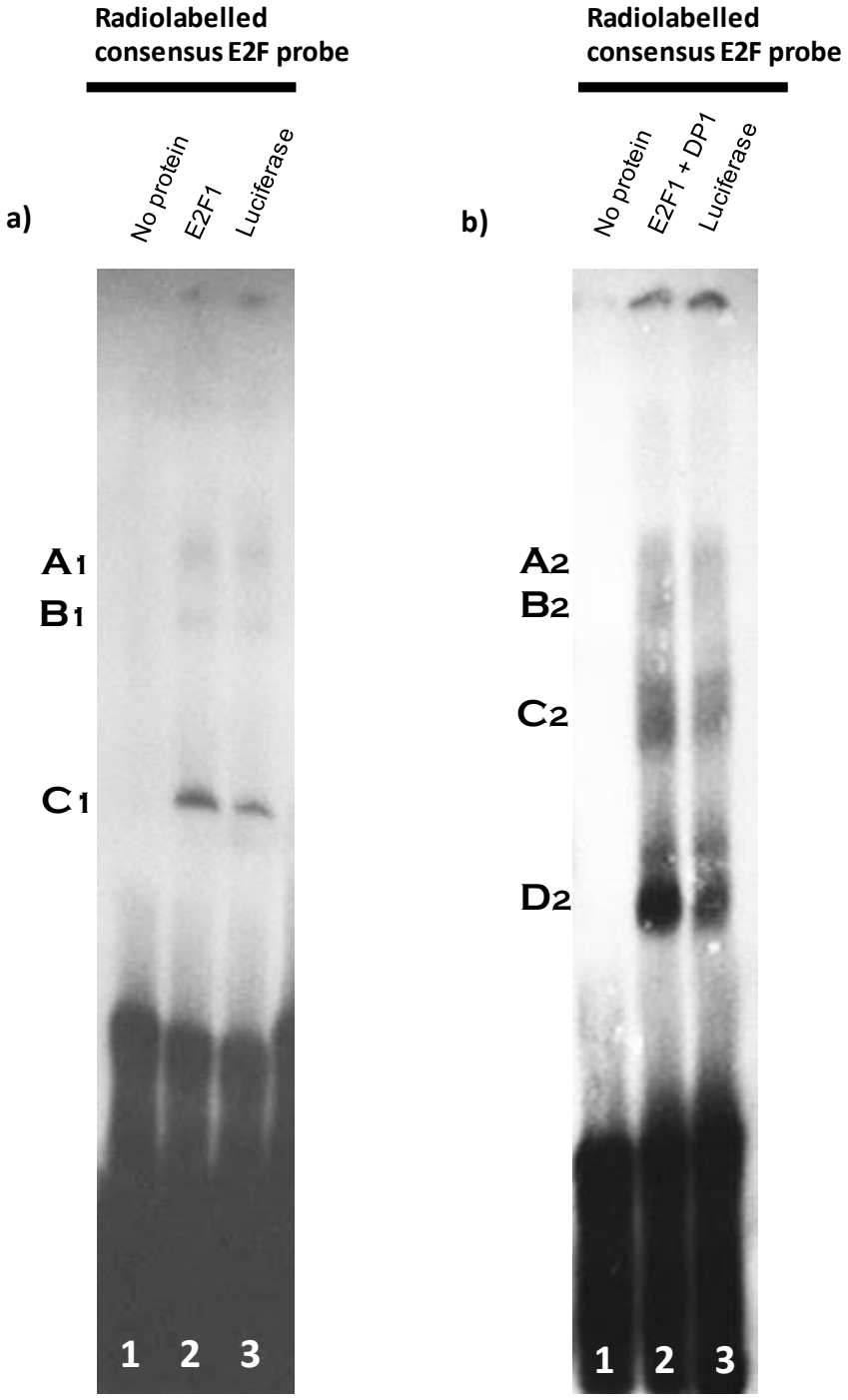

Appendix Figure 2: EMSA with *in vitro* translated proteins. The ability of *in vitro* translated E2F1 to bind to a consensus E2F site was tested by EMSA analysis. **a)** *in vitro* translated E2F1 protein incubated on its own with the radiolabelled consensus E2F probe. **b)** *in vitro* translated E2F1 protein incubated with *in vitro* translated DP1 protein incubated with the radiolabelled E2F consensus probe. In both analysis luciferase protein was used as a control for proteins possibly contained in the transcription/translation rabbit reticulocyte lysate system machinery binding to the radiolabelled consensus E2F1 probe. When *in vitro* translated E2F1 protein is incubated with *in vitro* translated DP1, an additional bandshift was observed in comparison to luciferase control (bandshift B_2).

Bibliography

Abdolazimi Y, Stojanova Z, Segil N. 2016. Selection of cell fate in the organ of Corti involves the integration of Hes/Hey signaling at the Atoh1 promoter. *Development* 143: 841-850.

Adams MR, Sears R, Nuckolls F, Leone G, Nevins JR. 2000. Complex Transcriptional Regulatory Mechanisms Control Expression of the E2F3 Locus. *Molecular and Cellular Biology* 20: 3633-3639.

Alder J, Lee KJ, Jessell TM, Hatten ME. 1999. Generation of cerebellar granule neurons in vivo by transplantation of BMP-treated neural progenitor cells. *Nature Neuroscience* 2: 535-540.

Adler HJ, Raphael Y. 1996. New hair cells arise from supporting cell conversion in the acoustically damaged chick inner ear. *Neuroscience Letters* 205: 17-20.

Ahmed M, Wong EY, Sun J, Xu J, Wang F, Xu PX. 2012a. Eya1-Six1 interaction is sufficient to induce hair cell fate in the cochlea by activating Atoh1 expression in cooperation with Sox2. *Developmental cell* 22: 377-390.

Akazawa C, Ishibashi M, Shimizu C, Nakanishi S, Kageyama R. 1995. A Mammalian Helix-Loop-Helix Factor Structurally Related to the Product of Drosophila Proneural Gene atonal Is a Positive Transcriptional Regulator Expressed in the Developing Nervous System. *Journal of Biological Chemistry* 270: 8730-8738.

Akiyama T, Ohuchi T, Sumida S, Matsumoto K, Toyoshima K. 1992. Phosphorylation of the retinoblastoma protein by cdk2. *Proceedings of the National Academy of Sciences of the United States of America* 89: 7900-7904.

Alberts B, Johnson, A., Lewis, J., Raff, M., Roberts, K. and Walter, P. . 2002. Molecular biology of the cell. 4th edn. *Annals of Botany* 91: 401-401.

Alla V, Engelmann D, Niemetz A, Pahnke J, Schmidt A, Kunz M, Emmrich S, Steder M, Koczan D, Pützer BM. 2010. E2F1 in Melanoma Progression and Metastasis. *Journal of the National Cancer Institute* 102: 127-133.

Allen BL, Taatjes DJ. 2015. The Mediator complex: a central integrator of transcription. *Nat Rev Mol Cell Biol* 16: 155-166.

Alsina B, Abelló G, Ulloa E, Henrique D, Pujades C, Giraldez F. 2004. FGF signaling is required for determination of otic neuroblasts in the chick embryo. *Developmental Biology* 267: 119-134.

Alsina B, Abelló G. 2007. Establishment of a proneural field in the inner ear. *The International journal of developmental biology* 51: 483 - 493.

Alvarez IS, Navascués J. 1990. Shaping, invagination, and closure of the chick embryo otic vesicle: Scanning electron microscopic and quantitative study. *The Anatomical Record* 228: 315-326.

Arney KL, Fisher AG. 2004. Epigenetic aspects of differentiation. Journal of Cell Science 117: 4355-4363.

Arnold JS, Braunstein EM, Ohyama T, Groves AK, Adams JC, Brown MC, Morrow BE. 2006. Tissue-specific roles of Tbx1 in the development of the outer, middle and inner ear, defective in 22q11DS patients. *Human Molecular Genetics* 15: 1629-1639.

Ashcroft M, Taya Y, Vousden KH. 2000. Stress Signals Utilize Multiple Pathways To Stabilize p53. *Molecular and Cellular Biology* 20: 3224-3233.

Attwooll C, Denchi E, Helin K. 2004. The E2F family: specific functions and overlapping interests. *EMBO J* 23: 4709 - 4716.

Ayrault O, Zhao H, Zindy F, Qu C, Sherr CJ, Roussel MF. 2010. Atoh1 Inhibits Neuronal Differentiation and Collaborates with Gli1 to Generate Medulloblastoma-Initiating Cells. *Cancer Research* 70: 5618-5627.

Bagchi S, Weinmann R, Raychaudhuri P. 1991. The retinoblastoma protein copurifies with E2F-I, an E1A-regulated inhibitor of the transcription factor E2F. *Cell* 65: 1063-1072.

Bancroft M, Bellairs R. 1977. Placodes of the chick embryo studied by SEM. *Anat Embryol* 151: 97-108.

Bandara LR, La Thangue NB. 1991. Adenovirus E1a prevents the retinoblastoma gene product from complexing with a cellular transcription factor. *Nature* 351: 494-497.

Barber RD, Ronnett GV. 2000. Reconstructing smell. *Molecular neurobiology* 21: 161-173.

Bates S, Phillips AC, Clark PA, Stott F, Peters G, Ludwig RL, Vousden KH. 1998. p14ARF links the tumour suppressors RB and p53. *Nature* 395: 124-125.

Beijersbergen RL, Kerkhoven RM, Zhu L, Carlee L, Voorhoeve PM, Bernards R. 1994. E2F-4, a new member of the E2F gene family, has oncogenic activity and associates with p107 in vivo. *Genes & Development* 8: 2680-2690.

Ben-Arie N, Bellen HJ, Armstrong DL, McCall AE, Gordadze PR, Guo Q, Matzuk MM, Zoghbi HY. 1997. Math1 is essential for genesis of cerebellar granule neurons. Nature 390: 169-172.

Ben-Arie N, Hassan BA, Bermingham NA, Malicki DM, Armstrong D, Matzuk M, Bellen HJ, Zoghbi HY. 2000. Functional conservation of atonal and Math1 in the CNS and PNS. *Development* 127: 1039-1048

Ben-Arie N, McCall AE, Berkman S, Eichele G, Bellen HJ, Zoghbi HY. 1996. Evolutionary Conservation of Sequence and Expression of the bHLH Protein Atonal Suggests a Conserved Role in Neurogenesis. *Human Molecular Genetics* 5: 1207-1216.

Bergström B EH. 1973. The vestibular sensory cells and their innervation. *International Journal of Equilibrium Research* June: 27-32.

Bermingham NA, Hassan BA, Price SD, Vollrath MA, Ben-Arie N, Eatock RA, Bellen HJ, Lysakowski A, Zoghbi HY. 1999. Math1: An Essential Gene for the Generation of Inner Ear Hair Cells. *Science* 284: 1837-1841.

Bermingham NA, Hassan BA, Wang VY, Fernandez M, Banfi S, Bellen HJ, Fritzsch B, Zoghbi HY. 2001. Proprioceptor Pathway Development Is Dependent on MATH1. Neuron 30: 411-422.

Bilous RW, Murty G, Parkinson DB, Thakker RV, Coulthard MG, Burn J, Mathias D, Kendall-Taylor P. 1992. Autosomal Dominant Familial Hypoparathyroidism, Sensorineural Deafness, and Renal Dysplasia. New England Journal of Medicine 327: 1069-1074.

Bird A. 2002. DNA methylation patterns and epigenetic memory. *Genes & Development* 16: 6-21.

Bjerknes M, Cheng H. 2006. Neurogenin 3 and the enteroendocrine cell lineage in the adult mouse small intestinal epithelium. *Developmental Biology* 300: 722-735.

Blake MC, Azizkhan JC. 1989. Transcription factor E2F is required for efficient expression of the hamster dihydrofolate reductase gene in vitro and in vivo. *Molecular and Cellular Biology* 9: 4994-5002.

Boddy SL, Chen W, Romero-Guevara R, Kottam L, Bellantuono I, Rivolta MN. 2012. Inner ear progenitor cells can be generated in vitro from human bone marrow mesenchymal stem cells. Regenerative Medicine 7: 757-767.

Bok J, Bronner-Fraser M, Wu DK. 2005. Role of the hindbrain in dorsoventral but not anteroposterior axial specification of the inner ear. *Development* 132: 2115-2124.

Bok J. WCaDKW. 2007. Patterning and morphogenesis of the vertebrate inner ear. *The International journal of developmental biology* 51: 521 - 533.

Bonfig W, Krude H, Schmidt H. 2011. A novel mutation of LHX3 is associated with combined pituitary hormone deficiency including ACTH deficiency, sensorineural hearing loss, and short neck—a case report and review of the literature. European Journal of Pediatrics 170: 1017-1021.

Bossuyt W, Kazanjian A, De Geest N, Kelst SV, Hertogh GD, Geboes K, Boivin GP, Luciani J, Fuks F, Chuah M et al. 2009. Atonal homolog 1 Is a Tumor Suppressor Gene. *PLoS Biol* 7: e1000039.

Bradley DJ, Towle HC, Young WS. 1994. Alpha and beta thyroid hormone receptor (TR) gene expression during auditory neurogenesis: evidence for TR isoform-specific transcriptional regulation in vivo. *Proceedings of the National Academy of Sciences of the United States of America* 91: 439-443.

Brehm A, Miska EA, McCance DJ, Reid JL, Bannister AJ, Kouzarides T. 1998. Retinoblastoma protein recruits histone deacetylase to repress transcription. Nature 391.

Briggs KJ, Eberhart CG, Watkins DN. 2008. Just Say No to ATOH: How HIC1 Methylation Might Predispose Medulloblastoma to Lineage Addiction. *Cancer Research* 68: 8654-8656.

Bird A. 2002. DNA methylation patterns and epigenetic memory. *Genes & Development* 16: 6-21.

Brooker R, Hozumi K, Lewis J. 2006. Notch ligands with contrasting functions: Jagged1 and Delta1 in the mouse inner ear. *Development* 133: 1277-1286.

Brown RD. 1981. Comparative Acute Cochlear Toxicity of Intravenous Bumetanide and Furosemide in the Purebred Beagle. *The Journal of Clinical Pharmacology* 21: 620-627.

Bruce A. Sherf SLN, Rita R. Hannah and Keith V. Wood 1996. Dual-LuciferaseTM Reporter Assay: An Advanced Co-Reporter Technology Integrating Firefly and Renilla Luciferase Assays *Promega Notes Magazine* 57.

Bryant J, Goodyear RJ, Richardson GP. 2002. Sensory organ development in the inner ear: molecular and cellular mechanisms. *British Medical Bulletin* 63: 39-57.

Burton Q, Cole LK, Mulheisen M, Chang W, Wu DK. 2004. The role of Pax2 in mouse inner ear development. *Developmental Biology* 272: 161-175.

Cafaro J, Lee GS, Stone JS. 2007. Atoh1 expression defines activated progenitors and differentiating hair cells during avian hair cell regeneration. *Developmental Dynamics* 236: 156-170.

Cam H, Dynlacht B. 2003. Emerging roles for E2F: beyond the G1/S transition and DNA replication. *Cancer Cell* 3: 311 - 316.

Cartharius K, Frech K, Grote K, Klocke B, Haltmeier M, Klingenhoff A, Frisch M, Bayerlein M, Werner T. 2005. MatInspector and beyond: promoter analysis based on transcription factor binding sites. *Bioinformatics* 21: 2933-2942.

Cedar H. 1988. DNA methylation and gene activity. *Cell* 53: 3-4.

Cerqueira A, Martín A, Symonds CE, Odajima J, Dubus P, Barbacid M, Santamaría D. 2014. Genetic Characterization of the Role of the Cip/Kip Family of Proteins as Cyclin-Dependent Kinase Inhibitors and Assembly Factors. *Molecular and Cellular Biology* 34: 1452-1459.

Chang W, Lin Z, Kulessa H, Hebert J, Hogan BL, Wu DK. 2008. Bmp4 is essential for the formation of the vestibular apparatus that detects angular head movements. *PLoS Genet* 4: e1000050.

Chellappa R, Li S, Pauley S, Jahan I, Jin K, Xiang M. 2008. Barhl1 Regulatory Sequences Required for Cell-Specific Gene Expression and Autoregulation in the Inner Ear and Central Nervous System. Molecular and Cellular Biology 28: 1905-1914.

Chellappan SP, Hiebert S, Mudryj M, Horowitz JM, Nevins JR. 1991. The E2F transcription factor is a cellular target for the RB protein. *Cell* 65: 1053-1061.

Chen H-Z, Tsai S-Y, Leone G. 2009. Emerging roles of E2Fs in cancer: an exit from cell cycle control. Nat Rev Cancer 9: 785-797.

Chen M, Manley JL. 2009. Mechanisms of alternative splicing regulation: insights from molecular and genomics approaches. *Nature reviews Molecular cell biology* 10: 741-754.

Chen P, Johnson JE, Zoghbi HY, Segil N. 2002. The role of Math1 in inner ear development: Uncoupling the establishment of the sensory primordium from hair cell fate determination. *Development* 129: 2495-2505.

Chen P, Segil N. 1999. p27(Kip1) links cell proliferation to morphogenesis in the developing organ of Corti. *Development* 126: 1581-1590.

Chen W, Johnson SL, Marcotti W, Andrews PW, Moore HD, Rivolta MN. 2009. Human Fetal Auditory Stem Cells Can Be Expanded In Vitro and Differentiate Into Functional Auditory Neurons and Hair Cell-Like Cells. *Stem cells* 27: 1196-1204.

Chiaromonte F, Weber RJ, Roskin KM, Diekhans M, Kent WJ, Haussler D. 2003. The Share of Human Genomic DNA under Selection Estimated from Human–Mouse Genomic Alignments. *Cold Spring Harbor Symposia on Quantitative Biology* 68: 245-254.

Chien WW, Isgrig K, Roy S, Belyantseva IA, Drummond MC, May LA, Fitzgerald TS, Friedman TB, Cunningham LL. 2015. Gene therapy restores hair cell stereocilia morphology in inner ears of deaf whirler mice. *Mol Ther* doi:10.1038/mt.2015.150.

Chinwalla et al. 2002. Initial sequencing and comparative analysis of the mouse genome. *Nature* 420: 520-562.

Chong JL, Tsai SY, Sharma N, Opavsky R, Price R, Wu L, Fernandez SA, Leone G. 2009. E2f3a and E2f3b contribute to the control of cell proliferation and mouse development. *Mol Cell Biol* 29: 414-424.

Choo B, Kondrichin I, Parinov S, Emelyanov A, Go W, Toh W-c, Korzh V. 2006. Zebrafish transgenic Enhancer TRAP line database (ZETRAP). *BMC Developmental Biology* 6: 5.

Clarke AR, Maandag ER, van Roon M, van der Lugt NMT, van der Valk M, Hooper ML, Berns A, te Rielef H. 1992. Requirement for a functional Rb-1 gene in murine development. *Nature* 359: 328-330.

Classon M, Harlow E. 2002. The retinoblastoma tumour suppressor in development and cancer. *Nat Rev Cancer* 2: 910-917.

Cloud JE, Rogers C, Reza TL, Ziebold U, Stone JR, Picard MH, Caron AM, Bronson RT, Lees JA. 2002. Mutant Mouse Models Reveal the Relative Roles of E2F1 and E2F3 In Vivo. *Molecular and Cellular Biology* 22: 2663-2672.

Clough RL, Sud R, Davis-Silberman N, Hertzano R, Avraham KB, Holley M, Dawson SJ. 2004. Brn-3c (POU4F3) regulates BDNF and NT-3 promoter activity. *Biochemical and Biophysical Research Communications* 324: 372-381.

Cohen-Salmon M, El-Amraoui A, Leibovici M, Petit C. 1997. Otogelin: A glycoprotein specific to the acellular membranes of the inner ear. *Proceedings of the National Academy of Sciences of the United States of America* 94: 14450-14455.

Cole LK, Le Roux I, Nunes F, Laufer E, Lewis J, Wu DK. 2000. Sensory organ generation in the chicken inner ear: Contributions of Bone morphogenetic protein 4, Serrate1, and Lunatic fringe. *The Journal of Comparative Neurology* 424: 509-520.

Collin RWJ, Chellappa R, Pauw R-J, Vriend G, Oostrik J, van Drunen W, Huygen PL, Admiraal R, Hoefsloot LH, Cremers FPM et al. 2008. Missense Mutations in POU4F3 Cause Autosomal Dominant Hearing Impairment DFNA15 and Affect Subcellular Localization and DNA Binding. Human mutation 29: 545-554.

Cooper-Kuhn CM, Vroemen M, Brown J, Ye H, Thompson MA, Winkler J, Kuhn HG. 2002. Impaired Adult Neurogenesis in Mice Lacking the Transcription Factor E2F1. *Molecular and Cellular Neuroscience* 21: 312-323.

Corwin AKaJT. 1989. Cell Production in the Chicken Cochlea *THE JOURNAL OF COMPARATIVE NEUROLOGY* 281: 129-135.

Costa A, Sanchez-Guardado L, Juniat S, Gale JE, Daudet N, Henrique D. 2015. Generation of sensory hair cells by genetic programming with a combination of transcription factors. *Development* 142: 1948-1959.

Cotanche DA. 1987. Regeneration of the tectorial membrane in the chick cochlea following severe acoustic trauma. *Hearing Research* 30: 197-206.

D'Angelo A, Bluteau O, Garcia-Gonzalez MA, Gresh L, Doyen A, Garbay S, Robine S, Pontoglio M. 2010. Hepatocyte nuclear factor 1α and β control terminal differentiation and cell fate commitment in the gut epithelium. *Development* 137: 1573-1582.

Dagnino L, Fry CJ, Bartley SM, Farnham P, Gallie BL, Phillips RA. 1997. Expression patterns of the E2F family of transcription factors during mouse nervous system development. *Mechanisms of development* 66: 13-25.

Dallos. 1992. The active cochlea. *Journal of Neuroscience* December 12: 4575-4585.

Das PM, Singal R. 2004. DNA Methylation and Cancer. *Journal of Clinical Oncology* 22: 4632-4642.

Daudet N, Gibson R, Shang J, Bernard A, Lewis J, Stone J. 2009. Notch regulation of progenitor cell behavior in quiescent and regenerating auditory epithelium of mature birds. *Dev Biol* 326: 86-100.

Day D, Tuite M. 1998. Post-transcriptional gene regulatory mechanisms in eukaryotes: an overview. *Journal of Endocrinology* 157: 361-371.

De Bruin A, Maiti B, Jakoi L, Timmers C, Buerki R, Leone G. 2003. Identification and Characterization of E2F7, a Novel Mammalian E2F Family Member Capable of Blocking Cellular Proliferation. *Journal of Biological Chemistry* 278: 42041-42049.

DeGregori J, Leone G, Ohtani K, Miron A, Nevins JR. 1995. E2F-1 accumulation bypasses a G1 arrest resulting from the inhibition of G1 cyclin-dependent kinase activity. *Genes & Development* 9: 2873-2887.

Deol MS. 1964. The abnormalities of the inner ear in kreisler mice. *Journal of Embryology and Experimental Morphology* 12: 475-490.

Di Stefano L, Jensen MR, Helin K. 2003. E2F7, a novel E2F featuring DP-independent repression of a subset of E2F-regulated genes. *The EMBO Journal* 22: 6289-6298.

Dick FA, Rubin SM. 2013. Molecular mechanisms underlying RB protein function. Nat Rev Mol Cell Biol 14: 297-306.

Dimova DK, Dyson NJ. 2005. The E2F transcriptional network: old acquaintances with new faces. *Oncogene* 24: 2810-2826.

Doetzlhofer A, Avraham KB. 2016. Insights into inner ear-specific gene regulation: epigenetics and non-coding RNAs in inner ear development and regeneration. *Seminars in Cell & Developmental Biology*.

Dooling RJ, Fay, Richard R. 2000. Comparative Hearing: Birds and Reptiles. *Springer Handbook of Auditory Research*.

Driver EC, Sillers L, Coate TM, Rose MF, Kelley MW. 2013. The Atoh1-lineage gives rise to hair cells and supporting cells within the mammalian cochlea. *Developmental Biology* 376: 86-98.

Durán Alonso MB, Feijoo-Redondo A, Conde de Felipe M, Carnicero E, García AS, García-Sancho J, Rivolta MN, Giráldez F, Schimmang T. 2012. Generation of inner ear sensory cells from bone marrow-derived human mesenchymal stem cells. Regenerative Medicine 7: 769-783.

Dyson N. 1998. The regulation of E2F by pRB-family proteins. *Genes & Development* 12: 2245-2262.

Ebert PJ, Timmer JR, Nakada Y, Helms AW, Parab PB, Liu Y, Hunsaker TL, Johnson JE. 2003. Zic1 represses Math1 expression via interactions with the Math1 enhancer and modulation of Math1 autoregulation. *Development* 130: 1949-1959.

Erkman L, McEvilly RJ, Luo L, Ryan AK, Hooshmand F, O'Connell SM, Keithley EM, Rapaport DH, Ryan AF, Rosenfeld MG. 1996. Role of transcription factors a Brn-3.1 and Brn-3.2 in auditory and visual system development. *Nature* 381: 603-606.

Erol S. 2007. Aminoglycoside-Induced Ototoxicity. *Current Pharmaceutical Design* 13: 119-126.

Ewen ME, Sluss HK, Sherr CJ, Matsushime H, Kato J-y, Livingston DM. 1993. Functional interactions of the retinoblastoma protein with mammalian D-type cyclins. *Cell* 73: 487-497.

Faddis B. 2008. Structural and Functional Anatomy of the Outer Ear. In: Anatomy and Physiology of Hearing for Audiologists. *Thomson Delmar Learning Publishers, Clifton Park, NY*.

Fekete DM. 1996. Cell fate specification in the inner ear. *Current Opinion in Neurobiology* 6: 533-541.

Fekete DM, Wu DK. 2002. Revisiting cell fate specification in the inner ear. *Current Opinion in Neurobiology* 12: 35-42.

Fetoni AR, Picciotti PM, Paludetti G, Troiani D. 2011. Pathogenesis of presbycusis in animal models: A review. *Experimental Gerontology* 46: 413-425.

Fontemaggi G, Dell'Orso S, Trisciuoglio D, Shay T, Melucci E, Fazi F, Terrenato I, Mottolese M, Muti P, Domany E et al. 2009. The execution of the transcriptional axis mutant p53, E2F1 and ID4 promotes tumor neo-angiogenesis. *Nat Struct Mol Biol* 16: 1086-1093.

Forge A, Li L, Corwin JT, Nevill G. 1993. Ultrastructural Evidence for Hair Cell Regeneration in the Mammalian Inner Ear. *Science* 259: 1616-1619.

Forge A, Wright T. 2002. The molecular architecture of the inner ear. *British Medical Bulletin* 63: 5-24.

Freeman S, Chrysostomou E, Kawakami K, Takahashi Y, Daudet N. 2012. Tol2-mediated gene transfer and in ovo electroporation of the otic placode: a powerful and versatile approach for investigating embryonic development and regeneration of the chicken inner ear. *Methods in molecular biology* 916: 127-139.

Freeman SD, Daudet N. 2012. Artificial induction of Sox21 regulates sensory cell formation in the embryonic chicken inner ear. *PLoS ONE* 7: e46387.

Frisch T, Sørensen MS, Overgaard S, Lind M, Bretlau P. 1998. Volume-Referent Bone Turnover Estimated From the Interlabel Area Fraction After Sequential Labeling. *Bone* 22: 677-682.

Frucht CS, Uduman M, Duke JL, Kleinstein SH, Santos-Sacchi J, Navaratnam DS. 2010. Gene Expression Analysis of Forskolin Treated Basilar Papillae Identifies MicroRNA181a as a Mediator of Proliferation. *PLoS ONE* 5: e11502.

Gaubatz S, Lees JA, Lindeman GJ, Livingston DM. 2001. E2F4 Is Exported from the Nucleus in a CRM1-Dependent Manner. *Molecular and Cellular Biology* 21: 1384-1392.

Gerlach LM, Hutson MR, Germiller JA, Nguyen-Luu D, Victor JC, Barald KF. 2000. Addition of the BMP4 antagonist, noggin, disrupts avian inner ear development. *Development* 127: 45-54.

Giese K, Kingsley C, Kirshner JR, Grosschedl R. 1995. Assembly and function of a TCR alpha enhancer complex is dependent on LEF-1-induced DNA bending and multiple protein-protein interactions. *Genes & Development* 9: 995-1008.

Gilmore TD. 2006. Introduction to NF-[kappa]B: players, pathways, perspectives. *Oncogene* 25: 6680-6684.

Ginsberg D, Vairo G, Chittenden T, Xiao ZX, Xu G, Wydner KL, DeCaprio JA, Lawrence JB, Livingston DM. 1994. E2F-4, a new member of the E2F transcription factor family, interacts with p107. *Genes & Development* 8: 2665-2679.

Girling R, Partridge JF, Bandara LR, Burden N, Totty NF, Hsuan JJ, La Thangue NB. 1993. A new component of the transcription factor DRTF1/E2F. *Nature* 362: 83-87.

Goodyear R, Richardson G. 1997. Pattern Formation in the Basilar Papilla: Evidence for Cell Rearrangement. *The Journal of Neuroscience* 17: 6289-6301.

Goodyear RJ, Gates R, Lukashkin AN, Richardson GP. 1999. Hair-cell numbers continue to increase in the utricular macula of the early posthatch chick. *Journal of Neurocytology* 28: 851-861.

Goodyear RJ, Marcotti W, Kros CJ, Richardson GP. 2005. Development and properties of stereociliary link types in hair cells of the mouse cochlea. *The Journal of Comparative Neurology* 485: 75-85.

Gowri D. Nayak HSKR, Richard J. Goodyear and Guy P. Richardson. 2007. Development of the hair bundle and mechanotransduction. *The International journal of developmental biology* 51: 597-608.

Graham A, Begbie J, McGonnell I. 2004. Significance of the cranial neural crest. *Developmental Dynamics* 229: 5-13.

Greenbaum D, Colangelo C, Williams K, Gerstein M. 2003. Comparing protein abundance and mRNA expression levels on a genomic scale. *Genome Biology* 4: 117-117.

Grewal SIS, Moazed D. 2003. Heterochromatin and Epigenetic Control of Gene Expression. *Science* 301: 798-802.

Grimmer MR, Weiss WA. 2008. BMPs oppose Math1 in cerebellar development and in medulloblastoma. *Genes & Development* 22: 693-699.

Groves AK. 2010. The challenge of hair cell regeneration. *Experimental Biology and Medicine* 235: 434-446.

Groves AK, Bronner-Fraser M. 2000. Competence, specification and commitment in otic placode induction. *Development* 127: 3489-3499.

Groves AK, Zhang KD, Fekete DM. 2013. The Genetics of Hair Cell Development and Regeneration. *Annual Review of Neuroscience* 36: null.

Grunstein M. 1998. Yeast Heterochromatin: Regulation of Its Assembly and Inheritance by Histones. *Cell* 93: 325-328.

Guasconi V YH, Ait-Si-Ali S. 2003. Transcription factors. *Atlas of Genetics and Cytogenetics in Oncology and Haematology* April 2003.

Gubbels SP, Woessner DW, Mitchell JC, Ricci AJ, Brigande JV. 2008. Functional auditory hair cells produced in the mammalian cochlea by in utero gene transfer. *Nature* 455: 537-541.

Guo H, Ingolia NT, Weissman JS, Bartel DP. 2010. Mammalian microRNAs predominantly act to decrease target mRNA levels. *Nature* 466: 835-840.

Haines ED. 2013. *Fundamental Neuroscience for Basic and Clinical Applications*.

Halaban R, Cheng E, Zhang Y, Mandigo C, Miglarese M. 1998. Release of cell cycle constraints in mouse melanocytes by overexpressed mutant E2F1E132 but not by deletion of p16INK4A or p21WAF1/CIP1. *Oncogene* 16: 2489 - 2501.

Hayashi T, Ray CA, Bermingham-McDonogh O. 2008. Fgf20 Is Required for Sensory Epithelial Specification in the Developing Cochlea. *Journal of Neuroscience* 28: 5991-5999.

Hardy M. 1938. The length of the organ of Corti in man. *American Journal of Anatomy* 62: 291-311.

Heintzman ND, Ren B. 2006. The gateway to transcription: identifying, characterizing and understanding promoters in the eukaryotic genome. *Cell Mol Life Sci* 64: 386-400.

Helin K, Lees JA, Vidal M, Dyson N, Harlow E, Fattaey A. 1992. A cDNA encoding a pRB-binding protein with properties of the transcription factor E2F. *Cell* 70: 337-350.

Helin K, Wu C, Fattaey A, Lees J, Dynlacht B, NGWU C, Harlow E. 1993. Heterodimerization of the transcription factors E2F-1 and DP-1 leads to cooperative trans-activation. *Genes Dev* 7: 1850 - 1861.

Hellman LM, Fried MG. 2007. Electrophoretic mobility shift assay (EMSA) for detecting protein-nucleic acid interactions. *Nat Protocols* 2: 1849-1861.

Heller N, Brändli AW. 1999. Xenopus Pax-2/5/8 orthologues: Novel insights into Pax Gene evolution and identification of Pax-8 as the earliest marker for otic and pronephric cell lineages. *Developmental Genetics* 24: 208-219.

Helms AW, Abney AL, Ben-Arie N, Zoghbi HY, Johnson JE. 2000. Autoregulation and multiple enhancers control Math1 expression in the developing nervous system. *Development* 127: 1185-1196.

Helms AW, Johnson JE. 1998. Progenitors of dorsal commissural interneurons are defined by MATH1 expression. *Development* 125: 919-928.

Henley SA, Dick FA. 2012. The retinoblastoma family of proteins and their regulatory functions in the mammalian cell division cycle. Cell Division 7: 1-14.

Hertzano R, Dror AA, Montcouquiol M, Ahmed ZM, Ellsworth B, Camper S, Friedman TB, Kelley MW, Avraham KB. 2007. Lhx3, a LIM domain transcription factor, is regulated by Pou4f3 in the auditory but not in the vestibular system. *European Journal of Neuroscience* 25: 999-1005.

Hertzano R, Montcouquiol M, Rashi-Elkeles S, Elkon R, Yücel R, Frankel WN, Rechavi G, Möröy T, Friedman TB, Kelley MW et al. 2004. Transcription profiling of inner ears from Pou4f3ddl/ddl identifies Gfi1 as a target of the Pou4f3 deafness gene. Human Molecular Genetics 13: 2143-2153.

Hidalgo-Sánchez Ma, Alvarado-Mallart R-M, Alvarez IS. 2000. Pax2, Otx2, Gbx2 and Fgf8 expression in early otic vesicle development. *Mechanisms of development* 95: 225-229.

Hijmans EM, Voorhoeve PM, Beijersbergen RL, van 't Veer LJ, Bernards R. 1995. E2F-5, a new E2F family member that interacts with p130 in vivo. *Molecular and Cellular Biology* 15: 3082-3089.

Hinds PW, Mittnacht S, Dulic V, Arnold A, Reed SI, Weinberg RA. 1992. Regulation of retinoblastoma protein functions by ectopic expression of human cyclins. *Cell* 70: 993-1006.

Holoch D, Moazed D. 2015. RNA-mediated epigenetic regulation of gene expression. *Nature reviews Genetics* **16**: 71-84.

Hozumi A, Yoshida R, Horie T, Sakuma T, Yamamoto T, Sasakura Y. 2013. Enhancer activity sensitive to the orientation of the gene it regulates in the chordate genome. *Dev Biol* 375: 79-91.

Hu X, Huang J, Feng L, Fukudome S, Hamajima Y, Lin J. 2010. Sonic hedgehog (SHH) promotes the differentiation of mouse cochlear neural progenitors via the Math1–Brn3.1 signaling pathway in vitro. *Journal of neuroscience research* 88: 927-935.

Hu Z, Luo X, Zhang L, Lu F, Dong F, Monsell E, Jiang H. 2012. Generation of human inner ear prosensory-like cells via epithelial-to-mesenchymal transition. *Regenerative medicine* 7: 663-673.

Iaquinta PJ, Lees JA. 2007. Life and death decisions by the E2F transcription factors. *Current opinion in cell biology* 19: 649-657.

Ikeda MA, Jakoi L, Nevins JR. 1996. A unique role for the Rb protein in controlling E2F accumulation during cell growth and differentiation. *Proceedings of the National Academy of Sciences of the United States of America* 93: 3215-3220.

Ikeda R, Pak K, Chavez E, Ryan AF. 2014. Transcription Factors with Conserved Binding Sites Near ATOH1 on the POU4F3 Gene Enhance the Induction of Cochlear Hair Cells. Molecular neurobiology doi:10.1007/s12035-014-8801-y.

Itoh M, Chitnis AB. 2001. Expression of proneural and neurogenic genes in the zebrafish lateral line primordium correlates with selection of hair cell fate in neuromasts. *Mechanisms of development* 102: 263-266.

Ivey-Hoyle M, Conroy R, Huber HE, Goodhart PJ, Oliff A, Heimbrook DC. 1993. Cloning and characterization of E2F-2, a novel protein with the biochemical properties of transcription factor E2F. *Molecular and Cellular Biology* 13: 7802-7812.

Izumikawa M, Batts SA, Miyazawa T, Swiderski DL, Raphael Y. 2008. Response of the flat cochlear epithelium to forced expression of Atoh1. *Hearing Research* 240: 52-56.

Izumikawa M, Minoda R, Kawamoto K, Abrashkin KA, Swiderski DL, Dolan DF, Brough DE, Raphael Y. 2005. Auditory hair cell replacement and hearing improvement by Atoh1 gene therapy in deaf mammals. *Nature medicine* 11: 271-276.

Jafar-Nejad H, Bellen HJ. 2004. Gfi/Pag-3/Senseless Zinc Finger Proteins: a Unifying Theme? Molecular and Cellular Biology 24: 8803-8812.

Jagger JD, Holley CM, Ashmore FJ. 1999. Ionic currents expressed in a cell line derived from the organ of Corti of the Immortomouse. *Pflügers Archiv* 438: 8-14.

Jarman AP AI. 1998. The specificity of proneural genes in determining Drosophila sense organ identity. *Mech Dev* 76(1-2): 117-125.

Jarman AP, Grau Y, Jan LY, Jan YN. 1993. atonal is a proneural gene that directs chordotonal organ formation in the Drosophila peripheral nervous system. *Cell* 73: 1307-1321.

Jarman AP, Grell EH, Ackerman L, Jan LY, Jan YN. 1994. atonal is the proneural gene for Drosophila photoreceptors. *Nature* 369: 398-400.

Jarman AP, Sun Y, Jan LY, Jan YN. 1995. Role of the proneural gene, atonal, in formation of Drosophila chordotonal organs and photoreceptors. *Development* 121: 2019-2030.

Jat PS, Noble MD, Ataliotis P, Tanaka Y, Yannoutsos N, Larsen L, Kioussis D. 1991. Direct derivation of conditionally immortal cell lines from an H-2Kb-tsA58 transgenic mouse. *Proceedings of the National Academy of Sciences of the United States of America* 88: 5096-5100.

Jen Y, Manova K, Benezra R. 1997. Each member of the Id gene family exhibits a unique expression pattern in mouse gastrulation and neurogenesis. *Developmental Dynamics* 208: 92-106.

Jiang H, Sha S-H, Schacht J. 2005. NF-κB pathway protects cochlear hair cells from aminoglycoside-induced ototoxicity. *Journal of neuroscience research* 79: 644-651.

Johnson DG, Schwarz JK, Cress WD, Nevins JR. 1993. Expression of transcription factor E2F1 induces quiescent cells to enter S phase. *Nature* 365: 349-352.

Jones C, Chen P. 2007. Planar cell polarity signaling in vertebrates. *BioEssays : news and reviews in molecular, cellular and developmental biology* 29: 120-132.

Jones JM, Montcouquiol M, Dabdoub A, Woods C, Kelley MW. 2006. Inhibitors of Differentiation and DNA Binding (Ids) Regulate Math1 and Hair Cell Formation during the Development of the Organ of Corti. *J Neurosci* 26: 550-558.

Jones S. 2004. An overview of the basic helix-loop-helix proteins. *Genome Biology* 5: 226-226.

Jorgensen, M. J, Mathiesen, C. 1988. The avian inner ear. Continuous production of hair cells in vestibular sensory organ, but not in the auditory papilla. Springer, Heidelberg, Allemagne.

Jun-ya Kato HM, Scott W. Hiebert, Mark E. Ewen, and Charles J. Sherr 1993. Direct binding of cyclin D to the retinoblastoma gene product (pRb) and pRb phosphorylation by the cyclin D-dependent kinase CDK4. *Genes & Development* 7: 331-342.

Juven-Gershon T, Kadonaga JT. 2010. Regulation of Gene Expression via the Core Promoter and the Basal Transcriptional Machinery. *Developmental biology* 339: 225-229.

Kaelin Jr WG, Pallas DC, DeCaprio JA, Kaye FJ, Livingston DM. 1991. Identification of cellular proteins that can interact specifically with the T/ElA-binding region of the retinoblastoma gene product. *Cell* 64: 521-532.

Kamaid A, Neves J, Giráldez F. 2010. Id Gene Regulation and Function in the Prosensory Domains of the Chicken Inner Ear: A Link between Bmp Signaling and Atoh1. *The Journal of Neuroscience* 30: 11426-11434.

Karin M, Lin A. 2002. NF-[kappa]B at the crossroads of life and death. *Nat Immunol* 3: 221-227.

Kawamoto K, Ishimoto S-I, Minoda R, Brough DE, Raphael Y. 2003. Math1 Gene Transfer Generates New Cochlear Hair Cells in Mature Guinea Pigs In Vivo. *The Journal of Neuroscience* 23: 4395-4400.

Kawamoto K, Izumikawa M, Beyer LA, Atkin GM, Raphael Y. 2009. Spontaneous hair cell regeneration in the mouse utricle following gentamicin ototoxicity. *Hearing Research* 247: 17-26.

Kazanjian A, Gross EA, Grimes HL. 2006. The growth factor independence-1 transcription factor: New functions and new insights. Critical Reviews in Oncology/Hematology 59: 85-97.

Kazanjian A, Noah T, Brown D, Burkart J, Shroyer NF. 2010. Atonal Homolog 1 Is Required for Growth and Differentiation Effects of Notch/γ-Secretase Inhibitors on Normal and Cancerous Intestinal Epithelial Cells. *Gastroenterology* 139: 918-928.e916

Kelley M, Talreja D, Corwin J. 1995. Replacement of hair cells after laser microbeam irradiation in cultured organs of corti from embryonic and neonatal mice. *The Journal of Neuroscience* 15: 3013-3026.

Kelley MW. 2006. Regulation of cell fate in the sensory epithelia of the inner ear. *Nature reviews Neuroscience* 7: 837-849.

Kelley MW. 2007. Cellular commitment and differentiation in the organ of Corti. *The International journal of developmental biology* 51: 571-583.

Kelley MW, Wu DK, Popper AN, Fay RR. 2005. Development of the Inner Ear. *Springer Handbook of Auditory Research* 26.

Kelley MW, Xu XM, Wagner MA, Warchol ME, Corwin JT. 1993. The developing organ of Corti contains retinoic acid and forms supernumerary hair cells in response to exogenous retinoic acid in culture. *Development* 119: 1041-1053.

Kherrouche Z, Blais A, Ferreira E, De Launoit Y, Monte D. 2006. ASK-1 (apoptosis signal-regulating kinase 1) is a direct E2F target gene. *The Biochemical journal* 396: 547-556.

Kiernan AE FD. 1997. In vivo gene transfer into the embryonic inner ear using retroviral vectors. *Audiology Neurootology* 1-2: 12-24.

Kiernan AE, Pelling AL, Leung KKH, Tang ASP, Bell DM, Tease C, Lovell-Badge R, Steel KP, Cheah KSE. 2005. Sox2 is required for sensory organ development in the mammalian inner ear. *Nature* 434: 1031-1035.

Kiernan AE, Xu J, Gridley T. 2006. The Notch Ligand JAG1 Is Required for Sensory Progenitor Development in the Mammalian Inner Ear. *PLoS Genetics* 2: e4.

Kim H-J, Won H-H, Park K-J, Hong SH, Ki C-S, Cho SS, Venselaar H, Vriend G, Kim J-W. 2013. SNP Linkage Analysis and Whole Exome Sequencing Identify a Novel *POU4F3* Mutation in Autosomal Dominant Late-Onset Nonsyndromic Hearing Loss (DFNA15). PLoS ONE 8: e79063.

Kim TH, Shivdasani RA. 2011. Genetic evidence that intestinal Notch functions vary regionally and operate through a common mechanism of Math1 repression. J *Biol Chem* 286: 11427-11433.

Kim YK, Lee AS. 1991. Identification of a 70-base-pair cell cycle regulatory unit within the promoter of the human thymidine kinase gene and its interaction with cellular factors. *Molecular and Cellular Biology* 11: 2296-2302.

Kingsley. 1999. The Auditory System. *Concise Text of Neuroscience, Lippincott Williams & Wilkins, Baltimore*: 393-432.

Koehler KR, Mikosz AM, Molosh AI, Patel D, Hashino E. 2013. Generation of inner ear sensory epithelia from pluripotent stem cells in 3D culture. *Nature* 500: 217-221.

Kornberg RD. 1999. Eukaryotic transcriptional control. *Trends in cell biology 9*: M46-M49.

Kovesdi I, Reichel R, Nevins JR. 1986. Identification of a cellular transcription factor involved in E1A trans-activation. *Cell* 45: 219-228.

Kovesdi I, Reichel R, Nevins JR. 1987. Role of an Adenovirus E2 Promoter Binding Factor in E1A-Mediated Coordinate Gene Control. *Proceedings of the National Academy of Sciences of the United States of America* 84: 2180-2184.

Krauss S, Johansen T, Korzh V, Fjose A. 1991. Expression of the zebrafish paired box gene pax[zf-b] during early neurogenesis. *Development* 113: 1193-1206.

Krizhanovsky V, Ben-Arie N. 2006. A novel role for the choroid plexus in BMP-mediated inhibition of differentiation of cerebellar neural progenitors. *Mechanisms of development* 123: 67-75.

Ku YC, Renaud NA, Veile RA, Helms C, Voelker CC, Warchol ME, Lovett M. 2014. The transcriptome of utricle hair cell regeneration in the avian inner ear. *The Journal of neuroscience : the official journal of the Society for Neuroscience* 34: 3523-3535.

Kusek JC, Greene RM, Pisano MM. 2001. Expression of the E2F and retinoblastoma families of proteins during neural differentiation. *Brain Research Bulletin* 54: 187-198.

Kwon H-J, Chung H-M. 2003. Yin Yang 1, a vertebrate Polycomb group gene, regulates antero-posterior neural patterning. *Biochemical and Biophysical Research Communications* 306: 1008-1013.

Lai HC, Klisch TJ, Roberts R, Zoghbi HY, Johnson JE. 2011. In vivo neuronal subtype-specific targets of Atoh1 (Math1) in dorsal spinal cord. *The Journal of neuroscience : the official journal of the Society for Neuroscience* 31: 10859-10871.

Landsberg RL, Awatramani RB, Hunter NL, Farago AF, DiPietrantonio HJ, Rodriguez CI, Dymecki SM. 2005. Hindbrain Rhombic Lip Is Comprised of Discrete Progenitor Cell Populations Allocated by Pax6. *Neuron* 48: 933-947.

Lanford PJ, Shailam R, Norton CR, Ridley T, Kelley MW. 2000. Expression of Math1 and HES5 in the Cochleae of Wildtype and Jag2 Mutant Mice. *JARO* 1: 161-171.

La Thangue NB. 1994. DRTFI/E2F: an expanding family of heterodimeric transcription factors implicated in cell cycle control *Elsevier Science Ltd* 19: 108-114.

Lee B, Bhinge A, Iyer V. 2011. Wide-ranging functions of E2F4 in transcriptional activation and repression revealed by genome-wide analysis. Nucleic Acids Res 39: 3558 - 3573.

Lee JS, Galvin KM, Shi Y. 1993. Evidence for physical interaction between the zinc-finger transcription factors YY1 and Sp1. *Proceedings of the National Academy of Sciences of the United States of America* 90: 6145-6149.

Lee KJ, Dietrich P, Jessell TM. 2000. Genetic ablation reveals that the roof plate is essential for dorsal interneuron specification. *Nature* 403: 734-740.

Lees JA, Saito M, Vidal M, Valentine M, Look T, Harlow E, Dyson N, Helin K. 1993. The retinoblastoma protein binds to a family of E2F transcription factors. *Molecular and Cellular Biology* 13: 7813-7825.

Legan PK, Lukashkina VA, Goodyear RJ, Kössl M, Russell IJ, Richardson GP. 2000. A Targeted Deletion in α-Tectorin Reveals that the Tectorial Membrane Is Required for the Gain and Timing of Cochlear Feedback. *Neuron* 28: 273-285.

Legan PK, Rau A, Keen JN, Richardson GP. 1997. The Mouse Tectorins: Modular matrix proteins of the inner ear homologous to components of the sperm-egg adhesion system. *Journal of Biological Chemistry* 272: 8791-8801.

Léger S, Brand M. 2002. Fgf8 and Fgf3 are required for zebrafish ear placode induction, maintenance and inner ear patterning. *Mechanisms of development* 119: 91-108.

Lelli A, Asai Y, Forge A, Holt JR, Géléoc GSG. 2009. Tonotopic Gradient in the Developmental Acquisition of Sensory Transduction in Outer Hair Cells of the Mouse Cochlea. *Journal of Neurophysiology* 101: 2961-2973.

León Y, Sanchez JA, Miner C, Ariza-McNaughton L, Represa JJ, Giraldez F. 1995a. Developmental Regulation of Fos-Protein during Proliferative Growth of the

Otic Vesicle and its Relation to Differentiation Induced by Retinoic Acid. *Developmental Biology* 167: 75-86.

León Y, Vazquez E, Sanz C, Vega JA, Mato JM, Giraldez F, Represa J, Varela-Nieto I. 1995b. Insulin-like growth factor-I regulates cell proliferation in the developing inner ear, activating glycosyl-phosphatidylinositol hydrolysis and Fos expression. *Endocrinology* 136: 3494-3503.

Leow CC, Romero MS, Ross S, Polakis P, Gao W-Q. 2004. Hath1, Down-Regulated in Colon Adenocarcinomas, Inhibits Proliferation and Tumorigenesis of Colon Cancer Cells. *Cancer Research* 64: 6050-6057.

Li J, Ran C, Li E, Gordon F, Comstock G, Siddiqui H, Cleghorn W, Chen H-Z, Kornacker K, Liu C-G et al. 2008. Synergistic Function of E2F7 and E2F8 Is Essential for Cell Survival and Embryonic Development. *Developmental cell* 14: 62-75.

Li S, Price SM, Cahill H, Ryugo DK, Shen MM, Xiang M. 2002. Hearing loss caused by progressive degeneration of cochlear hair cells in mice deficient for the Barhl1 homeobox gene. Development 129: 3523-3532.

Li X, Zhao X, Fang Y, Jiang X, Duong T, Fan C, Huang C-C, Kain SR. 1998. Generation of Destabilized Green Fluorescent Protein as a Transcription Reporter. *Journal of Biological Chemistry* 273: 34970-34975.

Lin Z, Cantos R, Patente M, Wu DK. 2005. Gbx2 is required for the morphogenesis of the mouse inner ear: a downstream candidate of hindbrain signaling. *Development* 132: 2309-2318.

Lindeman GJ, Dagnino L, Gaubatz S, Xu Y, Bronson RT, Warren HB, Livingston DM. 1998. A specific, nonproliferative role for E2F-5 in choroid plexus function revealed by gene targeting. *Genes & Development* 12: 1092-1098.

Liu W, Li G, Chien JS, Raft S, Zhang H, Chiang C, Frenz DA. 2002. Sonic Hedgehog Regulates Otic Capsule Chondrogenesis and Inner Ear Development in the Mouse Embryo. *Developmental Biology* 248: 240-250.

Liu X, Yan D. 2007. Ageing and hearing loss. *Journal of Pathology* 211: 188-197.

Logan N, Delavaine L, Graham A, Reilly C, Wilson J, Brummelkamp TR, Hijmans EM, Bernards R, La Thangue NB. 2004. E2F-7: a distinctive E2F family member with an unusual organization of DNA-binding domains. *Oncogene* 23: 5138-5150.

Logan N, Graham A, Zhao X, Fisher R, Maiti B, Leone G, Thangue NBL. 2005. E2F-8: an E2F family member with a similar organization of DNA-binding domains to E2F-7. *Oncogene* 24: 5000-5004.

Lopez I, Honrubia V, Lee S-C, Li G, Beykirch K. 1998. Hair cell recovery in the chinchilla crista ampullaris after gentamicin treatment: A quantitative approach. *Otolaryngology - Head and Neck Surgery* 119: 255-262.

Lu Z, Luo RZ, Peng H, Huang M, Nishmoto A, Hunt KK, Helin K, Liao WS, Yu Y. 2006. E2F-HDAC complexes negatively regulate the tumor suppressor gene ARHI in breast cancer. *Oncogene* 25: 230-239.

Lui JC, Baron J. 2013. Evidence that Igf2 down-regulation in post-natal tissues and up-regulation in malignancies is driven by transcription factor E2f3. *Proceedings of the National Academy of Sciences* 110: 6181-6186.

Luger K, Mader AW, Richmond RK, Sargent DF, Richmond TJ. 1997. Crystal structure of the nucleosome core particle at 2.8 A resolution. *Nature* 389: 251-260.

Luo RX, Postigo AA, Dean DC. 1998. Rb interacts with histone deacetylase to repress transcription. Cell 92.

Machold R, Fishell G. 2005. Math1 Is Expressed in Temporally Discrete Pools of Cerebellar Rhombic-Lip Neural Progenitors. Neuron 48: 17-24.

Magae J, Wu CL, Illenye S, Harlow E, Heintz NH. 1996. Nuclear localization of DP and E2F transcription factors by heterodimeric partners and retinoblastoma protein family members. Journal of Cell Science 109: 1717-1726.

Magnaghi L, Groisman R, Naguibneva I, Robin P, Lorain S, Le Villain JP, Troalen F, Trouche D, Harel-Bellan A. 1998. Retinoblastoma protein represses transcription by recruiting a histone deacetylase. Nature 391.

Mann DJ, Jones NC. 1996. E2F-1 but not E2F-4 can overcome p16-induced G1 cell-cycle arrest. *Current Biology* 6: 474-483.

Mannoor MS, Jiang Z, James T, Kong YL, Malatesta KA, Soboyejo WO, Verma N, Gracias DH, McAlpine MC. 2013. 3D Printed Bionic Ears. *Nano Letters* 13: 2634-2639.

Mansour SL, Goddard JM, Capecchi MR. 1993. Mice homozygous for a targeted disruption of the proto-oncogene int-2 have developmental defects in the tail and inner ear. *Development* 117: 13-28.

Mantela J, Jiang Z, Ylikoski J, Fritzsch B, Zacksenhaus E, Pirvola U. 2005. The retinoblastoma gene pathway regulates the postmitotic state of hair cells of the mouse inner ear. *Development* 132: 2377-2388.

Marfori M, Mynott A, Ellis JJ, Mehdi AM, Saunders NFW, Curmi PM, Forwood JK, Bodén M, Kobe B. 2011. Molecular basis for specificity of nuclear import and prediction of nuclear localization. *Biochimica et Biophysica Acta (BBA) - Molecular Cell Research* 1813: 1562-1577.

Maricich SM, Wellnitz SA, Nelson AM, Lesniak DR, Gerling GJ, Lumpkin EA, Zoghbi HY. 2009. Merkel Cells are Essential for Light Touch Responses. *Science* (New York, NY) 324: 1580-1582.

Mark M, Lufkin T, Vonesch JL, Ruberte E, Olivo JC, Dolle P, Gorry P, Lumsden A, Chambon P. 1993. Two rhombomeres are altered in Hoxa-1 mutant mice. *Development* 119: 319-338.

Maroon H, Walshe J, Mahmood R, Kiefer P, Dickson C, Mason I. 2002. Fgf3 and Fgf8 are required together for formation of the otic placode and vesicle. *Development* 129: 2099-2108.

Massari ME, Murre C. 2000. Helix-Loop-Helix Proteins: Regulators of Transcription in Eucaryotic Organisms. *Molecular and Cellular Biology* 20: 429-440.

Maston GA, Evans SK, Green MR. 2006. Transcriptional Regulatory Elements in the Human Genome. *Annual Review of Genomics and Human Genetics* 7: 29-59.

Masuda M, Pak K, Chavez E, Ryan AF. 2012. TFE2 and GATA3 enhance induction of POU4F3 and myosin VIIa positive cells in nonsensory cochlear epithelium by ATOH1. *Dev Biol* 372: 68-80.

Matei V, Pauley S, Kaing S, Rowitch D, Beisel KW, Morris K, Feng F, Jones K, Lee J, Fritzsch B. 2005. Smaller inner ear sensory epithelia in Neurog1 null mice are related to earlier hair cell cycle exit. *Developmental Dynamics* 234: 633-650.

Mayor CMB, Schwartz JR., Poliakov A., Rubin EM., Frazer KA., Pachter LS. and Dubchak I. 2000. VISTA: visualizing global DNA sequence alignments of arbitrary length. *Bioinformatics* 16.

McClellan KA, Ruzhynsky VA, Douda DN, Vanderluit JL, Ferguson KL, Chen D, Bremner R, Park DS, Leone G, Slack RS. 2007. Unique Requirement for Rb/E2F3 in Neuronal Migration: Evidence for Cell Cycle-Independent Functions. *Molecular and Cellular Biology* 27: 4825-4843.

Meraldi P, Lukas J, Fry AM, Bartek J, Nigg EA. 1999. Centrosome duplication in mammalian somatic cells requires E2F and Cdk2-Cyclin A. *Nat Cell Biol* 1: 88-93.

Merlo GR, Paleari L, Mantero S, Zerega B, Adamska M, Rinkwitz S, Bober E, Levi G. 2002. The Dlx5 Homeobox Gene Is Essential for Vestibular Morphogenesis in the Mouse Embryo through a BMP4-Mediated Pathway. *Developmental Biology* 248: 157-169.

Meyer BI, Gruss P. 1993. Mouse Cdx-1 expression during gastrulation. *Development* 117: 191-203.

Millimaki BB, Sweet EM, Dhason MS, Riley BB. 2007. Zebrafish atoh1 genes: classic proneural activity in the inner ear and regulation by Fgf and Notch. *Development* 134: 295-305.

Milton A, Luoto K, Ingram L, Munro S, Logan N, Graham AL, Brummelkamp TR, Hijmans EM, Bernards R, La Thangue NB. 2006. A functionally distinct member of the DP family of E2F subunits. *Oncogene* 25: 3212-3218.

Moberg K, Starz MA, Lees JA. 1996. E2F-4 switches from p130 to p107 and pRB in response to cell cycle reentry. *Molecular and Cellular Biology* 16: 1436-1449.

Möröy T. 2005. The zinc finger transcription factor Growth factor independence 1 (Gfi1). The International Journal of Biochemistry & Cell Biology 37: 541-546.

Morrison KM, Miesegaes GR, Lumpkin EA, Maricich SM. 2009. Mammalian Merkel cells are descended from the epidermal lineage. *Developmental Biology* 336: 76-83.

Morsli H, Choo D, Ryan A, Johnson R, Wu DK. 1998. Development of the Mouse Inner Ear and Origin of Its Sensory Organs. *The Journal of Neuroscience* 18: 3327-3335.

Morsli H, Tuorto F, Choo D, Postiglione MP, Simeone A, Wu DK. 1999. Otx1 and Otx2 activities are required for the normal development of the mouse inner ear. *Development* 126: 2335-2343.

Muller H, Bracken AP, Vernell R, Moroni MC, Christians F, Grassilli E, Prosperini E, Vigo E, Oliner JD, Helin K. 2001. E2Fs regulate the expression of genes involved in differentiation, development, proliferation, and apoptosis. *Genes Dev* 15: 267-285.

Müller H, Moroni MC, Vigo E, Petersen BO, Bartek J, Helin K. 1997. Induction of S-phase entry by E2F transcription factors depends on their nuclear localization. *Molecular and Cellular Biology* 17: 5508-5520.

Muller U, Barr-Gillespie PG. 2015. New treatment options for hearing loss. *Nat Rev Drug Discov* 14: 346-365.

Mulvaney JF, Amemiya Y, Freeman SD, Ladher RK, Dabdoub A. 2015. Molecular cloning and functional characterisation of chicken Atonal homologue 1: A comparison with human Atoh1. *Biology of the Cell* 107: 41-60.

Mulvaney J, Dabdoub A. 2012. Atoh1, an essential transcription factor in neurogenesis and intestinal and inner ear development: function, regulation, and context dependency. *Journal of the Association for Research in Otolaryngology : JARO* 13: 281-293.

Mutoh H, Sakamoto H, Hayakawa H, Arao Y, Satoh K, Nokubi M, Sugano K. 2006. The intestine-specific homeobox gene Cdx2 induces expression of the basic helix–loop–helix transcription factor Math1. *Differentiation; research in biological diversity* 74: 313-321.

Myat A, Henrique D, Ish-Horowicz D, Lewis J. 1996. A Chick Homologue ofSerrateand Its Relationship withNotchandDeltaHomologues during Central Neurogenesis. *Developmental Biology* 174: 233-247.

Nagy I, Monge A, Albinger-Hegyi A, Schmid S, Bodmer D. 2005. NF-kappaB is required for survival of immature auditory hair cells in vitro. *Journal of the Association for Research in Otolaryngology : JARO* 6: 260-268.

Namdaran P, Reinhart KE, Owens KN, Raible DW, Rubel EW. 2012. Identification of Modulators of Hair Cell Regeneration in the Zebrafish Lateral Line. *The Journal of Neuroscience* 32: 3516-3528.

Neves J, Uchikawa M, Bigas A, Giraldez F. 2012. The prosensory function of Sox2 in the chicken inner ear relies on the direct regulation of Atoh1. *PLoS ONE* 7: e30871.

Nevins J. 1998. Toward an understanding of the functional complexity of the E2F and retinoblastoma families. *Cell Growth Differ* 9: 585 - 593.

Nissen RM, Yan J, Amsterdam A, Hopkins N, Burgess SM. 2003. Zebrafish foxi one modulates cellular responses to Fgf signaling required for the integrity of ear and jaw patterning. *Development* 130: 2543-2554.

Nornes HO, Dressler GR, Knapik EW, Deutsch U, Gruss P. 1990. Spatially and temporally restricted expression of Pax2 during murine neurogenesis. *Development* 109: 797-809.

Novoradovsky A., Zhang V., Ghosh M., Hogrefe H., Sorge JA. and Gaasterland T. 2005. Computational Principles of Primer Design for Site Directed Mutagenesis. *Nanotech* 1: 532 - 535.

Ohyama T, Groves AK, Martin K. 2007. The first steps towards hearing: mechanisms of otic placode induction. *The International journal of developmental biology* 51: 463-472.

Ormondroyd E dlLS, La Thangue NB. 1995. A new member of the DP family, DP-3, with distinct protein products suggests a regulatory role for alternative splicing in the cell cycle transcription factor DRTF1/E2F. *Oncogene* 11: 1437.

Oshima K, Shin K, Diensthuber M, Peng AW, Ricci AJ, Heller S. 2010. Mechanosensitive Hair Cell-Like Cells from Embryonic and Induced Pluripotent Stem Cells. *Cell* 141: 704-716.

Pahl HL. 1999. Activators and target genes of Rel/NF-kB transcription factors. *Oncogene* 18: 6853 – 6866.

Palstra RJ, Grosveld F. 2012. Transcription factor binding at enhancers: shaping a genomic regulatory landscape in flux. *Frontiers in genetics* 3: 195.

Pan N, Jahan I, Kersigo J, Duncan JS, Kopecky B, Fritzsch B. 2012. A novel Atoh1 "self-terminating" mouse model reveals the necessity of proper Atoh1 level and duration for hair cell differentiation and viability. PLoS ONE 7: e30358.

Passamaneck YJ, Katikala L, Perrone L, Dunn MP, Oda-Ishii I, Di Gregorio A. 2009. Direct activation of a notochord cis-regulatory module by Brachyury and FoxA in the ascidian Ciona intestinalis. *Development (Cambridge, England)* 136: 3679-3689.

Pasteau S LL, Arnaud L, Trembleau A, Brun G. 1995. Isolation and characterization of a chicken homolog of the E2F-1 transcription factor. *Oncogene* October 19: 1475-1486.

Pauley S, Wright TJ, Pirvola U, Ornitz D, Beisel K, Fritzsch B. 2003. Expression and function of FGF10 in mammalian inner ear development. *Developmental Dynamics* 227: 203-215.

Pearson BE, Nasheuer HP, Wang TS. 1991. Human DNA polymerase alpha gene: sequences controlling expression in cycling and serum-stimulated cells. *Molecular and Cellular Biology* 11: 2081-2095.

Person RE, Li F-Q, Duan Z, Benson KF, Wechsler J, Papadaki HA, Eliopoulos G, Kaufman C, Bertolone SJ, Nakamoto B et al. 2003. Mutations in proto-oncogene GFI1 cause human neutropenia and target ELA2. Nature genetics 34: 308-312.

Peignon G, Durand A, Cacheux W, Ayrault O, Terris B, Laurent-Puig P, Shroyer NF, Van Seuningen I, Honjo T, Perret C et al. 2011. Complex interplay between β-catenin signalling and Notch effectors in intestinal tumorigenesis. *Gut* 60: 166-176.

Pfeffer PL, Gerster T, Lun K, Brand M, Busslinger M. 1998. Characterization of three novel members of the zebrafish Pax2/5/8 family: dependency of Pax5 and Pax8 expression on the Pax2.1 (noi) function. *Development* 125: 3063-3074.

Phillips AC, Ernst MK, Bates S, Rice NR, Vousden KH. 1999. E2F-1 Potentiates Cell Death by Blocking Antiapoptotic Signaling Pathways. *Molecular Cell* 4: 771-781.

Pickles JO. 1993. Early events in auditory processing. *Current Opinion in Neurobiology* 3: 558-562.

Pickles JO. 1998. An Introduction to the Physiology of Hearing. *Emerald Group Plublishing Limited*.

Plank J L, Dean A. 2014. Enhancer Function: Mechanistic and Genome-Wide Insights Come Together. *Molecular Cell* 55: 5-14.

Prabakaran S, Lippens G, Steen H, Gunawardena J. 2012. Post-translational modification: nature's escape from genetic imprisonment and the basis for dynamic information encoding. *Wiley interdisciplinary reviews Systems biology and medicine* 4: 565-583.

Pujades C, Kamaid A, Alsina B, Giraldez F. 2006. BMP-signaling regulates the generation of hair-cells. *Developmental Biology* 292: 55-67.

Purves D, Augustine G, Fitzpatrick D, Hall W, LaMantia A, McNamara J, White L. 2008. *Neuroscience, 4th Edition*.

Quandt K, Frech K, Karas H, Wingender E, Werner T. 1995. Matlnd and Matlnspector: new fast and versatile tools for detection of consensus matches in nucleotide sequence data. *Nucleic Acids Research* 23: 4878-4884.

Raft S, Koundakjian EJ, Quinones H, Jayasena CS, Goodrich LV, Johnson JE, Segil N, Groves AK. 2007. Cross-regulation of Ngn1 and Math1 coordinates the production of neurons and sensory hair cells during inner ear development. *Development* 134: 4405-4415.

Raft S, Nowotschin S, Liao J, Morrow BE. 2004. Suppression of neural fate and control of inner ear morphogenesis by Tbx1. *Development* 131: 1801-1812.

Raimundo N, Song L, Shutt TE, McKay SE, Cotney J, Guan MX, Gilliland TC, Hohuan D, Santos-Sacchi J, Shadel GS. 2012. Mitochondrial stress engages E2F1 apoptotic signaling to cause deafness. *Cell* 148: 716-726.

Rajab A, Kelberman D, de Castro SCP, Biebermann H, Shaikh H, Pearce K, Hall CM, Shaikh G, Gerrelli D, Grueters A et al. 2008. Novel mutations in LHX3 are associated with hypopituitarism and sensorineural hearing loss. Human Molecular Genetics 17: 2150-2159.

Ratajewski M, Pulaski L. 2009. YY1-dependent transcriptional regulation of the human GDAP1 gene. *Genomics* 94: 407-413.

Ryan AF. 1997. Transcription factors and the control of inner ear development. Seminars in Cell & Developmental Biology 8: 249-256.

Represa J, Sanchez A, Miner C, Lewis J, Giraldez F. 1990. Retinoic acid modulation of the early development of the inner ear is associated with the control of c-fos expression. *Development* 110: 1081-1090.

Riccomagno MM, Martinu L, Mulheisen M, Wu DK, Epstein DJ. 2002. Specification of the mammalian cochlea is dependent on Sonic hedgehog. *Genes & Development* 16: 2365-2378.

Riccomagno MM, Takada S, Epstein DJ. 2005. Wnt-dependent regulation of inner ear morphogenesis is balanced by the opposing and supporting roles of Shh. *Genes & Development* 19: 1612-1623.

Richardson GP, Russell IJ, Duance VC, Bailey AJ. 1987. Polypeptide composition of the mammalian tectorial membrane. *Hearing Research* 25: 45-60.

Rivolta MN. 2012. New strategies for the restoration of hearing loss: challenges and opportunities. *British Medical Bulletin* doi:10.1093/bmb/lds035.

Rivolta MN, Grix N, Lawlor P, Ashmore JF, Jagger DJ, Holley MC. 1998. Auditory hair cell precursors immortalized from the mammalian inner ear. *Proceedings of the Royal Society B: Biological Sciences* 265: 1595-1603.

Rivolta MN, Holley MC. 2002. Cell lines in inner ear research. *Journal of neurobiology* 53: 306-318.

Robledo RF, Lufkin T. 2006. Dlx5 and Dlx6 homeobox genes are required for specification of the mammalian vestibular apparatus. *genesis* 44: 425-437.

Rocha-Sanchez SM., Beisel KW. 2007. *The International Journal of Developmental Biology* 51 (6-7): 585-95.

Rose MF, Ren J, Ahmad KA, Chao H-T, Klisch TJ, Flora A, Greer JJ, Zoghbi HY. 2009. Math1 Is Essential for the Development of Hindbrain Neurons Critical for Perinatal Breathing. *Neuron* 64: 341-354.

Rubel EW, Dew LA, Roberson DW, Warchol ME, Corwin JT, Forge A, Li L, Nevill G. 1995. Mammalian Vestibular Hair Cell Regeneration. *Science* 267: 701-707.

Ruben. 1967. Development of the inner ear of the mouse: a radioautographic study of terminal mitoses. *Acta Otolaryngology* 220: 1-44.

Rubin SM. 2013. Deciphering the retinoblastoma protein phosphorylation code. Trends in Biochemical Sciences 38: 12-19.

Rüsch A, Ng L, Goodyear R, Oliver D, Lisoukov I, Vennström B, Richardson G, Kelley MW, Forrest D. 2001. Retardation of Cochlear Maturation and Impaired Hair Cell Function Caused by Deletion of All Known Thyroid Hormone Receptors. *The Journal of Neuroscience* 21: 9792-9800.

Ruzhynsky VA, McClellan KA, Vanderluit JL, Jeong Y, Furimsky M, Park DS, Epstein DJ, Wallace VA, Slack RS. 2007. Cell Cycle Regulator E2F4 Is Essential for the Development of the Ventral Telencephalon. *The Journal of Neuroscience* 27: 5926-5935.

Ryan AF. 1997. Transcription factors and the control of inner ear development. *Seminars in Cell & Developmental Biology* 8: 249-256.

Ryals BM., Rubel EW. 1988 Hair cell regeneration after acoustic trauma in adult Coturnix quail. *Science* Jun 24;240: 1774-1776.

Sage C, Huang M, Vollrath MA, Brown MC, Hinds PW, Corey DP, Vetter DE, Chen ZY. 2006. Essential role of retinoblastoma protein in mammalian hair cell development and hearing. *Proceedings of the National Academy of Sciences of the United States of America* 103: 7345-7350.

Sage J. 2000. Targeted disruption of the three Rb-related genes leads to loss of G1 control and immortalization. *Genes & Development* 14: 3037-3050.

Sainsbury S, Bernecky C, Cramer P. 2015. Structural basis of transcription initiation by RNA polymerase II. *Nat Rev Mol Cell Biol* 16: 129-143.

Saint-Germain N, Lee Y-H, Zhang Y, Sargent TD, Saint-Jeannet J-P. 2004. Specification of the otic placode depends on Sox9 function in Xenopus. *Development* 131: 1755-1763.

Sander JD, Joung JK. 2014. CRISPR-Cas systems for editing, regulating and targeting genomes. Nat Biotech 32: 347-355.

Sato Y, Kasai T, Nakagawa S, Tanabe K, Watanabe T, Kawakami K, Takahashi Y. 2007. Stable integration and conditional expression of electroporated transgenes in chicken embryos. *Developmental Biology* 305: 616-624.

Scheffer D, Sage C, Corey DP, Pingault V. 2007. Gene expression profiling identifies Hes6 as a transcriptional target of ATOH1 in cochlear hair cells. *FEBS Letters* 581: 4651-4656.

Schmid RM, Perkins ND, Duckett CS, Andrews PC, Nabel GJ. 1991. Cloning of an NF-[kappa]B subunit which stimulates HIV transcription in synergy with p65. *Nature* 352: 733-736.

Schwarz JK, Bassing CH, Kovesdi I, Datto MB, Blazing M, George S, Wang XF, Nevins JR. 1995. Expression of the E2F1 transcription factor overcomes type beta transforming growth factor-mediated growth suppression. *Proceedings of the National Academy of Sciences of the United States of America* 92: 483-487.

Seigel GM. 1999. The golden age of retinal cell culture. *Molecular Vision* 19; 5:4.

Seto E, Lewist B, Shenk T. 1993. Interaction between transcription factors Spl and YY1. *Nature* 365: 462-464.

Sherr CJ, Roberts JM. 1999. CDK inhibitors: positive and negative regulators of G1-phase progression. *Genes & Development* 13: 1501-1512.

Shi F, Cheng Y-f, Wang XL, Edge ASB. 2010. β-Catenin Up-regulates Atoh1 Expression in Neural Progenitor Cells by Interaction with an Atoh1 3′ Enhancer. *Journal of Biological Chemistry* 285: 392-400.

Shi Y, Seto E, Chang L-S, Shenk T. 1991. Transcriptional repression by YY1, a human GLI-Krüippel-related protein, and relief of repression by adenovirus E1A protein. *Cell* 67: 377-388.

Shou J, Zheng JL, Gao W-Q. 2003. Robust generation of new hair cells in the mature mammalian inner ear by adenoviral expression of Hath1. *Molecular and*

Shroyer NF, Wallis D, Venken KJT, Bellen HJ, Zoghbi HY. 2005. Gfi1 functions downstream of Math1 to control intestinal secretory cell subtype allocation and differentiation. Genes & Development 19: 2412-2417.

Sidorova N, Hung S, Rau DC. 2010. Stabilizing labile DNA-protein complexes in polyacrylamide gels. *Electrophoresis* 31: 648-653.

Siegfried Z, Simon I. 2010. DNA methylation and gene expression. *Wiley Interdisciplinary Reviews: Systems Biology and Medicine* 2: 362-371.

Slepecky NB. 1996. Structure of the mammalian cochlea. In: Dallos P, Popper A, Fay R, editors. The Cochlea. New York: Springer-Verlag. 44–129.

Slepecky NB, Savage JE, Cefaratti LK, Yoo TJ. 1992. Electron-microscopic localization of type II, IX, and V collagen in the organ of Corti of the gerbil. *Cell and tissue research* 267: 413-418.

Solomon KS, Kudoh T, Dawid IB, Fritz A. 2003. Zebrafish foxi1 mediates otic placode formation and jaw development. *Development* 130: 929-940.

Soni LE, Warren CM, Bucci C, Orten DJ, Hasson T. 2005. The unconventional myosin-VIIa associates with lysosomes. *Cell motility and the cytoskeleton* 62: 13-26.

Stegmaier P KA, Wingender E. 2004. Systematic DNA-binding domain classification of transcription factors. *Genome Informatics International Conference on Genome Informatics* 15 276–286.

Stewart MD, Jang C-W, Hong NW, Austin AP, Behringer RR. 2009. Dual fluorescent protein reporters for studying cell behaviors in vivo. *Genesis (New York, Ny : 2000)* 47: 708-717.

Stiewe T, Putzer BM. 2000. Role of the p53-homologue p73 in E2F1-induced apoptosis. *Nat Genet* 26: 464-469.

Stojanova ZP, Kwan T, Segil N. 2015. Epigenetic regulation of Atoh1 guides hair cell development in the mammalian cochlea. *Development* 142: 3529-3536.

Stone JS. 1998. Recent insights into regeneration of auditory and vestibular hair cells. *Current Opinion in Neurology* 11: 17-24.

Stone JS, Rubel EW. 2000. Cellular studies of auditory hair cell regeneration in birds. *Proceedings of the National Academy of Sciences* 97: 11714-11721.

Stone JS, Shang J-L, Tomarev S. 2003. Expression of Prox1 defines regions of the avian otocyst that give rise to sensory or neural cells. *The Journal of Comparative Neurology* 460: 487-502.

Street VA, Li J, Robbins CA, Kallman JC. 2011. A DNA Variant within the MYO7A Promoter Regulates YY1 Transcription Factor Binding and Gene Expression Serving as a Potential Dominant DFNA11 Auditory Genetic Modifier. *Journal of Biological Chemistry* 286: 15278-15286.

Sud R, Jones CM, Banfi S, Dawson SJ. 2005. Transcriptional regulation by Barhl1 and Brn-3c in organ-of-Corti-derived cell lines. Brain Res Mol Brain Res 141: 174-180.

Sun X-H, Baltimore D. 1991. An inhibitory domain of E12 transcription factor prevents DNA binding in E12 homodimers but not in E12 heterodimers. *Cell* 64: 459-470.

Sun Y, Jan LY, Jan YN. 1998. Transcriptional regulation of atonal during development of the Drosophila peripheral nervous system. *Development* 125: 3731-3740.

Takahashi Y, Rayman JB, Dynlacht BD. 2000. Analysis of promoter binding by the E2F and pRB families in vivo: distinct E2F proteins mediate activation and repression. Genes & Development 14: 804-816.

Tanaka M, Ueda A, Kanamori H, Ideguchi H, Yang J, Kitajima S, Ishigatsubo Y. 2002. Cell-cycle-dependent Regulation of Human aurora A Transcription Is Mediated by Periodic Repression of E4TF1. *Journal of Biological Chemistry* 277: 10719-10726.

Tao Y, Kassatly RF, Cress WD, Horowitz JM. 1997. Subunit composition determines E2F DNA-binding site specificity. *Molecular and Cellular Biology* 17: 6994-7007.

Taylor RR, Forge A. 2005. Hair cell regeneration in sensory epithelia from the inner ear of a urodele amphibian. *The Journal of Comparative Neurology* 484: 105-120.

Terrinoni A, Serra V, Bruno E, Strasser A, Valente E, Flores ER, van Bokhoven H, Lu X, Knight RA, Melino G. 2013. Role of p63 and the Notch pathway in cochlea development and sensorineural deafness. *Proceedings of the National Academy of Sciences of the United States of America* 110: 7300-7305.

Thompson DC, McPhillips H, Davis RL, Lieu TA, Homer CJ, Helfand M. 2001. Universal newborn hearing screening: Summary of evidence. *JAMA* 286: 2000-2010.

Tornari C, Towers ER, Gale JE, Dawson SJ. 2014. Regulation of the Orphan Nuclear Receptor *Nr2f2* by the DFNA15 Deafness Gene *Pou4f3*. *PLoS ONE* 9: e112247.

Torres M, Giráldez F. 1998. The development of the vertebrate inner ear. *Mechanisms of development* 71: 5-21.

Towers M, Fisunov G, Tickle C. 2009. Expression of E2F transcription factor family genes during chick wing development. *Gene Expression Patterns* 9: 528-531.

Towers ER, Kelly JJ, Sud R, Gale JE, Dawson SJ. 2011. Caprin-1 is a target of the deafness gene Pou4f3 and is recruited to stress granules in cochlear hair cells in response to ototoxic damage. *Journal of Cell Science* 124: 1145-1155.

Trainor P, Krumlauf R. 2000. Plasticity in mouse neural crest cells reveals a new patterning role for cranial mesoderm. *Nat Cell Biol* 2: 96-102.

Trimarchi JM, Fairchild B, Verona R, Moberg K, Andon N, Lees JA. 1998. E2F-6, a member of the E2F family that can behave as a transcriptional repressor. *Proceedings of the National Academy of Sciences of the United States of America* 95: 2850-2855.

Tsai KY, Hu Y, Macleod KF, Crowley D, Yamasaki L, Jacks T. 1998. Mutation of E2f-1 Suppresses Apoptosis and Inappropriate S Phase Entry and Extends Survival of Rb-Deficient Mouse Embryos. *Molecular Cell* 2: 293-304.

Uchida Y, Sugiura S, Ando F, Nakashima T, Shimokata H. 2011. Molecular genetic epidemiology of age-related hearing impairment. *Auris Nasus Larynx* 38: 657-665.

Urasaki A, Morvan G, Kawakami K. 2006. Functional Dissection of the Tol2 Transposable Element Identified the Minimal cis-Sequence and a Highly Repetitive Sequence in the Subterminal Region Essential for Transposition. *Genetics* 174: 639-649.

Usheva A, Shenk T. 1994. TATA-binding protein-independent initiation: YY1, TFIIB, and RNA polymerase II direct basal transcription on supercoiled template DNA. *Cell* 76: 1115-1121.

Vahava O, Morell R, Lynch ED, Weiss S, Kagan ME, Ahituv N, Morrow JE, Lee MK, Skvorak AB, Morton CC et al. 1998. Mutation in Transcription Factor POU4F3 Associated with Inherited Progressive Hearing Loss in Humans. Science 279: 1950-1954.

Van den Heuvel S, Dyson NJ. 2008. Conserved functions of the pRB and E2F families. *Nat Rev Mol Cell Biol* 9.

VanDussen KL, Samuelson LC. 2010. Mouse atonal homolog 1 directs intestinal progenitors to secretory cell rather than absorptive cell fate. Developmental Biology 346: 215-223.

Van Esch H, Groenen P, Nesbit MA, Schuffenhauer S, Lichtner P, Vanderlinden G, Harding B, Beetz R, Bilous RW, Holdaway I et al. 2000. GATA3 haplo-insufficiency causes human HDR syndrome. *Nature* 406: 419-422.

Van Eyken E, Van Camp G, Van Laer L. 2007. The Complexity of Age-Related Hearing Impairment: Contributing Environmental and Genetic Factors. *Audiology and Neurotology* 12: 345-358.

Van Keymeulen A, Mascre G, Youseff KK, Harel I, Michaux C, De Geest N, Szpalski C, Achouri Y, Bloch W, Hassan BA et al. 2009. Epidermal progenitors give rise to Merkel cells during embryonic development and adult homeostasis. *The Journal of Cell Biology* 187: 91-100.

Vernimmen D, Bickmore WA. 2015. The Hierarchy of Transcriptional Activation: From Enhancer to Promoter. *Trends in Genetics* 31: 696-708.

Verona R, Moberg K, Estes S, Starz M, Vernon JP, Lees JA. 1997. E2F activity is regulated by cell cycle-dependent changes in subcellular localization. *Molecular and Cellular Biology* 17: 7268-7282.

Vitelli F, Viola A, Morishima M, Pramparo T, Baldini A, Lindsay E. 2003. TBX1 is required for inner ear morphogenesis. *Human Molecular Genetics* 12: 2041-2048.

Wallis D, Hamblen M, Zhou Y, Venken KJT, Schumacher A, Grimes HL, Zoghbi HY, Orkin SH, Bellen HJ. 2003. The zinc finger transcription factor Gfi1, implicated in lymphomagenesis, is required for inner ear hair cell differentiation and survival. Development 130: 221-232.

Wang C-C, Tsai M-F, Hong T-M, Chang G-C, Chen C-Y, Yang W-M, Chen JJW, Yang P-C. 2005. The transcriptional factor YY1 upregulates the novel invasion suppressor HLJ1 expression and inhibits cancer cell invasion. *Oncogene* 24: 4081-4093.

Wang G-P, Chatterjee I, Batts SA, Wong HT, Gong T-W, Gong S-S, Raphael Y. 2010. Notch signaling and Atoh1 expression during hair cell regeneration in the mouse utricle. *Hearing Research* 267: 61-70.

Wang L, Wang R, Herrup K. 2007. E2F1 Works as a Cell Cycle Suppressor in Mature Neurons. *The Journal of Neuroscience* 27: 12555-12564.

Wang VY, Rose MF, Zoghbi HY. 2005. Math1 Expression Redefines the Rhombic Lip Derivatives and Reveals Novel Lineages within the Brainstem and Cerebellum. *Neuron* 48: 31-43.

Wang W, Grimmer JF, Van De Water TR, Lufkin T. 2004. Hmx2 and Hmx3 Homeobox Genes Direct Development of the Murine Inner Ear and Hypothalamus and Can Be Functionally Replaced by Drosophila Hmx. *Developmental cell* 7: 439-453.

Weinmann AS, Bartley SM, Zhang T, Zhang MQ, Farnham PJ. 2001. Use of Chromatin Immunoprecipitation To Clone Novel E2F Target Promoters. *Molecular and Cellular Biology* 21: 6820-6832.

Weiss S, Gottfried I, Mayrose I, Khare SL, Xiang M, Dawson SJ, Avraham KB. 2003. The DFNA15 Deafness Mutation Affects POU4F3 Protein Stability, Localization, and Transcriptional Activity. Molecular and Cellular Biology 23: 7957-7964.

Wiener FM, Ross DA. 1946. The Pressure Distribution in the Auditory Canal in a Progressive Sound Field. *The Journal of the Acoustical Society of America* 18: 401-408.

Woods C, Montcouquiol M, Kelley MW. 2004. Math1 regulates development of the sensory epithelium in the mammalian cochlea. *Nat Neurosci* 7: 1310-1318.

Workman JL, Kingston RE. 1998. Alteration of nucleosome structure as a mechanism of transcriptional regulation. *Annual Review of Biochemistry* 67: 545-579.

Wright E, Hargrave MR, Christiansen J, Cooper L, Kun J, Evans T, Gangadharan U, Greenfield A, Koopman P. 1995. The Sry-related gene Sox9 is expressed during chondrogenesis in mouse embryos. *Nat Genet* 9: 15-20.

Wu CL, Zukerberg LR, Ngwu C, Harlow E, Lees JA. 1995. In vivo association of E2F and DP family proteins. *Molecular and Cellular Biology* 15: 2536-2546.

Wu DK, Nunes FD, Choo D. 1998. Axial specification for sensory organs versus non-sensory structures of the chicken inner ear. *Development* 125: 11-20.

Wu L, Timmers C, Maiti B, Saavedra HI, Sang L, Chong GT, Nuckolls F, Giangrande P, Wright FA, Field SJ et al. 2001. The E2F1-3 transcription factors are essential for cellular proliferation. *Nature* 414: 457-462.

Xiang M, Gan L, Li D, Chen Z-Y, Zhou L, O'Malley BW, Klein W, Nathans J. 1997. Essential role of POU–domain factor Brn-3c in auditory and vestibular hair

cell development. *Proceedings of the National Academy of Sciences* 94: 9445-9450.

Xiang M, Gao WQ, Hasson T, Shin JJ. 1998. Requirement for Brn-3c in maturation and survival, but not in fate determination of inner ear hair cells. *Development* 125: 3935-3946.

Xu P-X, Adams J, Peters H, Brown MC, Heaney S, Maas R. 1999. Eya1-deficient mice lack ears and kidneys and show abnormal apoptosis of organ primordia. *Nat Genet* 23: 113-117.

Yamasoba T, Lin FR, Someya S, Kashio A, Sakamoto T, Kondo K. 2013. Current concepts in age-related hearing loss: Epidemiology and mechanistic pathways. *Hearing research* 303: 30-38.

Yang C, Bolotin E, Jiang T, Sladek FM, Martinez E. 2007. Prevalence of the initiator over the TATA box in human and yeast genes and identification of DNA motifs enriched in human TATA-less core promoters. *Gene* 389: 52-65.

Yang H, Xie X, Deng M, Chen X, Gan L. 2010. Generation and characterization of Atoh1-Cre knock-in mouse line. *genesis* 48: 407-413.

Yang Q, Bermingham NA, Finegold MJ, Zoghbi HY. 2001. Requirement of Math1 for Secretory Cell Lineage Commitment in the Mouse Intestine. *Science* 294: 2155-2158.

Yu W, Chan-On W, Teo M, Ong C, Cutcutache I, Allen G, Wong B, Myint S, Lim K, Voorhoeve PM et al. 2011. First somatic mutation of E2F1 in a critical DNA binding residue discovered in well-differentiated papillary mesothelioma of the peritoneum. *Genome Biology* 12: R96.

Zhang Y CS. 1995. Cloning and characterization of human DP2, a novel dimerization partner of E2F. *Oncogene* 10: 2085.

Zhao H, Ayrault O, Zindy F, Kim J-H, Roussel MF. 2008. Post-transcriptional down-regulation of Atoh1/Math1 by bone morphogenic proteins suppresses medulloblastoma development. *Genes & Development* 22: 722-727.

Zheng JL, Gao W-Q. 1997. Analysis of Rat Vestibular Hair Cell Development and Regeneration Using Calretinin as an Early Marker. *The Journal of Neuroscience* 17: 8270-8282.

Zheng JL, Gao W-Q. 2000. Overexpression of Math1 induces robust production of extra hair cells in post-natal rat inner ears. *Nat Neurosci* 3: 580-586.

Zheng W, Huang L, Wei Z-B, Silvius D, Tang B, Xu P-X. 2003. The role of Six1 in mammalian auditory system development. *Development* 130: 3989-4000.

Ziebold U, Reza T, Caron A, Lees JA. 2001. E2F3 contributes both to the inappropriate proliferation and to the apoptosis arising in Rb mutant embryos. *Genes & Development* 15: 386-391.

On line databases

Allen Brain Atlas: Website: © 2015 Allen Institute for Brain Science. Allen Brain Atlas [Internet]. Available from: http://www.brain-map.org.

ATOH1 expressing cell lines:
https://genevisible.com/cell-lines/HS/Gene%20Symbol/ATOH1

ClustalW2.1: http://www.ebi.ac.uk/Tools/msa/clustalw2

echick atlas: http://www.echickatlas.org/ecap/home.html

Emage: http://www.emouseatlas.org/emage

Ensembl genome browser: http://www.ensembl.org/index.html

GEISHA: Gallus Expression *In Situ* Hybridization Analysis
http://geisha.arizona.edu/geisha

GeneCardsSuite: http://www.genecards.org/cgi-bin/carddisp.pl?gene=ATOH1

Genomatix (MatInspector):
https://www.genomatix.de/online_help/help_matinspector/matinspector_help.html

mVista: http://genome.lbl.gov/vista/mvista/submit.shtml

Oligo Calc: http://biotools.nubic.northwestern.edu/OligoCalc.html

Quick Change Site-Directed Mutagenesis Primer Design:
http://www.genomics.agilent.com/primerDesignProgram.jsp.

Santa Cruz Biotechnology: E2F1 (C-20): sc-193datasheet.datasheets.scbt.com/sc-193.pdf